

WEAK DECAYS BEYOND LEADING LOGARITHMS

Gerhard Buchalla³, Andrzej J. Buras^{1,2}, Markus E. Lautenbacher^{1,4}

¹ *Physik Department, Technische Universität München,
D-85748 Garching, Germany.*

² *Max-Planck-Institut für Physik – Werner-Heisenberg-Institut,
Föhringer Ring 6, D-80805 München, Germany.*

³ *Theoretical Physics Department,
Fermi National Accelerator Laboratory,
P.O. Box 500, Batavia, IL 60510, USA.*

⁴ *SLAC Theory Group, Stanford University,
P.O. Box 4349, Stanford, CA 94309, USA.*

(November 1995)

to appear in Reviews of Modern Physics

Abstract

We review the present status of QCD corrections to weak decays beyond the leading logarithmic approximation including particle-antiparticle mixing and rare and CP violating decays. After presenting the basic formalism for these calculations we discuss in detail the effective hamiltonians for all decays for which the next-to-leading corrections are known. Subsequently, we present the phenomenological implications of these calculations. In particular we update the values of various parameters and we incorporate new information on m_t in view of the recent top quark discovery. One of the central issues in our review are the theoretical uncertainties related to renormalization scale ambiguities which are substantially reduced by including next-to-leading order corrections. The impact of this theoretical improvement on the determination of the Cabibbo-Kobayashi-Maskawa matrix is then illustrated in various cases.

Contents

I	Introduction	1
A	Preliminary Remarks	1
B	Outline	5
II	Standard Electroweak Model	8
A	Particles and Interactions	8
B	Standard Parametrization	9
C	Wolfenstein Parameterization Beyond Leading Order	10
D	Unitarity Triangle Beyond Leading Order	12
III	Basic Formalism	14
A	Renormalization of QCD	14
B	Operator Product Expansion in Weak Decays – Preliminaries	17
C	OPE and Short Distance QCD Effects	20
D	The Renormalization Group	26
1	Basic Concepts	26
2	Threshold Effects in LLA	28
3	Penguin Operators	29
E	Summary of Basic Formalism	30
F	Wilson Coefficients Beyond Leading Order	31
1	The RG Formalism	31
2	The Calculation of the Anomalous Dimensions	35
3	Renormalization Scheme Dependence	37
4	Discussion	39
5	Evanescence Operators	41
IV	Guide to Effective Hamiltonians	44
V	The Effective $\mu = 1$ Hamiltonian: Current-Current Operators	47
A	Operators	47
B	Wilson Coefficients and RG Evolution	47
VI	The Effective $\mu = 1$ Hamiltonian: Inclusion of QCD Penguin Operators	53
A	Operators	53
B	Wilson Coefficients	54
C	Renormalization Group Evolution and Anomalous Dimension Matrices	56
D	Quark Threshold Matching Matrix	57
E	Numerical Results for the $K \rightarrow \pi$ Wilson Coefficients in Pure QCD	57
F	The $B \rightarrow \pi$ Effective Hamiltonian in Pure QCD	59
G	Numerical Results for the $B \rightarrow \pi$ Wilson Coefficients in Pure QCD	60

VII	The Effective $B = 1$ Hamiltonian: Inclusion of Electroweak Penguin Operators	61
A	Operators	61
B	Wilson Coefficients	62
C	Renormalization Group Evolution and Anomalous Dimension Matrices	63
D	Quark Threshold Matching Matrix	66
E	Numerical Results for the $K \rightarrow \pi$ Wilson Coefficients	67
F	The $B = 1$ Effective Hamiltonian Including Electroweak Penguins	68
G	Numerical Results for the $B = 1$ Wilson Coefficients	71
VIII	The Effective Hamiltonian for $K_L \rightarrow \pi^0 e^+ e^-$	73
A	Operators	73
B	Wilson Coefficients	74
C	Renormalization Group Evolution and Anomalous Dimension Matrices	75
D	Quark Threshold Matching Matrix	76
E	Numerical Results for the $K_L \rightarrow \pi^0 e^+ e^-$ Wilson Coefficients	76
IX	The Effective Hamiltonian for $B \rightarrow X_s$	79
A	Operators	79
B	Wilson Coefficients	79
C	Renormalization Group Evolution and Anomalous Dimension Matrices	81
D	Results for the Wilson Coefficients	83
E	Numerical Analysis	83
X	The Effective Hamiltonian for $B \rightarrow X_s e^+ e^-$	85
A	Operators	85
B	Wilson Coefficients	85
C	Numerical Results	87
XI	Effective Hamiltonians for Rare K - and B -Decays	89
A	Overview	89
B	The Decay $K^+ \rightarrow \pi^+ \pi^0$	91
1	The Next-to-Leading Order Effective Hamiltonian	91
2	Z-Penguin and Box Contribution in the Top Sector	93
3	The Z -Penguin Contribution in the Charm Sector	94
4	The Box Contribution in the Charm Sector	96
5	Discussion	97
C	The Decay $(K_L \rightarrow \pi^+ \pi^-)_{SD}$	98
1	The Next-to-Leading Order Effective Hamiltonian	98
2	Discussion	99
D	The Decays $K_L \rightarrow \pi^0 \pi^0$, $B \rightarrow X_{s,d} \pi^0$ and $B_{s,d} \rightarrow \pi^+ \pi^-$	100
XII	The Effective Hamiltonian for $K^0 - \bar{K}^0$ Mixing	101
A	General Structure	101
B	The Top Contribution – \mathcal{M}_2	103
C	The Charm Contribution – \mathcal{M}_1	105
D	The Top-Charm Contribution – \mathcal{M}_3	108

E	Numerical Results	114
1	General Remarks	114
2	Results for ϵ_1 , ϵ_2 and ϵ_3	115
XIII	The Effective Hamiltonian for $B^0 - \bar{B}^0$ Mixing	118
A	General Structure	118
B	Numerical Results	119
XIV	Penguin Box Expansion for FCNC Processes	121
XV	Heavy Quark Effective Theory Beyond Leading Logs	124
A	General Remarks	124
B	Basic Concepts	124
C	Heavy-Light Currents	127
D	The Pseudoscalar Decay Constant in the Static Limit	129
E	$B \rightarrow 2$ Transitions in the Static Limit	130
XVI	Comments on Input Parameters	136
A	CKM Element V_{cb}	136
B	CKM Element Ratio V_{ub}/V_{cb}	136
C	Top Quark Mass m_t	136
XVII	Inclusive B Decays	138
A	General Remarks	138
B	b-Quark Decay Modes	139
C	The B Meson Semileptonic Branching Ratio	142
XVIII	ϵ_K, $B^0 - \bar{B}^0$ Mixing and the Unitarity Triangle	145
A	Basic Formula for ϵ_K	145
B	Basic Formula for $B^0 - \bar{B}^0$ Mixing	147
C	$\sin(2\beta)$ from ϵ_K and $B^0 - \bar{B}^0$ Mixing	148
D	Phenomenological Analysis	148
XIX	ϵ''/ϵ' Beyond Leading Logarithms	153
A	Basic Formulae	153
B	Hadronic Matrix Elements for $K \rightarrow \pi$	154
C	$\langle \pi Q_i K \rangle$ for $(V - A) \times (V - A)$ Operators	155
D	$\langle \pi Q_i K \rangle$ for $(V - A) \times (V + A)$ Operators	156
E	$\langle \pi Q_i K \rangle$ for $(V - A) \times (V - A)$ Operators	157
F	The Four Dominant Contributions to ϵ''/ϵ'	158
G	An Analytic Formula for ϵ''/ϵ'	160
H	Numerical Results	162
XX	$K_L - K_S$ Mass Difference and $\Delta I = 1/2$ Rule	167
A	$M(K_L - K_S)$	167
B	The $\Delta I = 1/2$ Rule	168

XXI	The Decay $K_L \rightarrow \pi^0 e^+ e^-$	170
A	General Remarks	170
B	Analytic Formula for $B(K_L \rightarrow \pi^0 e^+ e^-)_{\text{dir}}$	171
C	Numerical Analysis	172
D	The Indirectly CP Violating and CP Conserving Parts	174
E	Outlook	175
XXII	The Decay $B \rightarrow X_s$	177
A	General Remarks	177
B	The Decay $B \rightarrow X_s$ in the Leading Log Approximation	178
C	Looking at $B \rightarrow X_s$ Beyond Leading Logarithms	180
XXIII	The Decay $B \rightarrow X_s e^+ e^-$	182
A	General Remarks	182
B	The Differential Decay Rate	183
C	Numerical Analysis	184
XXIV	The Decays $K^+ \rightarrow \pi^+ \pi^0$ and $K_L \rightarrow \pi^0 \pi^0$	188
A	General Remarks on $K^+ \rightarrow \pi^+ \pi^0$	188
B	Master Formulae for $K^+ \rightarrow \pi^+ \pi^0$	188
C	Numerical Analysis of $K^+ \rightarrow \pi^+ \pi^0$	191
	1 Renormalization Scale Uncertainties	191
	2 Expectations for $B(K^+ \rightarrow \pi^+ \pi^0)$	193
D	General Remarks on $K_L \rightarrow \pi^0 \pi^0$	195
E	Master Formulae for $K_L \rightarrow \pi^0 \pi^0$	195
F	Numerical Analysis of $K_L \rightarrow \pi^0 \pi^0$	196
	1 Renormalization Scale Uncertainties	196
	2 Expectations for $B(K_L \rightarrow \pi^0 \pi^0)$	196
G	Unitarity Triangle from $K \rightarrow \pi \pi$	197
H	$\sin 2\beta$ from $K \rightarrow \pi \pi$	198
XXV	The Decays $K_L \rightarrow \pi^+ \pi^-$ and $K^+ \rightarrow \pi^+ \pi^- \pi^0$	200
A	General Remarks on $K_L \rightarrow \pi^+ \pi^-$	200
B	Master Formulae for $(K_L \rightarrow \pi^+ \pi^-)_{\text{SD}}$	200
C	Numerical Analysis of $(K_L \rightarrow \pi^+ \pi^-)_{\text{SD}}$	201
	1 Renormalization Scale Uncertainties	201
	2 Expectations for $B(K_L \rightarrow \pi^+ \pi^-)_{\text{SD}}$	203
D	General Remarks on $K^+ \rightarrow \pi^+ \pi^- \pi^0$	204
E	Master Formulae for ϵ_{LR}	205
F	Numerical Analysis of ϵ_{LR}	206
XXVI	The Decays $B \rightarrow X$ and $B \rightarrow \pi^+ \pi^-$	208
A	General Remarks	208
B	The Decays $B \rightarrow X_s$ and $B \rightarrow X_d$	208
C	The Decays $B_s \rightarrow \pi^+ \pi^-$ and $B_d \rightarrow \pi^+ \pi^-$	209

XXVII	Summary	211
A	Compilation of Numerical Input Parameters	214
	APPENDIXES	214

I. INTRODUCTION

A. Preliminary Remarks

Among the fundamental forces of nature the weak interactions clearly show the most complicated and diversified pattern from the point of view of our present day understanding represented by the Standard Model of particle physics. Although this theory of the strong and electroweak forces is capable of describing very successfully a huge amount of experimental information in a quantitative way and a great deal of phenomena at least qualitatively, there are many big question marks that remain. The most prominent among them like the problem of electroweak symmetry breaking and the origin of fermion masses and quark mixing are closely related to the part of the Standard Model describing weak interactions. Equally puzzling is the fact that whereas the discrete space-time symmetries C, P, CP and T are respected by strong and electromagnetic interactions, the weak force violates them all. Obviously, the weak interaction is the corner of the Standard Model that is least understood. The history of this field is full of surprises and still more of them might be expected in the future.

For these reasons big efforts have been and still are being undertaken in order to develop our theoretical understanding of weak interaction phenomena and to disentangle the basic mechanisms and parameters. An excellent laboratory for this enterprise is provided by the very rich phenomenology of weak meson decays.

The careful investigation of these decays is mandatory for further testing the Standard Model. Of particular importance is the determination of all Cabibbo-Kobayashi-Maskawa (CKM) parameters as a prerequisite for a decisive test of the consistency of the Standard Model ansatz including the unitarity of the CKM matrix and its compatibility with the quark masses. Many interesting issues within this context still remain unsettled. Let us just mention here the question of direct CP violation in non-leptonic K decays (" π^0 "), the yet completely unknown pattern of CP violation in the B system and the rare K and B decays, which are sensitive to the effects of virtual heavy particles, most notably the top quark, its mass and its weak couplings. Whether the CKM description of CP violation is correct, remains as an outstanding open question. It is clear that the need for a modification of the model is conceivable and that meson decay phenomena might provide a window for "new physics". However, independently of this possibility it is crucial to improve the theoretical predictions in the Standard Model itself, either to further establish its correctness, or to be able to make clear cut statements on its possible failure.

Now, for all attempts towards a theoretical understanding of these issues the obvious fact that the fundamental forces do not come in isolation is of crucial significance. Since hadrons are involved in the decays that are of interest here, QCD unavoidably gets into the game. In order to understand weak meson decays we have to understand the interplay of weak interactions with the strong forces.

To accomplish this task it is necessary to employ the field theoretical tools of the operator product expansion (OPE) (Wilson and Zimmermann, 1972) and the renormalization group (Stueckelberg and Petermann, 1953), (Gell-Mann and Low, 1954), (Ovsyannikov, 1956), (Symanzik, 1970), (Callan Jr, 1970), ('t Hooft, 1973), (Weinberg, 1973). The basic virtues of these two techniques may be characterized as follows. Consider the amplitude A for some weak meson decay process. Using the OPE formalism this amplitude can be represented as (Witten, 1977)

$$A = \langle H_{\text{eff}} \rangle = \sum_i C_i(\mu; M_W) \langle Q_i \rangle \quad (\text{I.1})$$

where it is factorized into the Wilson coefficient functions C_i and the matrix elements of local operators Q_i . In this process the W boson and other fields with mass bigger than the factorization scale are “integrated out”, that is removed from the theory as dynamical degrees of freedom. The effect of their existence is however implicitly taken into account in the Wilson coefficients. In a more intuitive interpretation one can view the expression $\sum_i C_i Q_i$ as an effective hamiltonian for the process considered, with Q_i as the effective vertices and C_i the corresponding coupling constants. Usually for weak decays only the operators of lowest dimension need to be taken into account. Contributions of higher dimensional operators are negligible since they are typically suppressed by powers of p^2/M_W^2 , where p is the momentum scale relevant for the decaying meson in question.

The essential point about the OPE is that it achieves a separation of the full problem into two distinct parts, the long-distance contributions contained in the operator matrix elements and the short-distance physics described by the Wilson coefficients. The renormalization scale separating the two regimes is typically chosen to be of the order $O(1 \text{ GeV})$ for kaon decays and a few GeV for the decays of D and B mesons. The physical amplitude A however cannot depend on μ . The μ dependence of the Wilson coefficients has to cancel the μ dependence present in $\langle Q_i \rangle$. In other words it is a matter of choice what exactly belongs to the matrix elements and what to the coefficient functions. This cancellation of μ dependence involves generally several terms in the expansion in (I.1).

The long-distance part in (I.1) deals with low energy strong interactions and therefore poses a very difficult problem. Many approaches, like lattice gauge theory, $1/N$ -expansion, QCD- and hadronic sum rules or chiral perturbation theory, have been used in the past to obtain qualitative insight and some quantitative estimates of relevant hadronic matrix elements. In addition heavy quark effective theory (HQET) and heavy quark expansions (HQE) have been widely used for B decays. Despite these efforts the problem is not yet solved satisfactorily.

In general in weak decays of mesons the hadronic matrix elements constitute the most important source of theoretical uncertainty. There are however a few special examples of semileptonic rare decays ($K^+ \rightarrow \pi^+ \nu \bar{\nu}$, $K_L \rightarrow \pi^0 \nu \bar{\nu}$, $B \rightarrow X_s \nu \bar{\nu}$) where the matrix elements needed can be extracted from well measured leading decays or calculated perturbatively or as in the case of $B_s \rightarrow \mu^+ \mu^-$ expressed fully in terms of meson decay constants. Thus practically the problem of long-distance QCD can be completely avoided. This makes these decay modes very attractive from a theoretical point of view, although due to very small branching ratios they are quite difficult to access experimentally today.

Contrary to the long-distance contributions the short-distance part can be analyzed systematically using well established field theoretical methods. Due to the asymptotic freedom property of QCD the strong interaction effects at short-distances are calculable in perturbation theory in the strong coupling $\alpha_s(\mu)$. In fact $\alpha_s(\mu)$ is small enough in the full range of relevant short distance scales of $O(M_W)$ down to $O(1 \text{ GeV})$ to serve as a reasonable expansion parameter. However the presence of large logarithms $\ln(M_W/\mu)$ multiplying $\alpha_s(\mu)$ (where $\mu = O(1 \text{ GeV})$) in the calculation of the coefficients $C_i(\mu; M_W)$ spoils the validity of the usual perturbation series. This is a characteristic feature of renormalizable quantum field theories when vastly different scales are present. It is therefore necessary to perform a renormalization group analysis which allows an efficient summation of logarithmic terms to all orders in perturbation theory. In this way the usual perturbation

theory is replaced by the renormalization group improved perturbation theory in which the leading order (LO) corresponds to summing the leading logarithmic terms $(\ln(M_W/m_c))^n$. Then at next-to-leading order (NLO), all terms of the form $(\ln(M_W/m_c))^n$ are summed in addition, and so on.

The evaluation of the short-distance coefficients in renormalization group improved perturbation theory is only a part of the entire problem, but one should stress that still it is indispensable to analyze this part systematically; the effective hamiltonians resulting from the short-distance analysis provide the necessary basis for any further computation of weak decay amplitudes. The long-distance matrix elements needed in addition can be treated separately and will hopefully be known with desirable accuracy one day.

The rather formal expression for the decay amplitudes given in (I.1) can always be cast in a form (Buchalla *et al.*, 1991)

$$A(M \rightarrow F) = \sum_i B_i V_{CKM}^i \frac{1}{Q_{CD}} F_i(m_t, m_c) \quad (I.2)$$

which is more useful for phenomenology. In writing (I.2) we have generalized (I.1) to include several CKM factors V_{CKM}^i . The functions $F_i(m_t, m_c)$ result from the evaluation of loop diagrams with internal top and charm exchanges and may also depend solely on m_t or m_c . In certain cases F_i are mass independent. The factors $\frac{1}{Q_{CD}}$ summarize short distance QCD corrections which can be calculated by the formal methods mentioned above. Finally B_i stand for nonperturbative factors related to the hadronic matrix elements of the contributing operators: the main theoretical uncertainty in the whole enterprise. A well known example of a B_i -factor is the renormalization group invariant parameter B_K relevant for $K^0 - \bar{K}^0$ mixing and the indirect CP violation in $K \rightarrow \pi$. It is worth noting that the short-distance QCD contributions by themselves have already an important impact on weak decay processes. In non-leptonic K-decays, for example, they help to explain the famous $|I = 1/2|$ rule and they generate penguin operators which are relevant for $B \rightarrow \pi$. They suppress the semileptonic branching ratio in heavy quark decays and produce a significant enhancement of the weak radiative process $B \rightarrow X_s \gamma$.

Starting with the pioneering work of (Gaillard and Lee, 1974a) and (Altarelli and Maiani, 1974), who calculated the first leading logarithmic QCD effects in weak decays, considerable efforts have been devoted to the calculation of short-distance QCD corrections to weak meson decay processes. The analysis has been extended to a large variety of particular modes. Of great interest are especially processes sensitive to the virtual contribution of heavy quarks, like the top. A classic example of this type is the 1974 analysis of (Gaillard and Lee, 1974b) of $K^0 - \bar{K}^0$ mixing and their estimate of the charm quark mass prior to its discovery, based on the dependence of the $S = 2$ transition on virtual charm. This calculation constitutes the prototype application for present day analyses of virtual top contributions in $B^0 - \bar{B}^0$ mixing, rare decays and CP violation, which are similar in spirit.

Until 1989 most of the calculations were done in LO, i.e. in the leading logarithmic approximation (Vainshtein *et al.*, 1977), (Gilman and Wise, 1979), (Gilman and Wise, 1980), (Guberina and Peccei, 1980). An exception was the important work of (Altarelli *et al.*, 1981) where the first NLO calculation in the theory of weak decays has been presented.

Today the effective hamiltonians for weak processes are available at the next-to-leading level for the most important and interesting cases due to a series of publications devoted to this enterprise beginning with the work of (Buras and Weisz, 1990). In table I we give a list of decays for which NLO QCD corrections are known at present. With the next-to-leading short-distance effects

included, weak decays have in a sense now achieved the status that the conceptually similar field of deep inelastic lepton nucleon scattering had attained more than a decade ago (Buras, 1980).

TABLE I. Processes for which NLO QCD corrections have been calculated by now.

Decay	Reference
F = 1 Decays	
current-current operators	(Altarelli <i>et al.</i> , 1981), (Buras and Weisz, 1990)
QCD penguin operators	(Buras <i>et al.</i> , 1993c), (Buras <i>et al.</i> , 1993a), (Ciuchini <i>et al.</i> , 1994a)
electroweak penguin operators	(Buras <i>et al.</i> , 1993c), (Buras <i>et al.</i> , 1993a), (Ciuchini <i>et al.</i> , 1994a)
magnetic penguin operators	(Misiak and Münz, 1995)
$B \rightarrow B' X e$	(Altarelli <i>et al.</i> , 1981), (Buchalla, 1993), (Bagan <i>et al.</i> , 1994), (Bagan <i>et al.</i> , 1995b)
Inclusive $S = 1$	(Jamin and Pich, 1994)
Particle-Antiparticle Mixing	
1	(Herrlich and Nierste, 1994)
$2 \rightarrow B$	(Buras <i>et al.</i> , 1990)
3	(Herrlich and Nierste, 1995a)
Rare K- and B-Meson Decays	
$K_L^0 \rightarrow 0, B \rightarrow 1^+ 1, B \rightarrow X_S$	(Buchalla and Buras, 1993a)
$K^+ \rightarrow +, K_L \rightarrow +$	(Buchalla and Buras, 1994a)
$K^+ \rightarrow +$	(Buchalla and Buras, 1994b)
$K_L \rightarrow 0 e^+ e$	(Buras <i>et al.</i> , 1994a)
$B \rightarrow X_S e^+ e$	(Misiak, 1995), (Buras and Münz, 1995)

Let us recall why NLO calculations are important for weak decays and why it is worthwhile to perform the very involved and complicated computations.

The NLO is first of all necessary to test the validity of perturbation theory. In LO all the $(\ln(M_W/m_s))^n$ terms are summed, yielding a result of $O(1)$; it is only at NLO where one obtains a truly perturbative $O(\alpha_s)$ correction relative to the LO and one can check whether it is small enough to justify the perturbative approach.

Without going to NLO the scheme specific QCD scale $\overline{m_s}$ extracted from various high energy processes cannot be used meaningfully in weak decays.

Due to renormalization group (RG) invariance the physical amplitudes do not depend on the exact scales μ_i at which quark masses (top) are defined or heavy particles are integrated out. However in perturbation theory RG invariance is broken through the truncation of the series by terms of the neglected order. Numerically the resulting scale ambiguities, representing the theoretical uncertainty of the short-distance part, are a serious problem for the LO which can be reduced considerably by going to NLO.

The Wilson coefficients are renormalization scheme dependent quantities. The scheme dependence is first “felt” at NLO whereas the LO is completely insensitive to this important feature. In particular this issue is essential for a proper matching of the short distance contributions to the long distance matrix elements as obtained from lattice calculations.

In some cases, particularly for $\pi^0, K_L \rightarrow \gamma e^+ e^-$ and $B \rightarrow X_s e^+ e^-$, the central issue of the top quark mass dependence is strictly speaking a NLO effect.

We would like to stress that short-distance QCD should be contrasted with an “intrinsically perturbative” theory like QED, where perturbation theory is almost the whole story since α_{QED} is exceedingly small. In QCD the coupling is much larger at interesting scales so that the conceptual questions like residual scale or scheme dependences, which are formally of the neglected higher order, become important numerically. Thus in this sense the question of higher order corrections is not only one of a quantitative improvement (of making precise predictions even more accurate, like in QED), but of a qualitative improvement as well.

We think that the time is appropriate to review the subject of QCD corrections to weak meson decays at the next-to-leading order level and to collect the most important results obtained in this field.

B. Outline

This review is divided into three parts, roughly speaking “basic concepts”, “technicalities” and “phenomenological applications”. The division is made especially for pedagogical reasons hoping to make the review as readable as possible to a wide audience of physicists.

In the first part we discuss the basic formalism necessary to obtain the effective hamiltonians for weak decays from the underlying full $SU(3) \times SU(2)_L \times U(1)_Y$ gauge theory of the Standard Model.

The second part constitutes a compendium of effective hamiltonians for all weak decays for which NLO corrections have been calculated in the literature and whose list is given in table I. We include also the discussion of the important decay $B \rightarrow X_s$ which is known only at the LO level.

The third part of our review then presents the phenomenological picture of weak decays beyond the leading logarithmic approximation using the results obtained in parts one and two.

We end our review of this exciting field with a brief summary of results and an outlook.

We are aware of the fact that some sections in this review are necessarily rather technical which is connected to the very nature of the subject of this review. We have however made efforts to present the material in a pedagogical fashion. Thus part one can be regarded as an elementary introduction to the formalism of QCD calculations which include renormalization group methods and the operator product expansion. Even if our compendium in part two looks rather technical at first sight, the guidelines to the effective hamiltonians presented in section IV should be helpful in following and using this important part of our review. In any case the phenomenological part three is almost self-contained and its material can be easily followed with the help of the guidelines in section IV without the necessity of fully understanding the details of NLO calculations.

Part One –

The Basic Formalism

In this first part we will discuss the basic formalism behind radiative corrections to weak decays.

In section II we recall those ingredients of the standard $SU(3) \times SU(2) \times U(1)$ model, which play an important role in subsequent sections. In particular we recall the Cabibbo-Kobayashi-Maskawa matrix in two useful parametrizations and we briefly describe the unitarity triangle.

In section III we outline the basic formalism for the calculation of QCD effects in weak decays. Beginning with the idea of effective field theories we introduce subsequently the techniques of the operator product expansion and the renormalization group. These important concepts are illustrated explicitly using the simple, but phenomenologically relevant example of current-current operators, which allows to demonstrate the procedure in a transparent way. The central issue in this formalism is the computation of the Wilson coefficients C_i of local operators in the LO and NLO approximation. This calculation involves the proper computation of C_i at $\mu = O(M_W)$ and the renormalization group evolution down to low energy scales $\mu \ll M_W$ relevant for the weak decays considered. The latter requires the evaluation of one-loop and two-loop anomalous dimensions of Q_i or more generally the anomalous dimension matrices, which describe the mixing of these operators under renormalization. We outline the steps for a consistent calculation of the Wilson coefficients C_i and formulate recipes for the determination of the anomalous dimensions of local operators. In section III F we give “master formulae” for the Wilson coefficients C_i , including NLO corrections. Since these formulae will be central for our review, we discuss their various properties in some detail. In particular we address the μ - and renormalization scheme dependences and we show on general grounds how these dependences are canceled by those present in the hadronic matrix elements.

II. STANDARD ELECTROWEAK MODEL

A. Particles and Interactions

Throughout this review we will work in the context of the three generation model of quarks and leptons based on the gauge group $SU(3) \times SU(2)_L \times U(1)_Y$ spontaneously broken down to $SU(3) \times U(1)_Q$. Here Y and Q denote the weak hypercharge and the electric charge generators, respectively. $SU(3)$ stands for QCD which will be discussed in more detail in the following section. Here we would like to recall certain features of the electroweak part of the Standard Model which will be important for our considerations.

The left-handed leptons and quarks are put in $SU(2)_L$ doublets

$$\begin{pmatrix} \nu_e \\ e \end{pmatrix}_L, \quad \begin{pmatrix} \nu_\mu \\ \mu \end{pmatrix}_L, \quad \begin{pmatrix} \nu_\tau \\ \tau \end{pmatrix}_L \quad (II.1)$$

$$\begin{pmatrix} u \\ d \end{pmatrix}_L, \quad \begin{pmatrix} c \\ s \end{pmatrix}_L, \quad \begin{pmatrix} t \\ b \end{pmatrix}_L \quad (II.2)$$

with the corresponding right-handed fields transforming as singlets under $SU(2)_L$. The primes are discussed below. The relevant electroweak charges Q , Y and the third component of the weak isospin T_3 are collected in table II.

TABLE II. Electroweak charges Q , Y and the third component of the weak isospin T_3 for quarks and leptons in the Standard Model.

	e_L	e_L	e_R	u_L	d_L	u_R	d_R
Q	0	1	1	2/3	1=3	2/3	1=3
T_3	1/2	1=2	0	1/2	1=2	0	0
Y	1	1	2	1/3	1/3	4/3	2=3

The electroweak interactions of quarks and leptons are mediated by the massive weak gauge bosons W^\pm and Z^0 and by the photon A . These interactions are summarized by the Lagrangian

$$\mathcal{L}_{int} = \mathcal{L}_{CC} + \mathcal{L}_{NC} \quad (II.3)$$

where

$$\mathcal{L}_{CC} = \frac{g_2}{2} (J^+ W^- + J^- W^+) \quad (II.4)$$

describes the *charged current* interactions and

$$\mathcal{L}_{NC} = e J^\mu A_\mu + \frac{g_2}{2 \cos \theta_W} J^0 Z_\mu \quad (II.5)$$

the *neutral current* interactions. Here e is the QED coupling constant, g_2 is the $SU(2)_L$ coupling constant and θ_W is the Weinberg angle. The currents are given as follows

$$J^+ = (ud^0)_V - A + (cs^0)_V - A + (tb^0)_V - A + (\bar{e}e)_V - A + (\bar{\nu}_\mu \nu_\mu)_V - A + (\bar{\nu}_\tau \nu_\tau)_V - A \quad (\text{II.6})$$

$$J^{\text{em}} = \sum_f Q_f \bar{f} f \quad (\text{II.7})$$

$$J^0 = \sum_f \bar{f} (\nu_f - a_f \gamma_5) f \quad (\text{II.8})$$

$$\nu_f = T_3^f - 2Q_f \sin^2 \theta_W \quad a_f = T_3^f \quad (\text{II.9})$$

where Q_f and T_3^f denote the charge and the third component of the weak isospin of the left-handed fermion f_L .

In our discussion of weak decays an important role is played by the Fermi constant:

$$\frac{G_F}{\sqrt{2}} = \frac{g_2^2}{8M_W^2} \quad (\text{II.10})$$

which has the value

$$G_F = 1.16639 \cdot 10^5 \text{ GeV}^{-2} \quad (\text{II.11})$$

Other values of the relevant parameters will be collected in appendix A.

The interactions between the gauge bosons are standard and can be found in any textbook on gauge theories.

The primes in (II.2) indicate that the weak eigenstates $(d^0; s^0; b^0)$ are not equal to the corresponding mass eigenstates $(d; s; b)$, but are rather linear combinations of the latter. This is expressed through the relation

$$\begin{pmatrix} d^0 \\ s^0 \\ b^0 \end{pmatrix} = \begin{pmatrix} V_{ud} & V_{us} & V_{ub} \\ V_{cd} & V_{cs} & V_{cb} \\ V_{td} & V_{ts} & V_{tb} \end{pmatrix} \begin{pmatrix} d \\ s \\ b \end{pmatrix} \quad (\text{II.12})$$

where the unitary matrix connecting these two sets of states is the Cabibbo-Kobayashi-Maskawa (CKM) matrix. Many parametrizations of this matrix have been proposed in the literature. We will use in this review two parametrizations: the standard parametrization recommended by the particle data group and the Wolfenstein parametrization.

B. Standard Parametrization

Let us introduce the notation $c_{ij} = \cos \theta_{ij}$ and $s_{ij} = \sin \theta_{ij}$ with i and j being generation labels ($i, j = 1, 2, 3$). The standard parametrization is then given as follows (Particle Data Group, 1994)

$$V = \begin{pmatrix} c_{12}c_{13} & s_{12}c_{13} & s_{13}e^{-i\delta} \\ -s_{12}c_{23} - c_{12}s_{23}s_{13}e^{i\delta} & c_{12}c_{23} - s_{12}s_{23}s_{13}e^{i\delta} & s_{23}c_{13} \\ s_{12}c_{23} - c_{12}s_{23}s_{13}e^{i\delta} & -s_{12}s_{23} - c_{12}c_{23}s_{13}e^{i\delta} & c_{23}c_{13} \end{pmatrix} \quad (\text{II.13})$$

where δ is the phase necessary for CP violation. s_{ij} and c_{ij} can all be chosen to be positive and may vary in the range $0 \leq s_{ij} \leq 1$. However the measurements of CP violation in K decays force δ to be in the range $0 < \delta < \pi$.

The extensive phenomenology of the last years has shown that s_{13} and s_{23} are small numbers: $\mathcal{O}(10^{-3})$ and $\mathcal{O}(10^{-2})$, respectively. Consequently to an excellent accuracy $c_{13} = c_{23} = 1$ and the four independent parameters are given as follows

$$s_{12} = |V_{us}|, \quad s_{13} = |V_{ub}|, \quad s_{23} = |V_{cb}| \quad (\text{II.14})$$

with the phase δ extracted from CP violating transitions or loop processes sensitive to $|V_{td}|$. The latter fact is based on the observation that for $\delta \neq 0$, as required by the analysis of CP violation, there is a one-to-one correspondence between δ and $|V_{td}|$ given by

$$|V_{td}| = \frac{\sqrt{a^2 + b^2 - 2ab \cos \delta}}{2} ; \quad a = |V_{cd} V_{cb}|, \quad b = |V_{ud} V_{ub}| \quad (\text{II.15})$$

C. Wolfenstein Parameterization Beyond Leading Order

We will also use the Wolfenstein parametrization (Wolfenstein, 1983). It is an approximate parametrization of the CKM matrix in which each element is expanded as a power series in the small parameter $\lambda = |V_{us}| = 0.22$

$$V = \begin{pmatrix} 1 - \frac{\lambda^2}{2} & \lambda & A \lambda^3 e^{i\phi} \\ -\lambda & 1 - \frac{\lambda^2}{2} & A \lambda^2 \\ A \lambda^3 (1 - \frac{\lambda^2}{2}) & A \lambda^2 & 1 \end{pmatrix} + \mathcal{O}(\lambda^4) \quad (\text{II.16})$$

and the set (II.14) is replaced by

$$\lambda; \quad A; \quad \phi; \quad \delta \quad (\text{II.17})$$

The Wolfenstein parameterization has several nice features. In particular it offers in conjunction with the unitarity triangle a very transparent geometrical representation of the structure of the CKM matrix and allows to derive several analytic results to be discussed below. This turns out to be very useful in the phenomenology of rare decays and of CP violation.

When using the Wolfenstein parametrization one should remember that it is an approximation and that in certain situations neglecting $\mathcal{O}(\lambda^4)$ terms may give wrong results. The question then arises how to find $\mathcal{O}(\lambda^4)$ and higher order terms? The point is that since (II.16) is only an approximation the *exact* definition of λ is not unique by terms of the neglected order $\mathcal{O}(\lambda^4)$. This is the reason why in different papers in the literature different $\mathcal{O}(\lambda^4)$ terms can be found. They simply correspond to different definitions of the expansion parameter λ . Obviously the physics does not depend on this choice. Here it suffices to find an expansion in λ which allows for simple relations between the parameters (II.14) and (II.17). This will also restore the unitarity of the CKM matrix which in the Wolfenstein parametrization as given in (II.16) is not satisfied exactly.

To this end we go back to (II.13) and we impose the relations (Buras *et al.*, 1994b)

$$s_{12} = \lambda, \quad s_{23} = A \lambda^2, \quad s_{13} e^{i\phi} = A \lambda^3 e^{i\phi} \quad (\text{II.18})$$

to *all orders* in λ . In view of the comments made above this can certainly be done. It follows that

$$\rho = \frac{s_{13}}{s_{12}s_{23}} \cos \delta = \frac{s_{13}}{s_{12}s_{23}} \sin \delta \quad (\text{II.19})$$

We observe that (II.18) and (II.19) represent simply the change of variables from (II.14) to (II.17). Making this change of variables in the standard parametrization (II.13) we find the CKM matrix as a function of $(\delta; A; \rho; \eta)$ which satisfies unitarity exactly! We also note that in view of $q_3 = 1 \pm \mathcal{O}(\epsilon^6)$ the relations between s_{ij} and v_{ij} in (II.14) are satisfied to high accuracy. The relations in (II.19) have been first used in (Schmidtler and Schubert, 1992). However, the improved treatment of the unitarity triangle presented below goes beyond the analysis of these authors.

The procedure outlined above gives automatically the corrections to the Wolfenstein parametrization in (II.16). Indeed expressing (II.13) in terms of Wolfenstein parameters using (II.18) and then expanding in powers of ϵ we recover the matrix in (II.16) and in addition find explicit corrections of $\mathcal{O}(\epsilon^4)$ and higher order terms. V_{ub} remains unchanged. The corrections to V_{us} and V_{cb} appear only at $\mathcal{O}(\epsilon^7)$ and $\mathcal{O}(\epsilon^8)$, respectively. For many practical purposes the corrections to the real parts can also be neglected. The essential corrections to the imaginary parts are:

$$V_{cd} = -iA^2 \epsilon^5 \quad V_{ts} = -iA^4 \quad (\text{II.20})$$

These two corrections have to be taken into account in the discussion of CP violation. On the other hand the imaginary part of V_{cs} which in our expansion in ϵ appears only at $\mathcal{O}(\epsilon^6)$ can be fully neglected.

In order to improve the accuracy of the unitarity triangle discussed below we will also include the $\mathcal{O}(\epsilon^5)$ correction to V_{td} which gives

$$V_{td} = A^3 (1 - \rho - i\eta) \quad (\text{II.21})$$

with

$$\rho = \rho (1 - \frac{\epsilon^2}{2}) \quad \eta = \eta (1 - \frac{\epsilon^2}{2}) \quad (\text{II.22})$$

In order to derive analytic results we need accurate explicit expressions for $\eta = V_{td} V_{ts}^*$ where $\eta = \eta_c + i\eta_t$. We have

$$\text{Im } \eta_t = \text{Im } \eta_c = A^2 \epsilon^5 \quad (\text{II.23})$$

$$\text{Re } \eta_c = \eta (1 - \frac{\epsilon^2}{2}) \quad (\text{II.24})$$

$$\text{Re } \eta_t = \eta (1 - \frac{\epsilon^2}{2}) A^2 \epsilon^5 (1 - \rho) \quad (\text{II.25})$$

Expressions (II.23) and (II.24) represent to an accuracy of 0.2% the exact formulae obtained using (II.13). The expression (II.25) deviates by at most 2% from the exact formula in the full range of parameters considered. In order to keep the analytic expressions in the phenomenological applications in a transparent form we have dropped a small $\mathcal{O}(\epsilon^7)$ term in deriving (II.25). After inserting the expressions (II.23)–(II.25) in exact formulae for quantities of interest, further expansion in ϵ should not be made.

D. Unitarity Triangle Beyond Leading Order

The unitarity of the CKM matrix provides us with several relations of which

$$V_{ud}V_{ub} + V_{cd}V_{cb} + V_{td}V_{tb} = 0 \quad (\text{II.26})$$

is the most useful one. In the complex plane the relation (II.26) can be represented as a triangle, the so-called “unitarity–triangle” (UT). Phenomenologically this triangle is very interesting as it involves simultaneously the elements V_{ub} , V_{cb} and V_{td} which are under extensive discussion at present.

In the usual analyses of the unitarity triangle only terms $O(\lambda^3)$ are kept in (II.26) (Buras and Harlander, 1992), (Nir, 1992), (Harris and Rosner, 1992), (Schmidtler and Schubert, 1992), (Dib *et al.*, 1990), (Ali and London, 1995). It is however straightforward to include the next-to-leading $O(\lambda^5)$ terms (Buras *et al.*, 1994b). We note first that

$$V_{cd}V_{cb} = A^3 + O(\lambda^7): \quad (\text{II.27})$$

Thus to an excellent accuracy $V_{cd}V_{cb}$ is real with $\text{Im} V_{cd}V_{cb} = A^3$. Keeping $O(\lambda^5)$ corrections and rescaling all terms in (II.26) by A^{-3} we find

$$\frac{1}{A^3}V_{ud}V_{ub} = \rho + i\eta \quad ; \quad \frac{1}{A^3}V_{td}V_{tb} = 1 - \rho - i\eta \quad (\text{II.28})$$

with ρ and η defined in (II.22). Thus we can represent (II.26) as the unitarity triangle in the complex $(\rho; \eta)$ plane. This is shown in fig. 1. The length of the side CB which lies on the real axis equals unity when eq. (II.26) is rescaled by $V_{cd}V_{cb}$. We observe that beyond the leading order in λ the point A *does not* correspond to $(\rho; \eta)$ but to $(\bar{\rho}; -\bar{\eta})$. Clearly within 3% accuracy $\rho = \bar{\rho}$ and $\eta = -\bar{\eta}$. Yet in the distant future the accuracy of experimental results and theoretical calculations may improve considerably so that the more accurate formulation given here will be appropriate.

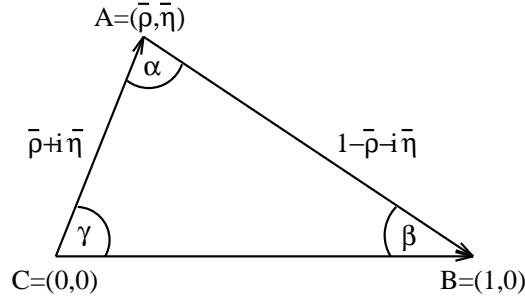


FIG. 1. Unitarity triangle in the complex $(\rho; \eta)$ plane.

Using simple trigonometry one can calculate $\sin(2\beta)$, $\beta = \arg(-V_{td}V_{tb}/V_{cd}V_{cb})$, in terms of $(\rho; \eta)$ with the result:

$$\sin(2\beta) = \frac{2(\eta^2 + \rho^2 - \eta)}{(\eta^2 + \rho^2)(1 - \rho^2 + \eta^2)} \quad (\text{II.29})$$

$$\sin(2\beta) = \frac{2(1 - \rho^2)}{(1 - \rho^2 + \eta^2)^2} \quad (\text{II.30})$$

$$\sin(2\theta) = \frac{2\sin\theta\cos\theta}{\sin^2\theta + \cos^2\theta} = \frac{2\sin\theta\cos\theta}{1} \quad (\text{II.31})$$

The lengths CA and BA in the rescaled triangle of fig. 1 to be denoted by R_b and R_t , respectively, are given by

$$R_b = \frac{V_{ud}V_{ub}}{V_{cd}V_{cb}} = \frac{1}{\sin^2\theta + \cos^2\theta} = (1 - \frac{1}{2}\sin^2\theta) \frac{V_{ub}}{V_{cb}} \quad (\text{II.32})$$

$$R_t = \frac{V_{td}V_{tb}}{V_{cd}V_{cb}} = \frac{1}{(1 - \sin^2\theta) + \sin^2\theta} = \frac{1}{\cos^2\theta} \frac{V_{td}}{V_{cb}} \quad (\text{II.33})$$

The expressions for R_b and R_t given here in terms of $(\theta; \gamma)$ are excellent approximations. Clearly R_b and R_t can also be determined by measuring two of the angles α_i :

$$R_b = \frac{\sin(\alpha_c)}{\sin(\alpha_b)} = \frac{\sin(\alpha_c + \alpha_a)}{\sin(\alpha_a)} = \frac{\sin(\alpha_c)}{\sin(\alpha_c + \alpha_a)} \quad (\text{II.34})$$

$$R_t = \frac{\sin(\alpha_c)}{\sin(\alpha_b)} = \frac{\sin(\alpha_c + \alpha_a)}{\sin(\alpha_a)} = \frac{\sin(\alpha_c)}{\sin(\alpha_c + \alpha_a)} \quad (\text{II.35})$$

III. BASIC FORMALISM

A. Renormalization of QCD

As already emphasized in the introduction, the effects of QCD play an important role in the phenomenology of weak decays of hadrons. In fact in the theoretical analysis of these decays the investigation of QCD corrections is the most difficult and extensive part. In the present subsection we shall therefore briefly recall basic features of perturbative QCD and its renormalization. Thereby we will concentrate on those aspects, that will be needed for the present review. We will also take the opportunity to introduce for later reference the expressions for the running coupling, the running mass and the corresponding renormalization group functions.

The Lagrangian density of QCD reads

$$\begin{aligned} \mathcal{L}_{\text{QCD}} = & \frac{1}{4} (\partial_\mu A^a_\nu - \partial_\nu A^a_\mu) (\partial^\mu A^{a\nu} - \partial^\nu A^{a\mu}) - \frac{1}{2} (\partial_\mu A^a_\nu)^2 \\ & + \bar{q} (i \not{D} - m_q) q + \bar{c}^a \partial_\mu \partial^\mu c^a \\ & - \frac{g}{2} f^{abc} (\partial_\mu A^a_\nu - \partial_\nu A^a_\mu) A^{b\mu} A^{c\nu} - \frac{g^2}{4} f^{abc} f^{ade} A^a_\mu A^b_\nu A^{c\mu} A^{d\nu} \\ & + g \bar{q}_i T^a_{ij} q_j A^a + g f^{abc} (\partial_\mu c^a - \partial^a c_\mu) b^{b\mu} A^c_\mu \end{aligned} \quad (\text{III.1})$$

Here $q = (q_1; q_2; q_3)$ is the color triplet of quark flavor q , $q = u, d, s, c, b, t$, g is the QCD coupling, A^a_μ the gluon field, c^a the ghost field and ξ the gauge parameter. T^a , f^{abc} ($a, b, c = 1, \dots, 8$) are the generators and structure constants of $SU(3)$, respectively. From this Lagrangian one may read off the Feynman rules for QCD, e.g. $ig T^a_{ij}$ for the quark-gluon vertex.

In order to deal with divergences that appear in quantum (loop) corrections to Green functions, the theory has to be regularized to have an explicit parametrization of the singularities and subsequently renormalized to render the Green functions finite. For these purposes we will employ:

Dimensional regularization (DR) by continuation to $D = 4 - 2\epsilon$ space-time dimensions (Bollini and Giambiagi, 1972a), (Bollini and Giambiagi, 1972b), ('t Hooft and Veltman, 1972a), (Ashmore, 1972), (Cicuta and Montaldi, 1972).

Subtraction of divergences in the minimal subtraction scheme \overline{MS} ('t Hooft, 1973) or the modified minimal subtraction scheme $\overline{\overline{MS}}$ (Bardeen *et al.*, 1978).

To eliminate the divergences one has to renormalize the fields and parameters in the Lagrangian, in general through

$$\begin{aligned} A^a_0 &= Z_3^{1/2} A^a & q_0 &= Z_q^{1/2} q & c^a_0 &= Z_3^{1/2} c^a \\ g_0 &= Z_g g & m_0 &= Z_m m \end{aligned} \quad (\text{III.2})$$

The index "0" indicates unrenormalized quantities. The factors Z are the renormalization constants. The scale μ has been introduced to make g dimensionless in $D = 4 - 2\epsilon$ dimensions. Since we will not consider Green functions with external ghosts, we will not need the ghost field renormalization. We also do not need the gauge parameter renormalization if we are dealing with gauge independent quantities, as e.g. Wilson coefficient functions.

A straightforward way to implement renormalization is provided by the counterterm method.

Thereby the parameters and fields in the original Lagrangian, which are to be considered as unrenormalized (bare) quantities, are reexpressed through renormalized ones by means of (III.2) from the very beginning. For instance, the quark kinetic term becomes

$$L_F = \bar{q} i \not{\partial} q - m_0 \bar{q} q - \bar{q} i \not{A} q - m \bar{q} q + (Z_q - 1) \bar{q} i \not{\partial} q - (Z_q Z_m - 1) m \bar{q} q \quad (\text{III.3})$$

The advantage then is, that only renormalized quantities are present in the Lagrangian. The counterterms $(Z - 1)$, appearing in addition, can be formally treated as interaction terms that contribute to Green functions calculated in perturbation theory. The Feynman rule for the counterterms in (III.3), for example, reads (p is the quark momentum)

$$i(Z_q - 1) \not{p} - i(Z_q Z_m - 1) m \quad (\text{III.4})$$

The constants Z_i are then determined such that they cancel the divergences in the Green functions according to the chosen renormalization scheme. In an analogous way all renormalization constants can be fixed by considering the appropriate Green functions.

Of central importance for the study of perturbative QCD effects are the renormalization group equations, which govern the dependence of renormalized parameters and Green functions on the renormalization scale μ . These differential equations are easily derived from the definition (III.2) by using the fact that bare quantities are μ -independent. In this way one finds that the renormalized coupling $g(\mu)$ obeys (Gross, 1976)

$$\frac{d}{d \ln \mu} g(\mu) = \beta(g(\mu)) \quad (\text{III.5})$$

where

$$\beta(g) = -g \left(\frac{1}{Z_g} \frac{dZ_g}{d \ln \mu} \right) = -g + \gamma(g) \quad (\text{III.6})$$

which defines the β function. (III.5) is valid in arbitrary dimensions. In four dimensions $\beta(g)$ reduces to $\gamma(g)$. Similarly, the anomalous dimension of the mass, γ_m , defined through

$$\frac{d \ln m(\mu)}{d \ln \mu} = \gamma_m(g(\mu)) \quad (\text{III.7})$$

is given by

$$\gamma_m(g) = \frac{1}{Z_m} \frac{dZ_m}{d \ln \mu} \quad (\text{III.8})$$

In the \overline{MS} -scheme, where just the pole terms in ϵ are present in the renormalization constants Z_i , these can be expanded as follows

$$Z_i = 1 + \sum_{k=1}^{\infty} \frac{1}{\epsilon^k} Z_{i,k}(g) \quad (\text{III.9})$$

Using (III.5), (III.6) one finds

$$\frac{1}{Z_g} \frac{dZ_g}{d \ln \mu} = -2g^2 \frac{\partial Z_{g,1}(g)}{\partial g^2} \quad (\text{III.10})$$

which allows a direct calculation of the renormalization group functions from the $1/\epsilon$ -pole part of the renormalization constants. Along these lines one obtains at the two loop level, required for next-to-leading order calculations,

$$g(\mu) = g_0 \frac{g^3}{16\pi^2} + g_1 \frac{g^5}{(16\pi^2)^2} \quad (\text{III.11})$$

In terms of

$$s = \frac{g^2}{4} \quad (\text{III.12})$$

we have

$$\frac{d s}{d \ln \mu} = 2 g_0 \frac{s}{4} + 2 g_1 \frac{s^3}{(4\pi^2)^2} \quad (\text{III.13})$$

Similarly, the two-loop expression for the quark mass anomalous dimension can be written as

$$\gamma_m(s) = \gamma_{m0} \frac{s}{4} + \gamma_{m1} \frac{s^2}{4} \quad (\text{III.14})$$

We also give the $1/\epsilon$ -pole part Z_{qf1} of the quark field renormalization constant Z_q to $O(s^2)$, which we will need later on

$$Z_{qf1} = a_1 \frac{s}{4} + a_2 \frac{s^2}{4} \quad (\text{III.15})$$

The coefficients in eqs. (III.13) – (III.15) read

$$g_0 = \frac{11N - 2f}{3}, \quad g_1 = \frac{34}{3}N^2 - \frac{10}{3}Nf - 2C_F f, \quad C_F = \frac{N^2 - 1}{2N} \quad (\text{III.16})$$

$$\gamma_{m0} = 6C_F, \quad \gamma_{m1} = C_F - 3C_F + \frac{97}{3}N - \frac{10}{3}f \quad (\text{III.17})$$

$$a_1 = -C_F, \quad a_2 = C_F - \frac{3}{4}C_F - \frac{17}{4}N + \frac{1}{2}f \quad (\text{III.18})$$

N is the number of colors, f the number of quark flavors. The coefficients are given in the $\overline{\text{MS}}$ scheme. However, g_0 , g_1 , γ_{m0} and a_1 are scheme independent. The expressions for a_1 and a_2 in (III.18) are valid in Feynman gauge, $\epsilon = 4$.

At two-loop order the solution of the renormalization group equation (III.13) for $s(\mu)$ can always be written in the form

$$s(\mu) = \frac{4}{g_0 \ln \frac{\mu^2}{\Lambda^2}} \left[1 + \frac{2}{g_0} \frac{\ln \ln \frac{\mu^2}{\Lambda^2}}{\ln \frac{\mu^2}{\Lambda^2}} + \frac{1}{g_0^2} \frac{\ln^2 \ln \frac{\mu^2}{\Lambda^2}}{\ln^2 \frac{\mu^2}{\Lambda^2}} \right] \quad (\text{III.19})$$

Eq. (III.19) gives the running coupling constant at NLO. $s(\mu)$ vanishes as $\mu \rightarrow \Lambda$ due to asymptotic freedom. We remark that, in accordance with the two-loop accuracy, (III.19) is valid

up to terms of the order $O(1/\ln^3 \mu^2 = \mu^2)$. For the purpose of counting orders in $1/\ln^2 \mu^2 = \mu^2$ the double logarithmic expression $\ln \ln^2 \mu^2 = \mu^2$ may formally be viewed as a constant. Note that an additional term $\text{const} \cdot \ln^2 \mu^2 = \mu^2$, which is of the same order as the next-to-leading correction term in (III.19), can always be absorbed into a multiplicative redefinition of \bar{m}_S . Hence the choice of the form (III.19) is possible without restriction, but one should keep in mind that the definition of \bar{m}_S is related to this particular choice. The introduction of the \overline{MS} scheme and the corresponding definition of \overline{m}_S and its relation to $m_{\overline{MS}}$ is discussed in section III F 4. Finally we write down the two-loop expression for the running quark mass in the \overline{MS} (\overline{MS}) scheme, which results from integrating (III.7)

$$m(\mu) = m(\mu_0) \left(\frac{s(\mu)}{s(\mu_0)} \right)^{\frac{\gamma_0}{2\beta_0}} \left[1 + \frac{\gamma_1}{2\beta_0} \frac{1}{s(\mu_0)} - \frac{1}{2\beta_0^2} \frac{s(\mu)}{s(\mu_0)} \right] \quad (III.20)$$

B. Operator Product Expansion in Weak Decays – Preliminaries

Weak decays of hadrons are mediated through the weak interactions of their quark constituents, whose strong interactions, binding the constituents into hadrons, are characterized by a typical hadronic energy scale of the order of 1 GeV . Our goal is therefore to derive an effective low energy theory describing the weak interactions of quarks. The formal framework to achieve this is provided by the operator product expansion (OPE). In order to introduce the main ideas behind it, let us consider the simple example of the quark level transition $c \rightarrow s u d$, which is relevant for Cabibbo-allowed decays of D mesons. Disregarding QCD effects for the moment, the tree-level W-exchange amplitude for $c \rightarrow s u d$ is simply given by

$$\begin{aligned} A &= i \frac{G_F}{2} V_{cs} V_{ud} \frac{M_W^2}{k^2} (sc)_{V-A} (ud)_{V-A} \\ &= i \frac{G_F}{2} V_{cs} V_{ud} (sc)_{V-A} (ud)_{V-A} + O\left(\frac{k^2}{M_W^2}\right) \end{aligned} \quad (III.21)$$

where $(V-A)$ refers to the Lorentz structure $(1 - \gamma_5)$.

Since k , the momentum transfer through the W propagator, is very small as compared to the W mass M_W , terms of the order $O(k^2/M_W^2)$ can safely be neglected and the full amplitude A can be approximated by the first term on the r.h.s. of (III.21). Now this term may obviously be also obtained from an effective hamiltonian defined by

$$H_{\text{eff}} = \frac{G_F}{2} V_{cs} V_{ud} (sc)_{V-A} (ud)_{V-A} + \dots \quad (III.22)$$

where the ellipsis denotes operators of higher dimensions, typically involving derivative terms, which can in principle be chosen so as to reproduce the terms of higher order in k^2/M_W^2 of the full amplitude in (III.21). This exercise already provides us with a simple example of an OPE. The product of two charged current operators is expanded into a series of local operators, whose contributions are weighted by effective coupling constants, the Wilson coefficients.

A more formal basis for this procedure may be given by considering the generating functional for Green functions in the path integral formalism. The part of the generating functional relevant for the present discussion is, up to an overall normalizing factor, given by

$$Z_W = \int [dW^+] [dW^-] \exp(i \int d^4x L_W) \quad (\text{III.23})$$

where L_W is the Lagrangian density containing the kinetic terms of the W boson field and its interaction with charged currents

$$L_W = \frac{1}{2} (\partial_\mu W^+_\nu - \partial_\nu W^+_\mu) (\partial^\mu W^-_\nu - \partial^\nu W^-_\mu) + M_W^2 W^+_\mu W^-_\mu + \frac{g_2}{2} (J^+_\mu W^-_\mu + J^-_\mu W^+_\mu) \quad (\text{III.24})$$

$$J^+ = V_{pn} \bar{p} (1 - \gamma_5) n \quad p = (u; c; t) \quad n = (d; s; b) \quad J^- = (J^+)^Y \quad (\text{III.25})$$

Since we are not interested in Green functions with external W lines, we have not introduced external source terms for the W fields. In the present argument we will furthermore choose the unitary gauge for the W field for definiteness, however physical results do not depend on this choice.

Introducing the operator

$$K(x; y) = \int d^4z \langle 0 | T \{ \partial_\mu W^+_\nu(x) \partial^\mu W^-_\nu(y) \} | 0 \rangle \quad (\text{III.26})$$

we may, after discarding a total derivative in the W kinetic term, rewrite (III.23) as

$$Z_W = \int [dW^+] [dW^-] \exp i \int d^4x d^4y W^+_\mu(x) K(x; y) W^-_\mu(y) + i \frac{g_2}{2} \int d^4x J^+_\mu W^-_\mu + J^-_\mu W^+_\mu \quad (\text{III.27})$$

The inverse of K , denoted by Δ , and defined through

$$\int d^4y K(x; y) \Delta(y; z) = g \delta^{(4)}(x - z) \quad (\text{III.28})$$

is just the W propagator in the unitary gauge

$$\Delta(x; y) = \int \frac{d^4k}{(2\pi)^4} \tilde{\Delta}(k) e^{-ik(x-y)} \quad (\text{III.29})$$

$$\tilde{\Delta}(k) = \frac{1}{k^2 - M_W^2} g \frac{k_\mu k_\nu}{M_W^2} \quad (\text{III.30})$$

Performing the gaussian functional integration over $W_\mu(x)$ in (III.27) explicitly, this expression simplifies to

$$Z_W = \exp \left[i \int d^4x \frac{g_2^2}{8} J^+_\mu(x) \Delta(x; y) J^-_\nu(y) d^4y \right] \quad (\text{III.31})$$

This result implies a nonlocal action functional for the quarks

$$S_{n1} = \int d^4x L_{kin} - \frac{g_2^2}{8} \int d^4x d^4y J^-(x) (x;y) J^+(y) \quad (III.32)$$

where the first piece represents the quark kinetic terms and the second their charged current interactions.

We can now formally expand this second, nonlocal term in powers of $1/M_W^2$ to yield a series of local interaction operators of dimensions that increase with the order in $1/M_W^2$. To lowest order

$$(x;y) = \frac{g}{M_W^2} (4) (x-y) \quad (III.33)$$

and the second term in (III.32) becomes

$$\frac{g_2^2}{8M_W^2} \int d^4x J^-(x) J^+(x) \quad (III.34)$$

corresponding to the usual effective charged current interaction Lagrangian

$$L_{int,eff} = \frac{G_F}{2} J^- J^+ (x) = \frac{G_F}{2} V_{pn} V_{p^0 n^0} (np)_V - A (p^0 n^0)_V - A \quad (III.35)$$

which contains, among other terms, the leading contribution to (III.22).

The simple considerations we have presented so far already illustrate several of the basic aspects of the general approach.

Formally, the procedure to approximate the interaction term in (III.32) by (III.34) is an example of a short-distance OPE. The product of the local operators $J^-(x)$ and $J^+(y)$, to be taken at short-distances due to the convolution with the massive, short-range W propagator $(x;y)$ (compare (III.33)), is expanded into a series of composite local operators, of which the leading term is shown in (III.34).

The dominant contributions in the short-distance expansion come from the operators of lowest dimension. In our case these are four-fermion operators of dimension six, whereas operators of higher dimensions can usually be neglected in weak decays.

Note that, as far as the charged current weak interaction is concerned, no approximation is involved yet in the nonlocal interaction term in (III.32), except that we do not consider higher order weak corrections or processes with external W boson states. Correspondingly, the OPE series into which the nonlocal interaction is expanded, is equivalent to the original theory, when considered to all orders in $1/M_W^2$. In other words, the full series will reproduce the complete Green functions for the charged current weak interactions of quarks. The truncation of the operator series then yields a systematic approximation scheme for low energy processes, neglecting contributions suppressed by powers of k^2/M_W^2 . In this way one is able to construct low energy effective theories for weak decays.

In going from the full to the effective theory the W boson is removed as an explicit, dynamical degree of freedom. This step is often referred to as “integrating out” the W boson, a terminology which is very obvious in the path integral language discussed above. Alternatively one could of course use the canonical operator formalism, where the W field instead of being integrated out, gets “contracted out” through the application of Wick’s theorem.

The effective local four-fermion interaction terms are a modern version of the classic Fermi-theory of weak interactions.

An intuitive interpretation of the OPE formalism discussed so far is, that from the point of view of low energy dynamics, the effects of a short-range exchange force mediated by a heavy boson approximately corresponds to a point interaction.

The presentation we have given illustrates furthermore, that the approach of evaluating the relevant Green functions (or amplitudes) directly in order to construct the OPE, as in (III.21), actually gives the same result as the more formal technique employing path integrals. While the latter can give some useful insight into the general aspects of the method, the former is more convenient for practical calculations and we will make use of it throughout the discussion to follow.

Up to now we have not talked about the strong interactions among quarks, which have of course to be taken into account. They are described by QCD and can at short-distances be calculated in perturbation theory, due to the property of asymptotic freedom of QCD. The corresponding gluon exchange contributions constitute quantum corrections to the simplified picture sketched above, which can in this sense be viewed as a classical approximation. We will describe the incorporation of QCD corrections and related additional features they imply for the OPE in the following section.

C. OPE and Short Distance QCD Effects

We will now take up the discussion of QCD quantum corrections at short-distances to the OPE for weak decays. A crucial point for this enterprise is the property of asymptotic freedom of QCD. This allows one to treat the short-distance corrections, that is the contribution of hard gluons at energies of the order $O(M_W)$ down to hadronic scales $\sim 1 \text{ GeV}$, in perturbation theory. In the following, we will always restrict ourselves to the leading dimension six operators in the OPE and omit the negligible contributions of higher dimensional operators. Staying with our example of $c \rightarrow s$ transitions, recall that we had for the amplitude without QCD

$$A_0 = \frac{G_F}{2} V_{cs} V_{ud} (s_i c_i)_{V-A} (u_j d_j)_{V-A} \quad (\text{III.36})$$

where the summation over repeated color indices is understood. This result leads directly to the effective hamiltonian of (III.22) where the color indices have been suppressed. If we now include QCD effects, the effective hamiltonian, constructed to reproduce the low energy approximation of the exact theory, is generalized to

$$H_{\text{eff}} = \frac{G_F}{2} V_{cs} V_{ud} (C_1 Q_1 + C_2 Q_2) \quad (\text{III.37})$$

where

$$Q_1 = (s_i c_j)_{V-A} (u_j d_i)_{V-A} \quad (\text{III.38})$$

$$Q_2 = (s_i c_i)_{V-A} (u_j d_j)_{V-A} \quad (\text{III.39})$$

The essential features of this hamiltonian are:

In addition to the original operator Q (with index 2 for historical reasons) a new operator Q_1 with the same flavor form but different color structure is generated. This is because a gluon linking the two color singlet weak current lines can “mix” the color indices due to the following relation for the color charges T_{ij}^a

$$T_{ik}^a T_{jl}^a = \frac{1}{2N} \delta_{ik} \delta_{jl} + \frac{1}{2} \delta_{il} \delta_{jk} \quad (\text{III.40})$$

The Wilson coefficients G and C_2 , the coupling constants for the interaction terms Q_1 and Q_2 , become calculable nontrivial functions of s , M_W and the renormalization scale μ . If QCD is neglected they have the trivial form $C_1 = 0$, $C_2 = 1$ and (III.37) reduces to (III.22).

In order to obtain the final result for the hamiltonian (III.37), we have to calculate the coefficients $C_{1,2}$. These are determined by the requirement that the amplitude A in the full theory be reproduced by the corresponding amplitude in the effective theory (III.37), thus

$$A = \frac{G_F}{2} V_{cs} V_{ud} (C_1 h_{Q_1} + C_2 h_{Q_2}) \quad (\text{III.41})$$

If we calculate the amplitude A and, to the same order in s , the matrix elements of operators h_{Q_1} , h_{Q_2} via (III.41). This procedure is called *matching* the full theory onto the effective theory (III.37).

Here we use the term “amplitude” in the meaning of “amputated Green function”. Correspondingly operator matrix elements are – within this perturbative context – amputated Green functions with operator insertion. In a diagrammatic language these amputated Green functions are given by Feynman graphs, but without gluonic self energy corrections in external legs, like e.g. in figs. 2 and 3 for the full and effective theory, respectively. In the present example penguin diagrams do not contribute due to the flavor structure of the $c \rightarrow s$ transition.

Evaluating the current-current diagrams of fig. 2 (a)–(c), we find for the full amplitude A to $O(s)$

$$A = \frac{G_F}{2} V_{cs} V_{ud} \left[1 + 2C_F \frac{s}{4} \ln \frac{2}{p^2} S_2 + \frac{3}{N} \frac{s}{4} \ln \frac{M_W^2}{p^2} S_2 - \frac{3}{4} \frac{s}{4} \ln \frac{M_W^2}{p^2} S_1 \right] \quad (\text{III.42})$$

Here we have introduced the spinor amplitudes

$$S_1 = (s_i c_j)_{V-A} (u_j d_i)_{V-A} \quad (\text{III.43})$$

$$S_2 = (s_i c_i)_{V-A} (u_j d_j)_{V-A} \quad (\text{III.44})$$

which are just the tree level matrix elements of Q_1 and Q_2 . We have employed the Feynman gauge ($\epsilon = 1$) and taken all external quark lines massless and carrying the off-shell momentum p . Furthermore we have kept only logarithmic corrections $s \ln$ and discarded constant contributions of order $O(s)$, which corresponds to the leading log approximation. The necessary renormalization of the quark fields in the \overline{MS} -scheme is already incorporated into (III.42). It has removed a $1/\epsilon$ singularity in the first term of (III.42), which therefore carries an explicit ϵ -dependence.

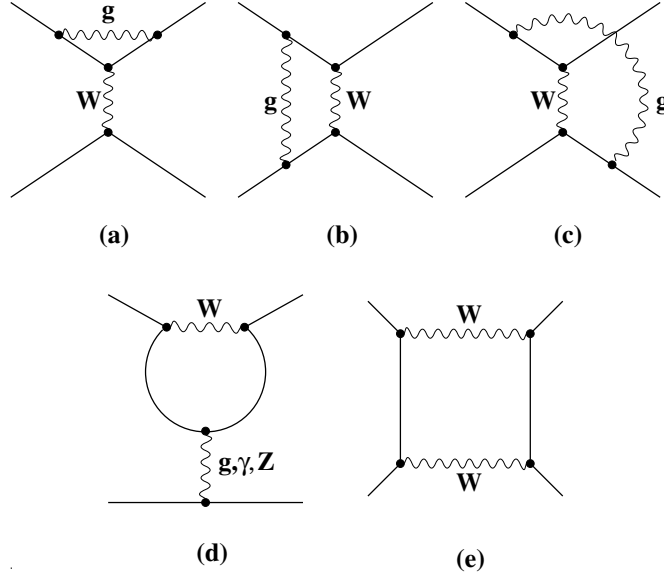


FIG. 2. One-loop current-current (a)–(c), penguin (d) and box (e) diagrams in the full theory. For pure QCD corrections as considered in this section and e.g. in VI the γ - and Z -contributions in diagram (d) and the diagram (e) are absent. Possible left-right or up-down reflected diagrams are not shown.

Under the same conditions, the unrenormalized current-current matrix elements of the operators Q_1 and Q_2 are from fig. 3 (a)-(c) found to be

$$\langle Q_1 \rangle^{(0)} = \left(1 + 2C_F \frac{s}{4} \right) \left(\frac{1}{n} + \ln \frac{2}{p^2} \right) S_1 + \frac{3}{N} \left(\frac{s}{4} \right) \left(\frac{1}{n} + \ln \frac{2}{p^2} \right) S_1 + \frac{3}{4} \left(\frac{s}{4} \right) \left(\frac{1}{n} + \ln \frac{2}{p^2} \right) S_2 \quad (\text{III.45})$$

$$\langle Q_2 \rangle^{(0)} = \left(1 + 2C_F \frac{s}{4} \right) \left(\frac{1}{n} + \ln \frac{2}{p^2} \right) S_2 + \frac{3}{N} \left(\frac{s}{4} \right) \left(\frac{1}{n} + \ln \frac{2}{p^2} \right) S_2 + \frac{3}{4} \left(\frac{s}{4} \right) \left(\frac{1}{n} + \ln \frac{2}{p^2} \right) S_1 \quad (\text{III.46})$$

Again, the divergences in the first terms are eliminated through field renormalization. However, in contrast to the full amplitude, the resulting expressions are still divergent. Therefore an additional multiplicative renormalization, referred to as *operator renormalization*, is necessary:

$$Q_i^{(0)} = Z_{ij} Q_j \quad (\text{III.47})$$

Since (III.45) and (III.46) each involve both S_1 and S_2 , the renormalization constant is in this case a 2×2 matrix Z . The relation between the unrenormalized ($\langle Q_i \rangle^{(0)}$) and the renormalized amputated Green functions ($\langle Q_i \rangle$) is then

$$\langle Q_i \rangle^{(0)} = Z_q^{-2} Z_{ij} \langle Q_j \rangle \quad (\text{III.48})$$

From (III.45), (III.46) and (III.15) we read off (MS-scheme)

$$Z = 1 + \frac{s}{4} \frac{1}{n} \begin{pmatrix} 3-N & 3 \\ 3 & 3-N \end{pmatrix} \quad (\text{III.49})$$

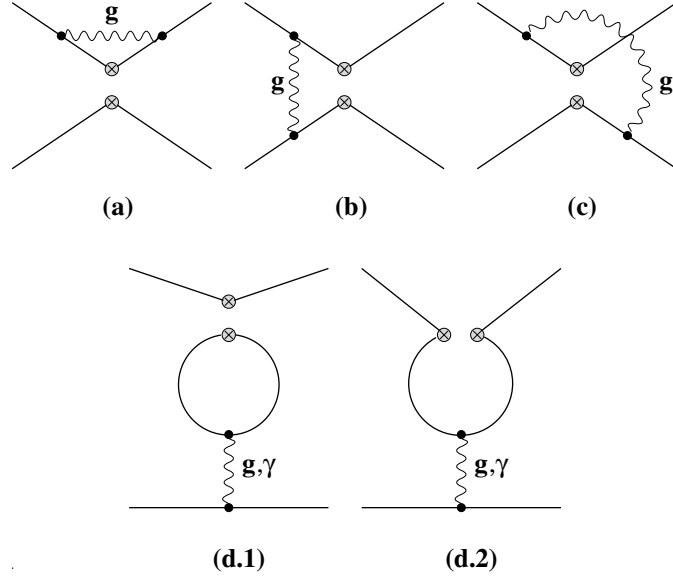


FIG. 3. One loop current-current (a)–(c) and penguin (d) diagrams contributing to the LO anomalous dimensions and matching conditions in the effective theory. The 4-vertex “ \otimes ” denotes the insertion of a 4-fermion operator Q_i . For pure QCD corrections as considered in this section and e.g. in VI the contributions from \otimes in diagrams (d.1) and (d.2) are absent. Again, possible left-right or up-down reflected diagrams are not shown.

It follows that the renormalized matrix elements $\langle Q_i \rangle$ are given by

$$\langle Q_1 \rangle = 1 + 2C_F \frac{s}{4} \ln \frac{s}{p^2} S_1 + \frac{3}{N} \frac{s}{4} \ln \frac{s}{p^2} S_1 - \frac{3}{4} \frac{s}{4} \ln \frac{s}{p^2} S_2 \quad (\text{III.50})$$

$$\langle Q_2 \rangle = 1 + 2C_F \frac{s}{4} \ln \frac{s}{p^2} S_2 + \frac{3}{N} \frac{s}{4} \ln \frac{s}{p^2} S_2 - \frac{3}{4} \frac{s}{4} \ln \frac{s}{p^2} S_1 \quad (\text{III.51})$$

Inserting $\langle Q_i \rangle$ into (III.41) and comparing with (III.42) we derive

$$C_1 = -\frac{3}{4} \frac{s}{4} \ln \frac{M_W^2}{2} \quad C_2 = 1 + \frac{3}{N} \frac{s}{4} \ln \frac{M_W^2}{2} \quad (\text{III.52})$$

We would like to digress and add a comment on the renormalization of the interaction terms in the effective theory. The commonly used convention is to introduce via (III.48) the renormalization constants Z_{ij} , defined to absorb the divergences of the operator matrix elements. It is however instructive to view this renormalization in a slightly different, but of course equivalent way, corresponding to the standard counterterm method in perturbative renormalization. Consider, as usual, the hamiltonian of the effective theory as the starting point with fields and coupling constants as bare quantities, which are renormalized according to ($q=s, c, u, d$)

$$q^{(0)} = Z_q^{1=2} q \quad (\text{III.53})$$

$$C_i^{(0)} = Z_{ij}^c C_j \quad (\text{III.54})$$

Then the hamiltonian (III.37) is essentially (omitting the factor $\frac{G_F}{2} V_{cs} V_{ud}$)

$$C_i^{(0)} Q_i(q^{(0)}) = Z_q^2 Z_{ij}^c C_j Q_i = C_i Q_i + (Z_q^2 Z_{ij}^c - \delta_{ij}) C_j Q_i \quad (\text{III.55})$$

that is, it can be written in terms of renormalized couplings and fields $(C_i Q_i)$, plus counterterms. The argument $q^{(0)}$ in the first term in (III.55) indicates that the interaction term Q_i is composed of bare fields. Calculating the amplitude with the hamiltonian (III.55), which includes the counterterms, we get the finite renormalized result

$$Z_q^2 Z_{ij}^c C_j h_{Q_i}^{(0)} = C_j h_{Q_j} \quad (\text{III.56})$$

Hence (compare (III.48))

$$Z_{ij}^c = Z_{ji}^{-1} \quad (\text{III.57})$$

In short, it is sometimes useful to keep in mind that one can think of the “operator renormalization”, which sounds like a new concept, in terms of the completely equivalent, but customary, renormalization of the coupling constants C_i , as in any field theory.

Now that we have presented in quite some detail the derivation of the Wilson coefficients in (III.52), we shall discuss and interpret the most important aspects of the short-distance expansion for weak decays, which can be studied very transparently on the explicit example we have given.

First of all a further remark about the phenomenon of operator mixing that we encountered in our example. This occurs because gluonic corrections to the matrix element of the original operator Q_2 are not just proportional to Q_2 itself, but involve the additional structure Q_1 (and vice versa). Therefore, besides a Q_2 -counterterm, a counterterm Q_1 is needed to renormalize this matrix element – the operators in question are said to mix under renormalization. This however is nothing new in principle. It is just an algebraic generalization of the usual concepts. Indeed, if we introduce a different operator basis $Q = (Q_2 \quad Q_1)^T$ (with coefficients $C = C_2 \quad C_1$) the renormalization becomes diagonal and matrix elements of Q_+ and Q_- are renormalized multiplicatively. In this new basis the OPE reads

$$A = A_+ + A_- = \frac{G_F}{2} V_{cs} V_{ud} (C_+ h_{Q_+} + C_- h_{Q_-}) \quad (\text{III.58})$$

where $(S = (S_2 \quad S_1)^T)$

$$A = \frac{G_F}{2} V_{cs} V_{ud} \left(1 + 2C_F \frac{s}{4} \ln \frac{s}{p^2} \right) S + \left(\frac{3}{N} - 3 \right) \frac{s}{4} \ln \frac{M_W^2}{p^2} S \quad (\text{III.59})$$

and

$$h_{Q_i} = \left(1 + 2C_F \frac{s}{4} \ln \frac{s}{p^2} \right) S + \left(\frac{3}{N} - 3 \right) \frac{s}{4} \ln \frac{s}{p^2} S \quad (\text{III.60})$$

$$C = 1 + \left(\frac{3}{N} - 3 \right) \frac{s}{4} \ln \frac{M_W^2}{s} \quad (\text{III.61})$$

In the calculation of the amplitude A in (III.42) and of the matrix elements in (III.45) and (III.46) the off-shell momentum p of the external quark legs represents an infrared regulator. The logarithmic infrared divergence of the gluon correction diagrams (figs. 2(a)–(c) and 3(a)–(c)) as $p^2 \rightarrow 0$ is evident from (III.42), (III.45) and (III.46). A similar observation can be made for the M_W dependence of the full amplitude A . We see that (III.42) is logarithmically divergent in the limit $M_W \rightarrow 1$. This behaviour is reflected in the ultraviolet divergences (persisting after field renormalization) of the matrix elements (III.45), (III.46) in the effective theory, whose local interaction terms correspond to the weak interactions in the infinite M_W limit as they are just the leading contribution of the $1/M_W$ operator product expansion. This also implies, that the characteristic logarithmic functional dependence of the leading $O(1/M_W)$ corrections is closely related to the divergence structure of the effective theory, that is to the renormalization constants Z_{ij} .

The most important feature of the OPE is that it provides a factorization of short-distance (coefficients) and long-distance (operator matrix elements) contributions. This is clearly exhibited in our example. The dependence of the amplitude (III.42) on p^2 , representing the long-distance structure of A , is fully contained in the matrix elements of the local operators Q_i (III.50), (III.51), whereas the Wilson coefficients C_i in (III.52) are free from this dependence. Essentially, this factorization has the form (see (III.59) – (III.61))

$$(1 + {}_sG \ln \frac{M_W^2}{p^2}) = (1 + {}_sG \ln \frac{M_W^2}{2}) (1 + {}_sG \ln \frac{2}{p^2}) \quad (\text{III.62})$$

that is, amplitude = coefficient function \times operator matrix element. Hereby the logarithm on the l.h.s. is split according to

$$\ln \frac{M_W^2}{p^2} = \ln \frac{M_W^2}{2} + \ln \frac{2}{p^2} \quad (\text{III.63})$$

Since the logarithmic behaviour results from the integration over some virtual loop momentum, we may – roughly speaking – rewrite this as

$$\int_{p^2}^{M_W^2} \frac{dk^2}{k^2} = \int_2^{M_W^2} \frac{dk^2}{k^2} + \int_{p^2}^2 \frac{dk^2}{k^2} \quad (\text{III.64})$$

which illustrates that the coefficient contains the contributions from large virtual momenta of the loop correction from scales 1 GeV to M_W , whereas the low energy contributions are separated into the matrix elements.

Of course, the latter can not be calculated in perturbation theory for transitions between physical meson states. The point is, that we have calculated the OPE for unphysical off-shell quark external states only to extract the Wilson coefficients, which we need to construct the effective hamiltonian (III.37). For this purpose the fact that we have considered an unphysical amplitude is irrelevant since the coefficient functions do not depend on the external states, but represent the short-distance structure of the theory. Once we have extracted the coefficients and written down the effective hamiltonian, the latter can be used – at least in principle – to evaluate the physically interesting decay amplitudes by means of some nonperturbative approach.

In interpreting the role of the scale μ we may distinguish two different aspects. From the point of view of the effective theory μ is just a renormalization scale, introduced in the process of renormalizing the effective local interaction terms by the dimensional method. On the other hand, from the point of view of the full theory, μ acts as the scale at which the full contribution is separated into a low energy and a high energy part, as is evident from the above discussion. For this reason μ is sometimes also called the *factorization scale*.

In our case the infrared structure of the amplitude is characterized by the off-shell momentum p . In general one could work with any other arbitrary momentum configuration, on-shell or off-shell, with or without external quark mass, with infrared divergences regulated by off-shell momenta, quark masses, a fictitious gluon mass or by dimensional regularization. In the case of off-shell momenta the amplitude is furthermore dependent on the gauge parameter of the gluon field. All these things belong to the infrared or long-distance structure of the amplitude. Therefore the dependence on these choices is the same for the full amplitude and for the operator matrix elements and drops out in the coefficient functions. To check that this is really the case for a particular choice is of crucial importance for practical calculations. On the other hand one may use this freedom and choose the treatment of external lines according to convenience or taste. Sometimes it may however seem preferable to keep a slightly more inconvenient dependence on external masses and/or gluon gauge in order to have a useful check that this dependence does indeed cancel out for the Wilson coefficients one is calculating.

D. The Renormalization Group

1. Basic Concepts

So far we have computed the Wilson coefficient functions (III.61) in ordinary perturbation theory. This, however, is not sufficient for the problem at hand. The appropriate scale at which to normalize the hadronic matrix elements of local operators is a low energy scale – low compared to the weak scale M_W – of a few GeV typically. In our example of charm decay $\mu = O(m_c)$. For such a low scale the logarithm $\ln(M_W^2/\mu^2)$ multiplying $\alpha_s(\mu)$ in the expression (III.61) becomes large. Although $\alpha_s(\mu)$ by itself is a valid expansion parameter down to scales of $O(1 \text{ GeV})$, say, this is not longer true for the combination $\alpha_s(\mu) \ln(M_W^2/\mu^2)$. In fact, for our example (III.61) the first order correction term amounts for $\mu = 1 \text{ GeV}$ to 65 – 130% although $\alpha_s=4$ 4%. The reason for this breakdown of the naive perturbative expansion lies ultimately in the appearance of largely disparate scales M_W and μ in the problem at hand.

This situation can be considerably improved by employing the method of the renormalization group (RG). The renormalization group is the group of transformations between different choices of the renormalization scale μ . The renormalization group equations describe the change of renormalized quantities, Green functions and parameters, with μ in a differential form. As we shall illustrate below, solving these differential equations allows, in the leading logarithmic approximation (LLA), to sum up the terms $(\alpha_s \ln(M_W/\mu))^n$ to all orders n ($n = 0; \dots; 1$) in perturbation theory. This leads to the RG improved perturbation theory. Going one step beyond in this modified expansion, to the next-to-leading logarithmic approximation (NLLA), the summation is extended

to all terms $\alpha_s (\alpha_s \ln(M_W = \mu))^\eta$, and so on. In this context it is useful to consider $\alpha_s \ln(M_W = \mu)$ with a large logarithm $\ln(M_W = \mu)$ as a quantity of order $\mathcal{O}(1)$

$$\alpha_s \ln \frac{M_W}{\mu} = \mathcal{O}(1) \quad M_W \quad (III.65)$$

Therefore the series in powers of $\alpha_s \ln(M_W = \mu)$ cannot be truncated. Summed to all orders it yields again a contribution of order $\mathcal{O}(1)$. Correspondingly the next-to-leading logs $\alpha_s (\alpha_s \ln(M_W = \mu))^\eta$ represent an $\mathcal{O}(\alpha_s)$ perturbative correction to the leading term.

The renormalization group equation for the Wilson coefficient functions follows from the fact, that the unrenormalized Wilson coefficients $C^{(0)} = Z_C C$ ($C^T = (C_1; C_2)$) are μ -independent. Defining the matrix of anomalous dimensions by

$$= Z^{-1} \frac{d}{d \ln} Z \quad (III.66)$$

and recalling that $Z_C^T = Z^{-1}$, we obtain the renormalization group equation

$$\frac{d}{d \ln} C(\mu) = -\gamma^T(\alpha_s) C(\mu) \quad (III.67)$$

The solution of (III.67) may formally be written in terms of a μ -evolution matrix U as

$$C(\mu) = U(\mu; M_W) C(M_W) \quad (III.68)$$

From (III.49) and (III.66) we have to first order in α_s

$$(\alpha_s) = \frac{\alpha_s}{4} C^{(0)} = \frac{\alpha_s}{4} \begin{pmatrix} 6-N & 6 \\ 6 & 6-N \end{pmatrix} \quad (III.69)$$

or in the diagonal basis

$$(\alpha_s) = \frac{\alpha_s}{4} C^{(0)} \quad C^{(0)} = \begin{pmatrix} N & 1 \\ 0 & N \end{pmatrix} \quad (III.70)$$

Note that if we neglect QCD loop corrections completely, the couplings C are independent of μ . The nontrivial μ -dependence of C expressed in (III.67) is a genuine quantum effect. It implies an anomalous scaling behaviour for the dimensionless coefficients, i.e. one that is different from the classical theory. For this reason the factor γ is called anomalous (scale) dimension (compare (III.67) with $\frac{d}{d \ln} \mu^n = n \mu^n$ for an n -dimensional μ -dependent term μ^n).

Using (III.13) the RG equation (III.67) is easily solved with the result

$$C(\mu) = \frac{\alpha_s(M_W)}{\alpha_s(\mu)} \left(\frac{\mu}{M_W} \right)^{\frac{\gamma^{(0)}}{2\beta_0}} C(M_W) \quad (III.71)$$

At a scale $\mu = M_W$ no large logarithms are present and $C(M_W)$ can therefore be calculated in ordinary perturbation theory. From (III.61) we have to the order needed for the LLA

$$C(M_W) = 1 \quad (III.72)$$

(III.71) and (III.72) give the final result for the coefficients in the leading log approximation of RG improved perturbation theory.

At this point one should emphasize, that the choice of the high energy matching scale $\mu_W = M_W$ is of course not unique. The only requirement is that the choice of μ_W must not introduce large logs $\ln(M_W = \mu_W)$ in order not to spoil the applicability of the usual perturbation theory. Therefore μ_W should be of order $O(M_W)$. The logarithmic correction in (III.61) is then $O(\alpha_s)$ and is neglected in LLA. Then, still, $C(\mu_W) = 1$ and

$$C(\mu) = \frac{s(\mu_W)^{\frac{1}{2} \frac{(0)}{0}}}{s(\mu)^{\frac{1}{2} \frac{(0)}{0}}} = \frac{s(M_W)^{\frac{1}{2} \frac{(0)}{0}}}{s(\mu)^{\frac{1}{2} \frac{(0)}{0}}} (1 + O(\alpha_s)) \quad (\text{III.73})$$

A change of μ_W around the value of M_W causes an ambiguity of $O(\alpha_s)$ in the coefficient. This ambiguity represents a theoretical uncertainty in the determination of $C(\mu)$. In order to reduce it, it is necessary to go beyond the leading order. At NLO the scale ambiguity is then reduced from $O(\alpha_s)$ to $O(\alpha_s^2)$. We will come back to this point below. Presently, we will set $\mu_W = M_W$, but it is important to keep the related uncertainty in mind.

Taking into account the leading order solution of the RG equation (III.13) for the coupling, which can be expressed in the form

$$s(\mu) = \frac{s(\mu_0)}{1 + \frac{s(\mu_0)}{4} \ln \frac{\mu^2}{\mu_0^2}} \quad (\text{III.74})$$

we may rewrite (III.71) as

$$C(\mu) = \frac{1}{1 + \frac{s(\mu_0)}{4} \ln \frac{\mu^2}{\mu_0^2}} \frac{1}{s(\mu_0)^{\frac{1}{2} \frac{(0)}{0}}} \quad (\text{III.75})$$

(III.75) contains the logarithmic corrections $s \ln(M_W^2 = \mu^2)$ to all orders in α_s . This shows very clearly that the leading log corrections have been summed up to all orders in perturbation theory by solving the RG equation. In particular, if we again expand (III.75) in powers of α_s , keeping the first term only we recover (III.61). This observation demonstrates, that the RG method allows to obtain solutions, which go beyond the conventional perturbation theory.

Before concluding this subsection, we would like to introduce still two generalizations of the approach developed so far, which will appear in the general discussion below.

2. Threshold Effects in LLA

First we may generalize the renormalization group evolution from M_W down to m_c to include the threshold effect of heavy quarks like b or t as follows

$$C(\mu) = U^{(f=4)}(\mu; m_b) U^{(f=5)}(m_b; \mu) C(\mu_W) \quad (\text{III.76})$$

which is valid for the LLA. In our example of the $c \rightarrow s$ transition the top quark gives no contribution at all. Being heavier (but comparable) in mass than the W , it is simply removed from

the theory along with the W-boson. In a first step the coefficients at the initial scale $\mu_W = M_W$ are evolved down to $\mu_b = m_b$ in an effective theory with five quark flavors ($f = 5$). Then, again in the spirit of the effective field theory technique, for scales below μ_b also the bottom quark is removed as an explicit degree of freedom from the effective theory, yielding a new effective theory with only four “active” quark flavors left. The matching corrections between both theories can be calculated in ordinary perturbation theory at the scale μ_b , since due to $\mu_b = m_b$ no large logs can occur in this procedure. For the same reason matching corrections ($\mathcal{O}(\alpha_s)$) can be neglected in LLA and the coefficients at μ_b , $C(\mu_b)$, simply serve as the initial values for the RG evolution in the four quark theory down to $\mu_c = m_c$. In addition, continuity of the running coupling across the threshold μ_b is imposed by the requirement

$$g_{sf=4}(\mu_b; \alpha_s^{(4)}) = g_{sf=5}(\mu_b; \alpha_s^{(5)}) \quad (\text{III.77})$$

which defines different QCD scales μ_f for each effective theory.

Neglecting the b-threshold, as we did before (III.68), one may just perform the full evolution from μ_W to μ_c in an effective four flavor theory. It turns out that in some cases the difference of these two approaches is even negligible.

We would like to add a comment on this effective field theory technique. At the first sight the idea to “remove by hand” heavy degrees of freedom may look somewhat artificial. However it appears quite natural when not viewed from the evolution from high towards low energies but vice versa (which actually corresponds to the historical way). Suppose only the “light” quarks u, d, s, c were known. Then in the attempt to formulate a theory of their weak interactions one would be lead to a generalized Fermi theory with (effective) four quark coupling constants to be determined somehow. Of course, we are in the lucky position to know the underlying theory in the form of the Standard Model. Therefore we can actually derive the coupling constants of the low energy effective theory from “first principles”. This is exactly what is achieved technically by going through a series of effective theories, removing heavy degrees of freedom successively, by means of a step-by-step procedure.

3. Penguin Operators

A second, but very important issue is the generation of QCD penguin operators (Vainshtein *et al.*, 1977). Consider for example the local operator $(s_i u_j)_{V-A} (u_j d_i)_{V-A}$, which is directly induced by W-boson exchange. In this case, additional QCD correction diagrams, the penguin diagrams (d.1) and (d.2) with a gluon in fig. 3, contribute and as a consequence six operators are involved in the mixing under renormalization instead of two. These read

$$\begin{aligned} Q_1 &= (s_i u_j)_{V-A} (u_j d_i)_{V-A} \\ Q_2 &= (s_i u_i)_{V-A} (u_j d_j)_{V-A} \\ Q_3 &= (s_i d_i)_{V-A} \sum_q (q_j q_j)_{V-A} \\ Q_4 &= (s_i d_j)_{V-A} \sum_q (q_j q_i)_{V-A} \\ Q_5 &= (s_i d_i)_{V-A} \sum_q (q_j q_j)_{V+A} \\ Q_6 &= (s_i d_j)_{V-A} \sum_q (q_j q_i)_{V+A} \end{aligned} \quad (\text{III.78})$$

The sum over q runs over all quark flavors that exist in the effective theory in question. The operators Q_1 and Q_2 are just the ones we have encountered in subsection III C, but with the c -quark replaced by u . This modified flavor structure gives rise to the gluon penguin type diagrams

shown in fig. 3 (d). Since the gluon coupling is of course flavor conserving, it is clear that penguins cannot be generated from the operator $(sc)_V - A (ud)_V - A$. The penguin graphs induce the new local interaction vertices $Q_3; \dots; Q_6$, which have the same quantum numbers. Their structure is easily understood. The flavor content is determined by the $(sd)_V - A$ current in the upper part and by a $\bar{q}_q(qq)_V$ vector current due to the gluon coupling in the lower. This vector structure is for convenience decomposed into a $(V - A)$ and a $(V + A)$ part. For each of these, two different color forms arise due to the color structure of the exchanged gluon (see (III.40)). Together this yields the four operators $Q_3; \dots; Q_6$.

For all operators $Q_1; \dots; Q_6$ all possible QCD corrections (that is all amputated Green functions with insertion of Q_i) of the current-current (fig. 3 (a)–(c)) as well as of the penguin type (fig. 3 (d.1) and (d.2)) have to be evaluated. In this process no new operators are generated, so that $Q_1; \dots; Q_6$ form a complete set. They “close under renormalization”. In analogy to the case of subsection III C the divergent parts of these Green functions determine, after field renormalization, the operator renormalization constants, which in the present case form a 6×6 matrix. The calculation of the corresponding anomalous dimension matrix and the renormalization group analysis then proceeds in the usual way. We will see that the inclusion of higher order electroweak interactions requires the introduction of still more operators.

E. Summary of Basic Formalism

We think that after this rather detailed discussion of the methods required for the short-distance calculations in weak decays, it is useful to give at this point a concise summary of the material covered so far. At the same time this may serve as an outline of the necessary procedure for practical calculations. Furthermore it will also provide a starting point for the extension of the formalism from the LLA considered until now to the NLLA to be presented in the next subsection.

Ultimately our goal is the evaluation of weak decay amplitudes involving hadrons in the framework of a low energy effective theory, of the form

$$iH_{\text{eff}} = \frac{G_F}{2} V_{CKM} h_Q^T () iC ()$$

The procedure for this calculation can be divided into the following three steps.

Step 1: Perturbation Theory

Calculation of Wilson coefficients $C (\mu_W)$ at $\mu_W = M_W$ to the desired order in α_s . Since logarithms of the form $\ln (\mu_W / M_W)$ are not large, this can be performed in ordinary perturbation theory. It amounts to matching the full theory onto a five quark effective theory.

Step 2: RG Improved Perturbation Theory

Calculation of the anomalous dimensions of the operators

Solution of the renormalization group equation for $C (\mu)$

Evolution of the coefficients from μ_W down to the appropriate low energy scale

$$C (\mu) = U (\mu ; \mu_W) C (\mu_W)$$

Step 3: Non-Perturbative Regime

Calculation of hadronic matrix elements $\langle Q_i \rangle$, normalized at the appropriate low energy scale, by means of some non-perturbative method.

Important issues in this procedure are:

The OPE achieves a *factorization* of short- and long distance contributions.

- Correspondingly, in order to disentangle the short-distance from the long-distance part and to extract $C_i(\mu_W)$ in actual calculations, a proper *matching* of the full onto the *effective theory* has to be performed.
- Similar comments apply to the matching of an effective theory with n_f quark flavors to a theory with $(n_f - 1)$ flavors during the RG evolution to lower scales.
- Furthermore, factorization implies, that the μ -dependence and also the dependence on the renormalization scheme, which appears beyond the leading order, cancel between C_i and $\langle Q_i \rangle$.
- Since the top quark is integrated out along with the W, the coefficients $C_i(\mu_W)$ in general contain also the full dependence on the top quark mass m_t .

A *summation of large logs* by means of the RG method is necessary. More specifically, in the n -th order of renormalization group improved perturbation theory the terms of the form

$$C_i^{(n)}(\mu) = C_i^{(0)}(\mu) \ln \frac{M_W}{\mu} \ln^k \frac{M_W}{\mu}$$

are summed to all orders in k ($k=0, 1, 2, \dots$). This approach is justified as long as $\ln \frac{M_W}{\mu}$ is small enough, which requires that μ not be too low, typically not less than 1 GeV .

F. Wilson Coefficients Beyond Leading Order

1. The RG Formalism

We are now going to extend the renormalization group formalism for the coefficient functions to the next-to-leading order level. Subsequently we will discuss important aspects of the resulting formulae, in particular the scale- and scheme dependences and their cancellation.

To have something specific in mind, we may consider the calculation for the $S = 1$ effective hamiltonian for nonleptonic decays, which without QCD effects and for low energy is given by

$$H_{\text{eff}}^{S=1} = \frac{G_F}{2} V_{us} V_{ud} (su)_{V-A} (ud)_{V-A} \quad (\text{III.79})$$

At higher energies of course also the charm, bottom and top quark have to be taken into account. The Feynman diagrams contributing to $O(\alpha_s)$ corrections to this hamiltonian are shown in fig. 2 and 3. Including current-current- as well as penguin type corrections, the relevant operator basis consists of the six operators in (III.78).

On the one hand, this particular case is very important by itself since it provides the theoretical

basis for a large variety of different decay modes. On the other hand we will at this stage keep the discussion fairly general, so that all important features of a general validity are exhibited. In addition, the central formulae of this subsection will be used at several places later on, if at times extended or modified to match the specific cases in question. In part two of this report we will give a more detailed discussion of the hamiltonians relevant for various decays. Here, we would rather like to concentrate on the presentation of the OPE and renormalization group formalism.

The effective hamiltonian for nonleptonic decays may be written in general as

$$H_{\text{eff}} = \frac{G_F}{\sqrt{2}} \sum_i C_i(\mu) Q_i(\mu) + \frac{G_F}{\sqrt{2}} \mathcal{Q}^T(\mu) \mathcal{C}(\mu) \quad (\text{III.80})$$

where the index i runs over all contributing operators, in our example $Q_1; \dots; Q_6$ of (III.78). It is straightforward to apply H_{eff} to D- and B-meson decays as well by changing the quark flavors appropriately. For the time being we omit CKM parameters, which can be reinserted later on. μ is some low energy scale of the order $O(1 \text{ GeV})$, $O(m_c)$ and $O(m_b)$ for K-, D- and B-meson decays, respectively. The argument μ of the operators $Q_i(\mu)$ means, that their matrix elements are to be normalized at scale μ .

The Wilson coefficient functions are given by

$$\mathcal{C}(\mu) = U(\mu; \mu_W) \mathcal{C}(\mu_W) \quad (\text{III.81})$$

The coefficients at the scale $\mu_W = O(M_W)$ can be evaluated in perturbation theory. The evolution matrix U then includes the renormalization group improved perturbative contributions from the scale μ_W down to μ .

In the first step we determine $\mathcal{C}(\mu_W)$ from a comparison of the amputated Green function with appropriate external lines in the full theory with the corresponding amplitude in the effective theory. At NLO we have to calculate to $O(\alpha_s)$, including non-logarithmic, constant terms. The full amplitude results from the current-current- and penguin type diagrams in fig. 2, is finite after field renormalization and can be written as

$$A = \frac{G_F}{\sqrt{2}} S^T (\mathcal{A}^{(0)} + \frac{s(\mu_W)}{4} \mathcal{A}^{(1)}) \quad (\text{III.82})$$

Here S denotes the tree level matrix elements of the operators \mathcal{Q} . In the effective theory (III.80) the current-current- and penguin corrections of fig. 3 have to be calculated for all the operators Q_i . In this case, besides the field renormalization, a renormalization of operators is necessary

$$Z_q^2 h\mathcal{Q}_i^{(0)} = Z h\mathcal{Q}_i \quad (\text{III.83})$$

where the matrix Z absorbes those divergences of the Green functions with operator \mathcal{Q} insertion, that are not removed by the field renormalization. The renormalized matrix elements of the operators can then to $O(\alpha_s)$ be written as

$$h\mathcal{Q}(\mu_W)_i = (1 + \frac{s(\mu_W)}{4} r) S \quad (\text{III.84})$$

and the amplitude in the effective theory to the same order becomes

$$A_{\text{eff}} = \frac{G_F}{2} S^T \left(1 + \frac{s(\mu_W)}{4} r^T \right) C(\mu_W) \quad (\text{III.85})$$

Equating (III.82) and (III.85) we obtain

$$C(\mu_W) = \tilde{A}^{(0)} + \frac{s(\mu_W)}{4} (\tilde{A}^{(1)} - r^T \tilde{A}^{(0)}) \quad (\text{III.86})$$

In general $\tilde{A}^{(1)}$ in (III.82) involves logarithms $\ln(M_W^2 = p^2)$ where p denotes some global external momentum for the amplitudes in fig. 2. On the other hand, the matrix r in (III.84), characterizing the radiative corrections to $h\mathcal{Q}(\mu_W)$, includes $\ln(p^2 = \frac{2}{W})$. As we have seen in subsection III C, these logarithms combine to $\ln(M_W^2 = \frac{2}{W})$ in the Wilson coefficient (III.86). For $\mu_W = M_W$ this logarithm vanishes altogether. For $\mu_W = O(M_W)$ the expression $\ln(M_W^2 = \frac{2}{W})$ is a “small logarithm” and the correction $s \ln(M_W^2 = \frac{2}{W})$, which could be neglected in LLA, has to be kept in the perturbative calculation at NLO together with constant pieces of order $O(s)$.

In the second step, the renormalization group equation for C

$$\frac{d}{d \ln} C(\mu) = -\gamma^T(g) C(\mu) \quad (\text{III.87})$$

has to be solved with boundary condition (III.86). The solution is written with the help of the U -matrix as in (III.81), where $U(\mu; \mu_W)$ obeys the same equation as $C(\mu)$ in (III.87). The general solution is easily written down iteratively

$$U(\mu; \mu_W) = 1 + \int_{\mu_W}^{\mu} dg_1 \frac{\gamma^T(g_1)}{g_1} + \int_{\mu_W}^{\mu} dg_1 \int_{\mu_W}^{g_1} dg_2 \frac{\gamma^T(g_1)}{g_1} \frac{\gamma^T(g_2)}{g_2} + \dots \quad (\text{III.88})$$

which using $dg = d \ln \mu = -\gamma(g)$ is readily seen to solve the renormalization group equation

$$\frac{d}{d \ln} U(\mu; \mu_W) = -\gamma^T(g) U(\mu; \mu_W) \quad (\text{III.89})$$

The series in (III.88) can be more compactly expressed by introducing the notion of g -ordering

$$U(\mu; \mu_W) = T_g \exp \int_{\mu_W}^{\mu} dg^0 \frac{\gamma^0(g)}{g^0} \quad (\text{III.90})$$

where in the case $g(\mu) > g(\mu_W)$ the g -ordering operator T_g is defined through

$$T_g f(g_1) \dots f(g_n) = \sum_{\text{perm}} (g_{i_1} \dots g_{i_2}) (g_{i_2} \dots g_{i_3}) \dots (g_{i_{n-1}} \dots g_n) f(g_{i_1}) \dots f(g_{i_n}) \quad (\text{III.91})$$

and brings about an ordering of the factors $f(g_i)$ such that the coupling constants increase from right to left. The sum in (III.91) runs over all permutations $f_{i_1}; \dots; i_n$ of $f_1; 2; \dots; n$. The T_g ordering is necessary since in general the anomalous dimension matrices at different couplings do not commute beyond the leading order, $[\gamma(g_1); \gamma(g_2)] \neq 0$.

At next-to-leading order we have to keep the first two terms in the perturbative expansions for $\gamma(g)$ (see (III.11)) and $\gamma(g)$

$$\gamma(g) = \gamma^{(0)} \frac{s}{4} + \gamma^{(1)} \frac{s^2}{4} \quad (\text{III.92})$$

To this order the evolution matrix $U(\mu; m)$ is given by (Buras *et al.*, 1992)

$$U(\mu; m) = \left(1 + \frac{s(\mu)}{4} J\right) U^{(0)}(\mu; m) \left(1 - \frac{s(m)}{4} J\right) \quad (\text{III.93})$$

$U^{(0)}$ is the evolution matrix in leading logarithmic approximation and the matrix J expresses the next-to-leading corrections to this evolution. We have

$$U^{(0)}(\mu; m) = V \left[\frac{s(m)}{s(\mu)} \right]^{\frac{1}{2} \tilde{\gamma}_D^{(0)}} V^{-1} \quad (\text{III.94})$$

where V diagonalizes $\tilde{\gamma}_D^{(0)T}$

$$\tilde{\gamma}_D^{(0)} = V^{-1} \tilde{\gamma}_D^{(0)T} V \quad (\text{III.95})$$

and $\tilde{\gamma}_D^{(0)}$ is the vector containing the diagonal elements of the diagonal matrix $\tilde{\gamma}_D^{(0)}$. If we define

$$G = V^{-1} \tilde{\gamma}_D^{(0)T} V \quad (\text{III.96})$$

and a matrix H whose elements are

$$H_{ij} = \tilde{\gamma}_{ij}^{(0)} \frac{1}{2} \frac{G_{ij}}{2 + \tilde{\gamma}_i^{(0)} + \tilde{\gamma}_j^{(0)}} \quad (\text{III.97})$$

the matrix J is given by

$$J = V H V^{-1} \quad (\text{III.98})$$

The fact that (III.93) is indeed a solution of the RG equation (III.89) to the order considered is straightforwardly verified by differentiation with respect to $\ln \mu$. Combining now the initial values (III.86) with the evolution matrix (III.93) we obtain

$$C(\mu) = \left(1 + \frac{s(\mu)}{4} J\right) U^{(0)}(\mu; m) \left[\tilde{A}^{(0)} + \frac{s(m)}{4} \tilde{A}^{(1)} - (\tilde{r}^T + J) \tilde{A}^{(0)} \right] \quad (\text{III.99})$$

Using (III.99) we can calculate for example the coefficients at a scale $\mu = m_b = O(m_b)$, working in an effective five flavor theory, $f = 5$. If we have to evolve the coefficients to still lower values, we would like to formulate a new effective theory for $\mu < m_b$ where now also the b -quark is removed as an explicit degree of freedom. To calculate the coefficients in this new four flavor theory at the scale m_b , we have to determine the matching corrections at this scale.

We follow the same principles as in the case of integrating out the W -boson and require

$$h_Q^f(m) i^T C_f(m) = h_Q^{f-1}(m) i^T C_{f-1}(m) \quad (\text{III.100})$$

in the general case of a change from an f -flavor to a $(f-1)$ -flavor theory at a scale m . The “full amplitude” on the l.h.s., which is now in an f -flavor effective theory, is expanded into matrix elements of the new $(f-1)$ -flavor theory, multiplied by new Wilson coefficients C_{f-1} . From (III.84), determining the matrix elements of operators to $O(\mu^{-s})$, one finds

$$h\mathcal{Q}_f(m)i = (1 + \frac{s(m)}{4}) r h\mathcal{Q}_{f-1}(m)i \quad (\text{III.101})$$

where

$$r = r^{(f)} - r^{(f-1)} \quad (\text{III.102})$$

In (III.102) we have made explicit the dependence of the matrix r on the number of quark flavors which enters in our example via the penguin contributions. From (III.100) and (III.101) we find

$$\mathcal{C}_{f-1}(m) = M(m) \mathcal{C}_f(m) \quad (\text{III.103})$$

with

$$M(m) = 1 + \frac{s(m)}{4} r^T \quad (\text{III.104})$$

The general renormalization group matrix U in (III.93), now evaluated for $(f-1)$ flavors, can be used to evolve $\mathcal{C}_{f-1}(m)$ to lower values of the renormalization scale. It is clear that no large logarithms can appear in (III.104) and that therefore the matching corrections, expressed in the matrix $M(m)$ can be computed in usual perturbation theory. We note that this type of matching corrections enters in a nontrivial way for the first time at the NLO level. In the LLA $M = 1$ and one can simply omit the b -flavor components in the penguin operators when crossing the b -threshold.

We also remark that the correction matrix M introduces a small discontinuity of the coefficients, regarded as functions of μ , at the matching scale m . This is however not surprising. In any case the $\mathcal{C}(\mu)$ are not physical quantities and their discontinuity precisely cancels the effect of removing the heavy quark flavor from the operators, which evidently is a “discontinuous” step. Hence, physical amplitudes are not affected and indeed the behaviour of \mathcal{C} at the matching scale ensures that the same physical result will be obtained, whether we choose to calculate in the f -flavor- or in the $(f-1)$ -flavor theory for scales around the matching scale m .

To conclude we will write down how the typical final result for the coefficient functions at 1 GeV , appropriate for K -decays, looks like, if we combine all the contributions discussed above. Then we can write

$$\mathcal{C}(\mu) = U_3(\mu; c) M(c) U_4(\mu; b) M(b) U_5(\mu; w) \mathcal{C}(w) \quad (\text{III.105})$$

where U_f is the evolution matrix for f active flavors. In the following discussion we will not always include the flavor thresholds when writing the expression for the RG evolution. It is clear, that they can be added in a straightforward fashion.

2. The Calculation of the Anomalous Dimensions

The matrix of anomalous dimensions is the most important ingredient for the renormalization group calculation of the Wilson coefficient functions. In the following we will summarize the essential steps of its calculation.

Recall that the evaluation of the amputated Green functions with insertion of the operators \mathcal{Q} gives the relation

$$h\mathcal{Q} i^{(0)} = Z_q^{-2} Z h\mathcal{Q} i - Z_{GF} h\mathcal{Q} i \quad (III.106)$$

$h\mathcal{Q} i^{(0)}$, $h\mathcal{Q} i$ denote the unrenormalized and renormalized Green functions, respectively. Z_q is the quark field renormalization constant and Z is the renormalization constant matrix of the operators \mathcal{Q} .

The anomalous dimensions are given by

$$(\mathcal{g}) = Z^{-1} \frac{d}{d \ln \mu} Z \quad (III.107)$$

In the \overline{MS} (or \overline{MS}) scheme the renormalization constants are chosen to absorb the pure pole divergences $1/\epsilon^k$ ($D = 4 - 2\epsilon$), but no finite parts. Z can then be expanded in inverse powers of ϵ as follows

$$Z = 1 + \sum_{k=1}^{\infty} \frac{1}{\epsilon^k} Z_k(\mathcal{g}) \quad (III.108)$$

Using the expression for the β -function (III.6), valid for arbitrary ϵ we derive the useful formula (Floratos *et al.*, 1977)

$$(\mathcal{g}) = -2\mathcal{g} \frac{\partial Z_1(\mathcal{g})}{\partial \mathcal{g}^2} = -2 \frac{\partial Z_1(\epsilon, s)}{\partial \epsilon} \quad (III.109)$$

Similarly to (III.108) we expand

$$Z_q = 1 + \sum_{k=1}^{\infty} \frac{1}{\epsilon^k} Z_{q,k}(\mathcal{g}) \quad (III.110)$$

$$Z_{GF} = 1 + \sum_{k=1}^{\infty} \frac{1}{\epsilon^k} Z_{GF,k}(\mathcal{g}) \quad (III.111)$$

From the calculation of the unrenormalized Green functions (III.106) we immediately obtain Z_{GF} . What we need to compute (\mathcal{g}) is $Z_1(\mathcal{g})$ (III.109). From (III.106), (III.108), (III.110), (III.111) we find

$$Z_1 = 2Z_{q,1} + Z_{GF,1} \quad (III.112)$$

At next-to-leading order we have from the $1/\epsilon$ poles of the unrenormalized Green functions

$$Z_{GF,1} = b_1 \frac{s}{4} + b_2 \frac{s}{4}^2 \quad (III.113)$$

The corresponding expression for the well known factor $Z_{q,1}$ has been quoted in (III.15). Using (III.15), (III.109), (III.112), (III.113) we finally obtain for the one- and two-loop anomalous dimension matrices $^{(0)}$ and $^{(1)}$ in (III.92)

$$^{(0)}_{ij} = -2[a_{ij} + (b_1)_{ij}] \quad (III.114)$$

$$^{(1)}_{ij} = -4[a_{2,ij} + (b_2)_{ij}] \quad (III.115)$$

(III.114) and (III.115) may be used as recipes to immediately extract the anomalous dimensions from the divergent parts of the unrenormalized Green functions.

3. Renormalization Scheme Dependence

A further issue, which becomes important at next-to-leading order is the dependence of unphysical quantities, like the Wilson coefficients and the anomalous dimensions, on the choice of the renormalization scheme. This scheme dependence arises because the renormalization prescription involves an arbitrariness in the finite parts to be subtracted along with the ultraviolet singularities. Two different schemes are then related by a finite renormalization. Considering the quantities, which we encountered in subsection III F 1, the following of them are independent of the renormalization scheme

$$Q_2 = (s_i u_i)_{V-A} (u_j d_j)_{V-A} \quad \text{or} \quad \tilde{Q}_2 = (s_i d_j)_{V-A} (u_j u_i)_{V-A} \quad (\text{III.116})$$

whereas

$$r, \gamma^{(1)}, J, C, h\tilde{Q} \quad (\text{III.117})$$

are scheme dependent.

In the framework of dimensional regularization one example of how such a scheme dependence can occur is the treatment of γ_5 in D dimensions. Possible choices are the “naive dimensional regularization” (NDR) scheme with γ_5 taken to be anticommuting or the ‘t-Hooft–Veltman (HV) scheme (‘t Hooft and Veltman, 1972b), (Breitenlohner and Maison, 1977) with non-anticommuting γ_5 . Another example is the use of operators in a color singlet or a non-singlet form, such as

$$Q_2 = (s_i u_i)_{V-A} (u_j d_j)_{V-A} \quad \text{or} \quad \tilde{Q}_2 = (s_i d_j)_{V-A} (u_j u_i)_{V-A} \quad (\text{III.118})$$

where i, j are color indices. In $D = 4$ dimensions these operators are equivalent since they are related by a Fierz transformation. In the NDR scheme however these two choices yield different results for $r, \gamma^{(1)}$ and J and thus constitute two different schemes, related by a nontrivial finite renormalization. On the other hand, both choices give the same $r, \gamma^{(1)}$ and J if the HV scheme is employed.

Let us now discuss the question of renormalization scheme dependences in explicit terms in order to obtain an overview on how the scheme dependences arise, how various quantities transform under a change of the renormalization scheme and how the cancellation of scheme dependences is guaranteed for physically relevant quantities.

First of all, it is clear that the product

$$h\tilde{Q}(\mu) i^T C(\mu) \quad (\text{III.119})$$

representing the full amplitude, is independent of the renormalization scheme chosen. This is simply due to the fact, that it is precisely the factorization of the amplitude into Wilson coefficients and matrix elements of operators by means of the operator product expansion, which introduces the scheme dependence of C and $h\tilde{Q} i$. In other words, the scheme dependence of C and $h\tilde{Q} i$ represents the arbitrariness one has in splitting the full amplitude into coefficients and matrix elements and the scheme independence of the combined product (III.119) is manifest in the construction of the operator product expansion.

More explicitly, these quantities are in different schemes (primed and unprimed) related by

$$h\mathcal{Q}i^0 = (1 + \frac{s}{4})h\mathcal{Q}i \quad \mathcal{C}^0 = (1 - \frac{s}{4}s^T)\mathcal{C} \quad (\text{III.120})$$

where s is a constant matrix. (III.120) represents a finite renormalization of \mathcal{C} and $h\mathcal{Q}i$. From (III.84) we immediately obtain

$$r^0 = r + s \quad (\text{III.121})$$

Furthermore from

$$h\mathcal{Q}(i)^T \mathcal{C}(j) = h\mathcal{Q}(i)^T U(j; M_W) \mathcal{C}(M_W) \quad (\text{III.122})$$

we have

$$U^0(j; M_W) = (1 - \frac{s(i)}{4}s^T)U(j; M_W)(1 + \frac{s(M_W)}{4}s^T) \quad (\text{III.123})$$

A comparison with (III.93) yields

$$J^0 = J - s^T \quad (\text{III.124})$$

The renormalization constant matrix in the primed scheme, Z^0 , follows from (III.120) and (III.106)

$$Z^0 = Z(1 - \frac{s}{4}s) \quad (\text{III.125})$$

Recalling the definition of the matrix of anomalous dimensions, (III.107) and (III.92), we derive

$$^{(0)}0 = ^{(0)} \quad ^{(1)}0 = ^{(1)} + [s; ^{(0)}] + 2_0 s \quad (\text{III.126})$$

With these general formulae at hand it is straightforward to clarify the cancellation of scheme dependences in all particular cases. Alternatively, they may be used to transform scheme dependent quantities from one scheme to another, if desired, or to check the compatibility of results obtained in different schemes.

In particular we immediately verify from (III.121) and (III.124) the scheme independence of the matrix $r^T + J$. This means that in the expression for \mathcal{C} in (III.99) the factor on the right hand side of $U^{(0)}$, related to the “upper end” of the evolution, is independent of the renormalization scheme, as it must be. The same is true for $U^{(0)}$. On the other hand \mathcal{C} still depends on the renormalization scheme through the matrix J to the left of $U^{(0)}$. As is evident from (III.120), this dependence is compensated for by the corresponding scheme dependence of the matrix elements of operators so that a physically meaningful result for the decay amplitudes is obtained. To ensure a proper cancellation of the scheme dependence the matrix elements have to be evaluated in the same scheme (renormalization, μ , form of operators) as the coefficient functions, which is a nontrivial task for the necessary non-perturbative computations. In other words, beyond the leading order the matching between short- and long-distance contributions has to be performed properly not only with respect to the scale μ , but also with respect to the renormalization scheme employed.

4. Discussion

We will now specialize the presentation of the general formalism to the case of a single operator (that is without mixing). This situation is e.g. relevant for the operators Q_+ and Q_- with four different quark flavors, which we encountered in section III C. The resulting simplifications are useful in order to display some more details of the structure of the calculation and to discuss the most salient features of the NLO analysis in a transparent way. In the case where only one single operator contributes, the amplitude in the full theory (dynamical W-boson) may be written as (see (III.82))

$$A = \frac{G_F}{\sqrt{2}} \left(1 + \frac{s(\mu_W)}{4} \right) \frac{^{(0)}}{2} \ln \frac{M_W^2}{p^2} + \tilde{A}^{(1)} S \quad (\text{III.127})$$

where we have made the logarithmic dependence on the W mass explicit. In the effective theory the amplitude reads

$$\begin{aligned} A_{\text{eff}} &= \frac{G_F}{\sqrt{2}} C(\mu_W) h_Q(\mu_W) i \\ &= \frac{G_F}{\sqrt{2}} C(\mu_W) \left(1 + \frac{s(\mu_W)}{4} \right) \frac{^{(0)}}{2} \ln \frac{p^2}{\mu_W^2} + \frac{!}{E} \ln 4 + \frac{\#}{r} S \end{aligned} \quad (\text{III.128})$$

The divergent pole term $1/\epsilon$ has been subtracted minimally. A comparison of (III.127) and (III.128) yields the Wilson coefficient

$$C(\mu_W) = 1 + \frac{s(\mu_W)}{4} \frac{^{(0)}}{2} \ln \frac{M_W^2}{\mu_W^2} + \frac{!}{E} \ln 4 + B \quad (\text{III.129})$$

where

$$B = \tilde{A}^{(1)} - \frac{\#}{r} \quad (\text{III.130})$$

In the leading log approximation we had simply $C(\mu_W) = 1$. By contrast at NLO the $O(\epsilon)$ correction has to be taken into account in addition. This correction term exhibits the following new features:

The expression $\frac{!}{E} \ln 4$, which is characteristic to dimensional regularization appears. It is proportional to $^{(0)}$.

A constant term B is present. B depends on the factorization scheme chosen.

An explicit logarithmic dependence on the matching scale μ_W shows up.

We discuss these points one by one.

First, the term $\frac{!}{E} \ln 4$ is characteristic for the \overline{MS} scheme. It can be eliminated by going from the \overline{MS} - to the \overline{MS} scheme. This issue is well known in the literature. We find it however useful to briefly repeat the definition of the \overline{MS} scheme in the present context, since this is an important point for NLO analyses.

Consider the RG solution for the coefficient

$$C(\mu) = \left(1 + \frac{s(\mu)}{4}\right)^J \frac{s(\mu_W)}{s(\mu)}^{\frac{\#}{2} \frac{(0)}{0}} \left(1 + \frac{s(\mu_W)}{4}\right)^{\frac{(0)}{2}} \ln \frac{M_W^2}{\mu^2} + E \ln 4 + B \frac{\#}{J} \quad (\text{III.131})$$

This represents the solution for the \overline{MS} scheme. Therefore in (III.131) $s = \overline{s_{\overline{MS}}}$. The redefinition of $\overline{s_{\overline{MS}}}$ through

$$\overline{s_{\overline{MS}}} = \overline{s_{\overline{MS}}} \left(1 + \frac{(E \ln 4)}{4} \overline{s_{\overline{MS}}} \right) \quad (\text{III.132})$$

is a finite renormalization of the coupling, which defines the \overline{MS} scheme. Since

$$[\overline{s_{\overline{MS}}}(\mu_W)]^{\frac{(0)}{2} \frac{\#}{0}} = [\overline{s_{\overline{MS}}}(\mu_W)]^{\frac{(0)}{2} \frac{\#}{0}} \left(1 + \frac{(E \ln 4)}{2} \overline{s_{\overline{MS}}}(\mu_W) \right)^{\frac{\#}{4}} \quad (\text{III.133})$$

we see, that this transformation eliminates, to the order considered, the $E \ln 4$ term in (III.131). At the lower end of the evolution the same redefinition yields a factor

$$1 - \frac{(E \ln 4)}{2} \overline{s_{\overline{MS}}}(\mu) \quad (\text{III.134})$$

which removes the corresponding factor from the matrix element (see (III.128))

$$h_Q(\mu) i_{\overline{MS}} = \left(1 + \frac{(E \ln 4)}{2} \overline{s_{\overline{MS}}}(\mu) \right)^{\frac{\#}{4}} h_Q(\mu) i_{\overline{MS}} \quad (\text{III.135})$$

At the next-to-leading log level we are working, the transformation (III.132) is equivalent to a redefinition of the scale according to

$$\frac{2}{\overline{MS}} = 4 e^{-E \frac{2}{\overline{MS}}} \quad (\text{III.136})$$

as one can verify with the help of (III.19). In practice, one can just drop the $(E \ln 4)$ terms in (III.131). Then $s(\mu)$ and $s(\mu_W)$ are to be taken in the \overline{MS} scheme. Throughout the present report it is always understood that the transformation to \overline{MS} has been performed. Then

$$C(\mu) = \left(1 + \frac{s(\mu)}{4}\right)^J \frac{s(\mu_W)}{s(\mu)}^{\frac{\#}{2} \frac{(0)}{0}} \left(1 + \frac{s(\mu_W)}{4}\right)^{\frac{(0)}{2}} \ln \frac{M_W^2}{\mu^2} + B \frac{\#}{J} \quad (\text{III.137})$$

Second, from the issue of the $\overline{MS} - \overline{MS}$ transformation, or more generally an arbitrary redefinition of s (or J) one should distinguish the renormalization scheme dependence due to the ambiguity in the renormalization of the operator. It suggests itself to use for the latter the term “factorization scheme dependence”. This is the scheme dependence we have discussed in section III F 3. A change in the factorization scheme transforms $^{(1)}$, B and J as

$$^{(1)0} = ^{(1)} + 2 \frac{0}{0} s \quad B^0 = B - s \quad J^0 = J - s \quad (\text{III.138})$$

where s is a constant number. This follows from the formulae in section III F 3 and from the definition of B in (III.130). Note that in the case of a single operator the relation between $^{(1)}$ and J simplifies to

$$J = \frac{1}{2} \frac{1}{\mu_0} \left(\frac{1}{\mu_0} \right)^{(0)} \left(\frac{1}{\mu_0} \right)^{(1)} \quad (III.139)$$

Obviously the scheme dependence cancels in the difference $B - J$ in (III.137).

Third, due to the explicit μ_w dependence in the $O(\mu_s)$ correction term the coefficient function is, to the order considered, independent of the precise value of the matching scale μ_w , as it must be. Indeed

$$\frac{d}{d \ln \mu_w} C(\mu_s) = O(\mu_s^2) \quad (III.140)$$

since

$$\frac{d}{d \ln \mu_w} s(\mu_w) = 2 \mu_0 \frac{s(\mu_w)^2}{4} + O(\mu_s^3) \quad (III.141)$$

In the same way one can also convince oneself that the coefficient function is independent of the heavy quark threshold scales, up to terms of the neglected order.

Of course the dependence on the low energy scale remains and has to be matched with the corresponding dependence of the operator matrix element.

All the points we have mentioned here apply in an analogous manner also to the case with operator mixing, only the algebra is then slightly more complicated.

We would like to stress once again that it is only at the NLO level, that these features enter the analysis in a nontrivial way, as should be evident from the presentation we have given above.

5. Evanescent Operators

Finally, we would like to mention the so called *evanescent* operators. These are operators which exist in $D \neq 4$ dimensions but vanish in $D = 4$. It has been stressed in (Buras and Weisz, 1990) that a correct calculation of two-loop anomalous dimensions requires a proper treatment of these operators. This discussion has been extended in (Dugan and Grinstein, 1991) and further generalized in (Herrlich and Nierste, 1995b). In view of a rather technical nature of this aspect we refer the interested reader to the papers quoted above.

Part Two –

The Effective Hamiltonians

The second part constitutes a compendium of effective hamiltonians for weak decays. We will deal with all decays for which NLO corrections have been calculated in the literature and whose list is given in table I. This includes a listing of the initial conditions $C_i(M_W)$, a listing of all one-loop and two-loop anomalous dimension matrices and finally tables of numerical values of the relevant Wilson coefficients as functions of \overline{MS} , m_t and the renormalization schemes considered. In certain cases we are able to give analytic formulae for C_i .

We will discuss all effective hamiltonians one by one. With the help of the master formulae and the procedure of section III it is easy to see similarities and differences between various cases. Our compendium includes also the $b \rightarrow s$ and $b \rightarrow sg$ transitions which although known only in the leading logarithmic approximation deserve special attention.

Finally, as a preparation for the third part we give a brief description of the “Penguin-Box Expansion” (PBE), which can be regarded as a version of OPE particularly suited for the study of the m_t dependence in weak decays.

In addition we have also included a section on NLO QCD calculations in the context of HQET. This chapter lies somewhat outside our main line of presentation. Also a comprehensive discussion of HQET is clearly beyond the scope of the present paper. However, we would like to illustrate the application of the general formalism for short distance QCD corrections within this framework and summarize a few important NLO results that have been obtained in HQET.

IV. GUIDE TO EFFECTIVE HAMILTONIANS

In order to facilitate the presentation of effective hamiltonians in weak decays we give a complete compilation of the relevant operators below. Divided into six classes, these operators play a dominant role in the phenomenology of weak decays. The six classes are given as follows

Current-Current Operators (fig. 4 (a)):

$$Q_1 = (s_i u_j)_{V-A} (u_j d_i)_{V-A} \quad Q_2 = (su)_{V-A} (ud)_{V-A} \quad (IV.1)$$

QCD-Penguins Operators (fig. 4 (b)):

$$Q_3 = (sd)_{V-A} \sum_q (qq)_{V-A} \quad Q_4 = (s_i d_j)_{V-A} \sum_q (q_j q_i)_{V-A} \quad (IV.2)$$

$$Q_5 = (sd)_{V-A} \sum_q (qq)_{V+A} \quad Q_6 = (s_i d_j)_{V-A} \sum_q (q_j q_i)_{V+A} \quad (IV.3)$$

Electroweak-Penguins Operators (fig. 4 (c)):

$$Q_7 = \frac{3}{2} (sd)_{V-A} \sum_q e_q (qq)_{V+A} \quad Q_8 = \frac{3}{2} (s_i d_j)_{V-A} \sum_q e_q (q_j q_i)_{V+A} \quad (IV.4)$$

$$Q_9 = \frac{3}{2} (sd)_{V-A} \sum_q e_q (qq)_{V-A} \quad Q_{10} = \frac{3}{2} (s_i d_j)_{V-A} \sum_q e_q (q_j q_i)_{V-A} \quad (IV.5)$$

Magnetic-Penguins Operators (fig. 4 (d)):

$$Q_7 = \frac{e}{8} m_b s_i (1 + \gamma_5) b_i F \quad Q_{8G} = \frac{g}{8} m_b s_i (1 + \gamma_5) T_{ij}^a b_j G^a \quad (IV.6)$$

$S = 2$ and $B = 2$ Operators (fig. 4 (e)):

$$Q(S=2) = (sd)_{V-A} (sd)_{V-A} \quad Q(B=2) = (bd)_{V-A} (bd)_{V-A} \quad (IV.7)$$

Semi-Leptonic Operators (fig. 4 (f)):

$$Q_{7V} = (sd)_{V-A} (ee)_V \quad Q_{7A} = (sd)_{V-A} (ee)_A \quad (IV.8)$$

$$Q_{9V} = (bs)_{V-A} (ee)_V \quad Q_{10A} = (bs)_{V-A} (ee)_A \quad (IV.9)$$

$$Q(\quad) = (sd)_{V-A} (\quad)_{V-A} \quad Q(\quad) = (sd)_{V-A} (\quad)_{V-A} \quad (IV.10)$$

where indices in color singlet currents have been suppressed for simplicity.

For illustrative purposes, typical diagrams in the full theory from which the operators (IV.1)–(IV.10) originate are shown in fig. 4.

The operators listed above will enter our review in a systematic fashion. We begin in section V with the presentation of the effective hamiltonians involving the current-current operators Q_1 and Q_2 only. These effective hamiltonians are given in (V.4), (V.5) and (V.6) for $B = 1$, $C = 1$ and $S = 1$ non-leptonic decays, respectively.

In section VI we will generalize the hamiltonians (V.4) and (V.6) to include the QCD-penguin operators Q_3 – Q_6 . The corresponding expressions are given in (VI.32) and (VI.1), respectively. This generalization does not affect the Wilson coefficients of Q_1 and Q_2 .

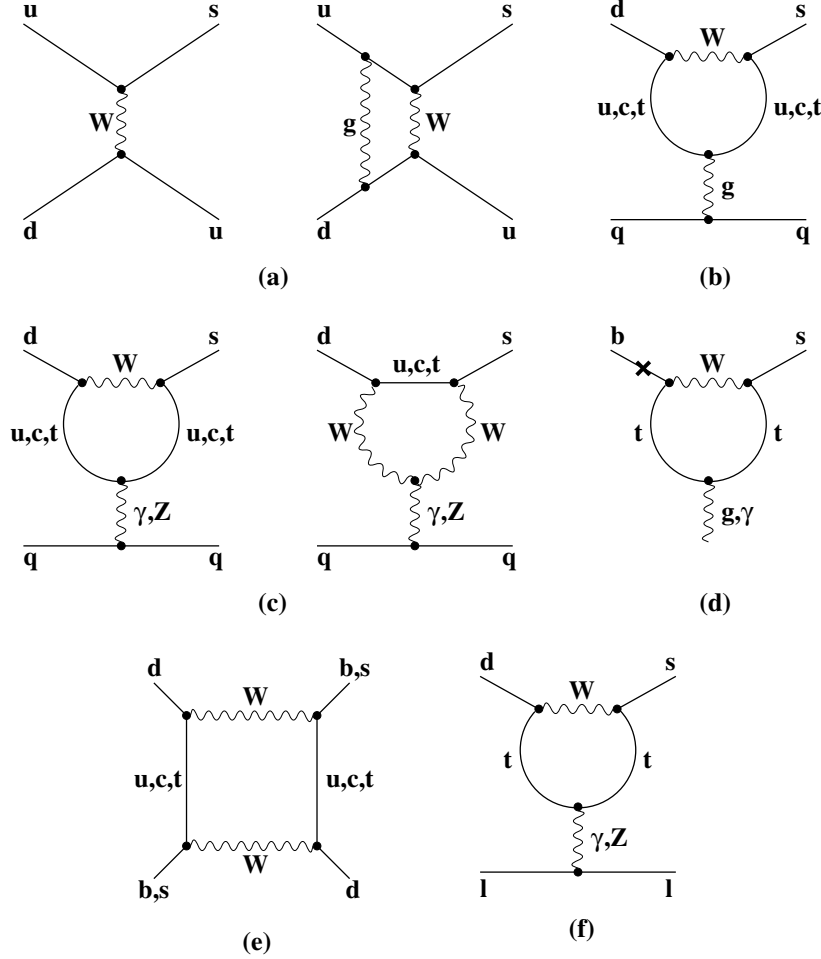


FIG. 4. Typical diagrams in the full theory from which the operators (IV.1)–(IV.10) originate. The cross in diagram (d) means a mass-insertion. It indicates that magnetic penguins originate from the mass-term on the external line in the usual QCD or QED penguin diagrams.

Next in section VII the $S = 1$ and $B = 1$ hamiltonians of section VI will be generalized to include the electroweak penguin operators $Q_7 - Q_{10}$. These generalized hamiltonians are given in (VII.1) and (VII.37) for $S = 1$ and $B = 1$ non-leptonic decays, respectively. The inclusion of the electroweak penguin operators implies the inclusion of QED effects. Consequently the coefficients of the operators $Q_1 - Q_6$ given in this section will differ slightly from the ones presented in the previous sections.

In section VIII the effective hamiltonian for $K_L \rightarrow \pi^0 e^+ e^-$ will be presented. It is given in (VIII.1). This hamiltonian can be considered as a generalization of the $S = 1$ hamiltonian (VI.1) presented in section VI to include the semi-leptonic operators Q_{7V} and Q_{7A} . This generalization does not modify the numerical values of the $S = 1$ coefficients C_i ($i = 1, \dots, 6$) given in section VI.

In section IX we will discuss the effective hamiltonian for $B \rightarrow X_S$. It is written down in (IX.1). This hamiltonian can be considered as a generalization of the $B = 1$ hamiltonian (VI.32) to include the magnetic penguin operators Q_7 and Q_{8G} . This generalization does not modify the numerical values of the $B = 1$ coefficients C_i ($i = 1, \dots, 6$) from section VI.

In section X we present the effective hamiltonian for $B \rightarrow X_s e^+ e^-$. It is to be found in (X.1) and can be considered as the generalization of the $B \rightarrow X_s$ hamiltonian to include the semi-leptonic operators Q_{9V} and Q_{10A} . The coefficients C_i ($i = 1; \dots; 6; 7; 8G$) given in section IX are not affected by this generalization.

In section XI the effective hamiltonians for $K^+ \rightarrow \pi^+ \pi^0$, $K_L \rightarrow \pi^+ \pi^-$, $K_L \rightarrow \pi^0 \pi^0$ ($B \rightarrow X_{s\pi^0}$) and $B \rightarrow 1^+ 1^-$ will be discussed. They are given in (XI.4), (XI.44), (XI.56) and (XI.57) respectively. Each of these hamiltonians involves only a single operator: Q_1 or Q_2 for $K^+ \rightarrow \pi^+ \pi^0$ ($K_L \rightarrow \pi^0 \pi^0$) and $K_L \rightarrow \pi^+ \pi^-$ with analogous operators for $B \rightarrow X_{s\pi^0}$ and $B \rightarrow 1^+ 1^-$.

Finally, sections XII and XIII present the effective hamiltonians for $S = 2$ and $B = 2$ transitions, respectively. These hamiltonians involve the operators Q_1 ($S = 2$) and Q_2 ($B = 2$) and can be found in (XII.1) and (XIII.1).

In table III we give the list of effective hamiltonians to be presented below, the equations in which they can be found and the list of operators entering different hamiltonians.

TABLE III. Compilation of various processes, equation no. of the corresponding effective hamiltonians and contributing operators.

Process	Cf. Equation	Contributing Operators
$F = 1, F = B; C; S$ current-current	(V.4)–(V.6)	$Q_1; Q_2$
$F = 1$ pure QCD	(VI.1), (VI.32)	$Q_1; \dots; Q_6$
$F = 1$ QCD and electroweak	(VII.1), (VII.37)	$Q_1; \dots; Q_{10}$
$K_L \rightarrow \pi^0 e^+ e^-$	(VIII.1)	$Q_1; \dots; Q_6; Q_{7V}; Q_{7A}$
$B \rightarrow X_s$	(IX.1)	$Q_1; \dots; Q_6; Q_7; Q_{8G}$
$B \rightarrow X_s e^+ e^-$	(X.1)	$Q_1; \dots; Q_6; Q_7; Q_{8G}; Q_{9V}; Q_{10A}$
$K^+ \rightarrow \pi^+ \pi^0$, $(K_L \rightarrow \pi^+ \pi^-)_{SD}$, $K_L \rightarrow \pi^0 \pi^0$, $B \rightarrow X_{s\pi^0}$, $B \rightarrow 1^+ 1^-$	(XI.4), (XI.44), (XI.56) (XI.57)	Q_1 ; Q_2
$K^0 - \bar{K}^0$ mixing	(XII.1)	Q_1 ($S = 2$)
$B^0 - \bar{B}^0$ mixing	(XIII.1)	Q_2 ($B = 2$)

V. THE EFFECTIVE $F = 1$ HAMILTONIAN: CURRENT-CURRENT OPERATORS

A. Operators

We begin our compendium by presenting the parts of effective hamiltonians involving the current-current operators only. These operators will be generally denoted by Q_1 and Q_2 , although their flavour structure depends on the decay considered. To be specific we will consider

$$Q_1 = (\bar{b}_i c_j)_{V-A} (u_j d_i)_{V-A} \quad Q_2 = (\bar{b}_i c_i)_{V-A} (u_j d_j)_{V-A} \quad (V.1)$$

$$Q_1 = (\bar{s}_i c_j)_{V-A} (u_j d_i)_{V-A} \quad Q_2 = (\bar{s}_i c_i)_{V-A} (u_j d_j)_{V-A} \quad (V.2)$$

$$Q_1 = (\bar{s}_i u_j)_{V-A} (u_j d_i)_{V-A} \quad Q_2 = (\bar{s}_i u_i)_{V-A} (u_j d_j)_{V-A} \quad (V.3)$$

for $B = 1$, $C = 1$ and $S = 1$ decays respectively. Then the corresponding effective hamiltonians are given by

$$H_{\text{eff}} (B = 1) = \frac{G_F}{\sqrt{2}} V_{cb} V_{ud} [\mathbb{C}_1 () Q_1 + C_2 () Q_2] \quad (= O(m_b)) \quad (V.4)$$

$$H_{\text{eff}} (C = 1) = \frac{G_F}{\sqrt{2}} V_{cs} V_{ud} [\mathbb{C}_1 () Q_1 + C_2 () Q_2] \quad (= O(m_c)) \quad (V.5)$$

$$H_{\text{eff}} (S = 1) = \frac{G_F}{\sqrt{2}} V_{us} V_{ud} [\mathbb{C}_1 () Q_1 + C_2 () Q_2] \quad (= O(1 \text{ GeV})) \quad (V.6)$$

As we will see in subsequent sections these hamiltonians have to be generalized to include also penguin operators. This however will not change the Wilson coefficients $\mathbb{C}_1 ()$ and $C_2 ()$ except for small $O ()$ corrections in a complete analysis which includes also electroweak penguin operators. For this reason it is useful to present the results for $C_{1,2}$ separately as they can be used in a large class of decays.

When analyzing Q_1 and Q_2 in isolation, it is useful to work with the operators Q_{\pm} and their coefficients z_{\pm} defined by

$$Q_{\pm} = \frac{1}{2} (Q_2 \pm Q_1) \quad z_{\pm} = C_2 \pm C_1 : \quad (V.7)$$

Q_+ and Q_- do not mix under renormalization and the expression for $z_{\pm} ()$ is very simple.

B. Wilson Coefficients and RG Evolution

The initial conditions for z_{\pm} at $\mu = M_W$ are obtained using the matching procedure between the full (fig. 2 (a)–(c)) and effective (fig. 3 (a)–(c)) theory summarized in section III F 1. Given the initial conditions for z_{\pm} at scale $\mu = M_W$

$$Z(M_W) = 1 + \frac{s(M_W)}{4} B \quad (V.8)$$

and using the NLO RG evolution formula (III.99) for the case without mixing one finds for the Wilson coefficients of Q at some scale

$$Z(\mu) = \left(1 + \frac{s(\mu)}{4} J \right)^{\#} \left(\frac{s(M_W)}{s(\mu)} \right)^{\#_d} \left(1 + \frac{s(M_W)}{4} B \right)^{\#} J \quad (V.9)$$

with

$$J = \frac{d}{d_0} - 1 - \frac{(1)}{2 d_0} \quad d = \frac{(0)}{2 d_0}; \quad (V.10)$$

where the coefficients d_0 and d_1 of the QCD β -function are given in (III.16). Furthermore the LO and NLO expansion coefficients for the anomalous dimensions of Q in (V.10) and the coefficients B in (V.8) are given by

$$(0) = -12 \frac{N-1}{2N} \quad (V.11)$$

$$(1) = \frac{N-1}{2N} - 21 \frac{57}{N} - \frac{19}{3} N - \frac{4}{3} f - 2 d_0 \quad (V.12)$$

$$B = \frac{N-1}{2N} [11 + \dots] \quad (V.13)$$

with N being the number of colors. Here we have introduced the parameter f which conveniently distinguishes between various renormalization schemes

$$f = \begin{cases} 0 & \text{NDR} \\ 4 & \text{HV} \end{cases} \quad (V.14)$$

Thus, using $N = 3$ in the following, J in (V.10) can also be written as

$$J = (J)_{\text{NDR}} + \frac{3}{6} - 1 = (J)_{\text{NDR}} - \frac{(0)}{12} \quad (V.15)$$

Setting (1) , B and d_1 to zero gives the leading logarithmic approximation (Altarelli and Maiani, 1974), (Gaillard and Lee, 1974a).

The NLO calculations in the NDR scheme and in the HV scheme have been presented in (Buras and Weisz, 1990). In writing (V.12) we have incorporated the $2 J^{(1)}$ correction in the HV scheme resulting from the non-vanishing two-loop anomalous dimension of the weak current.

$$J^{(1)} = \begin{cases} 0 & \text{NDR} \\ \frac{N^2-1}{N} 2 d_0 & \text{HV} \end{cases} \quad (V.16)$$

The NLO corrections (1) in the dimensional reduction scheme (DRED) have been first considered in (Altarelli *et al.*, 1981) and later confirmed in (Buras and Weisz, 1990). Here one has $f =$

6 N. This value for β in DRED incorporates also a finite renormalization of α_s in order to work in all schemes with the usual \overline{MS} coupling.

As already discussed in section III F 3, the expression $(B \rightarrow J)$ is scheme independent. The scheme dependence of the Wilson coefficients $z_i(\mu)$ originates then entirely from the scheme dependence of J at the lower end of the evolution which can be seen explicitly in (V.15).

In order to exhibit the μ dependence on the same footing as the scheme dependence, it is useful to rewrite (V.9) in the case of B-decays as follows:

$$z_i(\mu) = \left(1 + \frac{\alpha_s(\mu_b)}{4} J(\mu) \right)^{\beta_d} \left(\frac{\alpha_s(M_W)}{\alpha_s(\mu_b)} \right)^{\beta_d} \left(1 + \frac{\alpha_s(M_W)}{4} (B \rightarrow J) \right)^{\beta_d} \quad (V.17)$$

with

$$J(\mu) = (J)_{NDR} - \frac{(0)}{12} + \frac{(0)}{2} \ln\left(\frac{\mu^2}{m_b^2}\right) \quad (V.18)$$

summarizing both the renormalization scheme dependence and the μ -dependence. Note that in the first parenthesis in (V.17) we have set $\alpha_s(\mu) = \alpha_s(\mu_b)$ as the difference in the scales in this correction is still of higher order. We also note that a change of the renormalization scheme can be compensated by a change in β . From (V.18) we find generally

$$z_i = (z_i)_{NDR} \exp^{\beta_d} \frac{(i)}{12} \quad (V.19)$$

where i denotes a given scheme. From (V.14) we then have

$$(H \rightarrow V) = (H \rightarrow V)_{NDR} \exp \frac{1}{3} \quad (V.20)$$

Evidently the change in β relating HV and NDR¹ is the same for z_+ and z_- and consequently for $C_i(\mu)$.

This discussion shows that a meaningful analysis of the μ dependence of $C_i(\mu)$ can only be made simultaneously with the analysis of the scheme dependence.

The coefficients $C_i(\mu)$ for B-decays can now be calculated using

$$C_1(\mu) = \frac{z_+(\mu) - z_-(\mu)}{2} \quad C_2(\mu) = \frac{z_+(\mu) + z_-(\mu)}{2} \quad (V.21)$$

To this end we set $\mu = 5$ in the formulae above and use the two-loop $\alpha_s(\mu)$ of eq. (III.19) with $\frac{(5)}{\overline{MS}}$. The actual numerical values used for $\alpha_s(M_Z)$ or equivalently $\frac{(5)}{\overline{MS}}$ are collected in appendix A together with other numerical input parameters.

In the case of D-decays and K-decays the relevant scales are $\mu = O(m_c)$ and $\mu = O(1 \text{ GeV})$, respectively. In order to calculate $C_i(\mu)$ for these cases one has to evolve these coefficients first

¹The relation $(\beta_d)_{DRED} = (\beta_d)_{NDR} \exp \frac{2-1}{4}$ between NDR and DRED is more involved. In any case $(\beta_d)_{HV}$ and $(\beta_d)_{DRED}$ are larger than $(\beta_d)_{NDR}$.

from $\mu = O(m_b)$ further down to $\mu = O(m_c)$ in an effective theory with $f = 4$. Matching $\frac{(5)}{s}(m_b) = \frac{(4)}{s}(m_b)$ we find to a very good approximation $\frac{(4)}{M_S} = (325 \pm 110) \text{ MeV}$. Unfortunately, the necessity to evolve $C_1(\mu)$ from $\mu = M_W$ down to $\mu = m_c$ in two different effective theories ($f = 5$ and $f = 4$) and eventually in the case of K-decays with $f = 3$ for $\mu < m_c$ makes the formulae for $C_1(\mu)$ in D-decays and K-decays rather complicated. They can be found in (Buras *et al.*, 1993b). Fortunately all these complications can be avoided by a simple trick, which reproduces the results of (Buras *et al.*, 1993b) to better than 1.5%. In order to find $C_1(\mu)$ for $1 \text{ GeV} < \mu < 2 \text{ GeV}$ one can simply use the master formulae given above with $\frac{(5)}{M_S}$ replaced by $\frac{(4)}{M_S}$ and an “effective” number of active flavours $f = 4.15$. The latter effective value for f allows to obtain a very good agreement with (Buras *et al.*, 1993b). This can be verified by comparing the results presented here with those in tables X and XII where no “tricks” have been used. The nice feature of this method is that the μ and renormalization scheme dependences of $C_1(\mu)$ can still be studied in simple terms.

The numerical coefficients $C_1(\mu)$ for B-decays are shown in tables IV and V for different μ and $\frac{(5)}{M_S}$. In addition to the results for the NDR and HV renormalization schemes we show the LO values². The corresponding results for K-decays and D-decays are given in tables VI and VII.

TABLE IV. The coefficient $C_1(\mu)$ for B-decays.

[GeV]	$\frac{(5)}{M_S} = 140 \text{ MeV}$			$\frac{(5)}{M_S} = 225 \text{ MeV}$			$\frac{(5)}{M_S} = 310 \text{ MeV}$		
	LO	NDR	HV	LO	NDR	HV	LO	NDR	HV
4.0	-0.274	-0.175	-0.211	-0.310	-0.197	-0.239	-0.341	-0.216	-0.264
5.0	-0.244	-0.151	-0.184	-0.274	-0.169	-0.208	-0.300	-0.185	-0.228
6.0	-0.221	-0.133	-0.164	-0.248	-0.148	-0.184	-0.269	-0.161	-0.201
7.0	-0.203	-0.118	-0.148	-0.226	-0.132	-0.166	-0.246	-0.143	-0.181
8.0	-0.188	-0.106	-0.135	-0.209	-0.118	-0.151	-0.226	-0.128	-0.164

TABLE V. The coefficient $C_2(\mu)$ for B-decays.

[GeV]	$\frac{(5)}{M_S} = 140 \text{ MeV}$			$\frac{(5)}{M_S} = 225 \text{ MeV}$			$\frac{(5)}{M_S} = 310 \text{ MeV}$		
	LO	NDR	HV	LO	NDR	HV	LO	NDR	HV
4.0	1.121	1.074	1.092	1.141	1.086	1.107	1.158	1.096	1.120
5.0	1.105	1.062	1.078	1.121	1.072	1.090	1.135	1.080	1.101
6.0	1.093	1.054	1.069	1.107	1.062	1.079	1.118	1.068	1.087
7.0	1.084	1.047	1.061	1.096	1.054	1.069	1.106	1.059	1.077
8.0	1.077	1.042	1.055	1.087	1.047	1.062	1.096	1.052	1.069

²The results for the DRED scheme can be found in (Buras, 1995).

From tables IV–IX we observe:

The scheme dependence of the Wilson coefficients is sizable. This is in particular the case of C_1 which vanishes in the absence of QCD corrections.

The differences between LO and NLO results in the case of $\overline{\text{MS}}$ are large showing the importance of next-to-leading corrections. In fact in the NDR scheme the corrections may be as large as 70%. This comparison of LO and NLO coefficients can however be questioned because for the chosen values of $\frac{(4)}{\overline{\text{MS}}}(\mu_Z) = 0.135 - 0.009$ to be compared with $\frac{(4)}{\overline{\text{MS}}}(\mu_Z) = 0.117 - 0.007$ (Bethke, 1994), (Webber, 1994). Consequently the difference in LO and NLO results for C_1 originates partly in the change in the value of the QCD coupling.

In view of the latter fact it is instructive to show also the LO results in which the next-to-leading expression for α_s is used. We give some examples in tables VIII and IX. Now the differences between LO and NLO results is considerably smaller although still as large as 30–40% in the case of C_1 and the NDR scheme.

In any case the inclusion of NLO corrections in NDR and HV schemes weakens the impact of QCD on the Wilson coefficients of current–current operators. It is however important to keep in mind that such a behavior is specific to the scheme chosen and will in general be different in other schemes, reflecting the unphysical nature of the Wilson coefficient functions.

TABLE VI. The coefficient $C_1(\mu)$ for K-decays and D-decays.

$[\mu \text{ eV}]$	$\frac{(4)}{\overline{\text{MS}}} = 215 \text{ MeV}$			$\frac{(4)}{\overline{\text{MS}}} = 325 \text{ MeV}$			$\frac{(4)}{\overline{\text{MS}}} = 435 \text{ MeV}$		
	LO	NDR	HV	LO	NDR	HV	LO	NDR	HV
1.00	−0.602	−0.410	−0.491	−0.742	−0.510	−0.631	−0.899	−0.632	−0.825
1.25	−0.529	−0.356	−0.424	−0.636	−0.430	−0.523	−0.747	−0.512	−0.642
1.50	−0.478	−0.319	−0.379	−0.565	−0.378	−0.457	−0.653	−0.439	−0.543
1.75	−0.439	−0.291	−0.346	−0.514	−0.340	−0.410	−0.587	−0.390	−0.478
2.00	−0.409	−0.269	−0.320	−0.475	−0.311	−0.375	−0.537	−0.353	−0.431

We have made the whole discussion without invoking HQET (cf. section XV). It is sometimes stated in the literature that at $\mu = m_b$ in the case of B-decays one *has to* switch to HQET. In this case for $\mu < m_b$ the anomalous dimensions differ from those given above. We should however stress that switching to HQET can be done at any $\mu < m_b$ provided the logarithms $\ln(\mu/m_b)$ in \mathcal{H}_{ij} do not become too large. Similar comments apply to D-decays with respect to $\mu = m_c$. Of course the coefficients C_i calculated in HQET for $\mu < m_b$ are different from the coefficients presented here. However the corresponding matrix elements \mathcal{H}_{ij} in HQET are also different so that the physical amplitudes remain unchanged.

TABLE VII. The coefficient C_2 () for K-decays and D-decays.

[GeV]	$\frac{(4)}{M_S} = 215 \text{ M eV}$			$\frac{(4)}{M_S} = 325 \text{ M eV}$			$\frac{(4)}{M_S} = 435 \text{ M eV}$		
	LO	NDR	HV	LO	NDR	HV	LO	NDR	HV
1.00	1.323	1.208	1.259	1.422	1.275	1.358	1.539	1.363	1.506
1.25	1.274	1.174	1.216	1.346	1.221	1.282	1.426	1.277	1.367
1.50	1.241	1.152	1.187	1.298	1.188	1.237	1.358	1.228	1.296
1.75	1.216	1.136	1.167	1.264	1.165	1.207	1.313	1.196	1.252
2.00	1.198	1.123	1.152	1.239	1.148	1.185	1.279	1.174	1.221

 TABLE VIII. C_1^{LO} and C_2^{LO} for B-decays with s in NLO.

[GeV]	$\frac{(5)}{M_S} = 140 \text{ M eV}$		$\frac{(5)}{M_S} = 225 \text{ M eV}$		$\frac{(5)}{M_S} = 310 \text{ M eV}$	
	C_1	C_2	C_1	C_2	C_1	C_2
4.0	-0.244	1.105	-0.274	1.121	-0.301	1.135
5.0	-0.217	1.091	-0.243	1.105	-0.265	1.116
6.0	-0.197	1.082	-0.220	1.093	-0.239	1.102

 TABLE IX. C_1^{LO} and C_2^{LO} for K and D-decays with s in NLO.

[GeV]	$\frac{(4)}{M_S} = 215 \text{ M eV}$		$\frac{(4)}{M_S} = 325 \text{ M eV}$		$\frac{(4)}{M_S} = 435 \text{ M eV}$	
	C_1	C_2	C_1	C_2	C_1	C_2
1.0	-0.524	1.271	-0.664	1.366	-0.851	1.502
1.5	-0.413	1.201	-0.493	1.250	-0.579	1.307
2.0	-0.354	1.165	-0.412	1.200	-0.469	1.235

VI. THE EFFECTIVE $F = 1$ HAMILTONIAN: INCLUSION OF QCD PENGUIN OPERATORS

In section V we have restricted ourselves to current-current operators when considering QCD corrections to the effective $F = 1$ ($F = B; C; S$) hamiltonian for weak decays.

As already mentioned in section III D 3 e.g. for the $S = 1$ case the special flavour structure of $Q_2 = (su)_{V-A} (ud)_{V-A}$ allows not only for QCD corrections of the current-current type as in fig. 3 (a)–(c) from which the by now well known second current-current operator Q_1 is created. For a complete treatment of QCD corrections all possible ways of attaching a gluon to the initial weak $F = 1$ transition operator Q_2 have to be taken into account. Therefore attaching gluons to Q_2 in the form of diagrams (d.1) and (d.2) in fig. 3, generates a completely new set of four-quark operators, the so-called QCD penguin operators, usually denoted as $Q_3; \dots; Q_6$ ³. This procedure is often referred to as inserting Q_2 into type-1 and type-2 penguin diagrams.

The $S = 1$ effective hamiltonian for $K \rightarrow \pi$ at scales $\mu < m_c$ then reads

$$H_{\text{eff}}(S = 1) = \frac{G_F}{2} V_{us} V_{ud}^* \sum_{i=1}^6 (z_i(\mu) + \gamma_i(\mu)) Q_i; \quad (\text{VI.1})$$

with

$$= \frac{V_{ts} V_{td}^*}{V_{us} V_{ud}^*}; \quad (\text{VI.2})$$

The set of four-quark operators $Q_i(\mu)$ and Wilson coefficients $z_i(\mu)$ and $\gamma_i(\mu)$ will be discussed one by one in the subsections below.

A. Operators

The basis of four-quark operators for the $S = 1$ effective hamiltonian in (VI.1) is given in explicit form by

$$\begin{aligned} Q_1 &= (s_i u_j)_{V-A} (u_j d_i)_{V-A}; \\ Q_2 &= (su)_{V-A} (ud)_{V-A}; \\ Q_3 &= (sd)_{V-A} (qq)_{V-A}; \\ Q_4 &= (s_i d_j)_{V-A} (q_j q_i)_{V-A}; \\ Q_5 &= (sd)_{V-A} (qq)_{V+A}; \\ Q_6 &= (s_i d_j)_{V-A} (q_j q_i)_{V+A}; \end{aligned} \quad (\text{VI.3})$$

³Obviously, whether or not it is possible to form a closed fermion loop as in a type-1 insertion or to connect the two currents to yield a continuous fermion line as required for a type-2 insertion strongly depends on the flavour structure of the operator considered. E.g. for Q_2 only the type-2 penguin diagram contributes. This feature can be exploited to obtain NLO anomalous dimension matrices in the NDR scheme without the necessity of calculating closed fermion loops with γ_5 (Buras *et al.*, 1993c), (Buras *et al.*, 1993a).

As already mentioned, this basis closes under QCD renormalization.

For $m_b < m_c$ the sums over active quark flavours in (VI.3) run over u, d and s . However, when $m_b > m_c$ is considered also $q = c$ has to be included. Moreover, in this case two additional current–current operators have to be taken into account

$$Q_1^c = (s_i c_j)_{V-A} (c_j d_i)_{V-A} ; \quad Q_2^c = (sc)_{V-A} (cd)_{V-A} ; \quad (VI.4)$$

and the effective hamiltonian takes the form

$$H_e(S=1) = \frac{G_F}{2} V_{us} V_{ud} \left(1 + \sum_{i=1}^6 z_i(\mu) \right) (Q_i - Q_i^c) + \sum_{i=1}^6 v_i(\mu) Q_i^{\#} \quad (VI.5)$$

B. Wilson Coefficients

For the Wilson coefficients $y_i(\mu)$ and $z_i(\mu)$ in eq. (VI.1) one has

$$y_i(\mu) = v_i(\mu) - z_i(\mu) ; \quad (VI.6)$$

The coefficients z_i and v_i are the components of the six dimensional column vectors $\mathbf{v}(\mu)$ and $\mathbf{z}(\mu)$. Their RG evolution is given by

$$\mathbf{v}(\mu) = U_3(\mu; m_c) M(m_c) U_4(m_c; m_b) M(m_b) U_5(m_b; M_W) \mathbf{C}(M_W) ; \quad (VI.7)$$

$$\mathbf{z}(\mu) = U_3(\mu; m_c) \mathbf{z}(m_c) ; \quad (VI.8)$$

Here $U_f(m_1; m_2)$ denotes the full NLO evolution matrix for f active flavours. $M(m_i)$ is the matching matrix at quark threshold m_i given in eq. (III.104). These two matrices will be discussed in more detail in subsections VIC and VID, respectively.

The initial values $\mathbf{C}(M_W)$ necessary for the RG evolution of $\mathbf{v}(\mu)$ in eq. (VI.7) can be found according to the procedure of matching the effective (fig. 3) onto the full theory (fig. 2) as summarized in section III F. For the NDR scheme one obtains (Buras *et al.*, 1992)

$$C_1(M_W) = \frac{11}{2} - \frac{s(M_W)}{4} ; \quad (VI.9)$$

$$C_2(M_W) = 1 - \frac{11}{6} - \frac{s(M_W)}{4} ; \quad (VI.10)$$

$$C_3(M_W) = -\frac{s(M_W)}{24} \mathbb{E}_0(\mathbf{x}_t) ; \quad (VI.11)$$

$$C_4(M_W) = -\frac{s(M_W)}{8} \mathbb{E}_0(\mathbf{x}_t) ; \quad (VI.12)$$

$$C_5(M_W) = -\frac{s(M_W)}{24} \mathbb{E}_0(\mathbf{x}_t) ; \quad (VI.13)$$

$$C_6(M_W) = -\frac{s(M_W)}{8} \mathbb{E}_0(\mathbf{x}_t) ; \quad (VI.14)$$

where

$$E_0(x) = \frac{2}{3} \ln x + \frac{x(18 - 11x - x^2)}{12(1-x)^3} + \frac{x^2(15 - 16x + 4x^2)}{6(1-x)^4} \ln x; \quad (\text{VI.15})$$

$$E_0(x_t) = E_0(x) - \frac{2}{3} \quad (\text{VI.16})$$

with

$$x_t = \frac{m_t^2}{M_W^2}; \quad (\text{VI.17})$$

Here $E_0(x)$ results from the evaluation of the gluon penguin diagrams.

The initial values $C(M_W)$ in the HV scheme can be found in (Buras *et al.*, 1992).

In order to calculate the initial conditions $z(m_c)$ for $z_i(\mu)$ in eq. (VI.8) one has to consider the difference $Q_2^u - Q_2^c$ of Q_2 -type current-current operators as can be seen explicitly in (VI.5). Due to the GIM mechanism the coefficients $z_i(\mu)$ of penguin operators Q_i , $i \notin 1;2$ are zero in 5- and 4-flavour theories. The evolution for scales $\mu > m_c$ involves then only the current-current operators $Q_i^u - Q_i^c$, $i = 1;2$, with initial conditions at scale $\mu = M_W$

$$z_1(M_W) = C_1(M_W); \quad z_2(M_W) = C_2(M_W); \quad (\text{VI.18})$$

$Q_{1,2}^u - Q_{1,2}^c$ and $Q_{1,2}^c$ do not mix with each other under renormalization. We then find

$$\begin{pmatrix} z_1(m_c) \\ z_2(m_c) \end{pmatrix} = U_4(m_c; m_b) M(m_b) U_5(m_b; M_W) \begin{pmatrix} z_1(M_W) \\ z_2(M_W) \end{pmatrix}; \quad (\text{VI.19})$$

where this time the evolution matrices $U_{4,5}$ contain only the 2×2 anomalous dimension submatrices describing the mixing between current-current operators. The matching matrix $M(m_b)$ is then also only the corresponding 2×2 submatrix of the full 6×6 matrix in (VI.27). For the particular case of (VI.19) it simplifies to a unit matrix. When the charm quark is integrated out the operators $Q_{1,2}^c$ disappear from the effective hamiltonian and the coefficients $z_i(\mu)$, $i \notin 1;2$ for penguin operators become non-zero. In order to calculate $z_i(m_c)$ for penguin operators a proper matching between effective 4- and 3-quark theories, that is between (VI.5) and (VI.1), has to be made. For the 3-quark theory one obtains in the NDR scheme (Buras *et al.*, 1993b)

$$z(m_c) = \begin{pmatrix} 0 \\ z_1(m_c) \\ z_2(m_c) \\ s=(24)F_s(m_c) \\ s=(8)F_s(m_c) \\ s=(24)F_s(m_c) \\ s=(8)F_s(m_c) \end{pmatrix} \begin{pmatrix} 1 \\ C \\ C \\ C \\ C \\ C \\ C \end{pmatrix}; \quad (\text{VI.20})$$

where

$$F_s(m_c) = \frac{2}{3} z_2(m_c) \quad (\text{VI.21})$$

In the HV scheme $z_{1,2}$ are modified and one has $F_s(m_c) = 0$ or $z_i(m_c) = 0$ for $i \notin 1;2$.

C. Renormalization Group Evolution and Anomalous Dimension Matrices

The general RG evolution matrix $U(\mu_1; \mu_2)$ from scale μ_2 down to $\mu_1 < \mu_2$ reads in pure QCD

$$U(\mu_1; \mu_2) = T_g \exp \int_{g(\mu_2)}^{g(\mu_1)} dg^0 \frac{T_s(g^0)}{(g^0)}; \quad (\text{VI.22})$$

with $T_s(g^2)$ being the full 6×6 QCD anomalous dimension matrix for $Q_1; \dots; Q_6$.

For the case at hand it can be expanded in terms of T_s as follows

$$T_s(g^2) = \frac{T_s^{(0)}}{4} + \frac{T_s^{(1)}}{(4)^2} + \dots \quad (\text{VI.23})$$

Explicit expressions for $T_s^{(0)}$ and $T_s^{(1)}$ will be given below.

Using eq. (VI.23) the general QCD evolution matrix $U(\mu_1; \mu_2)$ of eq. (VI.22) can be written as in (III.93) (Buras *et al.*, 1992).

$$U(\mu_1; \mu_2) = \left[1 + \frac{T_s(\mu_1)}{4} J \right] U^{(0)}(\mu_1; \mu_2) \left[1 - \frac{T_s(\mu_2)}{4} J \right]; \quad (\text{VI.24})$$

where $U^{(0)}(\mu_1; \mu_2)$ denotes the evolution matrix in the leading logarithmic approximation and J summarizes the next-to-leading correction to this evolution. Therefore, the full matrix $U(\mu_1; \mu_2)$ sums logarithms $(\mu_2/\mu_1)^n$ and $(\mu_2/\mu_1)^n$ with $n = \ln(\mu_2^2/\mu_1^2)$. Explicit expressions for $U^{(0)}(\mu_1; \mu_2)$ and J are given in eqs. (III.94)–(III.98).

The LO anomalous dimension matrix $T_s^{(0)}$ of eq. (VI.23) has the explicit form (Gaillard and Lee, 1974a), (Altarelli and Maiani, 1974), (Vainshtein *et al.*, 1977), (Gilman and Wise, 1979), (Guberina and Peccei, 1980)

$$T_s^{(0)} = \begin{pmatrix} 0 & \frac{6}{N} & 6 & 0 & 0 & 0 & 0 & 1 \\ 6 & \frac{6}{N} & \frac{2}{3N} & \frac{2}{3} & \frac{2}{3N} & \frac{2}{3} & & \\ 0 & 0 & \frac{22}{3N} & \frac{22}{3} & \frac{4}{3N} & \frac{4}{3} & & \\ 0 & 0 & 6 & \frac{2f}{3N} + \frac{6}{N} + \frac{2f}{3} & \frac{2f}{3N} & \frac{2f}{3} & & \\ 0 & 0 & 0 & 0 & \frac{6}{N} & 6 & & \\ 0 & 0 & \frac{2f}{3N} & \frac{2f}{3} & \frac{2f}{3N} & \frac{6(1+N^2)}{N} + \frac{2f}{3} & & \end{pmatrix} \quad (\text{VI.25})$$

The NLO anomalous dimension matrix $T_s^{(1)}$ of eq. (VI.23) reads in the NDR scheme (Buras *et al.*, 1992), (Ciuchini *et al.*, 1994a)

$$\begin{array}{c}
\begin{array}{c} 0 \\ \vdots \\ \text{A} \end{array}
\begin{array}{ccccccc}
\frac{21}{2} & \frac{2f}{9} & \frac{7}{2} + \frac{2f}{3} & \frac{79}{9} & \frac{7}{3} & \frac{65}{9} & \frac{7}{3} \\
\frac{7}{2} + \frac{2f}{3} & \frac{21}{2} & \frac{2f}{9} & \frac{202}{243} & \frac{1354}{81} & \frac{1192}{243} & \frac{904}{81} \\
0 & 0 & \frac{5911}{486} + \frac{71f}{9} & \frac{5983}{162} + \frac{f}{3} & \frac{2384}{243} & \frac{71f}{9} & \frac{1808}{81} + \frac{f}{3} \\
0 & 0 & \frac{379}{18} + \frac{56f}{243} & \frac{91}{6} + \frac{808f}{81} & \frac{130}{9} & \frac{502f}{243} & \frac{14}{3} + \frac{646f}{81} \\
0 & 0 & \frac{61f}{9} & \frac{11f}{3} & \frac{71}{3} + \frac{61f}{9} & & 99 + \frac{11f}{3} \\
0 & 0 & \frac{682f}{243} & \frac{106f}{81} & \frac{225}{2} + \frac{1676f}{243} & \frac{1343}{6} + \frac{1348f}{81} &
\end{array}
\begin{array}{c} \vdots \\ 1 \end{array}
\end{array}
\quad (VI.26)$$

In (VI.25) and (VI.26) f denotes the number of active quark flavours at a certain scale μ . The corresponding results for $\gamma_s^{(1)}$ in the HV scheme can either be obtained by direct calculation or by using the relation (III.126). They can be found in (Buras *et al.*, 1992), (Ciuchini *et al.*, 1994a) where also the N dependence of $\gamma_s^{(1)}$ is given.

D. Quark Threshold Matching Matrix

As discussed in section III F 1 in general a matching matrix $M_s(m)$ has to be included in the RG evolution at NLO when going from a f -flavour effective theory to a $(f-1)$ -flavour effective theory at quark threshold $\mu = m$ (Buras *et al.*, 1992), (Buras *et al.*, 1993b).

For the $S = 1$ decay $K \rightarrow \pi$ in pure QCD one has (Buras *et al.*, 1992)

$$M_s(m) = 1 + \frac{\gamma_s(m)}{4} r_s^T : \quad (VI.27)$$

At the quark thresholds $m = m_b$ and $m = m_c$ the matrix r_s reads

$$r_s^T = \frac{5}{9} P (0; 0; 0; 1; 0; 1) \quad (VI.28)$$

with

$$P^T = (0; 0; \frac{1}{3}; 1; \frac{1}{3}; 1) : \quad (VI.29)$$

E. Numerical Results for the $K \rightarrow \pi$ Wilson Coefficients in Pure QCD

Tables X–XII give the $S = 1$ Wilson coefficients for $Q_1; \dots; Q_6$ in pure QCD. We observe a visible scheme dependence for all NLO Wilson coefficients. Notably we find γ_6 to be smaller in the HV than in the NDR scheme. In addition all coefficients, especially z_1 and $y_3; \dots; y_6$, show a strong dependence on $\overline{m_s}$. Next, at NLO the absolute values for $z_{1,2}$ and y_i are suppressed relative to their LO results, except for y_5 in HV and $y_{4,6}$ in NDR for $\mu > m_c$. The latter behaviour is related to the effect of the matching matrix $M_s(m_c)$ absent for $\mu > m_c$.

TABLE X. $S = 1$ Wilson coefficients at $\mu = 1 \text{ GeV}$ for $m_t = 170 \text{ GeV}$. $y_1 = y_2 = 0$.

Scheme	$\frac{(4)}{M_S} = 215 \text{ MeV}$			$\frac{(4)}{M_S} = 325 \text{ MeV}$			$\frac{(4)}{M_S} = 435 \text{ MeV}$		
	LO	NDR	HV	LO	NDR	HV	LO	NDR	HV
z_1	-0.602	-0.407	-0.491	-0.743	-0.506	-0.636	-0.901	-0.622	-0.836
z_2	1.323	1.204	1.260	1.423	1.270	1.362	1.541	1.352	1.515
z_3	0.003	0.007	0.004	0.004	0.013	0.007	0.006	0.022	0.015
z_4	-0.008	-0.022	-0.010	-0.012	-0.034	-0.016	-0.016	-0.058	-0.029
z_5	0.003	0.006	0.003	0.004	0.007	0.004	0.005	0.009	0.005
z_6	-0.009	-0.021	-0.009	-0.013	-0.034	-0.014	-0.018	-0.058	-0.025
y_3	0.029	0.023	0.026	0.036	0.031	0.036	0.045	0.040	0.048
y_4	-0.051	-0.046	-0.048	-0.060	-0.056	-0.059	-0.069	-0.066	-0.072
y_5	0.012	0.004	0.013	0.013	-0.001	0.016	0.014	-0.013	0.020
y_6	-0.084	-0.076	-0.070	-0.111	-0.109	-0.096	-0.145	-0.166	-0.136

TABLE XI. $S = 1$ Wilson coefficients at $\mu = m_c = 1.3 \text{ GeV}$ for $m_t = 170 \text{ GeV}$ and $f = 3$ effective flavours. z_3, z_4, z_5, z_6 are numerically irrelevant relative to z_1, z_2 . $y_1 = y_2 = 0$.

Scheme	$\frac{(4)}{M_S} = 215 \text{ MeV}$			$\frac{(4)}{M_S} = 325 \text{ MeV}$			$\frac{(4)}{M_S} = 435 \text{ MeV}$		
	LO	NDR	HV	LO	NDR	HV	LO	NDR	HV
z_1	-0.518	-0.344	-0.411	-0.621	-0.412	-0.504	-0.727	-0.487	-0.614
z_2	1.266	1.166	1.207	1.336	1.208	1.269	1.411	1.258	1.346
y_3	0.026	0.021	0.024	0.032	0.027	0.031	0.039	0.035	0.040
y_4	-0.050	-0.046	-0.048	-0.059	-0.056	-0.058	-0.068	-0.067	-0.070
y_5	0.013	0.007	0.013	0.015	0.005	0.016	0.016	0.001	0.018
y_6	-0.075	-0.067	-0.062	-0.095	-0.088	-0.079	-0.118	-0.116	-0.102

For y_3, \dots, y_5 there is no visible m_t dependence in the range $m_t = (170 \pm 15) \text{ GeV}$. For z_3, z_4, z_5, z_6 there is a relative variation of $O(1.5\%)$ for in/decreasing m_t . Finally, a comment on the Wilson coefficients in the HV Scheme as presented here is appropriate. As we have mentioned in section VB, the two-loop anomalous dimensions of the weak current in the HV scheme does not vanish. This peculiar feature of the HV scheme is also felt in $\gamma_s^{(1)}$. The diagonal terms in $\gamma_s^{(1)}$ acquire additional universal large $O(N^2)$ terms $(44=3)N^2$ which are absent in the NDR scheme. These artificial terms can be removed by working with $\gamma_s^{(1)} - 2\gamma_J^{(1)}$ instead of $\gamma_s^{(1)}$. This procedure, adopted in this review and in (Buras *et al.*, 1993b), corresponds effectively to a finite renormalization of operators which changes the coefficient of $\gamma_s=4$ in $C_2^{HV}(\mu_W)$ from $13=2$ to $7=6$. The Rome group (Ciuchini *et al.*, 1994a) has chosen not to make this additional finite renormalization and consequently their coefficients in the HV scheme differ from the HV coefficients presented here by a universal factor. They can be found by using

$$C_{\text{Rome}}^{HV}(\mu) = 1 - \frac{\gamma_s^{(1)}}{4} 4C_F C^{HV}(\mu) \quad (\text{VI.30})$$

TABLE XII. $S = 1$ Wilson coefficients at $\mu = 2 \text{ GeV}$ for $m_t = 170 \text{ GeV}$. For $\mu > m_c$ the GIM mechanism gives $z_i = 0$, $i = 3, \dots, 6$. $y_1 = y_2 = 0$.

	$\frac{(4)}{M.S.} = 215 \text{ MeV}$			$\frac{(4)}{M.S.} = 325 \text{ MeV}$			$\frac{(4)}{M.S.} = 435 \text{ MeV}$		
Scheme	LO	NDR	HV	LO	NDR	HV	LO	NDR	HV
z_1	-0.411	-0.266	-0.318	-0.477	-0.309	-0.374	-0.541	-0.350	-0.430
z_2	1.199	1.121	1.151	1.240	1.145	1.185	1.282	1.170	1.220
y_3	0.019	0.019	0.018	0.023	0.023	0.022	0.027	0.027	0.026
y_4	-0.040	-0.046	-0.039	-0.046	-0.054	-0.045	-0.052	-0.062	-0.052
y_5	0.011	0.010	0.011	0.012	0.010	0.013	0.013	0.010	0.015
y_6	-0.055	-0.057	-0.047	-0.067	-0.070	-0.056	-0.078	-0.085	-0.067

Clearly this difference is compensated by the corresponding difference in the hadronic matrix elements of the operators Q_i .

F. The $B = 1$ Effective Hamiltonian in Pure QCD

An important application of the formalism developed in the previous subsections is for the case of B -meson decays. The LO calculation can be found e.g. in (Ponce, 1981), (Grinstein, 1989) where the importance of NLO calculations has already been pointed out. This section can be viewed as the generalization of Grinstein's analysis beyond the LO approximation. We will focus on the $B = 1$, $C = 0$ part of the effective hamiltonian which is of particular interest for the study of CP violation in decays to CP self-conjugate final states. The part of the hamiltonian inducing $B = 1$, $C = 1$ transitions involves no penguin operators and has already been discussed in V.

At tree-level the effective hamiltonian of interest here is simply given by

$$H_e (B = 1) = \frac{G_F}{2} \sum_{q=u,c} \sum_{q^0=d,s} V_{qb} V_{qq^0}^* \bar{q} q \sum_V (q q^0)_V : \quad (\text{VI.31})$$

The cases $q^0 = d$ and $q^0 = s$ can be treated separately and have the same Wilson coefficients $C_i(\mu)$. Therefore we will restrict the discussion to $q^0 = d$ in the following.

Using unitarity of the CKM matrix, $\sum_u + \sum_c + \sum_t = 0$ with $\sum_i = V_{ib} V_{id}^*$, and the fact that $Q_{1,2}^u$ and $Q_{1,2}^c$ have the same initial conditions at $\mu = M_W$ one obtains for the effective $B = 1$ hamiltonian at scales $\mu = O(m_b)$

$$H_e (B = 1) = \frac{G_F}{2} f_c [C_1(\mu) Q_1^c(\mu) + C_2(\mu) Q_2^c(\mu)] + \sum_u [C_1(\mu) Q_1^u(\mu) + C_2(\mu) Q_2^u(\mu)] + \sum_{i=3}^6 C_i(\mu) Q_i(\mu) : \quad (\text{VI.32})$$

Here

$$\begin{aligned}
Q_1^q &= b_i q_j \gamma_{V-A} (q_j d_i)_{V-A} ; \\
Q_2^q &= b_i q_j \gamma_{V-A} (q d)_{V-A} ; \\
Q_3 &= b_i d_j \gamma_{V-A}^q (q q)_{V-A} ; \\
Q_4 &= b_i d_j \gamma_{V-A}^q (q_j q_i)_{V-A} ; \\
Q_5 &= b_i d_j \gamma_{V-A}^q (q q)_{V+A} ; \\
Q_6 &= b_i d_j \gamma_{V-A}^q (q_j q_i)_{V+A} ;
\end{aligned} \tag{VI.33}$$

where the summation runs over $q = u; d; s; c; b$

The corresponding $B = 1$ Wilson coefficients at scale $\mu = O(m_b)$ are simply given by a truncated version of eq. (VI.7)

$$C(m_b) = U_5(m_b; M_W) C(M_W) : \tag{VI.34}$$

Here U_5 is the 6×6 RG evolution matrix of eq. (VI.24) for $f = 5$ active flavours. The initial conditions $C(M_W)$ are identical to those of (VI.9)–(VI.14) for the $S = 1$ case.

G. Numerical Results for the $B = 1$ Wilson Coefficients in Pure QCD

TABLE XIII. $B = 1$ Wilson coefficients at $\mu = \overline{m}_b(m_b) = 4.40 \text{ GeV}$ for $m_t = 170 \text{ GeV}$.

Scheme	$\overline{m}_S^{(5)} = 140 \text{ MeV}$			$\overline{m}_S^{(5)} = 225 \text{ MeV}$			$\overline{m}_S^{(5)} = 310 \text{ MeV}$		
	LO	NDR	HV	LO	NDR	HV	LO	NDR	HV
C_1	-0.272	-0.164	-0.201	-0.307	-0.184	-0.227	-0.337	-0.202	-0.250
C_2	1.120	1.068	1.087	1.139	1.078	1.101	1.155	1.087	1.113
C_3	0.012	0.012	0.011	0.013	0.013	0.012	0.015	0.015	0.014
C_4	-0.026	-0.031	-0.026	-0.030	-0.035	-0.029	-0.032	-0.038	-0.032
C_5	0.008	0.008	0.008	0.009	0.009	0.009	0.009	0.009	0.010
C_6	-0.033	-0.035	-0.029	-0.038	-0.041	-0.033	-0.042	-0.046	-0.036

Table XIII lists the $B = 1$ Wilson coefficients for $Q_1^{u,c}; Q_2^{u,c}; Q_3; \dots; Q_6$ in pure QCD. C_1, C_4 and C_6 show a $O(20\%)$ scheme dependence while this dependence is much weaker for the rest of the coefficients.

Similarly to the $S = 1$ case the numerical values for $B = 1$ Wilson coefficients are sensitive to the value of \overline{m}_S used to determine α_s for the RG evolution. The sensitivity is however less pronounced than in the $S = 1$ case due to the higher value $\mu = \overline{m}_b(m_b)$ of the renormalization scale.

Finally, one finds no visible m_t dependence in the range $m_t = (170 \pm 15) \text{ GeV}$.

VII. THE EFFECTIVE $S = 1$ HAMILTONIAN: INCLUSION OF ELECTROWEAK PENGUIN OPERATORS

Similarly to the creation of the penguin operators $Q_3; \dots; Q_6$ through QCD corrections the inclusion of electroweak corrections, shown in figs. 2 (d) and (e), generates a set of new operators, the so-called electroweak penguin operators. For the $S = 1$ decay $K \rightarrow \pi \pi$ they are usually denoted by $Q_7; \dots; Q_{10}$.

This means that although now we will have to deal with technically more involved issues like an extended operator basis or the possibility of mixed QCD-QED contributions the underlying principles in performing the RG evolution will closely resemble those used in section VI for pure QCD. Obviously, the fundamental step has already been made when going from current-current operators only in section V, to the inclusion of QCD penguins in section VI. Hence, in this section we will wherever possible only point out the differences between the pure 6×6 QCD and the combined 10×10 QCD-QED case.

The full $S = 1$ effective hamiltonian for $K \rightarrow \pi \pi$ at scales $\mu < m_c$ reads including QCD and QED corrections⁴

$$H_{\text{eff}}(S = 1) = \frac{G_F}{2} V_{us} V_{ud}^* \sum_{i=1}^X (z_i(\mu) + y_i(\mu)) Q_i(\mu); \quad (\text{VII.1})$$

with $\sum_{i=1}^X V_{ts} V_{td}^* = (V_{us} V_{ud}^*)$.

A. Operators

The basis of four-quark operators for the $S = 1$ effective hamiltonian in (VII.1) is given by $Q_1; \dots; Q_6$ of (VI.3) and the electroweak penguin operators

$$\begin{aligned} Q_7 &= \frac{3}{2} (sd)_{V-A} \sum_q e_q (qq)_{V+A}; \\ Q_8 &= \frac{3}{2} (s_i d_j)_{V-A} \sum_q e_q (q_j q_i)_{V+A}; \\ Q_9 &= \frac{3}{2} (sd)_{V-A} \sum_q e_q (qq)_{V-A}; \\ Q_{10} &= \frac{3}{2} (s_i d_j)_{V-A} \sum_q e_q (q_j q_i)_{V-A}; \end{aligned} \quad (\text{VII.2})$$

Here, e_q denotes the quark electric charge reflecting the electroweak origin of $Q_7; \dots; Q_{10}$. The basis $Q_1; \dots; Q_{10}$ closes under QCD and QED renormalization. Finally, for $m_b > \mu > m_c$ the operators Q_1^c and Q_2^c of eq. (VI.4) have to be included again similarly to the case of pure QCD.

⁴In principle also operators $Q_{11} = \frac{g_s}{16\pi^2} m_s \bar{s} \gamma^\mu T^a G_a (1 - \gamma_5) d$ and $Q_{12} = \frac{ee_d}{16\pi^2} m_s \bar{s} \gamma^\mu F (1 - \gamma_5) d$ should be considered for $K \rightarrow \pi \pi$. However, as shown in (Bertolini *et al.*, 1995a) their numerical contribution is negligible. Therefore Q_{11} and Q_{12} will not be included here for $K \rightarrow \pi \pi$.

B. Wilson Coefficients

As far as formulae for Wilson coefficients are concerned the generalization of section VI B to the present case is to a large extent straightforward.

First, due to the extended operator basis $\mathbf{v}(\)$ and $\mathbf{z}(\)$ in eqs. (VI.7) and (VI.8) are now ten dimensional column vectors. Furthermore, the substitution

$$U_f(m_1; m_2) \rightarrow U_f(m_1; m_2; \)$$

has to be made in the RG evolution equations (VI.7), (VI.8) and (VI.19). Here $U_f(m_1; m_2; \)$ denotes the full 10×10 QCD- QED RG evolution matrix for f active flavours. $U_f(m_1; m_2; \)$ will still be discussed in more detail in subsection VII C.

The extended initial values $C(M_W)$ including now $O(\)$ corrections and additional entries for $Q_7; \dots; Q_{10}$ can be obtained from the usual matching procedure between figs. 2 and 3. They read in the NDR scheme (Buras *et al.*, 1993b)

$$C_1(M_W) = \frac{11}{2} \frac{s(M_W)}{4}; \quad (VII.3)$$

$$C_2(M_W) = 1 - \frac{11}{6} \frac{s(M_W)}{4} - \frac{35}{18} \frac{1}{4}; \quad (VII.4)$$

$$C_3(M_W) = -\frac{s(M_W)}{24} E_0(x_t) + \frac{1}{6 \sin^2 W} [2B_0(x_t) + C_0(x_t)]; \quad (VII.5)$$

$$C_4(M_W) = \frac{s(M_W)}{8} E_0(x_t); \quad (VII.6)$$

$$C_5(M_W) = -\frac{s(M_W)}{24} E_0(x_t); \quad (VII.7)$$

$$C_6(M_W) = -\frac{s(M_W)}{8h} E_0(x_t); \quad (VII.8)$$

$$C_7(M_W) = \frac{1}{6} [4C_0(x_t) + \tilde{B}_0(x_t)]; \quad (VII.9)$$

$$C_8(M_W) = 0; \quad (VII.10)$$

$$C_9(M_W) = \frac{1}{6} [4C_0(x_t) + \tilde{B}_0(x_t) + \frac{1}{\sin^2 W} (10B_0(x_t) - 4C_0(x_t))]; \quad (VII.11)$$

$$C_{10}(M_W) = 0; \quad (VII.12)$$

where

$$B_0(x) = \frac{1}{4} \left[\frac{x}{1-x} + \frac{x \ln x}{(x-1)^2} \right]; \quad (VII.13)$$

$$C_0(x) = \frac{x}{8} \left[\frac{x}{1-x} + \frac{3x+2}{(x-1)^2} \ln x \right]; \quad (VII.14)$$

$$D_0(x) = \frac{4}{9} \ln x + \frac{19x^3 + 25x^2}{36(x-1)^3} + \frac{x^2(5x^2 - 2x - 6)}{18(x-1)^4} \ln x; \quad (VII.15)$$

$$\tilde{B}_0(x_t) = D_0(x_t) - \frac{4}{9}; \quad (VII.16)$$

$\mathbb{E}_0(x_t)$ and x_t have already been defined in eqs. (VI.16) and (VI.17), respectively. Here $B_0(x)$ results from the evaluation of the box diagrams, $C_0(x)$ from the Z^0 -penguin, $D_0(x)$ from the photon penguin and $E_0(x)$ in $\mathbb{E}_0(x_t)$ from the gluon penguin diagrams.

The initial values $C(M_W)$ in the HV scheme can be found in (Buras *et al.*, 1993b).

Finally, the generalization of (VI.20) to the $Q_1; \dots; Q_{10}$ basis reads (Buras *et al.*, 1993b)

$$\mathbf{z}(m_c) = \begin{pmatrix} 0 & z_1(m_c) & 1 \\ \vdots & z_2(m_c) & \vdots \\ \vdots & s=(24)F_s(m_c) & \vdots \\ \vdots & s=(8)F_s(m_c) & \vdots \\ \vdots & s=(24)F_s(m_c) & \vdots \\ \vdots & s=(8)F_s(m_c) & \vdots \\ \vdots & = (6)F_e(m_c) & \vdots \\ \vdots & 0 & \vdots \\ \vdots & = (6)F_e(m_c) & \vdots \\ \vdots & 0 & \vdots \end{pmatrix}; \quad (\text{VII.17})$$

with $F_s(m_c)$ given by (VI.21) and

$$F_e(m_c) = \frac{4}{9} (3z_1(m_c) + z_2(m_c)) ; \quad (\text{VII.18})$$

In the HV scheme, in addition to $z_{1,2}$ differing from their NDR values, one has $F_s(m_c) = F_e(m_c) = 0$ and, consequently, $z_i(m_c) = 0$ for $i \notin \{1, 2\}$.

C. Renormalization Group Evolution and Anomalous Dimension Matrices

Besides an extended operator basis the main difference between the pure QCD case of section VI and the present case consists in the additional presence of QED contributions to the RG evolution. This will make the actual formulae for the RG evolution matrices more involved, however the underlying concepts developed in sections V and VI remain the same.

Similarly to (VI.22) for pure QCD the general RG evolution matrix $U(m_1; m_2;)$ from scale m_2 down to $m_1 < m_2$ can be written formally as⁵

$$U(m_1; m_2;) = T_g \exp \int_{g(m_2)}^{g(m_1)} dg^0 \frac{T(g^0;)}{(g^0)} ; \quad (\text{VII.19})$$

with $(g^2;)$ being now the full 10×10 anomalous dimension matrix including QCD and QED contributions.

For the case at hand $(g^2;)$ can be expanded in the following way

$$(g^2;) = s(g^2) + \frac{1}{4} (g^2) + \dots ; \quad (\text{VII.20})$$

⁵We neglect the running of the electromagnetic coupling, which is a very good approximation (Buchalla *et al.*, 1990).

with the pure s -expansion of $s(g^2)$ given in (VI.23). The term present due to QED corrections has the expansion

$$(g^2) = e^{(0)} + \frac{s}{4} s^{(1)} + \dots \quad (\text{VII.21})$$

Using (VII.20)–(VII.21) the general RG evolution matrix $U(m_1; m_2; s)$ of eq. (VII.19) may then be decomposed as follows

$$U(m_1; m_2; s) = U(m_1; m_2) + \frac{s}{4} R(m_1; m_2); \quad (\text{VII.22})$$

Here $U(m_1; m_2)$ represents the pure QCD evolution already encountered in section VI but now generalized to an extended operator basis. $R(m_1; m_2)$ describes the additional evolution in the presence of the electromagnetic interaction. $U(m_1; m_2)$ sums the logarithms $(s\tau)^n$ and $s(\tau)^n$ with $\tau = \ln(m_2^2/m_1^2)$, whereas $R(m_1; m_2)$ sums the logarithms $\tau(s\tau)^n$ and $(\tau)^n$.

The formula for $U(m_1; m_2)$ has already been given in (VI.24). The leading order formula for $R(m_1; m_2)$ can be found in (Buchalla *et al.*, 1990) except that there a different overall normalization (relative factor 4 in R) has been used. Here we give the general expression for $R(m_1; m_2)$ (Buras *et al.*, 1993b)

$$R(m_1; m_2) = \int_{g(m_2)}^{g(m_1)} dg^0 \frac{U(m_1; m^0)^T (g^0) U(m^0; m_2)}{(g^0)} \quad (\text{VII.23})$$

$$= \frac{2}{0} V K^{(0)}(m_1; m_2) + \frac{1}{4} \sum_{i=1}^3 K_i^{(1)}(m_1; m_2) V^{-1};$$

with $g^0 = g(m^0)$.

The matrix kernels in (VII.23) are defined by

$$(K^{(0)}(m_1; m_2))_{ij} = \frac{M_{ij}^{(0)}}{a_i a_j} \frac{s(m_2)}{s(m_1)} \frac{1}{s(m_1)} \frac{s(m_2)}{s(m_1)} \frac{1}{s(m_2)}; \quad (\text{VII.24})$$

$$K_1^{(1)}(m_1; m_2)_{ij} = \sum_{i \neq j}^8 \frac{M_{ij}^{(1)}}{a_i a_j} \frac{s(m_2)}{s(m_1)} \frac{s(m_2)}{s(m_1)} \frac{1}{s(m_1)} \frac{1}{s(m_2)}; \quad (\text{VII.25})$$

$$= \sum_{i=j}^8 \frac{M_{ii}^{(1)}}{a_i} \ln \frac{s(m_1)}{s(m_2)} \frac{1}{s(m_1)} \frac{1}{s(m_2)}$$

$$K_2^{(1)}(m_1; m_2) = s(m_2) K^{(0)}(m_1; m_2) H; \quad (\text{VII.26})$$

$$K_3^{(1)}(m_1; m_2) = s(m_1) H K^{(0)}(m_1; m_2) \quad (\text{VII.27})$$

with

$$M^{(0)} = V^{-1} e^{(0)T} V; \quad (\text{VII.28})$$

$$M^{(1)} = V^{-1} s^{(1)T} \frac{1}{0} e^{(0)T} + \sum_i \frac{1}{e^{(0)T}} J_i V;$$

The matrix H is defined in (III.97).

After this formal description we now give explicit expressions for the 10×10 LO and NLO anomalous dimension matrices $s^{(0)}$, $e^{(0)}$, $s^{(1)}$ and $s_\infty^{(1)}$. The values quoted for the NLO matrices are in the NDR scheme (Buras *et al.*, 1993c), (Buras *et al.*, 1993a), (Ciuchini *et al.*, 1994a). The corresponding results for $s^{(1)}$ and $s_\infty^{(1)}$ in the HV scheme can either be obtained by direct calculation or by using the QCD/QED version of eq. (III.126) given in (Buras *et al.*, 1993a). They can be found in (Buras *et al.*, 1993c), (Buras *et al.*, 1993a) and (Ciuchini *et al.*, 1993a), (Ciuchini *et al.*, 1994a).

The 6×6 submatrices for $Q_1; \dots; Q_6$ of the full LO and NLO 10×10 QCD matrices $s^{(0)}$ and $s^{(1)}$ are identical to the corresponding 6×6 matrices already given in eqs. (VI.25) and (VI.26), respectively. Next, $Q_1; \dots; Q_6$ do not mix to $Q_7; \dots; Q_{10}$ under QCD and hence

$$h_{s^{(0)}}^{ij} = h_{s^{(1)}}^{ij} = 0 \quad i = 1; \dots; 6 \quad j = 7; \dots; 10 : \quad (\text{VII.29})$$

The remaining entries for rows 7–10 in $s^{(0)}$ (Bijnens and Wise, 1984) and $s^{(1)}$ (Buras *et al.*, 1993c), (Ciuchini *et al.*, 1994a) are given in tables XIV and XV, respectively. There u and d ($f = u + d$) denote the number of active up- and down-type quark flavours.

TABLE XIV. Rows 7–10 of the LO anomalous dimension matrix $s^{(0)}$.

$(i; j)$	1	2	3	4	5	6	7	8	9	10
7	0	0	0	0	0	0	$\frac{6}{N}$	6	0	0
8	0	0	$\frac{2(u-d=2)}{3N}$	$\frac{2(u-d=2)}{3}$	$\frac{2(u-d=2)}{3N}$	$\frac{2(u-d=2)}{3}$	0	$\frac{6(1+N^2)}{N}$	0	0
9	0	0	$\frac{2}{3N}$	$\frac{2}{3}$	$\frac{2}{3N}$	$\frac{2}{3}$	0	0	$\frac{6}{N}$	6
10	0	0	$\frac{2(u-d=2)}{3N}$	$\frac{2(u-d=2)}{3}$	$\frac{2(u-d=2)}{3N}$	$\frac{2(u-d=2)}{3}$	0	0	6	$\frac{6}{N}$

TABLE XV. Rows 7–10 of the NLO anomalous dimension matrix $s^{(1)}$ for $N = 3$ and NDR.

$(i; j)$	1	2	3	4	5
7	0	0	$\frac{61(u-d=2)}{9}$	$\frac{11(u-d=2)}{3}$	$\frac{83(u-d=2)}{9}$
8	0	0	$\frac{682(u-d=2)}{243}$	$\frac{106(u-d=2)}{81}$	$\frac{704(u-d=2)}{243}$
9	0	0	$\frac{202}{243} + \frac{73(u-d=2)}{9}$	$\frac{1354}{81} + \frac{(u-d=2)}{3}$	$\frac{1192}{243} + \frac{71(u-d=2)}{9}$
10	0	0	$\frac{79}{9} + \frac{106(u-d=2)}{243}$	$\frac{7}{3} + \frac{826(u-d=2)}{81}$	$\frac{65}{9} + \frac{502(u-d=2)}{243}$

$(i; j)$	6	7	8	9	10
7	$\frac{11(u-d=2)}{3}$	$\frac{71}{3} + \frac{22f}{9}$	$99 + \frac{22f}{3}$	0	0
8	$\frac{736(u-d=2)}{81}$	$\frac{225}{2} + 4f$	$\frac{1343}{6} + \frac{68f}{9}$	0	0
9	$\frac{904}{81} + \frac{(u-d=2)}{3}$	0	0	$\frac{21}{2} + \frac{2f}{9}$	$\frac{7}{2} + \frac{2f}{3}$
10	$\frac{7}{3} + \frac{646(u-d=2)}{81}$	0	0	$\frac{7}{2} + \frac{2f}{3}$	$\frac{21}{2} + \frac{2f}{9}$

The full 10×10 matrices $e^{(0)}$ (Lusignoli, 1989) and $s_\infty^{(1)}$ (Buras *et al.*, 1993a), (Ciuchini *et al.*, 1994a) can be found in tables XVI and XVII, respectively.

TABLE XVI. The LO anomalous dimension matrix $\gamma_e^{(0)}$.

(i; j)	1	2	3	4	5	6	7	8	9	10
1	$\frac{8}{3}$	0	0	0	0	0	$\frac{16N}{27}$	0	$\frac{16N}{27}$	0
2	0	$\frac{8}{3}$	0	0	0	0	$\frac{16}{27}$	0	$\frac{16}{27}$	0
3	0	0	0	0	0	0	$\frac{16}{27} + \frac{16N(u-d=2)}{27}$	0	$\frac{88}{27} + \frac{16N(u-d=2)}{27}$	0
4	0	0	0	0	0	0	$\frac{16N}{27} + \frac{16(u-d=2)}{27}$	0	$\frac{16N}{27} + \frac{16(u-d=2)}{27}$	$\frac{8}{3}$
5	0	0	0	0	0	0	$\frac{8}{3} + \frac{16N(u-d=2)}{27}$	0	$\frac{16N(u-d=2)}{27}$	0
6	0	0	0	0	0	0	$\frac{16(u-d=2)}{27}$	$\frac{8}{3}$	$\frac{16(u-d=2)}{27}$	0
7	0	0	0	0	$\frac{4}{3}$	0	$\frac{4}{3} + \frac{16N(u+d=4)}{27}$	0	$\frac{16N(u+d=4)}{27}$	0
8	0	0	0	0	0	$\frac{4}{3}$	$\frac{16(u+d=4)}{27}$	$\frac{4}{3}$	$\frac{16(u+d=4)}{27}$	0
9	0	0	$\frac{4}{3}$	0	0	0	$\frac{8}{27} + \frac{16N(u+d=4)}{27}$	0	$\frac{28}{27} + \frac{16N(u+d=4)}{27}$	0
10	0	0	0	$\frac{4}{3}$	0	0	$\frac{8N}{27} + \frac{16(u+d=4)}{27}$	0	$\frac{8N}{27} + \frac{16(u+d=4)}{27}$	$\frac{4}{3}$

D. Quark Threshold Matching Matrix

Extending the matching matrix $M(m)$ of (VI.27) to the simultaneous presence of QCD and QED corrections yields

$$M(m) = 1 + \frac{s(m)}{4} r_s^T + \frac{e^2}{4} r_e^T : \quad (\text{VII.30})$$

At scale $\mu = m_b$ the matrices r_s and r_e read

$$r_s^T = \frac{5}{18} P(0;0;0; \quad 2;0; \quad 2;0;1;0;1) \quad (\text{VII.31})$$

$$r_e^T = \frac{10}{81} P(0;0;6;2;6;2; \quad 3; \quad 1; \quad 3; \quad 1) \quad (\text{VII.32})$$

and at $\mu = m_c$

$$r_s^T = \frac{5}{9} P(0;0;0;1;0;1;0;1;0;1) \quad (\text{VII.33})$$

$$r_e^T = \frac{40}{81} P(0;0;3;1;3;1;3;1;3;1) \quad (\text{VII.34})$$

with eq. (VI.29) generalized to

$$P^T = (0;0; \quad \frac{1}{3};1; \quad \frac{1}{3};1;0;0;0;0) ; \quad (\text{VII.35})$$

$$P^T = (0;0;0;0;0;0;1;0;1;0) : \quad (\text{VII.36})$$

TABLE XVII. The NLO anomalous dimension matrix $_{\overline{se}}^{(1)}$ for $N = 3$ and NDR.

(i; j)	1	2	3	4	5
1	$\frac{194}{9}$	$\frac{2}{3}$	$\frac{88}{243}$	$\frac{88}{81}$	$\frac{88}{243}$
2	$\frac{25}{3}$	$\frac{49}{9}$	$\frac{556}{729}$	$\frac{556}{243}$	$\frac{556}{729}$
3	0	0	$\frac{1690}{729} + \frac{136(u-d=2)}{243}$	$\frac{1690}{243} + \frac{136(u-d=2)}{81}$	$\frac{232}{729} + \frac{136(u-d=2)}{243}$
4	0	0	$\frac{641}{243} + \frac{388u}{729} + \frac{32d}{729}$	$\frac{655}{81} + \frac{388u}{243} + \frac{32d}{243}$	$\frac{88}{243} + \frac{388u}{729} + \frac{32d}{729}$
5	0	0	$\frac{136(u-d=2)}{243}$	$\frac{136(u-d=2)}{81}$	2 $\frac{136(u-d=2)}{243}$
6	0	0	$\frac{748u}{729} + \frac{212d}{729}$	$\frac{748u}{243} + \frac{212d}{243}$	3 $\frac{748u}{729} + \frac{212d}{729}$
7	0	0	$\frac{136(u+d=4)}{243}$	$\frac{136(u+d=4)}{81}$	$\frac{116}{9} + \frac{136(u+d=4)}{243}$
8	0	0	$\frac{748u}{729} + \frac{106d}{729}$	$\frac{748u}{243} + \frac{106d}{243}$	1 $\frac{748u}{729} + \frac{106d}{729}$
9	0	0	$\frac{7012}{729} + \frac{136(u+d=4)}{243}$	$\frac{764}{243} + \frac{136(u+d=4)}{81}$	$\frac{116}{729} + \frac{136(u+d=4)}{243}$
10	0	0	$\frac{1333}{243} + \frac{388u}{729} + \frac{16d}{729}$	$\frac{107}{81} + \frac{388u}{243} + \frac{16d}{243}$	$\frac{44}{243} + \frac{388u}{729} + \frac{16d}{729}$

(i; j)	6	7	8	9	10
1	$\frac{88}{81}$	$\frac{152}{27}$	$\frac{40}{9}$	$\frac{136}{27}$	$\frac{56}{9}$
2	$\frac{556}{243}$	$\frac{484}{729}$	$\frac{124}{27}$	$\frac{3148}{729}$	$\frac{172}{27}$
3	$\frac{232}{243} + \frac{136(u-d=2)}{81}$	$\frac{3136}{729} + \frac{104(u-d=2)}{27}$	$\frac{64}{27} + \frac{88(u-d=2)}{9}$	$\frac{20272}{729} + \frac{184(u-d=2)}{27}$	$\frac{112}{27} + \frac{8(u-d=2)}{9}$
4	$\frac{88}{81} + \frac{388u}{243} + \frac{32d}{243}$	$\frac{152}{27} + \frac{3140u}{729} + \frac{656d}{729}$	$\frac{40}{9} + \frac{100u}{27} + \frac{16d}{27}$	$\frac{170}{27} + \frac{908u}{729} + \frac{1232d}{729}$	$\frac{14}{3} + \frac{148u}{27} + \frac{80d}{27}$
5	6 + $\frac{136(u-d=2)}{81}$	$\frac{232}{9} + \frac{104(u-d=2)}{27}$	$\frac{40}{3} + \frac{88(u-d=2)}{9}$	$\frac{184(u-d=2)}{27}$	$\frac{8(u-d=2)}{9}$
6	7 + $\frac{748u}{243} + \frac{212d}{243}$	2 $\frac{5212u}{729} + \frac{4832d}{729}$	$\frac{182}{9} + \frac{188u}{27} + \frac{160d}{27}$	$\frac{2260u}{729} + \frac{2816d}{729}$	$\frac{140u}{27} + \frac{64d}{27}$
7	$\frac{20}{3} + \frac{136(u+d=4)}{81}$	$\frac{134}{9} + \frac{104(u+d=4)}{27}$	$\frac{38}{3} + \frac{88(u+d=4)}{9}$	$\frac{184(u+d=4)}{27}$	$\frac{8(u+d=4)}{9}$
8	$\frac{91}{9} + \frac{748u}{243} + \frac{106d}{243}$	2 $\frac{5212u}{729} + \frac{2416d}{729}$	$\frac{154}{9} + \frac{188u}{27} + \frac{80d}{27}$	$\frac{2260u}{729} + \frac{1408d}{729}$	$\frac{140u}{27} + \frac{32d}{27}$
9	$\frac{116}{243} + \frac{136(u+d=4)}{81}$	$\frac{1568}{729} + \frac{104(u+d=4)}{27}$	$\frac{32}{27} + \frac{88(u+d=4)}{9}$	$\frac{5578}{729} + \frac{184(u+d=4)}{27}$	$\frac{38}{27} + \frac{8(u+d=4)}{9}$
10	$\frac{44}{81} + \frac{388u}{243} + \frac{16d}{243}$	$\frac{76}{27} + \frac{3140u}{729} + \frac{328d}{729}$	$\frac{20}{9} + \frac{100u}{27} + \frac{8d}{27}$	$\frac{140}{27} + \frac{908u}{729} + \frac{616d}{729}$	$\frac{28}{9} + \frac{148u}{27} + \frac{40d}{27}$

E. Numerical Results for the \overline{MS} Wilson Coefficients

Tables XVIII–XX give the $S = 1$ Wilson coefficients for $Q_1; \dots; Q_{10}$ in the mixed case of QCD and QED.

The coefficients for the current-current and QCD penguin operators $Q_1; \dots; Q_6$ are only very weakly affected by the extension of the operator basis to the electroweak penguin operators $Q_7; \dots; Q_{10}$. Therefore the discussion for $Q_1; \dots; Q_6$ given in connection with tables X–XII for the case of pure QCD basically still holds and will not be repeated here.

For the remaining coefficients of $Q_7; \dots; Q_{10}$ one finds a moderate scheme dependence for y_7 , y_9 and y_{10} , but a $O(9\%)$ one for y_8 . The notable feature of y_6 being larger in NDR than in HV still holds, but is now confronted with an exactly opposite dependence for the other important $S = 1$ Wilson coefficient y_8 which is in addition enhanced over its LO value.

The particular dependence of y_6 and y_8 with respect to scheme, LO/NLO and m_t (see below) should be kept in mind for the later discussion of "Q=" in section XIX.

TABLE XVIII. $S = 1$ Wilson coefficients at $\mu = 1 \text{ GeV}$ for $m_t = 170 \text{ GeV}$. $y_1 = y_2 = 0$.

Scheme	$\frac{(4)}{M_S} = 215 \text{ MeV}$			$\frac{(4)}{M_S} = 325 \text{ MeV}$			$\frac{(4)}{M_S} = 435 \text{ MeV}$		
	LO	NDR	HV	LO	NDR	HV	LO	NDR	HV
z_1	-0.607	-0.409	-0.494	-0.748	-0.509	-0.640	-0.907	-0.625	-0.841
z_2	1.333	1.212	1.267	1.433	1.278	1.371	1.552	1.361	1.525
z_3	0.003	0.008	0.004	0.004	0.013	0.007	0.006	0.023	0.015
z_4	-0.008	-0.022	-0.010	-0.012	-0.035	-0.017	-0.017	-0.058	-0.029
z_5	0.003	0.006	0.003	0.004	0.008	0.004	0.005	0.009	0.005
z_6	-0.009	-0.022	-0.009	-0.013	-0.035	-0.014	-0.018	-0.059	-0.025
$z_7 =$	0.004	0.003	-0.003	0.008	0.011	-0.002	0.011	0.021	-0.001
$z_8 =$	0	0.008	0.006	0.001	0.014	0.010	0.001	0.027	0.017
$z_9 =$	0.005	0.007	0	0.008	0.018	0.005	0.012	0.034	0.011
$z_{10} =$	0	-0.005	-0.006	-0.001	-0.008	-0.010	-0.001	-0.014	-0.017
y_3	0.030	0.025	0.028	0.038	0.032	0.037	0.047	0.042	0.050
y_4	-0.052	-0.048	-0.050	-0.061	-0.058	-0.061	-0.071	-0.068	-0.074
y_5	0.012	0.005	0.013	0.013	-0.001	0.016	0.014	-0.013	0.021
y_6	-0.085	-0.078	-0.071	-0.113	-0.111	-0.097	-0.148	-0.169	-0.139
$y_7 =$	0.027	-0.033	-0.032	0.036	-0.032	-0.030	0.043	-0.031	-0.027
$y_8 =$	0.114	0.121	0.133	0.158	0.173	0.188	0.216	0.254	0.275
$y_9 =$	-1.491	-1.479	-1.480	-1.585	-1.576	-1.577	-1.700	-1.718	-1.722
$y_{10} =$	0.650	0.540	0.547	0.800	0.690	0.699	0.968	0.892	0.906

We also note that in the range of m_t considered here, y_7 is very small, y_9 is essentially unaffected by NLO QCD corrections and y_{10} is suppressed for m_c . It should also be stressed that y_9 and y_{10} are substantially larger than y_8 although, as we will see in the analysis of Q_8 , the operator Q_8 is more important than Q_9 and Q_{10} for this ratio.

Next, one infers from tables XVIII–XX that also in the mixed QCD/QED case the Wilson coefficients show a strong dependence on $\overline{M_S}$.

In contrast to the coefficients y_3, \dots, y_6 for QCD penguins, y_7, \dots, y_{10} for the electroweak penguins show a sizeable m_t dependence in the range $m_t = (170 \text{ -- } 15) \text{ GeV}$. With in/decreasing m_t there is a relative variation of $O(19\%)$ and $O(10\%)$ for the absolute values of y_7 and $y_{9,10}$, respectively. This is illustrated further in figs. 5 and 6 where the m_t dependence of these coefficients is shown explicitly. This strong m_t -dependence originates in the Z^0 -penguin diagrams. The m_t -dependence of y_9 and y_{10} can be conveniently parametrized by a linear function to an accuracy better than 0.5% . Details of this m_t -parametrization can be found in table XXI.

Finally, in tables XVIII–XX one observes again the usual feature of decreasing Wilson coefficients with increasing scale μ .

F. The $B = 1$ Effective Hamiltonian Including Electroweak Penguins

Finally we present in this section the Wilson coefficient functions of the $B = 1$, $C = 0$ hamiltonian, including the effects of electroweak penguin contributions (Buras *et al.*, 1993b).

TABLE XIX. $S = 1$ Wilson coefficients at $\mu = m_c = 1.3 \text{ GeV}$ for $m_t = 170 \text{ GeV}$ and $f = 3$ effective flavours. z_3, y_3, y_{10} are numerically irrelevant relative to $z_{1,2}, y_1 = y_2 = 0$.

	$\frac{(4)}{M_S} = 215 \text{ MeV}$			$\frac{(4)}{M_S} = 325 \text{ MeV}$			$\frac{(4)}{M_S} = 435 \text{ MeV}$		
Scheme	LO	NDR	HV	LO	NDR	HV	LO	NDR	HV
z_1	-0.521	-0.346	-0.413	-0.625	-0.415	-0.507	-0.732	-0.490	-0.617
z_2	1.275	1.172	1.214	1.345	1.216	1.276	1.420	1.265	1.354
y_3	0.027	0.023	0.025	0.034	0.029	0.033	0.041	0.036	0.042
y_4	-0.051	-0.048	-0.049	-0.061	-0.057	-0.060	-0.070	-0.068	-0.072
y_5	0.013	0.007	0.014	0.015	0.005	0.016	0.017	0.001	0.018
y_6	-0.076	-0.068	-0.063	-0.096	-0.089	-0.081	-0.120	-0.118	-0.103
$y_7 =$	0.030	-0.031	-0.031	0.039	-0.030	-0.028	0.048	-0.029	-0.026
$y_8 =$	0.092	0.103	0.112	0.121	0.136	0.145	0.155	0.179	0.189
$y_9 =$	-1.428	-1.423	-1.423	-1.490	-1.479	-1.479	-1.559	-1.548	-1.549
$y_{10} =$	0.558	0.451	0.457	0.668	0.547	0.553	0.781	0.656	0.664

TABLE XX. $S = 1$ Wilson coefficients at $\mu = 2 \text{ GeV}$ for $m_t = 170 \text{ GeV}$. For $\mu > m_c$ the GIM mechanism gives $z_i = 0, i = 3, \dots, 10, y_1 = y_2 = 0$.

	$\frac{(4)}{M_S} = 215 \text{ MeV}$			$\frac{(4)}{M_S} = 325 \text{ MeV}$			$\frac{(4)}{M_S} = 435 \text{ MeV}$		
Scheme	LO	NDR	HV	LO	NDR	HV	LO	NDR	HV
z_1	-0.413	-0.268	-0.320	-0.480	-0.310	-0.376	-0.544	-0.352	-0.432
z_2	1.206	1.127	1.157	1.248	1.151	1.191	1.290	1.176	1.227
y_3	0.021	0.020	0.019	0.025	0.024	0.023	0.028	0.028	0.027
y_4	-0.041	-0.046	-0.040	-0.047	-0.055	-0.046	-0.053	-0.063	-0.053
y_5	0.011	0.010	0.012	0.012	0.011	0.013	0.014	0.011	0.015
y_6	-0.056	-0.058	-0.047	-0.068	-0.071	-0.057	-0.079	-0.086	-0.068
$y_7 =$	0.031	-0.023	-0.020	0.037	-0.019	-0.020	0.042	-0.016	-0.019
$y_8 =$	0.068	0.076	0.084	0.084	0.094	0.102	0.101	0.113	0.121
$y_9 =$	-1.357	-1.361	-1.357	-1.393	-1.389	-1.389	-1.430	-1.419	-1.423
$y_{10} =$	0.442	0.356	0.360	0.513	0.414	0.419	0.581	0.472	0.477

These effects play a role in certain penguin-induced B meson decays as discussed in (Fleischer, 1994a), (Fleischer, 1994b), (Deshpande *et al.*, 1995), (Deshpande and He, 1995).

The generalization of the $B = 1, C = 0$ hamiltonian in pure QCD (VI.32) to incorporate also electroweak penguin operators is straightforward. One obtains

$$\begin{aligned}
 H_e (B = 1) = & \frac{G_F}{2} f_c [C_1 (Q_1^c) + C_2 (Q_2^c)] + \frac{G_F}{2} f_u [C_1 (Q_1^u) + C_2 (Q_2^u)] \\
 & + \sum_{i=3}^{10} C_i (Q_i) g :
 \end{aligned} \tag{VII.37}$$

TABLE XXI. Coefficients in linear m_t -parametrization $y_i = a + b$ ($m_t = 170 \text{ GeV}$) of Wilson coefficients y_9 and y_{10} at scale $\mu = m_c$ for $\frac{(4)}{M_S} = 325 \text{ MeV}$.

	$y_9 =$		$y_{10} =$	
	a	b	a	b
LO	0.189	-1.682	-0.111	0.780
NDR	0.129	-1.611	-0.128	0.676
HV	0.129	-1.611	-0.121	0.676

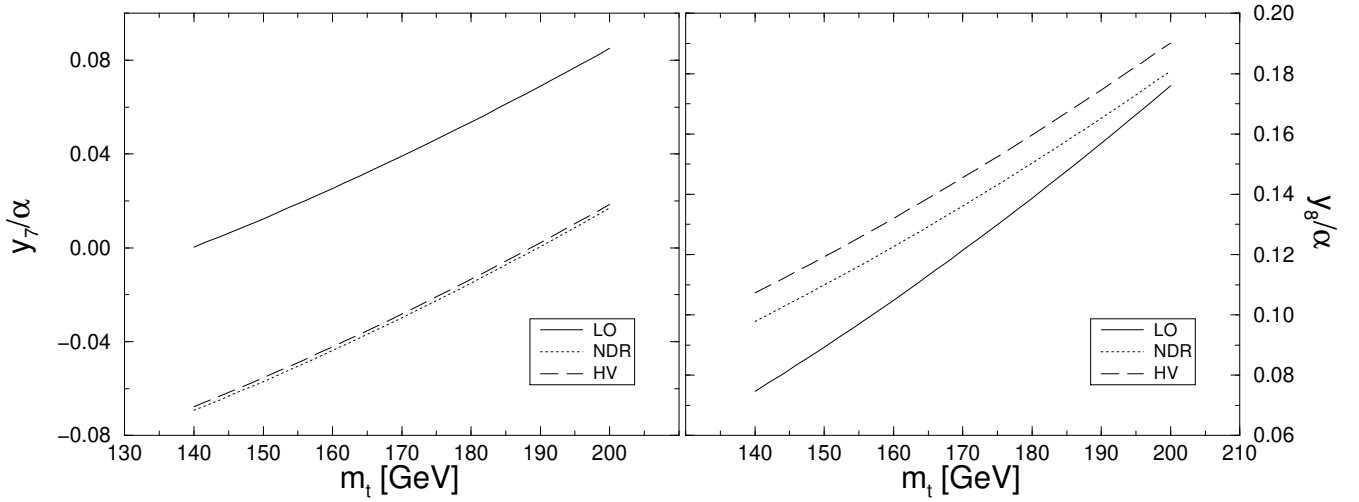


FIG. 5. Wilson coefficients $y_7(m_c)$ and $y_8(m_c)$ as functions of m_t for $\frac{(4)}{M_S} = 325 \text{ MeV}$.

where the operator basis now includes the electroweak penguin operators

$$\begin{aligned}
 Q_7 &= \frac{3}{2} b d_{V A}^X e_q (q q)_{V+A} ; \\
 Q_8 &= \frac{3}{2} b_i d_j^X e_q (q_j q_i)_{V+A} ; \\
 Q_9 &= \frac{3}{2} b d_{V A}^X e_q (q q)_{V A} ; \\
 Q_{10} &= \frac{3}{2} b_i d_j^X e_q (q_j q_i)_{V A}
 \end{aligned} \tag{VII.38}$$

in addition to (VI.33). The Wilson coefficients at $\mu = m_b$ read

$$C(m_b) = U_5(m_b; M_W;) C(M_W) : \tag{VII.39}$$

where U_5 is the 10×10 evolution matrix of (VII.22) for $f = 5$ flavors. The $C(M_W)$ are given in (VII.3) – (VII.12) in the NDR scheme.

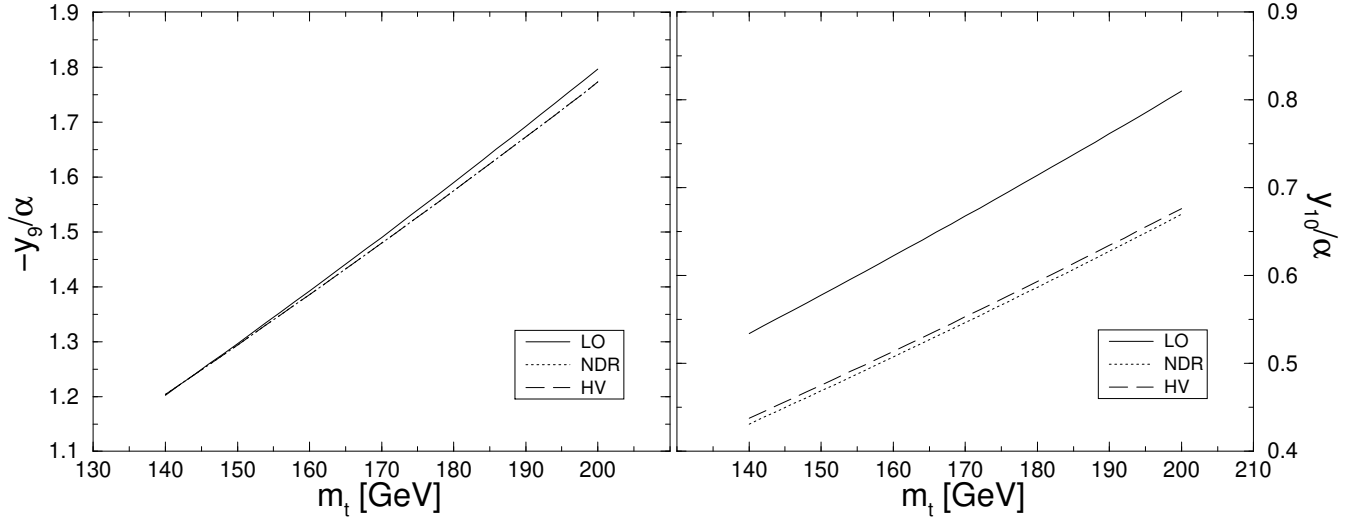


FIG. 6. Wilson coefficients $y_9(m_c)=$ and $y_{10}(m_c)=$ as a function of m_t for $\frac{(4)}{M_S} = 325 \text{ MeV}$.

G. Numerical Results for the $B = 1$ Wilson Coefficients

TABLE XXII. $B = 1$ Wilson coefficients at $\mu_b = m_b = 4.40 \text{ GeV}$ for $m_t = 170 \text{ GeV}$.

	$\frac{(5)}{M_S} = 140 \text{ MeV}$			$\frac{(5)}{M_S} = 225 \text{ MeV}$			$\frac{(5)}{M_S} = 310 \text{ MeV}$		
Scheme	LO	NDR	HV	LO	NDR	HV	LO	NDR	HV
C_1	-0.273	-0.165	-0.202	-0.308	-0.185	-0.228	-0.339	-0.203	-0.251
C_2	1.125	1.072	1.091	1.144	1.082	1.105	1.161	1.092	1.117
C_3	0.013	0.013	0.012	0.014	0.014	0.013	0.016	0.016	0.015
C_4	-0.027	-0.031	-0.026	-0.030	-0.035	-0.029	-0.033	-0.039	-0.033
C_5	0.008	0.008	0.008	0.009	0.009	0.009	0.009	0.009	0.010
C_6	-0.033	-0.036	-0.029	-0.038	-0.041	-0.033	-0.043	-0.046	-0.037
$C_7=$	0.042	-0.003	0.006	0.045	-0.002	0.005	0.047	-0.001	0.005
$C_8=$	0.041	0.047	0.052	0.048	0.054	0.060	0.054	0.061	0.067
$C_9=$	-1.264	-1.279	-1.269	-1.280	-1.292	-1.283	-1.294	-1.303	-1.296
$C_{10}=$	0.291	0.234	0.237	0.328	0.263	0.266	0.360	0.288	0.291

Table XXII lists the $B = 1$ Wilson coefficients for $Q_1^{uc}; Q_2^{uc}; Q_3; \dots; Q_{10}$ in the mixed case of QCD and QED.

Similarly to the $S = 1$ case the coefficients for the current-current and QCD penguin operators $Q_1; \dots; Q_6$ are only very weakly affected by the extension of the operator basis to the electroweak penguin operators $Q_7; \dots; Q_{10}$. Therefore the discussion of $C_1; \dots; C_6$ in connection with table XIII is also valid for the present case.

Here we therefore restrict our discussion to the coefficients $C_7; \dots; C_{10}$ of the operators $Q_7; \dots; Q_{10}$ in the extended basis.

The coefficients $C_7; \dots; C_{10}$ show a visible dependence on the scheme, $\overline{\text{MS}}$ and LO/NLO. However, this dependence is less pronounced for the coefficient C_9 than it is for $C_{7,8,10}$. This is noteworthy since in B-meson decays C_9 usually resides in the dominant electroweak penguin contribution (Fleischer, 1994a), (Fleischer, 1994b), (Deshpande *et al.*, 1995), (Deshpande and He, 1995).

In contrast to $C_1; \dots; C_6$ the additional coefficients $C_7; \dots; C_{10}$ show a non negligible m_t dependence in the range $m_t = (170 \text{ } 15) \text{ GeV}$. With in/decreasing m_t there is similarly to the $S = 1$ case a relative variation of $O(19\%)$ and $O(10\%)$ for the absolute values of C_8 and $C_{9,10}$, respectively.

Since the coefficients C_9 and C_{10} play an important role in B decays we show in fig. 7 their m_t dependence explicitly. Again the m_t -dependence can be parametrized by a linear function to an accuracy better than 0.5% . Details of the m_t -parametrization are given in table XXIII.

TABLE XXIII. Coefficients in linear m_t -parametrization $C_i = a + b(m_t - 170 \text{ GeV})$ of Wilson coefficients C_9 and C_{10} at scale $\mu_b = 4.4 \text{ GeV}$ for $\frac{(5)}{\overline{\text{MS}}} = 225 \text{ MeV}$.

	C_9		C_{10}	
	a	b	a	b
LO	0.152	-1.434	-0.056	0.385
NDR	0.109	-1.403	-0.065	0.328
HV	0.117	-1.403	-0.062	0.328

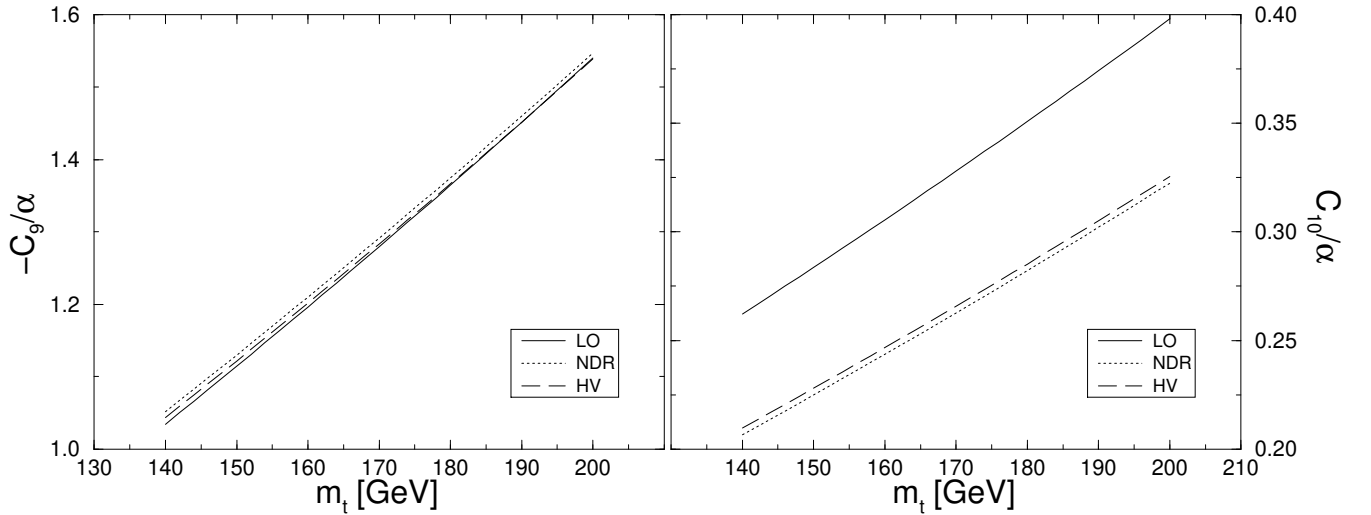


FIG. 7. Wilson coefficients C_9 and C_{10} at $\mu_b = \bar{m}_b(m_b) = 4.4 \text{ GeV}$ as a function of m_t for $\frac{(5)}{\overline{\text{MS}}} = 225 \text{ MeV}$.

VIII. THE EFFECTIVE HAMILTONIAN FOR $K_L \rightarrow \pi^0 e^+ e^-$

The $S = 1$ effective hamiltonian for $K_L \rightarrow \pi^0 e^+ e^-$ at scales $\mu < m_c$ is given by

$$H_e(S=1) = \frac{G_F}{2} V_{us} V_{ud}^* \sum_{i=1}^6 C_i^{7V} (Q_i + \gamma_A(M_W) Q_{7A}(M_W)) \quad (VIII.1)$$

with

$$C_i = \frac{V_{ts} V_{td}^*}{V_{us} V_{ud}^*} \quad (VIII.2)$$

A. Operators

In (VIII.1) $Q_{1,2}$ denote the $S = 1$ current-current and Q_3, \dots, Q_6 the QCD penguin operators of eq. (VI.3). For scales $\mu > m_c$ again the current-current operators $Q_{1,2}^C$ of eq. (VI.4) have to be taken into account.

The new operators specific to the decay $K_L \rightarrow \pi^0 e^+ e^-$ are

$$Q_{7V} = (sd)_V (ee)_V \quad (VIII.3)$$

$$Q_{7A} = (sd)_V (ee)_A \quad (VIII.4)$$

They originate through the γ - and Z^0 -penguin and box diagrams of fig. 2.

It is convenient to introduce the auxiliary operator

$$Q_{7V}^0 = (\gamma_5)_V (sd)_V (ee)_V \quad (VIII.5)$$

and work for the renormalization group analysis in the basis $Q_1, \dots, Q_6, Q_{7V}^0$. The factor γ_5 in the definition of Q_{7V}^0 implies that in this new basis the anomalous dimension matrix will be a function of γ_5 alone. At the end of the renormalization group analysis, this factor will be put back into the Wilson coefficient $C_{7V}(\mu)$ of the operator Q_{7V} in eq. (VIII.3). There is no need to include a similar factor in Q_{7A} as this operator does not mix under renormalization with the remaining operators. Since Q_{7A} has no anomalous dimension its Wilson coefficient is μ -independent.

In principle one can think of including the electroweak four-quark penguin operators Q_7, \dots, Q_{10} of eq. (VII.2) in H_e of (VIII.1). However, their Wilson coefficients and matrix elements for the decay $K_L \rightarrow \pi^0 e^+ e^-$ are both of order $O(\alpha_s)$ implying that these operators eventually would enter the amplitude $A(K_L \rightarrow \pi^0 e^+ e^-)$ at $O(\alpha_s^2)$. To the order considered here this contribution is thus negligible. This should be distinguished from the case of $K \rightarrow \pi \ell^+ \ell^-$ discussed in section VII. There, in spite of being suppressed by γ_5 relative to QCD penguin operators, the electroweak penguin operators have to be included in the analysis because of the additional enhancement factor $R \approx A_0 \approx A_2 \approx 22$ present in the formula for $"0"$ (see section XIX). Such an enhancement factor is not present in the $K_L \rightarrow \pi^0 e^+ e^-$ case and the electroweak penguin operators can be safely neglected.

Concerning the Wilson coefficients, the electroweak four-quark penguin operators would also affect through mixing under renormalization the coefficients C_3, \dots, C_6 at $O(\alpha_s)$ and C_{7V} at $O(\alpha_s^2)$.

Since the corresponding matrix elements are $\mathcal{O}(\alpha_s^2)$ and $\mathcal{O}(\alpha_s)$, respectively, we again obtain a negligible $\mathcal{O}(\alpha_s^2)$ effect in $\mathcal{A}(K_L \rightarrow \pi^0 e^+ e^-)$.

In summary, the electroweak four-quark penguin operators Q_7, \dots, Q_{10} can safely be neglected in the following discussion of $H_e(S=1)$ for $K_L \rightarrow \pi^0 e^+ e^-$.

We also neglect the “magnetic moment” operators. These operators, being of dimension five, do not influence the Wilson coefficients of the operators Q_1, \dots, Q_6 , Q_{7V} and Q_{7A} . Since their contributions to $K_L \rightarrow \pi^0 e^+ e^-$ are suppressed by an additional factor m_s , they appear strictly speaking at higher order in chiral perturbation theory. On the other hand the magnetic moment type operators play a crucial role in $b \rightarrow s$ and $b \rightarrow d$ transitions as discussed in sections IX and XXII. They also have to be kept in the decay $B \rightarrow X_s e^+ e^-$.

B. Wilson Coefficients

Eqs. (VI.6)–(VI.8) remain valid in the case of $K_L \rightarrow \pi^0 e^+ e^-$ with $U_F(m_1; m_2)$ and $M(m_1)$ now denoting 7×7 matrices in the $Q_1, \dots, Q_6, Q_{7V}^0$ basis. The Wilson coefficients are given by seven-dimensional column vectors $\mathbf{z}(\mu)$ and $\mathbf{v}(\mu)$ having components $(z_1, \dots, z_6, z_{7V}^0)$ and $(v_1, \dots, v_6, v_{7V}^0)$, respectively. Here

$$\mathbf{v}_{7V}^0(\mu) = \frac{s(\mu)}{s(\mu_W)} \mathbf{v}_{7V}(\mu); \quad \mathbf{z}_{7V}^0(\mu) = \frac{s(\mu)}{s(\mu_W)} \mathbf{z}_{7V}(\mu) \quad (\text{VIII.6})$$

are the rescaled Wilson coefficients of the auxiliary operator Q_{7V}^0 used in the renormalization group evolution.

The initial conditions $C_1(\mu_W), \dots, C_6(\mu_W)$, $z_1(\mu_W)$, $z_2(\mu_W)$ and $z_1(m_c), \dots, z_6(m_c)$ for the four-quark operators Q_1, \dots, Q_6 are readily obtained from eqs. (VI.9)–(VI.14), (VI.18) and (VI.20).

The corresponding initial conditions for the remaining operators Q_{7V}^0 and Q_{7A} specific to $K_L \rightarrow \pi^0 e^+ e^-$ are then given in the NDR scheme by

$$C_{7V}^0(\mu_W) = \frac{s(\mu_W)}{2} \frac{C_0(x_t) - B_0(x_t)}{\sin^2 \theta_W} - \frac{D_0(x_t) - 4C_0(x_t)}{2} \quad (\text{VIII.7})$$

and

$$C_{7A}(\mu_W) = Y_{7A}(\mu_W) = \frac{B_0(x_t) - C_0(x_t)}{2 \sin^2 \theta_W} \quad (\text{VIII.8})$$

In order to find $z_{7V}^0(m_c)$ which results from the diagrams of fig. 3, we simply have to rescale the NDR result for $z_7(m_c)$ in eq. (VII.17) by a factor of $\frac{s(m_c)}{s(\mu_W)}$. This yields

$$z_{7V}^0(m_c) = \frac{s(m_c)}{2} F_e(m_c) \quad (\text{VIII.9})$$

C. Renormalization Group Evolution and Anomalous Dimension Matrices

Working in the rescaled basis $Q_1; \dots; Q_6, Q_{7V}^0$ the anomalous dimension matrix has per construction a pure $O(\epsilon_s)$ expansion

$$= \frac{\epsilon_s}{4} {}^{(0)} + \frac{\epsilon_s^2}{(4)^2} {}^{(1)} + \dots; \quad (\text{VIII.10})$$

where ${}^{(0)}$ and ${}^{(1)}$ are 7×7 matrices. The evolution matrices $U_F(m_1; m_2)$ in eqs. (VI.7) and (VI.8) are for the present case simply given by (VI.24) and (III.94)–(III.98).

The 6×6 submatrix of ${}^{(0)}$ involving the operators $Q_1; \dots; Q_6$ has already been given in eq. (VI.25). Here we only give the remaining entries of ${}^{(0)}$ related to the additional presence of the operator Q_{7V}^0

$$\begin{aligned} {}_{17}^{(0)} &= \frac{16}{9}N & {}_{27}^{(0)} &= \frac{16}{9} \\ {}_{37}^{(0)} &= \frac{16}{9}N \quad u \quad \frac{d}{2} \quad \frac{1}{N} & {}_{47}^{(0)} &= \frac{16}{9} \quad u \quad \frac{d}{2} \quad N \\ {}_{57}^{(0)} &= \frac{16}{9}N \quad u \quad \frac{d}{2} & {}_{67}^{(0)} &= \frac{16}{9} \quad u \quad \frac{d}{2} \\ {}_{77}^{(0)} &= 2_0 = \frac{22}{3}N + \frac{4}{3}f & {}_{7i}^{(0)} &= 0 \quad i = 1; \dots; 6 \end{aligned} \quad (\text{VIII.11})$$

where N denotes the number of colours. These elements have been first calculated in (Gilman and Wise, 1980) except that ${}_{37}^{(0)}$ and ${}_{47}^{(0)}$ have been corrected in (Eeg and Picek, 1988), (Flynn and Randall, 1989a).

The 6×6 submatrix of ${}^{(1)}$ involving the operators $Q_1; \dots; Q_6$ has already been presented as ${}_{s}^{(1)}$ in eq. (VI.26) and the seventh column of ${}^{(1)}$ is given as follows in the NDR scheme (Buras *et al.*, 1994a)

$$\begin{aligned} {}_{17}^{(1)} &= \frac{8}{3} \quad 1 \quad N^2; \\ {}_{27}^{(1)} &= \frac{200}{81} \quad N \quad \frac{1}{N}; \\ {}_{37}^{(1)} &= \frac{8}{3} \quad u \quad \frac{d}{2} \quad 1 \quad N^2 + \frac{464}{81} \quad \frac{1}{N} \quad N; \\ {}_{47}^{(1)} &= u \frac{280}{81} + d \frac{64}{81} \quad \frac{1}{N} \quad N + \frac{8}{3} \quad N^2 \quad 1; \\ {}_{57}^{(1)} &= \frac{8}{3} \quad u \quad \frac{d}{2} \quad 1 \quad N^2; \\ {}_{67}^{(1)} &= u \frac{440}{81} \quad d \frac{424}{81} \quad N \quad \frac{1}{N}; \\ {}_{77}^{(1)} &= 2_1 = \frac{68}{3}N^2 + \frac{20}{3}Nf + 4C_F f \\ {}_{7i}^{(1)} &= 0 \quad i = 1; \dots; 6 \end{aligned} \quad (\text{VIII.12})$$

where $C_F = (N^2 - 1)/(2N)$. The corresponding results in the HV scheme can be found in (Buras *et al.*, 1994a).

D. Quark Threshold Matching Matrix

For the case of $K_L \rightarrow 0e^+e^-$ the matching matrix $M(\mu)$ has in the basis $Q_1; \dots; Q_6; Q_{7V}^0$ the form

$$M(\mu) = 1 + \frac{s(\mu)}{4} r_s^T \quad (\text{VIII.13})$$

where 1 and r_s^T are 7×7 matrices and μ is the scale of the quark threshold.

The 6×6 submatrix of $M(\mu)$ involving $Q_1; \dots; Q_6$ has been given in eq. (VI.28). The remaining entries of r_s can be found from the matrix r_s given in eqs. (VII.32) and (VII.34) by making a simple rescaling by $3/5$ as in the case of $z_7(\mu_c)$.

In summary, for the quark threshold $\mu = \mu_b$ the matrix r_s reads

$$r_s = \begin{pmatrix} 0 & 0 & 0 & 0 & 0 & 0 & 0 \\ 0 & 0 & 0 & 0 & 0 & 0 & 0 \\ 0 & 0 & 0 & 0 & 0 & 0 & \frac{20}{9} \\ 0 & 0 & \frac{5}{27} & \frac{5}{9} & \frac{5}{27} & \frac{5}{9} & \frac{20}{27} \\ 0 & 0 & 0 & 0 & 0 & 0 & \frac{20}{9} \\ 0 & 0 & \frac{5}{27} & \frac{5}{9} & \frac{5}{27} & \frac{5}{9} & \frac{20}{27} \\ 0 & 0 & 0 & 0 & 0 & 0 & 0 \end{pmatrix} : \quad (\text{VIII.14})$$

For $\mu = \mu_c$ the seventh column of r_s in (VIII.14) has to be multiplied by 2.

E. Numerical Results for the $K_L \rightarrow 0e^+e^-$ Wilson Coefficients

TABLE XXIV. $K_L \rightarrow 0e^+e^-$ Wilson coefficients for $Q_{7V,A}$ at $\mu = 1 \text{ GeV}$ for $\mu_t = 170 \text{ GeV}$. The corresponding coefficients for $Q_1; \dots; Q_6$ can be found in table X of section VI.

	$\frac{(4)}{M.S.} = 215 \text{ MeV}$			$\frac{(4)}{M.S.} = 325 \text{ MeV}$			$\frac{(4)}{M.S.} = 435 \text{ MeV}$		
Scheme	LO	NDR	HV	LO	NDR	HV	LO	NDR	HV
$z_{7V} =$	-0.014	-0.015	0.005	-0.024	-0.046	-0.003	-0.035	-0.084	-0.011
$y_{7V} =$	0.575	0.747	0.740	0.540	0.735	0.725	0.509	0.720	0.710
$y_{7A} =$	-0.700	-0.700	-0.700	-0.700	-0.700	-0.700	-0.700	-0.700	-0.700

In the case of $K_L \rightarrow 0e^+e^-$, due to $\gamma_i^{(0)} = \gamma_i^{(1)} = 0$, $i = 1; \dots; 6$ in eq. (VIII.11) and (VIII.12), respectively, the RG evolution of $Q_1; \dots; Q_6$ is completely unaffected by the additional presence of the operator Q_{7V} . The $K_L \rightarrow 0e^+e^-$ Wilson coefficients z_i and y_i , $i = 1; \dots; 6$ at scale $\mu = 1 \text{ GeV}$ can therefore be found in table X of section VI.

The $K_L \rightarrow 0e^+e^-$ Wilson coefficients for the remaining operators Q_{7V} and Q_{7A} are given in table XXIV. Some insight in the analytic structure of y_{7V} will be gained by studying the analogous decay $B \rightarrow X_s e^+e^-$ in section X and also in section XXI where the phenomenology of $K_L \rightarrow 0e^+e^-$ will be presented.

TABLE XXV. $K_L \rightarrow 0e^+e^-$ Wilson coefficients $z_{7V} =$ and $y_{7V} =$ for $m_t = 170 \text{ GeV}$ and various values of μ .

	$\frac{(4)}{\overline{MS}} = 215 \text{ M eV}$			$\frac{(4)}{\overline{MS}} = 325 \text{ M eV}$			$\frac{(4)}{\overline{MS}} = 435 \text{ M eV}$		
Scheme	LO	NDR	HV	LO	NDR	HV	LO	NDR	HV
[G eV]	$z_{7V} =$								
0.8	-0.031	-0.029	0.004	-0.053	-0.081	-0.012	-0.077	-0.149	-0.023
1.0	-0.014	-0.015	0.005	-0.024	-0.046	-0.003	-0.035	-0.084	-0.011
1.2	-0.004	-0.009	0.002	-0.006	-0.029	0	-0.009	-0.051	-0.002
[G eV]	$y_{7V} =$								
0.8	0.578	0.751	0.744	0.545	0.739	0.730	0.514	0.722	0.712
1.0	0.575	0.747	0.740	0.540	0.735	0.725	0.509	0.720	0.710
1.2	0.571	0.744	0.736	0.537	0.731	0.721	0.505	0.716	0.706

In table XXV we show the μ -dependence of $z_{7V} =$ and $y_{7V} =$. We find a pronounced scheme and μ -dependence for z_{7V} . This signals that these dependences have to be carefully addressed in the calculation of the CP conserving part in the $K_L \rightarrow 0e^+e^-$ amplitude. On the other hand, the scheme and μ -dependences for y_{7V} are below $O(1.5\%)$.

Similarly, z_{7V} shows a strong dependence on the choice of the QCD scale \overline{MS} while this dependence is small or absent for y_{7V} and y_{7A} , respectively.

Finally, as seen from eq. (VIII.9) z_{7V} is independent of m_t . However, with in/decreasing m_t in the range $m_t = (170 - 15) \text{ GeV}$ there is a relative variation of $O(3\%)$ and $O(14\%)$ for the absolute values of y_{7V} and y_{7A} , respectively. This is illustrated further in fig. 8 and table XXVI where the m_t dependence of these coefficients is shown explicitly. Accidentally for $m_t = 175 \text{ GeV}$ one finds $y_{7V} = y_{7A}$. Most importantly the impact of NLO corrections is to enhance the Wilson coefficient y_{7V} by roughly 25%. As we will see in section XXI this implies an enhancement of the direct CP violation in $K_L \rightarrow 0e^+e^-$.

TABLE XXVI. $K_L \rightarrow 0e^+e^-$ Wilson coefficients $y_{7V} =$ and $y_{7A} =$ for $\mu = 1.0 \text{ GeV}$ and various values of m_t .

	$y_{7V} =$									$y_{7A} =$
	$\frac{(4)}{\overline{MS}} = 215 \text{ M eV}$			$\frac{(4)}{\overline{MS}} = 325 \text{ M eV}$			$\frac{(4)}{\overline{MS}} = 435 \text{ M eV}$			
$m_t [\text{GeV}]$	LO	NDR	HV	LO	NDR	HV	LO	NDR	HV	
150	0.546	0.719	0.711	0.512	0.706	0.697	0.481	0.692	0.681	-0.576
160	0.560	0.733	0.726	0.526	0.721	0.711	0.495	0.706	0.696	-0.637
170	0.575	0.747	0.740	0.540	0.735	0.725	0.509	0.720	0.710	-0.700
180	0.588	0.761	0.753	0.554	0.748	0.739	0.523	0.734	0.723	-0.765
190	0.601	0.774	0.766	0.567	0.761	0.752	0.536	0.747	0.736	-0.833
200	0.614	0.786	0.779	0.580	0.774	0.764	0.549	0.760	0.749	-0.902

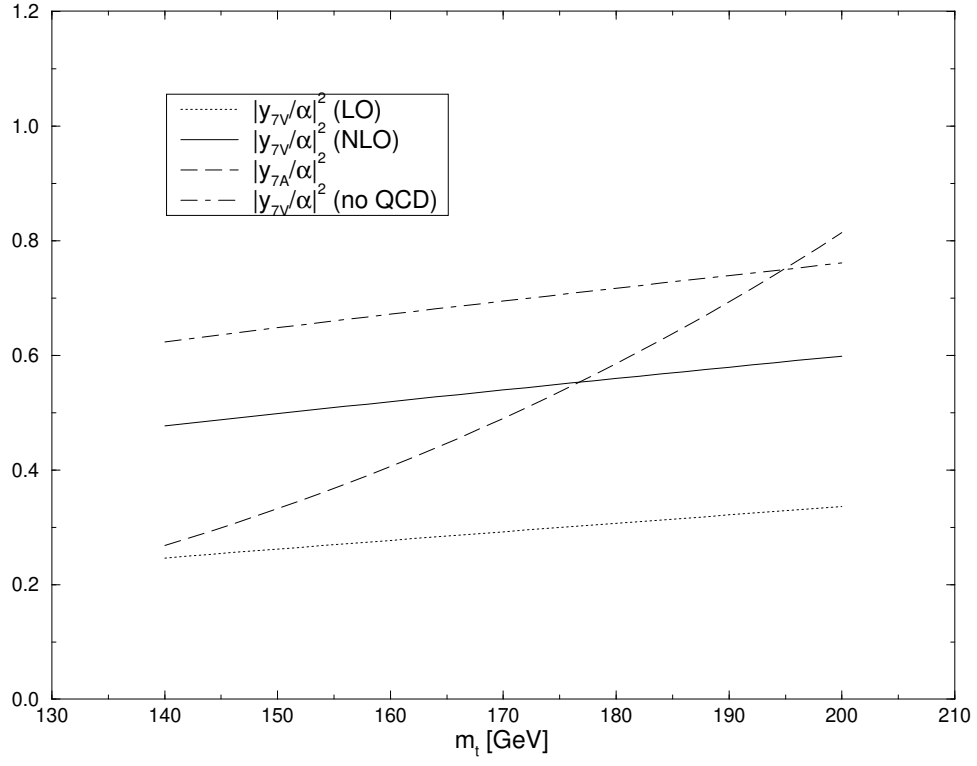


FIG. 8. Wilson coefficients $|y_{7V}/\alpha|^2 = j^2$ and $|y_{7A}/\alpha|^2 = j^2$ as a function of m_t for $\frac{(4)}{MS} = 325 \text{ MeV}$ at scale $\mu = 10 \text{ GeV}$.

IX. THE EFFECTIVE HAMILTONIAN FOR $B \rightarrow X_s$

The effective hamiltonian for $B \rightarrow X_s$ at scales $\mu = O(m_b)$ is given by

$$H_{\text{eff}}(b \rightarrow s) = \frac{G_F}{2} V_{ts} V_{tb}^* \sum_{i=1}^6 C_i(\mu) Q_i(\mu) + C_7(\mu) Q_7(\mu) + C_{8G}(\mu) Q_{8G}(\mu) \quad (\text{IX.1})$$

where in view of $|V_{us} V_{ub}| = |V_{ts} V_{tb}| < 0.02$ we have neglected the term proportional to $V_{us} V_{ub}^*$.

A. Operators

The complete list of operators is given as follows

$$\begin{aligned} Q_1 &= (s_i c_j)_{V-A} (c_j b_i)_{V-A} \\ Q_2 &= (sc)_{V-A} (\bar{c}b)_{V-A} \\ Q_3 &= (sb)_{V-A} (\bar{q}q)_{V-A} \\ Q_4 &= (s_i b_j)_{V-A} (\bar{q}_j q_i)_{V-A} \\ Q_5 &= (sb)_{V-A} (\bar{q}q)_{V+A} \\ Q_6 &= (s_i b_j)_{V-A} (\bar{q}_j q_i)_{V+A} \\ Q_7 &= \frac{e}{8} m_b s_i (1 + \gamma_5) b_i F \\ Q_{8G} &= \frac{g}{8} m_b s_i (1 + \gamma_5) T_{ij}^a b_j G^a \end{aligned} \quad (\text{IX.2})$$

The current-current operators $Q_{1,2}$ and the QCD penguin operators $Q_3; \dots; Q_6$ have been already contained in the usual $B \rightarrow 1$ hamiltonian presented in section VI F. The new operators Q_7 and Q_{8G} specific for $b \rightarrow s$ and $b \rightarrow sg$ transitions carry the name of magnetic penguin operators. They originate from the mass-insertion on the external b-quark line in the QCD and QED penguin diagrams of fig. 4 (d), respectively. In view of $m_s \ll m_b$ we do not include the corresponding contributions from mass-insertions on the external s-quark line.

B. Wilson Coefficients

A very peculiar feature of the renormalization group analysis of the set of operators in (IX.2) is that the mixing under (infinite) renormalization between the set $Q_1; \dots; Q_6$ and the operators $Q_7; Q_{8G}$ vanishes at the one-loop level. Consequently in order to calculate the coefficients $C_7(\mu)$ and $C_{8G}(\mu)$ in the leading logarithmic approximation, two-loop calculations of $O(\alpha_s^2)$ and $O(g_s^3)$ are necessary. The corresponding NLO analysis requires the evaluation of the mixing in question at the three-loop level. In view of this new feature it is useful to include additional couplings in the definition of Q_7 and Q_{8G} as done in (IX.2). In this manner the entries in the anomalous dimension matrix representing the mixing between $Q_1; \dots; Q_6$ and $Q_7; Q_{8G}$ at the two-loop level are $O(g_s^2)$

and enter the anomalous dimension matrix $\gamma_s^{(0)}$. Correspondingly the three-loop mixing between these two sets of operators enters the matrix $\gamma_s^{(1)}$.

The mixing under renormalization in the sector $Q_7; Q_{8G}$ proceeds in the usual manner and the corresponding entries in $\gamma_s^{(0)}$ and $\gamma_s^{(1)}$ result from one-loop and two-loop calculations, respectively.

At present, the coefficients C_7 and C_{8G} are only known in the leading logarithmic approximation. Consequently we are in the position to give here only their values in this approximation. The work on NLO corrections to C_7 and C_{8G} is in progress and we will summarize below what is already known about these corrections.

The peculiar feature of this decay mentioned above caused that the first fully correct calculation of the leading anomalous dimension matrix has been obtained only in 1993 (Ciuchini *et al.*, 1993b), (Ciuchini *et al.*, 1994c). It is instructive to clarify this right at the beginning. We follow here (Buras *et al.*, 1994c).

The point is that the mixing between the sets $Q_1; \dots; Q_6$ and $Q_7; Q_{8G}$ in $\gamma_s^{(0)}$ resulting from two-loop diagrams is generally regularization scheme dependent. This is certainly disturbing because the matrix $\gamma_s^{(0)}$, being the first term in the expansion for γ_s , is usually scheme independent. There is a simple way to circumvent this difficulty (Buras *et al.*, 1994c).

As noticed in (Ciuchini *et al.*, 1993b), (Ciuchini *et al.*, 1994c) the regularization scheme dependence of $\gamma_s^{(0)}$ in the case of $b \rightarrow s$ and $b \rightarrow sg$ is signaled in the one-loop matrix elements of $Q_1; \dots; Q_6$ for on-shell photons or gluons. They vanish in any 4-dimensional regularization scheme and in the HV scheme but some of them are non-zero in the NDR scheme. One has

$$hQ_i^{i_{\text{one loop}}} = y_i hQ_7^{i_{\text{tree}}}; \quad i = 1; \dots; 6 \quad (\text{IX.3})$$

and

$$hQ_i^{i_{\text{one loop}}^G} = z_i hQ_{8G}^{i_{\text{tree}}}; \quad i = 1; \dots; 6: \quad (\text{IX.4})$$

In the HV scheme all the y_i 's and z_i 's vanish, while in the NDR scheme $\mathbf{y} = (0; 0; 0; 0; \frac{1}{3}; 1)$ and $\mathbf{z} = (0; 0; 0; 0; 1; 0)$. This regularization scheme dependence is canceled by a corresponding regularization scheme dependence in $\gamma_s^{(0)}$ as first demonstrated in (Ciuchini *et al.*, 1993b), (Ciuchini *et al.*, 1994c). It should be stressed that the numbers y_i and z_i come from divergent, i.e. purely short-distance parts of the one-loop integrals. So no reference to the spectator-model or to any other model for the matrix elements is necessary here.

In view of all this it is convenient in the leading order to introduce the so-called “effective coefficients” (Buras *et al.*, 1994c) for the operators Q_7 and Q_{8G} which are regularization scheme independent. They are given as follows:

$$C_7^{(0)\text{eff}}(\mu) = C_7^{(0)}(\mu) + \sum_{i=1}^{X_6} y_i C_i^{(0)}(\mu): \quad (\text{IX.5})$$

and

$$C_{8G}^{(0)\text{eff}}(\mu) = C_{8G}^{(0)}(\mu) + \sum_{i=1}^{X_6} z_i C_i^{(0)}(\mu) \quad (\text{IX.6})$$

One can then introduce a scheme-independent vector

$$\vec{C}^{(0)\text{eff}}(\mu) = (C_1^{(0)}(\mu); \dots; C_6^{(0)}(\mu); C_7^{(0)\text{eff}}(\mu); C_{8G}^{(0)\text{eff}}(\mu)) : \quad (\text{IX.7})$$

From the RGE for $C^{(0)}(\mu)$ it is straightforward to derive the RGE for $C^{(0)eff}(\mu)$. It has the form

$$\frac{d}{d\mu} C_i^{(0)eff}(\mu) = \frac{s}{4} \gamma_{ji}^{(0)eff} C_j^{(0)eff}(\mu) \quad (IX.8)$$

where

$$\gamma_{ji}^{(0)eff} = \begin{cases} \gamma_{j7}^{(0)} + \sum_{k=1}^6 \gamma_{jk}^{(0)} \gamma_{7k}^{(0)} & i=7; j=1, \dots, 6 \\ \gamma_{j8}^{(0)} + \sum_{k=1}^6 \gamma_{jk}^{(0)} \gamma_{8k}^{(0)} & i=8; j=1, \dots, 6 \\ \gamma_{ji}^{(0)} & \text{otherwise.} \end{cases} \quad (IX.9)$$

The matrix $\gamma^{(0)eff}$ is a scheme-independent quantity. It equals the matrix which one would directly obtain from two-loop diagrams in the HV scheme. In order to simplify the notation we will omit the label “eff” in the expressions for the elements of this effective one loop anomalous dimension matrix given below and keep it only in the Wilson coefficients of the operators Q_7 and Q_{8G} .

This discussion clarifies why it took so long to find the correct leading anomalous dimension matrix for the $b \rightarrow s$ decay (Ciuchini *et al.*, 1993b), (Ciuchini *et al.*, 1994c). All previous calculations (Grinstein *et al.*, 1990), (Cella *et al.*, 1990), (Misiak, 1993), (Adel and Yao, 1993), (Adel and Yao, 1994) of the leading order QCD corrections to $b \rightarrow s$ used the NDR scheme setting unfortunately z_i and y_i to zero, or not including all operators or making other mistakes. The discrepancy between the calculation of (Grigjanis *et al.*, 1988) (DRED scheme) and (Grinstein *et al.*, 1990) (NDR scheme) has been clarified by (Misiak, 1994).

C. Renormalization Group Evolution and Anomalous Dimension Matrices

The coefficients $C_i(\mu)$ in (IX.1) can be calculated by using

$$C(\mu) = U_5(\mu; M_W) C(M_W) \quad (IX.10)$$

Here $U_5(\mu; M_W)$ is the 8×8 evolution matrix which is given in general terms in (III.93) with being this time an 8×8 anomalous dimension matrix. In the leading order $U_5(\mu; M_W)$ is to be replaced by $U_5^{(0)}(\mu; M_W)$ and the initial conditions by $C^{(0)}(M_W)$ given by (Grinstein *et al.*, 1990)

$$C_2^{(0)}(M_W) = 1 \quad (IX.11)$$

$$C_7^{(0)}(M_W) = \frac{3x_t^3}{4(x_t - 1)^4} \ln x_t + \frac{8x_t^3}{24(x_t - 1)^3} - \frac{5x_t^2 + 7x_t}{24(x_t - 1)^3} - \frac{1}{2} D_0^0(x_t) \quad (IX.12)$$

$$C_{8G}^{(0)}(M_W) = \frac{3x_t^2}{4(x_t - 1)^4} \ln x_t + \frac{x_t^3 + 5x_t^2 + 2x_t}{8(x_t - 1)^3} - \frac{1}{2} E_0^0(x_t) \quad (IX.13)$$

with all remaining coefficients being zero at $\mu = M_W$. The functions $D_0^0(x_t)$ and $E_0^0(x_t)$ are sometimes used in the literature. The 6×6 submatrix of $\gamma_s^{(0)}$ involving the operators $Q_1; \dots; Q_6$ is given in (VI.25). Here we only give the remaining non-vanishing entries of $\gamma_s^{(0)}$ (Ciuchini *et al.*, 1993b), (Ciuchini *et al.*, 1994c).

Denoting for simplicity $_{ij}^{(s)}$, the elements $_{i7}^{(0)}$ with $i = 1; \dots; 6$ are:

$$_{17}^{(0)} = 0; \quad _{27}^{(0)} = \frac{104}{27} C_F \quad (\text{IX.14})$$

$$_{37}^{(0)} = \frac{116}{27} C_F \quad _{47}^{(0)} = \frac{104}{27} u \quad \frac{58}{27} d \quad C_F \quad (\text{IX.15})$$

$$_{57}^{(0)} = \frac{8}{3} C_F \quad _{67}^{(0)} = \frac{50}{27} d \quad \frac{112}{27} u \quad C_F \quad (\text{IX.16})$$

The elements $_{i8}^{(0)}$ with $i = 1; \dots; 6$ are:

$$_{18}^{(0)} = 3; \quad _{28}^{(0)} = \frac{11}{9} N \quad \frac{29}{9} \frac{1}{N} \quad (\text{IX.17})$$

$$_{38}^{(0)} = \frac{22}{9} N \quad \frac{58}{9} \frac{1}{N} + 3f \quad _{48}^{(0)} = 6 + \frac{11}{9} N \quad \frac{29}{9} \frac{1}{N} \quad f \quad (\text{IX.18})$$

$$_{58}^{(0)} = 2N + \frac{4}{N} \quad 3f \quad _{68}^{(0)} = 4 \quad \frac{16}{9} N \quad \frac{25}{9} \frac{1}{N} \quad f \quad (\text{IX.19})$$

Finally the 2×2 one-loop anomalous dimension matrix in the sector $Q_7; Q_{8G}$ is given by (Grinstein *et al.*, 1990)

$$\begin{aligned} _{77}^{(0)} &= 8C_F & _{78}^{(0)} &= 0 \\ _{87}^{(0)} &= \frac{8}{3} C_F & _{88}^{(0)} &= 16C_F - 4N \end{aligned} \quad (\text{IX.20})$$

As we discussed above, the first correct calculation of the two-loop mixing between $Q_1; \dots; Q_6$ and Q_7, Q_{8G} has been presented in (Ciuchini *et al.*, 1993b), (Ciuchini *et al.*, 1994c) and confirmed subsequently in (Cella *et al.*, 1994a), (Cella *et al.*, 1994b), (Misiak, 1995). In order to extend these calculations beyond the leading order one would have to calculate $_{s}^{(1)}$ (see (III.92)) and $O(\epsilon_s)$ corrections to the initial conditions in (IX.12) and (IX.13). We summarize below the present status of this NLO calculation.

The 6×6 two-loop submatrix of $_{s}^{(1)}$ involving the operators $Q_1; \dots; Q_6$ is given in eq. (VI.26). The two-loop generalization of (IX.20) has been calculated only last year (Misiak and Münz, 1995). It is given for both NDR and HV schemes as follows

$$\begin{aligned} _{77}^{(1)} &= C_F \quad \frac{548}{9} N \quad 16C_F \quad \frac{56}{9} f \\ _{78}^{(1)} &= 0 \\ _{87}^{(1)} &= C_F \quad \frac{404}{27} N + \frac{32}{3} C_F + \frac{56}{27} f \\ _{88}^{(1)} &= \frac{458}{9} \quad \frac{12}{N^2} + \frac{214}{9} N^2 + \frac{56}{9} \frac{f}{N} \quad \frac{13}{9} fN \end{aligned} \quad (\text{IX.21})$$

The generalization of (IX.14)–(IX.19) to next-to-leading order requires three loop calculations which have not been done yet. The $O(\epsilon_s)$ corrections to $C_7(M_W)$ and $C_{8G}(M_W)$ have been considered in (Adel and Yao, 1993).

D. Results for the Wilson Coefficients

The leading order results for the Wilson Coefficients of all operators entering the effective hamiltonian in (IX.1) can be written in an analytic form. They are (Buras *et al.*, 1994c)

$$C_j^{(0)}(\mu) = \sum_{i=1}^{X^8} k_{ji} a_i \quad (j = 1; \dots; 6) \quad (\text{IX.22})$$

$$C_7^{(0)\text{eff}}(\mu) = \frac{16}{23} C_7^{(0)}(\mu_W) + \frac{8}{3} \frac{14}{23} \frac{16}{23} C_{8G}^{(0)}(\mu_W) + C_2^{(0)}(\mu_W) \sum_{i=1}^{X^8} h_i a_i; \quad (\text{IX.23})$$

$$C_{8G}^{(0)\text{eff}}(\mu) = \frac{14}{23} C_{8G}^{(0)}(\mu_W) + C_2^{(0)}(\mu_W) \sum_{i=1}^{X^8} h_i a_i; \quad (\text{IX.24})$$

with

$$= \frac{s(\mu_W)}{s(\mu)}; \quad (\text{IX.25})$$

and $C_7^{(0)}(\mu_W)$ and $C_{8G}^{(0)}(\mu_W)$ given in (IX.12) and (IX.13), respectively. The numbers a_i , k_{ji} , h_i and h_i are given in table XXVII.

TABLE XXVII.

i	1	2	3	4	5	6	7	8
a_i	$\frac{14}{23}$	$\frac{16}{23}$	$\frac{6}{23}$	$\frac{12}{23}$	0.4086	0.4230	0.8994	0.1456
k_{1i}	0	0	$\frac{1}{2}$	$\frac{1}{2}$	0	0	0	0
k_{2i}	0	0	$\frac{1}{2}$	$\frac{1}{2}$	0	0	0	0
k_{3i}	0	0	$\frac{1}{14}$	$\frac{1}{6}$	0.0510	0.1403	0.0113	0.0054
k_{4i}	0	0	$\frac{1}{14}$	$\frac{1}{6}$	0.0984	0.1214	0.0156	0.0026
k_{5i}	0	0	0	0	0.0397	0.0117	0.0025	0.0304
k_{6i}	0	0	0	0	0.0335	0.0239	0.0462	0.0112
h_i	2.2996	1.0880	$\frac{3}{7}$	$\frac{1}{14}$	0.6494	0.0380	0.0185	0.0057
h_i	0.8623	0	0	0	0.9135	0.0873	0.0571	0.0209

E. Numerical Analysis

The decay $B \rightarrow X_s$ is the only decay in our review for which the complete NLO corrections are not available. In presenting the numerical values for the Wilson coefficients a few remarks on the choice of μ_s should therefore be made. In the leading order the leading order expression for μ_s should be used. The question then is what to use for Q_{CD} in this expression. In other decays for which NLO corrections were available this was not important because LO results were secondary. We have therefore simply inserted our standard \overline{MS} values into the LO formula for μ_s . This procedure gives $s^{(5)}(\mu_Z) = 0.126; 0.136; 0.144$ for $\frac{s^{(5)}}{\overline{MS}} = 140 \text{ MeV}; 225 \text{ MeV}; 310 \text{ MeV}$,

respectively. In view of these high values of $\alpha_s^{(5)}(M_Z)$ we will proceed here differently. Following (Buras *et al.*, 1994c) we will use $\alpha_s^{(5)}(M_Z) = 0.110; 0.117; 0.124$ as in our NLO calculations, but we will evolve $\alpha_s(\mu)$ to $\alpha_s(m_b)$ using the leading order expressions. In short, we will use

$$\alpha_s(\mu) = \frac{\alpha_s(M_Z)}{1 - \beta_0 \alpha_s(M_Z) \ln(M_Z/\mu)} : \quad (\text{IX.26})$$

This discussion shows again the importance of the complete NLO calculation for this decay.

Before starting the discussion of the numerical values for the coefficients $C_7^{(0)\text{eff}}$ and $C_{8G}^{(0)\text{eff}}$, let us illustrate the relative numerical importance of the three terms in expression (IX.23) for $C_7^{(0)\text{eff}}$.

For instance, for $m_t = 170 \text{ GeV}$, $m_b = 5 \text{ GeV}$ and $\alpha_s^{(5)}(M_Z) = 0.117$ one obtains

$$\begin{aligned} C_7^{(0)\text{eff}}(\mu) &= 0.698 C_7^{(0)}(M_W) + 0.086 C_{8G}^{(0)}(M_W) - 0.156 C_2^{(0)}(M_W) \\ &= 0.698 (-0.193) + 0.086 (-0.096) - 0.156 = -0.299 : \end{aligned} \quad (\text{IX.27})$$

In the absence of QCD we would have $C_7^{(0)\text{eff}}(\mu) = C_7^{(0)}(M_W)$ (in that case one has $\beta_0 = 1$). Therefore, the dominant term in the above expression (the one proportional to $C_2^{(0)}(M_W)$) is the additive QCD correction that causes the enormous QCD enhancement of the $b \rightarrow s$ rate (Bertolini *et al.*, 1987), (Deshpande *et al.*, 1987). It originates solely from the two-loop diagrams. On the other hand, the multiplicative QCD correction (the factor 0.698 above) tends to suppress the rate, but fails in the competition with the additive contributions.

In the case of $C_{8G}^{(0)\text{eff}}$ a similar enhancement is observed

$$\begin{aligned} C_{8G}^{(0)\text{eff}}(\mu) &= 0.730 C_{8G}^{(0)}(M_W) - 0.073 C_2^{(0)}(M_W) \\ &= 0.730 (-0.096) - 0.073 = -0.143 : \end{aligned} \quad (\text{IX.28})$$

In table XXVIII we give the values of $C_7^{(0)\text{eff}}$ and $C_{8G}^{(0)\text{eff}}$ for different values of μ and $\alpha_s^{(5)}(M_Z)$. To this end (IX.26) has been used. A strong μ -dependence of both coefficients is observed. We will return to this dependence in section XXII.

TABLE XXVIII. Wilson coefficients $C_7^{(0)\text{eff}}$ and $C_{8G}^{(0)\text{eff}}$ for $m_t = 170 \text{ GeV}$ and various values of $\alpha_s^{(5)}(M_Z)$ and μ .

[GeV]	$\alpha_s^{(5)}(M_Z) = 0.110$		$\alpha_s^{(5)}(M_Z) = 0.117$		$\alpha_s^{(5)}(M_Z) = 0.124$	
	$C_7^{(0)\text{eff}}$	$C_{8G}^{(0)\text{eff}}$	$C_7^{(0)\text{eff}}$	$C_{8G}^{(0)\text{eff}}$	$C_7^{(0)\text{eff}}$	$C_{8G}^{(0)\text{eff}}$
2.5	-0.323	-0.153	-0.334	-0.157	-0.346	-0.162
5.0	-0.291	-0.140	-0.299	-0.143	-0.307	-0.147
7.5	-0.275	-0.133	-0.281	-0.136	-0.287	-0.139
10.0	-0.263	-0.129	-0.268	-0.131	-0.274	-0.133

X. THE EFFECTIVE HAMILTONIAN FOR $B \rightarrow X_s e^+ e^-$

The effective hamiltonian for $B \rightarrow X_s e^+ e^-$ at scales $\mu = O(m_b)$ is given by

$$H_e(b \rightarrow s e^+ e^-) = H_e(b \rightarrow s) \quad (X.1)$$

$$+ \frac{G_F}{2} V_{ts} V_{tb} [C_{9V}(\mu) Q_{9V}(\mu) + C_{10A}(\mu) Q_{10A}(\mu)]$$

where again we have neglected the term proportional to $V_{us} V_{ub}$ and $H_e(b \rightarrow s)$ is given in (IX.1).

A. Operators

In addition to the operators relevant for $B \rightarrow X_s$, there are two new operators

$$Q_{9V} = (sb)_V \rightarrow_A (ee)_V \quad Q_{10A} = (sb)_V \rightarrow_A (ee)_A \quad (X.2)$$

where V and A refer to γ and γ_5 , respectively.

They originate in the Z^0 - and γ -penguin diagrams with external ee of fig. 4(f) and from the corresponding box diagrams.

B. Wilson Coefficients

The coefficient $C_{10A}(\mu)$ is given by

$$C_{10A}(M_W) = \frac{1}{2} \mathcal{C}_{10}(M_W); \quad \mathcal{C}_{10}(M_W) = \frac{Y_0(x_t)}{\sin^2 \theta_W} \quad (X.3)$$

with $Y_0(x)$ given in (X.8). Since Q_{10A} does not renormalize under QCD, its coefficient does not depend on $\mu = O(m_b)$. The only renormalization scale dependence in (X.3) enters through the definition of the top quark mass. We will return to this issue in section XXIII C.

The coefficient $C_{9V}(\mu)$ has been calculated over the last years with increasing precision by several groups (Grinstein *et al.*, 1989), (Grigjanis *et al.*, 1989), (Cella *et al.*, 1991), (Misiak, 1993) culminating in two complete next-to-leading QCD calculations (Misiak, 1995), (Buras and Münz, 1995) which agree with each other.

In order to calculate the coefficient C_{9V} including next-to-leading order corrections we have to perform in principle a two-loop renormalization group analysis for the full set of operators contributing to (X.1). However, Q_{10A} is not renormalized and the dimension five operators Q_7 and Q_{8G} have no impact on C_{9V} . Consequently only a set of seven operators, Q_1, \dots, Q_6 and Q_{9V} , has to be considered. This is precisely the case of the decay $K_L \rightarrow \pi^0 e^+ e^-$ discussed in (Buras *et al.*, 1994a) and in section VIII, except for an appropriate change of quark flavours and the fact that now $\mu = O(m_b)$ instead of $\mu = O(1 \text{ GeV})$. Since the NLO analysis of $K_L \rightarrow \pi^0 e^+ e^-$ has already been presented in section VIII we will only give the final result for $C_{9V}(\mu)$. Because of the one step evolution from $\mu = M_W$ down to $\mu = m_b$ without any thresholds in between it is possible to find an analytic formula for $C_{9V}(\mu)$. Defining \mathcal{C}_9 by

$$C_{9V}(\mu) = \frac{1}{2} \mathcal{C}_9(\mu) \quad (X.4)$$

one finds (Buras and Münz, 1995) in the NDR scheme

$$\mathcal{C}_9^{NDR}(\mu) = P_0^{NDR} + \frac{Y_0(x_t)}{\sin^2 \theta_w} [4Z_0(x_t) + P_E E_0(x_t)] \quad (X.5)$$

with

$$P_0^{NDR} = \frac{1}{s(M_W)} \left(0.1875 + \sum_{i=1}^8 p_i x^{a_i+1} \right) + 1.2468 + \sum_{i=1}^8 x^{a_i} [r_i^{NDR} + s_i] \quad (X.6)$$

$$P_E = 0.1405 + \sum_{i=1}^8 q_i x^{a_i+1} : \quad (X.7)$$

The functions $Y_0(x)$ and $Z_0(x)$ are defined by

$$Y_0(x) = C_0(x) - B_0(x) \quad Z_0(x) = C_0(x) + \frac{1}{4} D_0(x) \quad (X.8)$$

with $B_0(x)$, $C_0(x)$ and $D_0(x)$ given in (VII.13), (VII.14) and (VII.15), respectively. $E_0(x)$ is given in eq. (VI.15). The powers a_i are the same as in table XXVII. The coefficients p_i , r_i^{NDR} , s_i , and q_i can be found in table XXIX. P_E is $O(10^{-2})$ and consequently the last term in (X.5) can be neglected. We keep it however in our numerical analysis. These results agree with (Misiak, 1995).

TABLE XXIX.

i	1	2	3	4	5	6	7	8
p_i	0.1875	0.1875	$\frac{80}{203}$	$\frac{8}{33}$	0.0433	0.1384	0.1648	0.0073
r_i^{NDR}	0	0	0.8966	0.1960	0.2011	0.1328	0.0292	0.1858
s_i	0	0	0.2009	0.3579	0.0490	0.3616	0.3554	0.0072
q_i	0	0	0	0	0.0318	0.0918	0.2700	0.0059
r_i^{HV}	0	0	0.1193	0.1003	0.0473	0.2323	0.0133	0.1799

In the HV scheme only the coefficients r_i are changed. They are given on the last line of table XXIX. Equivalently we can write

$$P_0^k = P_0^{NDR} + \sum_k \frac{4}{9} [3C_1^{(0)} + C_2^{(0)} - C_3^{(0)} - 3C_4^{(0)}] \quad (X.9)$$

with

$$C_k = \begin{cases} 0 & k = NDR \\ 1 & k = HV \end{cases} : \quad (X.10)$$

We note that

$$\sum_{i=1}^8 p_i = 0.1875; \quad \sum_{i=1}^8 q_i = 0.1405; \quad (X.11)$$

$$\sum_{i=1}^8 (r_i^k + s_i) = 1.2468 + \frac{4}{9} (1 + k); \quad \sum_{i=1}^8 p_i (a_i + 1) = \frac{16}{69}; \quad (X.12)$$

In this way for $k = 1$ one finds $P_E = 0$, $P_0^{NDR} = 4/9$ and $P_0^{HV} = 0$ in accordance with the initial conditions at $k = M_W$. Moreover, the second relation in (X.12) assures the correct large logarithm in P_0^{NDR} , i.e. $8/9 \ln(M_W)$.

The special feature of $C_{9V}(k)$ compared to the coefficients of the remaining operators contributing to $B \rightarrow X_s e^+ e^-$ is the large logarithm represented by $1/s$ in P_0 in (X.6). Consequently the renormalization group improved perturbation theory for C_{9V} has the structure $O(1/s) + O(1) + O(s) + \dots$; whereas the corresponding series for the remaining coefficients is $O(1) + O(s) + \dots$. Therefore in order to find the next-to-leading $O(1)$ term in the branching ratio for $B \rightarrow X_s e^+ e^-$, the full two-loop renormalization group analysis has to be performed in order to find C_{9V} , but the coefficients of the remaining operators should be taken in the leading logarithmic approximation. This is gratifying because the coefficient of the magnetic operator Q_7 is known only in the leading logarithmic approximation.

C. Numerical Results

In our numerical analysis we will use the two-loop expression for $1/s$ and the parameters collected in the appendix. Our presentation follows closely the one given in (Buras and Münz, 1995).

In table XXX we show the constant P_0 in (X.6) for different k and $\frac{(5)}{M_S}$, in the leading order corresponding to the first term in (X.6) and for the NDR and HV schemes as given by (X.6) and (X.9), respectively. In table XXXI we show the corresponding values for $C_9(k)$. To this end we set $m_t = 170 \text{ GeV}$.

TABLE XXX. The coefficient P_0 of C_9 for various values of $\frac{(5)}{M_S}$ and k .

[GeV]	$\frac{(5)}{M_S} = 140 \text{ MeV}$			$\frac{(5)}{M_S} = 225 \text{ MeV}$			$\frac{(5)}{M_S} = 310 \text{ MeV}$		
	LO	NDR	HV	LO	NDR	HV	LO	NDR	HV
2.5	2.053	2.928	2.797	1.933	2.846	2.759	1.835	2.775	2.727
5.0	1.852	2.625	2.404	1.788	2.591	2.395	1.736	2.562	2.388
7.5	1.675	2.391	2.127	1.632	2.373	2.127	1.597	2.358	2.128
10.0	1.526	2.204	1.912	1.494	2.194	1.917	1.469	2.185	1.921

We observe:

The NLO corrections to B enhance this constant relatively to the LO result by roughly 45% and 35% in the NDR and HV schemes, respectively. This enhancement is analogous to the one found in the case of $K_L \rightarrow 0 e^+ e^-$.

TABLE XXXI. Wilson coefficient \mathcal{C}_9 for $m_t = 170 \text{ GeV}$ and various values of $\frac{(5)}{M_S}$ and μ .

[GeV]	$\frac{(5)}{M_S} = 140 \text{ MeV}$			$\frac{(5)}{M_S} = 225 \text{ MeV}$			$\frac{(5)}{M_S} = 310 \text{ MeV}$		
	LO	NDR	HV	LO	NDR	HV	LO	NDR	HV
2.5	2.053	4.493	4.361	1.933	4.410	4.323	1.835	4.338	4.290
5.0	1.852	4.191	3.970	1.788	4.156	3.961	1.736	4.127	3.954
7.5	1.675	3.958	3.694	1.632	3.940	3.694	1.597	3.924	3.695
10.0	1.526	3.772	3.480	1.494	3.761	3.485	1.469	3.752	3.488

In calculating \mathcal{P} in the LO we have used $\alpha_s(\mu)$ at one-loop level. Had we used the two-loop expression for $\alpha_s(\mu)$ we would find for $\mu = 5 \text{ GeV}$ and $\frac{(5)}{M_S} = 225 \text{ MeV}$ the value $\mathcal{P}_0^{\text{LO}} = 1.98$. Consequently the NLO corrections would have smaller impact. Ref. (Grinstein *et al.*, 1989) including the next-to-leading term $\mathcal{O}(\alpha_s^2)$ would find \mathcal{P}_0 values roughly 20% smaller than $\mathcal{P}_0^{\text{NDR}}$ given in table XXX.

It is tempting to compare \mathcal{P} in table XXX with that found in the absence of QCD corrections. In the limit $\alpha_s \rightarrow 0$ we find $\mathcal{P}_0^{\text{NDR}} = 8/9 \ln(M_W/\mu) + 4/9$ and $\mathcal{P}_0^{\text{HV}} = 8/9 \ln(M_W/\mu)$ which for $\mu = 5 \text{ GeV}$ give $\mathcal{P}_0^{\text{NDR}} = 2.91$ and $\mathcal{P}_0^{\text{HV}} = 2.46$. Comparing these values with table XXX we conclude that the QCD suppression of \mathcal{P}_0 present in the leading order approximation is considerably weakened in the NDR treatment of α_s after the inclusion of NLO corrections. It is essentially removed for $\mu > 5 \text{ GeV}$ in the HV scheme.

The NLO corrections to \mathcal{C}_9 which include also the m_t -dependent contributions are large as seen in table XXXI. The results in HV and NDR schemes are by more than a factor of two larger than the leading order result $\mathcal{C}_9 = \mathcal{P}_0^{\text{LO}}$ which consistently should not include m_t -contributions. This demonstrates very clearly the necessity of NLO calculations which allow a consistent inclusion of the important m_t -contributions. For the same set of parameters the authors of (Grinstein *et al.*, 1989) would find \mathcal{C}_9 to be smaller than $\mathcal{C}_9^{\text{NDR}}$ by 10–15%.

The $\frac{(5)}{M_S}$ dependence of \mathcal{C}_9 is rather weak. On the other hand its μ dependence is sizable ($\sim 15\%$ in the range of μ considered) although smaller than in the case of the coefficients \mathcal{C}_7 and \mathcal{C}_{8G} given in table XXVIII. We also find that the m_t dependence of \mathcal{C}_9 is rather weak. Varying m_t between 150 GeV and 190 GeV changes \mathcal{C}_9 by at most 10%. This weak m_t dependence of \mathcal{C}_9 originates in the partial cancelation of m_t dependences between $Y_0(x_t)$ and $Z_0(x_t)$ in (X.5) as already seen in the case of $K_L \rightarrow \pi^0 e^+ e^-$ in fig. 8. Finally, the difference between $\mathcal{C}_9^{\text{NDR}}$ and $\mathcal{C}_9^{\text{HV}}$ is small and amounts to roughly 5%.

The dominant m_t -dependence in this decay originates in the m_t dependence of $\mathcal{C}_{10}(M_W)$. In fact, as can be seen in section VIII $\mathcal{C}_{10}(M_W) = 2 - y_{7A}$ with y_{7A} present in $K_L \rightarrow \pi^0 e^+ e^-$. The m_t dependence of y_{7A} is shown in fig. 8.

XI. EFFECTIVE HAMILTONIANS FOR RARE K - AND B -DECAYS

A. Overview

In the present section we will summarize the effective hamiltonians valid at next-to-leading logarithmic accuracy in QCD, which describe the semileptonic rare Flavour Changing Neutral Current (FCNC) transitions $K^+ \rightarrow \pi^+ \gamma$, $(K_L \rightarrow \pi^+ \gamma)_{SD}$, $K_L \rightarrow \pi^0 \gamma$, $B \rightarrow X_{s,d} \gamma$ and $B \rightarrow \ell^+ \ell^-$. These decay modes all are very similar in their structure and it is natural to discuss them together. On the other hand they differ from the decays $K \rightarrow \pi \ell^+ \ell^-$, $K \rightarrow \ell^+ \ell^-$, $B \rightarrow X_s \ell^+ \ell^-$ and $B \rightarrow X_s e^+ e^-$ discussed in previous sections. Before giving the detailed formulae, it will be useful to recall the most important general features of this class of processes first. In addition, characteristic differences between the specific modes will also become apparent from our presentation.

Within the Standard Model all the decays listed above are loop-induced semileptonic FCNC processes determined by Z^0 -penguin and box diagrams (fig. 2 (d) and (e)).

In particular, a distinguishing feature of the present class of decays is the absence of a photon penguin contribution. For the decay modes with neutrinos in the final state this is obvious, since the photon does not couple to neutrinos. For the mesons decaying into a charged lepton pair the photon penguin amplitude vanishes due to vector current conservation.

An important consequence is, that the decays considered here exhibit a hard GIM suppression, quadratic in (small) internal quark masses, which is a property of the Z^0 -penguin and box graphs. By contrast, the GIM suppression resulting from photon penguin contributions is logarithmic. Decays where the photon penguin contributes are for example $K_L \rightarrow \pi^0 e^+ e^-$ and $B \rightarrow X_s e^+ e^-$. The differences in the basic structure of these processes, resulting from the different pattern of GIM suppression, are the reason why we have discussed $K_L \rightarrow \pi^0 e^+ e^-$ and $B \rightarrow X_s e^+ e^-$ in a separate context.

The investigation of low energy rare decay processes allows to probe, albeit indirectly, high energy scales of the theory. Of particular interest is the sensitivity to properties of the top quark, its mass m_t and its CKM couplings V_{ts} and V_{td} .

A particular and very important advantage of the processes under discussion is, that theoretically clean predictions can be obtained. The reasons for this are:

- The low energy hadronic matrix elements required are just the matrix elements of quark currents between hadron states, which can be extracted from the leading (non-rare) semileptonic decays. Other long-distance contributions are negligibly small. An exception is the decay $K_L \rightarrow \pi^+ \pi^-$ receiving important contributions from the two-photon intermediate state, which are difficult to calculate reliably. However, the short-distance part $(K_L \rightarrow \pi^+ \pi^-)_{SD}$ alone, which we shall discuss here, is on the same footing as the other modes. The essential difficulty for phenomenological applications then is to separate the short-distance from the long-distance piece in the measured rate.
- According to the comments just made, the processes at hand are short-distance processes, calculable within a perturbative framework, possibly including renormalization group improvement. The necessary separation of the short-distance dynamics from the

low energy matrix elements is achieved by means of an operator product expansion. The scale ambiguities, inherent to perturbative QCD, essentially constitute the only theoretical uncertainties present in the analysis. These uncertainties are well under control as they may be systematically reduced through calculations beyond leading order.

The points made above emphasize, that the short-distance dominated loop-induced FCNC decays provide highly promising possibilities to investigate flavourdynamics at the quantum level. However, the very fact that these processes are based on higher order electroweak effects, which makes them interesting theoretically, at the same time implies, that the branching ratios will be very small and not easy to access experimentally.

The effective hamiltonians governing the decays $K^+ \rightarrow \pi^+ \pi^0$, $(K_L \rightarrow \pi^+ \pi^-)_{SD}$, $K_L \rightarrow \pi^0 \pi^0$, $B \rightarrow X_{s,d} \pi$, $B \rightarrow 11$, resulting from the Z^0 -penguin and box-type contributions, can all be written down in the following general form

$$H_{eff} = \frac{G_F}{2} \frac{1}{\sin^2 \theta_W} (c F(x_c) + t F(x_t)) (n n^0)_{V-A} (r r)_{V-A} \quad (XI.1)$$

where n, n^0 denote down-type quarks ($n; n^0 = d; s; b$ but $n \notin n^0$) and r leptons, $r = l; \bar{l}$ ($l = e; \mu; \tau$). The x_i are products of CKM elements, in the general case $x_i = V_{in} V_{in^0}$. Furthermore $x_i = m_i^2/M_W^2$.

The functions $F(x_i)$ describe the dependence on the internal up-type quark masses m_i (and on lepton masses if necessary) and are understood to include QCD corrections. They are increasing functions of the quark masses, a property that is particularly important for the top contribution. Crucial features of the structure of the hamiltonian are furthermore determined by the hard GIM suppression characteristic for this class of decays. First we note that the dependence of the hamiltonian on the internal quarks comes in the form

$$\sum_{i=u,c,t} F(x_i) = c(F(x_c) - F(x_u)) + t(F(x_t) - F(x_u)) \quad (XI.2)$$

where we have used the unitarity of the CKM matrix. Now, hard GIM suppression means that for $x \ll 1$ F behaves quadratically in the quark masses. In the present case we have

$$F(x) \approx x \ln x \quad \text{for } x \ll 1 \quad (XI.3)$$

The first important consequence is, that $F(x_u) = 0$ can be neglected. The hamiltonian acquires the form anticipated in (XI.1). It effectively consists of a charm and a top contribution. Therefore the relevant energy scales are M_W or m_t and, at least, m_c , which are large compared to Q_{CD} . This fact indicates the short-distance nature of these processes.

A second consequence of (XI.3) is that $F(x_c) \approx F(x_t) \approx O(10^{-3}) \ll 1$. Together with the weighting introduced by the CKM factors this relation determines the relative importance of the charm versus the top contribution in (XI.1). As seen in table XXXII a simple pattern emerges if one writes down the order of magnitude of c, t in terms of powers of the Wolfenstein expansion parameter λ .

For the CP-violating decay $K_L \rightarrow \pi^0 \pi^0$ and the B-decays the CKM factors c and t have the same order of magnitude. In view of $F(x_c) \approx F(x_t)$ the charm contribution is therefore

TABLE XXXII. Order of magnitude of CKM parameters relevant for the various decays, expressed in powers of the Wolfenstein parameter $\lambda = 0.22$. In the case of $K_L \rightarrow \pi^0$, which is CP-violating, only the imaginary parts of c_{cb} contribute.

	$K^+ \rightarrow \pi^+ \pi^0$ ($K_L \rightarrow \pi^+ \pi^-$) _{SD}	$K_L \rightarrow \pi^0$	$B \rightarrow X_s$ $B_s \rightarrow l^+ l^-$	$B \rightarrow X_d$ $B_d \rightarrow l^+ l^-$
c		($\text{Im } c_{cb}$) ⁵	2	3
t	5	($\text{Im } t_{cb}$) ⁵	2	3

negligible and these decays are entirely determined by the top sector.

For $K^+ \rightarrow \pi^+ \pi^0$ and $(K_L \rightarrow \pi^+ \pi^-)_{SD}$ on the other hand t_{cb} is suppressed compared to c_{cb} by a factor of order $O(\lambda^4) \sim O(10^{-3})$, which roughly compensates for the $O(10^3)$ enhancement of $F(x_t)$ over $F(x_c)$. Hence the top and charm contributions have the same order of magnitude and must both be taken into account.

In principle, as far as flavordynamics is concerned, the top and the charm sector have the same structure. The only difference comes from the quark masses. However, this difference has striking implications for the detailed formalism necessary to treat the strong interaction corrections. We have $m_t/M_W = O(1)$ and $m_c/M_W \ll 1$. Correspondingly the QCD coupling α_s is also somewhat smaller at m_t than at m_c . For the charm contribution this implies that one can work to lowest order in the mass ratio m_c/M_W . On the other hand, for the same reason, logarithmic QCD corrections $\alpha_s \ln M_W/m_c$ are large and have to be resummed to all orders in perturbation theory by renormalization group methods. On the contrary, no large logarithms are present in the top sector, so that ordinary perturbation theory is applicable, but all orders in m_t/M_W have to be taken into account. In fact we see that from the point of view of QCD corrections the charm and top contributions are quite “complementary” to each other, representing in a sense opposite limiting cases.

We are now ready to list the explicit expressions for the effective hamiltonians.

B. The Decay $K^+ \rightarrow \pi^+ \pi^0$

1. The Next-to-Leading Order Effective Hamiltonian

The final result for the effective hamiltonian inducing $K^+ \rightarrow \pi^+ \pi^0$ can be written as

$$H_{\text{eff}} = \frac{G_F}{2} \frac{1}{\sin^2 \theta_W} \sum_{l=e,\mu} X_{l\pi} V_{cs} V_{cd} X_{N_L}^1 + V_{ts} V_{td} X(x_t) (sd)_{V-A} (l\bar{l})_{V-A} : \quad (\text{XI.4})$$

The index $l=e, \mu$, denotes the lepton flavor. The dependence on the charged lepton mass, resulting from the box-graph, is negligible for the top contribution. In the charm sector this is the case only for the electron and the muon, but not for the τ -lepton.

The function $X(x)$, relevant for the top part, reads to $O(\lambda^2)$ and to all orders in $x = m^2/M_W^2$

$$X(x) = X_0(x) + \frac{s}{4} X_1(x) \quad (\text{XI.5})$$

with (Inami and Lim, 1981)

$$X_0(x) = \frac{x}{8} \left[\frac{2+x}{1-x} + \frac{3x}{(1-x)^2} \ln x \right] \quad (\text{XI.6})$$

and the QCD correction (Buchalla and Buras, 1993a)

$$\begin{aligned} X_1(x) = & \frac{23x + 5x^2}{3(1-x)^2} + \frac{4x^3}{(1-x)^3} + \frac{x}{(1-x)^3} \ln x \\ & + \frac{8x + 4x^2 + x^3}{2(1-x)^3} \ln^2 x - \frac{4x}{(1-x)^2} L_2(1-x) \\ & + 8x \frac{\partial X_0(x)}{\partial x} \ln x \end{aligned} \quad (\text{XI.7})$$

where $x = \frac{m_c^2}{M_W^2}$ with $m_c = O(m_t)$ and

$$L_2(1-x) = \int_1^x \frac{\ln t}{1-t} dt \quad (\text{XI.8})$$

The x -dependence in the last term in (XI.7) cancels to the order considered the x -dependence of the leading term $X_0(x)$.

The expression corresponding to $X(x_t)$ in the charm sector is the function X_{NL}^1 . It results from the RG calculation in NLLA and is given as follows:

$$X_{NL}^1 = C_{NL} - 4B_{NL}^{(1=2)} \quad (\text{XI.9})$$

C_{NL} and $B_{NL}^{(1=2)}$ correspond to the Z^0 -penguin and the box-type contribution, respectively. One has (Buchalla and Buras, 1994a)

$$\begin{aligned} C_{NL} = & \frac{x(m_c)}{32} K_c^{24} \left[\frac{48}{7} K_+ + \frac{24}{11} K_- + \frac{696}{77} K_{33} - \frac{4}{s_c^2} + \frac{15212}{1875} (1 - K_c^1) \right] \\ & + \frac{1}{m^2} \ln^2 \left[(16K_+ - 8K_-) \frac{1176244}{13125} K_+ + \frac{2302}{6875} K_- + \frac{3529184}{48125} K_{33} \right] \\ & + K \left[\frac{56248}{4375} K_+ + \frac{81448}{6875} K_- + \frac{4563698}{144375} K_{33} \right] \end{aligned} \quad (\text{XI.10})$$

where

$$K = \frac{s(M_W)}{s(m_c)} \quad K_c = \frac{s_c}{s(m_c)} \quad (\text{XI.11})$$

$$K_+ = K^{\frac{6}{25}} \quad K_- = K^{\frac{12}{25}} \quad K_{33} = K^{\frac{1}{25}} \quad (\text{XI.12})$$

$$\begin{aligned} B_{NL}^{(1=2)} = & \frac{x(m_c)}{4} K_c^{24} \left[3(1 - K_2) - \frac{4}{s_c^2} + \frac{15212}{1875} (1 - K_c^1) \right] \\ & + \frac{\ln^2}{m^2} \left[\frac{r \ln r}{1-r} - \frac{305}{12} + \frac{15212}{625} K_2 + \frac{15581}{7500} K_{K_2} \right] \end{aligned} \quad (\text{XI.13})$$

Here $K_2 = K^{1=25}$, $m = m_c$, $r = m_1^2 = m_c^2$ and m_l is the lepton mass. We will at times omit the index l of X_{NL}^1 . In (XI.10) – (XI.13) the scale is $\mu = O(m_c)$. The two-loop expression for $s(\mu)$ is given in (III.19). Again – to the considered order – the explicit $\ln(\mu^2 = m_c^2)$ terms in (XI.10) and (XI.13) cancel the μ -dependence of the leading terms.

These formulae give the complete next-to-leading effective hamiltonian for $K^+ \rightarrow \pi^+ \pi^0$. The leading order expressions (Novikov *et al.*, 1977), (Ellis and Hagelin, 1983), (Dib *et al.*, 1991), (Buchalla *et al.*, 1991) are obtained by replacing $X(x_t) \rightarrow X_0(x_t)$ and $X_{NL}^1 \rightarrow X_L$ with X_L found from (XI.10) and (XI.13) by retaining there only the $1 = s(\mu)$ terms. In LLA the one-loop expression should be used for s . This amounts to setting $\mu = 0$ in (III.19). The numerical values for X_{NL} for $\mu = m_c$ and several values of $\frac{(4)}{MS}$ and $m_c(m_c)$ are given in table XXXIII. The dependence will be discussed in part three.

TABLE XXXIII. The functions X_{NL}^e and X_{NL} for various $\frac{(4)}{MS}$ and m_c .

	$X_{NL}^e = 10^{-4}$			$X_{NL} = 10^{-4}$		
$\frac{(4)}{MS}$ [M eV] m_c [GeV]	1.25	1.30	1.35	1.25	1.30	1.35
215	10.55	11.40	12.28	7.16	7.86	8.59
325	9.71	10.55	11.41	6.32	7.01	7.72
435	8.75	9.59	10.45	5.37	6.05	6.76

2. Z-Penguin and Box Contribution in the Top Sector

For completeness we give here in addition the expressions for the Z^0 -penguin function $C(x)$ and the box function $B(x; 1=2)$ separately, which contribute to $X(x)$ in (XI.5) according to

$$X(x) = C(x) - 4B(x; 1=2) \quad (XI.14)$$

The functions C and B depend on the gauge of the W -boson. In 't Hooft–Feynman-gauge ($\epsilon = 1$) they read

$$C(x) = C_0(x) + \frac{s}{4} C_1(x) \quad (XI.15)$$

where (Inami and Lim, 1981)

$$C_0(x) = \frac{x}{8} \frac{6}{1-x} + \frac{3x+2}{(1-x)^2} \ln x \quad (XI.16)$$

and (Buchalla and Buras, 1993b)

$$C_1(x) = \frac{29x + 7x^2 + 4x^3}{3(1-x)^2} - \frac{x}{3(1-x)^2} \frac{35x^2 - 3x^3 - 3x^4}{(1-x)^2} \ln x \\ + \frac{20x^2 - x^3 + x^4}{2(1-x)^2} \ln^2 x + \frac{4x + x^3}{(1-x)^2} L_2(1-x) \\ + 8x \frac{\partial C_0(x)}{\partial x} \ln x \quad (XI.17)$$

Similarly

$$B(x; 1=2) = B_0(x) + \frac{s}{4} B_1(x; 1=2) \quad (\text{XI.18})$$

with the one-loop function (Inami and Lim, 1981)

$$B_0(x) = \frac{1}{4} \left[\frac{x}{1-x} + \frac{x}{(1-x)^2} \ln x \right] \quad (\text{XI.19})$$

and (Buchalla and Buras, 1993a)

$$B_1(x; 1=2) = \frac{13x + 3x^2}{3(1-x)^2} \frac{x}{3(1-x)^3} \ln x - \frac{x + 3x^2}{(1-x)^3} \ln^2 x + \frac{2x}{(1-x)^2} L_2(1-x) + 8x \frac{\partial B_0(x)}{\partial x} \ln x \quad (\text{XI.20})$$

The gauge dependence of C and B is canceled in the combination X (XI.14). The second argument in $B(x; 1=2)$ indicates the weak isospin of the external leptons (the neutrinos in this case).

3. The Z-Penguin Contribution in the Charm Sector

In the next two paragraphs we would like to summarize the essential ingredients of the RG calculation for the charm sector leading to (XI.10) and (XI.13). In particular we present the operators involved, the initial values for the RG evolution of the Wilson coefficients and the required two-loop anomalous dimensions. We will first treat the Z^0 -penguin contribution (XI.10) and discuss the box part (XI.13) subsequently. Further details can be found in (Buchalla and Buras, 1994a).

At renormalization scales of the order $O(M_W)$ and after integrating out the W - and Z -bosons the effective hamiltonian responsible for the Z^0 -penguin contribution of the charm sector is given by

$$H_{\text{eff}, Z}^{(Z)} = \frac{G_F}{2} \frac{1}{\sin^2 \theta_W} \sum_i c_i \frac{1}{M_W^2} (V_{i+} O_{i+} + V_i O_i + V_{i3} Q) \quad (\text{XI.21})$$

where the operator basis is

$$O_1 = i \bar{d} \gamma^\mu T^a ((s_i c_j)_{V-A} (c_j d_i)_{V-A}) (x) ((\bar{q}_k c_k)_{V-A} (\bar{l} l)_A) (0) \quad \text{fc ! ug} \quad (\text{XI.22})$$

$$O_2 = i \bar{d} \gamma^\mu T^a ((s_i c_1)_{V-A} (c_j d_j)_{V-A}) (x) ((\bar{q}_k c_k)_{V-A} (\bar{l} l)_A) (0) \quad \text{fc ! ug} \quad (\text{XI.23})$$

$$O = \frac{1}{2} (O_2 - O_1) \quad (\text{XI.24})$$

$$Q = \frac{m^2}{g^2} (sd)_{V-A} (\bar{l} l)_A \quad (\text{XI.25})$$

The Wilson coefficients at $\mu = M_W$ are $(\mathbf{v}^T = (v_1; v_2; v_3))$

$$\mathbf{v}(M_W) = \mathbf{v}^{(0)} + \frac{s(M_W)}{4} \mathbf{v}^{(1)} \quad (\text{XI.26})$$

$$\mathbf{v}^{(0)T} = (1; 1; 0) \quad (\text{XI.27})$$

$$\mathbf{v}^{(1)T} = (B_+; B_-; B_3) \quad (\text{XI.28})$$

where in the NDR scheme (\overline{MS} , anticommuting γ_5 in $D = 4$ dimensions)

$$B_{\pm} = 11 \frac{N}{2N} - 1, \quad B_3 = 16 \quad (\text{XI.29})$$

with N denoting the number of colors.

In the basis of operators $\{O_1; O_2; O_3\}$ the matrix of anomalous dimensions has the form

$$= \begin{pmatrix} 0 & 0 & 1 \\ B_+ & 0 & +3 \\ 0 & 0 & 33 \end{pmatrix} C_A \quad (\text{XI.30})$$

with the perturbative expansion

$$(\gamma_s) = \frac{s}{4} \gamma^{(0)} + \frac{s^2}{4} \gamma^{(1)} \quad (\text{XI.31})$$

The nonvanishing entries of the anomalous dimension matrix read

$$\begin{aligned} \gamma_{33}^{(0)} &= 2(\gamma_{m0} - \gamma_0) & \gamma_{33}^{(1)} &= 2(\gamma_{m1} - \gamma_1) \\ \gamma_{33}^{(0)} &= \frac{N-1}{6} & \gamma_{33}^{(1)} &= \frac{N-1}{2N} - 21 \frac{57}{N} - \frac{19}{3}N - \frac{4}{3}f \\ \gamma_3^{(0)} &= 8(N-1) & \gamma_3^{(1)} &= C_F(88N-48) \end{aligned} \quad (\text{XI.32})$$

where $\gamma_{m0}, \gamma_{m1}, \gamma_0, \gamma_1$ can be found in (III.17) and (III.16), respectively. The expressions $\gamma^{(1)}$ refer to the NDR scheme, consistent with the scheme chosen for $\mathbf{v}(M_W)$. Following the general method for the solution of the RG equations explained in section III F 1, we can compute the Wilson coefficients $\mathbf{v}(\mu)$ at a scale $\mu = O(m_c)$. It is convenient to work in an effective four-flavor theory ($f = 4$) in the full range of the RG evolution from M_W down to μ . The possible inclusion of a b -quark threshold would change the result for X_{NL} by not more than 0.1% and can therefore be safely neglected.

After integrating out the charm quark at the scale $\mu = O(m_c)$, the Z^0 -penguin part of the charm contribution to the effective hamiltonian becomes

$$H_{eff}^{(Z)} = \frac{G_F}{2} \frac{1}{\sin^2 \theta_W} C_{NL} (sd)_V A(\mu) \quad (\text{XI.33})$$

$$C_{NL} = \frac{x(\mu)}{32} \frac{1}{2} \left(1 - \ln \frac{\mu^2}{m^2} \right) + \gamma_{+3}^{(0)} K_+ + \gamma_3^{(0)} K + \frac{4}{s(\mu)} v_3(\mu) \quad (\text{XI.34})$$

The explicit expression for $v_3(\mu)$ as obtained from solving the RG equation is given in (Buchalla and Buras, 1994a). Inserting this expression in (XI.34), expressing the charm quark mass $m(\mu)$ in terms of $m(m)$ and setting $N = 3, f = 4$, we finally end up with (XI.10).

4. The Box Contribution in the Charm Sector

The RG analysis for the box contribution proceeds in analogy to the Z^0 -penguin case. The box part is even somewhat simpler. When the W boson is integrated out, the hamiltonian based on the box diagram reads

$$H_{\text{eff}\mathcal{R}}^{(B)} = \frac{G_F}{\sqrt{2}} \frac{1}{\sin^2 \theta_W} c \frac{1}{M_W^2} (c_1 O + c_2 Q) \quad (\text{XI.35})$$

$$O = \frac{1}{i} \int d^4 x T ((\bar{s}c)_{V-A} (\bar{l}l)_{V-A}) (x) (l \gamma_\mu A (\bar{s}d)_{V-A} (0)) \quad \text{fc ! ug} \quad (\text{XI.36})$$

with Q already given in (XI.25). The Wilson coefficients at M_W in the NDR scheme are given by

$$c^T(M_W) = (c_1(M_W); c_2(M_W)) = (1; 0) + \frac{s(M_W)}{4} (0; B_2) \quad B_2 = 36 \quad (\text{XI.37})$$

In the operator basis $\{O; Q\}$ the anomalous dimension matrix has the form

$$= \begin{pmatrix} 0 & 12 \\ 0 & 22 \end{pmatrix} \quad (\text{XI.38})$$

When expanded as

$$= \frac{s}{4} (0) + \frac{s}{4} (1) \quad (\text{XI.39})$$

the non-zero elements read (NDR scheme for (1))

$$\begin{aligned} \gamma_{22}^{(0)} &= 2 \begin{pmatrix} m_0 & 0 \end{pmatrix} & \gamma_{22}^{(1)} &= 2 \begin{pmatrix} m_1 & 1 \end{pmatrix} \\ \gamma_{12}^{(0)} &= 32 & \gamma_{12}^{(1)} &= 80 C_F \end{aligned} \quad (\text{XI.40})$$

Finally, after integrating out charm at $\mu = O(m_c)$

$$H_{\text{eff}\mathcal{R}}^{(B)} = \frac{G_F}{\sqrt{2}} \frac{1}{\sin^2 \theta_W} c 4 B_{NL}^{(l=2)} (\bar{s}d)_{V-A} (\bar{l}l)_{V-A} \quad (\text{XI.41})$$

$$B_{NL}^{(l=2)} = \frac{x(\mu)}{64} \left[16 \ln \frac{\mu^2}{m^2} + \frac{5}{4} + \frac{r \ln r}{1-r} \right] + \frac{4}{s(\mu)} c_2(\mu) \quad (\text{XI.42})$$

(XI.41) is written here for one neutrino flavor. The index $(l=2)$ refers to the weak isospin of the final state leptons. From this result (XI.13) can be derived ($N = 3, f = 4$). The explicit expression for $c_2(\mu)$ can be found in (Buchalla and Buras, 1994a).

Although Wilson coefficients and anomalous dimensions depend on the renormalization scheme, the final results in (XI.10) and (XI.13) are free from this dependence. The argument proceeds as in the general case presented in section III F 3.

5. Discussion

It is instructive to consider furthermore the function $X(x)$ in the limiting case of small masses ($x \ll 1$), keeping only terms linear in x and including $O(s)$ corrections:

$$X(x) \doteq \frac{3}{4}x \ln x - \frac{1}{4}x + \frac{s}{4} - 2x \ln^2 x - 7x \ln x - \frac{23 + 2s}{3}x \quad (\text{XI.43})$$

This simple and transparent expression can be regarded as a common limiting case of the top- and the charm contribution: On the one hand it follows from keeping only terms linear in x in the top function (XI.5). On the other hand it can be obtained (up to the last term in (XI.43) which is $O(sx)$ and goes beyond the NLLA) from expanding X_{NL} (XI.9) (for $m_t = 0$) to first order in s . This exercise provides one with a nice cross-check between the rather different looking functions X_{NL} and $X(x_t)$ of the charm- and the top sector. Viewed the other way around, (XI.43) may serve to further illustrate the complementary character of the calculations necessary in each of the two sectors. $X(x_t)$ is the generalization of (XI.43) that includes all the higher order mass terms. X_{NL} on the other hand generalizes (XI.43) to include all the leading logarithmic, $O(x \ln^{n+1} x)$, as well as the next-to-leading logarithmic $O(x \ln^n x)$ corrections, to all orders n in s . Of these only the terms with $n = 0$ and $n = 1$ are contained in (XI.43).

Applying the approximation (XI.43) to the charm part directly, one can furthermore convince oneself, that the $O(s)$ correction term would amount to more than 50% of the lowest order result. This observation illustrates very clearly the necessity to go beyond straightforward perturbation theory and to employ the RG summation technique. The importance of going still to next-to-leading order accuracy in the RG calculation is suggested by the relatively large size of the $O(x \ln x)$ term. Note also, that formally the non-logarithmic mass term ($x=4$) in (XI.43) is a next-to-leading order effect in the framework of RG improved perturbation theory. The same is true for the dependence on the charged lepton mass, which can be taken into account consistently only in NLLA.

A crucial issue is the residual dependence of the functions X_{NL} and $X(x_t)$ on the corresponding renormalization scales μ_c and μ_t . Since the quark current operator in (XI.1) has no anomalous dimension, its matrix elements do not depend on the renormalization scale. The same must then hold for the coefficient functions X_{NL} and $X(x_t)$. However, in practice this is only true up to terms of the neglected order in perturbation theory. The resulting scale ambiguities represent the theoretical uncertainties present in the calculation of the short-distance dominated processes under discussion. They can be systematically reduced by going to higher orders in the analysis. In table XXXIV we compare the order of the residual scale dependence in LLA and in NLLA for the top- and the charm contribution.

TABLE XXXIV. Residual scale ambiguity in the top and charm sector in LLA and NLLA.

	Top Sector ($\mu_t = O(m_t)$)	Charm Sector ($\mu_c = O(m_c)$)
LLA	$O(s)$	$O(x_c)$
NLLA	$O(s^2)$	$O(sx_c)$

For numerical investigations we shall use $1 \text{ GeV} \leq \mu_c \leq 3 \text{ GeV}$ for the renormalization scale $\mu_c = O(m_c)$ in the charm sector. Similarly, in the case of the top contribution we choose $\mu_t =$

$O(m_t)$ in the range $100 \text{ GeV} < m_t < 300 \text{ GeV}$ for $m_t = 170 \text{ GeV}$. Then, comparing LLA and NLLA, the theoretical uncertainty due to scale ambiguity is typically reduced from $O(10\%)$ to $O(1\%)$ in the top sector and from more than 50% to less than 20% in the charm sector. Here the quoted percentages refer to the total variation $(X_{\text{max}} - X_{\text{min}})/X_{\text{central}}$ of the functions $X(x_t)$ or X_{NL} within the range of scales considered. Phenomenological implications of this gain in accuracy will be discussed in section XXIV.

C. The Decay $(K_L \rightarrow \ell^+ \ell^-)_{SD}$

1. The Next-to-Leading Order Effective Hamiltonian

The analysis of $(K_L \rightarrow \ell^+ \ell^-)_{SD}$ proceeds in essentially the same manner as for $K^+ \rightarrow \ell^+ \ell^-$. The only difference is introduced through the reversed lepton line in the box contribution. In particular there is no lepton mass dependence, since only massless neutrinos appear as virtual leptons in the box diagram.

The effective hamiltonian in next-to-leading order can be written as follows:

$$H_{\text{eff}} = \frac{G_F}{2} \frac{1}{\sin^2 \theta_W} (V_{cs} V_{cd} Y_{NL} + V_{ts} V_{td} Y(x_t)) (sd)_{V-A} (\ell^+ \ell^-)_{V-A} + \text{h.c.} \quad (\text{XI.44})$$

The function $Y(x)$ is given by

$$Y(x) = Y_0(x) + \frac{s}{4} Y_1(x) \quad (\text{XI.45})$$

where (Inami and Lim, 1981)

$$Y_0(x) = \frac{x}{8} \left[\frac{4}{1-x} + \frac{3x}{(1-x)^2} \ln x \right] \quad (\text{XI.46})$$

and (Buchalla and Buras, 1993a)

$$\begin{aligned} Y_1(x) = & \frac{4x + 16x^2 + 4x^3}{3(1-x)^2} - \frac{4x - 10x^2 - x^3 - x^4}{(1-x)^3} \ln x \\ & + \frac{2x - 14x^2 + x^3 - x^4}{2(1-x)^3} \ln^2 x + \frac{2x + x^3}{(1-x)^2} L_2(1-x) \\ & + 8x \frac{\partial Y_0(x)}{\partial x} \ln x \end{aligned} \quad (\text{XI.47})$$

The RG expression Y_{NL} representing the charm contribution reads

$$Y_{NL} = C_{NL} B_{NL}^{(1=2)} \quad (\text{XI.48})$$

where C_{NL} is the Z^0 -penguin part given in (XI.10) and $B_{NL}^{(1=2)}$ is the box contribution in the charm sector, relevant for the case of final state leptons with weak isospin $T_3 = \pm 1/2$. One has (Buchalla and Buras, 1994a)

$$B_{NL}^{(1=2)} = \frac{x(m)}{4} K_c^{\frac{24}{25}} \left(3(1 - K_2) \frac{4}{s(\cdot)} + \frac{15212}{1875} (1 - K_c^{-1}) \right) \ln \frac{2}{m^2} + \frac{329}{12} + \frac{15212}{625} K_2 + \frac{30581}{7500} K K_2 \quad (XI.49)$$

Note the simple relation to $B_{NL}^{(1=2)}$ in (XI.13) (for $r = 0$)

$$B_{NL}^{(1=2)} - B_{NL}^{(1=2)} = \frac{x(m)}{2} K_c^{\frac{24}{25}} (K K_2 - 1) \quad (XI.50)$$

More details on the RG analysis in this case may be found in (Buchalla and Buras, 1994a).

TABLE XXXV. The function Y_{NL} for various $\frac{(4)}{MS}$ and m_c .

	$Y_{NL}=10^{-4}$		
$\frac{(4)}{MS}$ [M eV] n m _c [G eV]	1.25	1.30	1.35
215	3.09	3.31	3.53
325	3.27	3.50	3.73
435	3.40	3.64	3.89

2. Discussion

The gauge independent function Y can be decomposed into the Z^0 -penguin- and the box contribution

$$Y(x) = C(x) - B(x; 1=2) \quad (XI.51)$$

In Feynman-gauge for the W boson $C(x)$ is given in (XI.15). In the same gauge the box contribution reads

$$B(x; 1=2) = B_0(x) + \frac{s}{4} B_1(x; 1=2) \quad (XI.52)$$

with $B_0(x)$ from (XI.19) and

$$B_1(x; 1=2) = \frac{25x - 9x^2}{3(1 - x^2)} + \frac{11x + 5x^2}{3(1 - x^2)} \ln x - \frac{x + 3x^2}{(1 - x^2)} \ln^2 x + \frac{2x}{(1 - x^2)} L_2(1 - x) + 8x \frac{\partial B_0(x)}{\partial x} \ln x \quad (XI.53)$$

The equality $B(x; 1=2) = B(x; 1=2)$ at the one-loop level is a particular property of the Feynman-gauge. It is violated by $O(s)$ corrections. There is however a very simple relation between $B_1(x; 1=2)$ and $B_1(x; 1=2)$

$$B_1(x; 1=2) - B_1(x; 1=2) = 16B_0(x) \quad (XI.54)$$

We add a few comments on the most important differences between Y_{NL} and X_{NL} . Expanding Y_{NL} to first order in s we find

$$Y_{NL} = \frac{1}{2}x + \frac{s}{4}x \ln^2 x + O(sx) \quad (XI.55)$$

In contrast to X_{NL} both the terms of $O(x \ln x)$ and of $O(sx \ln x)$ are absent in Y_{NL} . The cancellation of the leading $O(x \ln x)$ terms between Z^0 -penguin and box contribution implies that the non-leading $O(x)$ term plays a much bigger role for Y_{NL} . A second consequence are the increased importance of QCD effects and the related larger sensitivity to m_c , resulting in a bigger theoretical uncertainty for Y_{NL} than it happened to be the case for X_{NL} . In addition, whereas $X(x_c)$ is suppressed by 30% through QCD effects, the zeroth order expression for Y is enhanced by as much as a factor of about 2.5. Nevertheless, QCD corrections included, X_{NL} still exceeds Y_{NL} by a factor of four, so that Y_{NL} is less important for $(K_L \rightarrow \pi^+ \pi^-)_{SD}$ than X_{NL} is for $K^+ \rightarrow \pi^+ \pi^-$. Although the impact of the bigger uncertainties in Y_{NL} is thus somewhat reduced in the complete result for $(K_L \rightarrow \pi^+ \pi^-)_{SD}$, the remaining theoretical uncertainty due to scale ambiguity is still larger than for $K^+ \rightarrow \pi^+ \pi^-$. It will be investigated numerically in section XXV. The numerical values for Y_{NL} for $m_c = m_c$ and several values of $\frac{(4)}{MS}$ and $m_c(m_c)$ are given in table XXXV.

D. The Decays $K_L \rightarrow \pi^0, B \rightarrow X_{sd}$ and $B_{sd} \rightarrow \pi^+ \pi^-$

After the above discussion it is easy to write down also the effective hamiltonians for $K_L \rightarrow \pi^0, B \rightarrow X_{sd}$ and $B_{sd} \rightarrow \pi^+ \pi^-$. As we have seen, only the top contribution is important in these cases and we can write

$$H_{eff} = \frac{G_F}{2} \frac{1}{\sin^2 \theta_w} V_{tn} V_{tn}^* X(x_t) (nn^0)_{V-A} + h.c. \quad (XI.56)$$

for the decays $K_L \rightarrow \pi^0, B \rightarrow X_s$ and $B \rightarrow X_d$, with $(nn^0) = (sd), (bs), (bd)$ respectively. Similarly

$$H_{eff} = \frac{G_F}{2} \frac{1}{\sin^2 \theta_w} V_{tn} V_{tn}^* Y(x_t) (nn^0)_{V-A} (ll)_{V-A} + h.c. \quad (XI.57)$$

for $B_s \rightarrow \pi^+ \pi^-$ and $B_d \rightarrow \pi^+ \pi^-$, with $(nn^0) = (bs), (bd)$. The functions X, Y are given in (XI.5) and (XI.45).

XII. THE EFFECTIVE HAMILTONIAN FOR $K^0 - \bar{K}^0$ MIXING

A. General Structure

The following chapter is devoted to the presentation of the effective hamiltonian for $S = 2$ transitions. This hamiltonian incorporates the short-distance physics contributing to $K^0 - \bar{K}^0$ mixing and is essential for the description of CP violation in the neutral K-meson system. Being a FCNC process, $K^0 - \bar{K}^0$ mixing can only occur at the loop level within the Standard Model. To lowest order it is induced through the box diagrams in fig. 4 (e). Including QCD corrections the effective low energy hamiltonian, to be derived from these diagrams, can be written as follows ($i = V_{is}V_{id}$)

$$H_{eff}^{S=2} = \frac{G_F^2}{16} M_W^2 \sum_{i,j} V_{is}^i V_{id}^j \left[S_0(x_c) + \frac{1}{2} S_0(x_t) + \frac{1}{2} S_0(x_c, x_t) \right] \times \left[1 + \frac{s(\mu)}{4} J_3(Q) + h.c. \right] \quad (XII.1)$$

This equation, together with (XII.31), (XII.10), (XII.68) for $i = 1, 2$ and $j = 3$ respectively, represents the complete next-to-leading order short-distance hamiltonian for $S = 2$ transitions. (XII.1) is valid for scales below the charm threshold $\mu_c = O(m_c)$. In this case $H_{eff}^{S=2}$ consists of a single four-quark operator

$$Q = (\bar{s}d)_{V-A} (\bar{s}d)_{V-A} \quad (XII.2)$$

which is multiplied by the corresponding coefficient function. It is useful and customary to decompose this function into a charm-, a top- and a mixed charm-top contribution, as displayed in (XII.1). This form is obtained upon eliminating x_u by means of CKM matrix unitarity and setting $x_u = 0$. The basic electroweak loop contributions without QCD correction are then expressed through the functions S_0 , which read (Inami and Lim, 1981)

$$S_0(x_c) = x_c \quad (XII.3)$$

$$S_0(x_t) = \frac{4x_t}{4(1-x_t)^2} - \frac{11x_t^2 + x_t^3}{2(1-x_t)^3} \quad (XII.4)$$

$$S_0(x_c, x_t) = x_c \ln \frac{x_t}{x_c} - \frac{3x_t}{4(1-x_t)} - \frac{3x_t^2 \ln x_t}{4(1-x_t)^2} \quad (XII.5)$$

Here again we keep only linear terms in $x_c \ll 1$, but of course all orders in x_t . Short-distance QCD effects are described through the correction factors α_s , β , γ and the explicitly μ -dependent terms in (XII.1). The discussion of these corrections will be the subject of the following sections.

Without QCD, i.e. in the limit $\alpha_s \rightarrow 0$, one has $\alpha_s[\mu] \rightarrow 0$. In general, the complete coefficient function multiplying Q in (XII.1) contains the QCD effects at high energies $\mu_W = O(M_W)$, $\mu_t = O(m_t)$ together with their RG evolution down to the scale $\mu = O(1 \text{ GeV})$. A common ingredient for the three different contributions in (XII.1) is the anomalous dimension of the operator Q and

the corresponding evolution of its coefficient. The Fierz symmetric flavor structure of Q implies that it acquires the same anomalous dimension as the Fierz symmetric operator $Q_+ = (Q_2 + Q_1)/2$ (see section V), explicitly

$$= \frac{s}{4} {}^{(0)} + \frac{s}{4} {}^{(1)} \quad (\text{XII.6})$$

$${}^{(0)} = \frac{N}{6} \frac{1}{N} \quad {}^{(1)} = \frac{N}{2N} \frac{1}{2N} \left(21 + \frac{57}{N} \right) \frac{19}{3} N + \frac{4}{3} f \quad (\overline{\text{NDR}}) \quad (\text{XII.7})$$

The resulting evolution of the coefficient of Q between general scales μ_1 and μ_2 then reads

$$C_Q(\mu_2) = \left[1 + \frac{s(\mu_2) - s(\mu_1)}{4} J_f \right]^{d_f} \frac{s(\mu_1)}{s(\mu_2)} C_Q(\mu_1) \quad (\text{XII.8})$$

where

$$d_f = \frac{{}^{(0)}}{2} \quad J_f = \frac{d_f}{0} \mu_1 \quad \frac{{}^{(1)}}{2} \mu_0 \quad (\text{XII.9})$$

depend on the number of active flavors f . At the lower end of the evolution $f = 3$. The terms in (XII.8) depending on $s(\mu)$ are factored out explicitly in (XII.1) to exhibit the μ -dependence of the coefficient function in the $f = 3$ regime, which has to cancel the corresponding μ -dependence of the hadronic matrix element of Q between meson states in physical applications. A similar comment applies to the scheme dependence entering J_f in (XII.9) through the scheme dependence of $d_f^{(1)}$. Splitting off the μ -dependence in (XII.1) is of course not unique. The way it is done belongs to the *definition* of the μ -factors.

Let us finally compare the structure of (XII.1) with the effective hamiltonians for rare decays discussed in chapter XI. Common features of both types of processes include:

Both are generated to lowest order via electroweak FCNC loop transitions involving heavy quarks.

They contain a charm and a top contribution.

The hamiltonian consists of a single dimension-6 operator.

Besides these similarities, however, there are also a few important differences, which have their root in the fact that the $S = 2$ box diagrams involve two distinct quark lines as compared to the single quark line in semileptonic rare decays:

The CKM parameter combinations λ_i appear quadratically in (XII.1) instead of only linearly.

(XII.1) in addition receives contributions from a mixed top-charm sector. This part in fact turns out to have the most involved structure of the three contributions.

The operator Q has a non-vanishing QCD anomalous dimension, resulting in a non-trivial scale and scheme dependence of the Wilson coefficient.

We will now present the complete next-to-leading order results for σ_2 , σ_1 and σ_3 in turn and discuss their most important theoretical features. The first leading log calculations of σ_1 have been presented in (Vainshtein *et al.*, 1976), (Novikov *et al.*, 1977) and of σ_2 in (Vysotskij, 1980). The complete leading log calculation including also σ_3 has been first performed in (Gilman and Wise, 1983). Leading order calculations in the presence of a heavy top can be found in (Kaufman *et al.*, 1989), (Flynn, 1990), (Datta *et al.*, 1990) and (Datta *et al.*, 1995).

The basic structure of the top quark sector in $H_{\text{eff}}^{S=2}$ is easy to understand. First the top quark is integrated out, along with the W , at a matching scale $\mu_t = O(m_t)$, leaving a m_t -dependent coefficient normalized at μ_t , multiplying the single operator Q . Subsequently the coefficient is simply renormalized down to scales $\mu = O(1 \text{ GeV})$ by means of (XII.8). Including NLO corrections the resulting QCD factor ρ from (XII.1) may be written (in \overline{MS}) as follows (Buras *et al.*, 1990)

where $m_0 = 6C_F$,

and

$$S_1^{(8)}(x) = \frac{64}{4(1-x)^2} + \frac{32}{2(1-x)^3} \ln x + \frac{x^2(4-7x+7x^2-2x^3)}{2(1-x)^4} \ln^2 x + \frac{2x(4-7x+7x^2+x^3)}{(1-x)^3} L_2(1-x) + \frac{16}{x} \frac{1}{6} L_2(1-x) \quad (\text{XII.13})$$

103

where the dilogarithm L_2 is defined in (XI.8).

In the expression (XII.10) we have taken into account the heavy quark thresholds at m_b and m_c in the RG evolution. As it must be, the dependence on the threshold scales is of the neglected order $O(\frac{2}{s})$. In fact the threshold ambiguity is here of $O(\frac{2}{s})$ also in LLA since $^{(0)}$ is flavor independent. It turns out that this dependence is also very weak numerically and we therefore set $\mu_c = m_c$ and $\mu_b = m_b$. Furthermore it is a good approximation to neglect the b-threshold completely using an effective 4-flavor theory from μ_t down to m_c . This can be achieved by simply substituting $m_b \rightarrow \mu_t$ in (XII.10).

The leading order expression for α_s is given by the first three factors on the r.h.s. of (XII.10). The fourth factor represents the next-to-leading order generalization. Let us discuss now the most interesting and important features of the NLO result for α_s exhibited in (XII.10).

α_s is proportional to the initial value of the Wilson coefficient function at $\mu_t = M_W$

$$S(x) = S_0(x) + \frac{s}{4} (S_1(x) + B_t S_0(x)) \quad (\text{XII.15})$$

which has to be extracted from the box graphs in fig. 4(e) and the corresponding gluon correction diagrams after a proper factorization of long- and short-distance contributions.

$S(x)$ in (XII.15) is similar to the functions $X(x)$ and $Y(x)$ in sections XI B 1 and XI C 1 except that $S(x)$ is scheme dependent due to the renormalization that is required for the operator \bar{Q} . This scheme dependence enters (XII.15) through the scheme dependent constant B_t , given in the NDR scheme in (XII.11). This scheme dependence is canceled in the combination $B_t \rightarrow J_5$ by the two-loop anomalous dimension contained in J_5 . Likewise the scheme dependence of J_F cancels in the differences $(J_F - J_{F-1})$ as is evident from the discussion of section III F 3.

A very important point is the dependence on the high energy matching scale μ_t . This dependence enters the NLO $\alpha_s(\mu_t)$ -correction in (XII.10) in two distinct ways: First as a term proportional to $^{(0)}$ and, secondly, in conjunction with m_0 . The first of these terms cancels to $O(\frac{2}{s})$ the μ_t -dependence present in the leading term $[\alpha_s(\mu_t)]^{6=23}$. The second, on the other hand, leads to an $O(\frac{2}{s}) \mu_t$ -dependence of α_s which is just the one needed to cancel the μ_t -ambiguity of the leading function $S_0(x_t(\mu_t))$ in the product $\alpha_s S_0(x_t)$, such that in total physical results become independent of μ_t to $O(\frac{2}{s})$. From these observations it is obvious that one may interpret μ_t in the first case as the initial scale of the RG evolution and in the second case as the scale at which the top quark mass is defined. These two scales need not necessarily have the same value.

The important point is, that to leading logarithmic accuracy the μ_t -dependence of both $\frac{L_0}{2}(\mu_t)$ and $S_0(x_t(\mu_t))$ remains uncompensated, leaving a disturbingly large uncertainty in the short-distance calculation.

It is interesting to note that in the limit $m_t \rightarrow M_W$ the dependence on μ_t enters α_s as $\ln \mu_t = m_t$, rather than $\ln \mu_t = M_W$. This feature provides a formal justification for choosing $\mu_t = O(m_t)$ instead of $\mu_t = O(M_W)$. An explicit expression for the large m_t limit in the similar case of α_{2B} may be found in section XIII.

Although at NLO the product ${}_2S_0(x_t)$ depends only very weakly on the precise value of x_t as long as it is of $O(m_t)$, the choice $x_t = m_t$ is again convenient: With this choice ${}_2$ becomes almost independent of the top quark mass m_t (m_t). By contrast, for $x_t = M_W$, say, ${}_2$ would decrease with rising m_t (m_t) in order to compensate for the increase of $S_0(x_t(M_W))$ due to the use of a – for high m_t – “unnaturally” low scale M_W .

As mentioned above the dependence of the Wilson coefficient on the low energy scale and the remaining scheme dependence (J_3) has been factored out explicitly in (XII.1). Therefore the QCD correction factor ${}_2$ is *by definition* scale and scheme independent on the lower end of the RG evolution.

C. The Charm Contribution – ${}_1$

The calculation of ${}_1$ beyond leading logs has been presented in great detail in (Herrlich and Nierste, 1994), (Herrlich, 1994). Our task here will be to briefly describe the basic procedure and to summarize the main results.

In principle the charm contribution is similar in structure to the top contribution. However, since the quark mass $m_c \ll M_W$, the charm degrees of freedom can no longer be integrated out simultaneously with the W boson, which would introduce large logarithmic corrections $\ln M_W/m_c$. To resum these logarithms one first constructs an effective theory at a scale $O(M_W)$, where the W boson is removed. The relevant operators are subsequently renormalized down to scales $\mu_c = O(m_c)$, where the charm quark is then integrated out. After this step only the operator Q (XII.2) remains and ${}_1$ is finally obtained as discussed in section XII A.

Let us briefly outline this procedure for the case at hand. After integrating out W the effective hamiltonian to first order in weak interactions, which is needed for the charm contribution, can be written as

$$H_c^{(1)} = \frac{G_F}{2} \sum_{q,q'=u,c} V_{q's} V_{qd}^* C_+ Q_+^{q'q} + C_- Q_-^{q'q} \quad (XII.16)$$

where we have introduced the familiar $S = 1$ four-quark operators in the multiplicatively renormalizable basis

$$Q^{q'q} = \frac{1}{2} \sum_{i,j} (s_i q_i^0)_{V-A} (q_j d_j)_{V-A} - (s_i q_j^0)_{V-A} (q_j d_i)_{V-A} \quad (XII.17)$$

We remark that no penguin operators appear in the present case due to GIM cancellation between charm quark and up quark contributions.

$S = 2$ transitions occur to second order in the effective interaction (XII.16). The $S = 2$ effective hamiltonian is therefore given by

$$H_{eff;c}^{S=2} = \frac{1}{2} \sum_Z d^4 x T H_c^{(1)}(x) H_c^{(1)}(0) \quad (XII.18)$$

Inserting (XII.16) into (XII.18), keeping only pieces that can contribute to the charm box diagrams and taking the GIM constraints into account, one obtains

$$H_{eff;c}^{S=2} = \frac{G_F^2}{2} \sum_{i,j=+} C_i C_j O_{ij} \quad (XII.19)$$

where

$$O_{ij} = \frac{1}{2} \int d^4x \, T \, Q_i^{\text{cc}}(x) Q_j^{\text{cc}}(0) - Q_i^{\text{uc}}(x) Q_j^{\text{cu}}(0) - Q_i^{\text{cu}}(x) Q_j^{\text{uc}}(0) + Q_i^{\text{uu}}(x) Q_j^{\text{uu}}(0) \quad (\text{XII.20})$$

From the derivation of (XII.19) it is evident, that the Wilson coefficients of the bilocal operators O_{ij} are simply given by the product $C_i C_j$ of the coefficients pertaining to the local operators Q_i , Q_j . The evolution of the C_i from M_W down to μ_c proceeds in the standard fashion and is described by equations of the type shown in (XII.8) with the appropriate anomalous dimensions inserted. In the following we list the required ingredients.

The Wilson coefficients at scale $\mu = M_W$ read

$$C(M_W) = 1 + \frac{s(M_W)}{4} B \quad (\text{XII.21})$$

$$B = 11 \frac{N}{2N} - 1 \quad (\text{NDR}) \quad (\text{XII.22})$$

The two-loop anomalous dimensions are

$$= \frac{s}{4}^{(0)} + \frac{s}{4}^{(1)} \quad (\text{XII.23})$$

$$^{(0)} = 6 \frac{N}{N} - 1 \quad ^{(1)} = \frac{N}{2N} - 1 - 21 \frac{57}{N} - \frac{19}{3} N - \frac{4}{3} f \quad (\text{NDR}) \quad (\text{XII.24})$$

For $i, j = +$; we introduce

$$d_i^{(f)} = \frac{1}{2} \frac{1}{0} \quad J_i^{(f)} = \frac{d_i^{(f)}}{0} - 1 \quad \frac{1}{2} \frac{1}{0} \quad (\text{XII.25})$$

and

$$d_{ij}^{(f)} = d_i^{(f)} + d_j^{(f)} \quad J_{ij}^{(f)} = J_i^{(f)} + J_j^{(f)} \quad (\text{XII.26})$$

The essential step consists in matching (XII.19) onto an effective theory without charm, which will contain the single operator $Q = (sd)_V A (sd)_V A$. In NLO this matching has to be performed to $O(\alpha_s)$. At a normalization scale μ_c it reads explicitly, expressed in terms of operator matrix elements ($i, j = +$;

$$h_{ij} = \frac{m_c^2(\mu_c)}{8} \frac{1}{2} \frac{1}{ij} + \frac{s(\mu_c)}{4} \frac{1}{ij} \ln \frac{m_c^2}{\mu_c^2} + \frac{1}{ij} h_{ij} \quad (\text{XII.27})$$

$$_{++} = \frac{N+3}{4} \quad + = + = \frac{N}{4} - 1 \quad = \frac{N}{4} - 1 \quad (\text{XII.28})$$

$$_{++} = 3(N-1)_{++} \quad + = + = 3(N+1)_{++} \quad = 3(N+3) \quad (\text{XII.29})$$

The c_{ij} are scheme dependent. In the NDR scheme they are given by (Herrlich and Nierste, 1994)

$$\begin{aligned} c_{++} &= (1 - \frac{N}{2}) \frac{N^2 - 6}{12N} + 3 \frac{N^2 + 2N + 13}{4N} \\ c_{+} &= c_{-} = (1 - \frac{N}{2}) \frac{N^2 + 2N - 2}{12N} + \frac{3N^2 + 13}{4N} \\ &= (1 - \frac{N}{2}) \frac{N^2 - 4N + 2}{12N} + \frac{3N^2 + 10N + 13}{4N} \end{aligned} \quad (\text{XII.30})$$

Now, starting from (XII.19), evolving C_i from M_W down to μ_c , integrating out charm at μ_c with the help of (XII.27), evolving the resulting coefficient according to (XII.8) and recalling the definition of c_1 in (XII.1), one finally obtains

$$\begin{aligned} c_1 &= [s(\mu_c)]^{\beta_3} \prod_{ij=+}^X \frac{s(m_b)}{s(\mu_c)} \frac{s(M_W)}{s(m_b)} \\ &\quad \times \left[c_{ij} + \frac{s(\mu_c)}{4} \ln \frac{\mu_c^2}{m_c^2} + c_{ij}^{(4)} J_{ij}^{(4)} + c_{ij}^{(5)} J_{ij}^{(5)} \right. \\ &\quad \left. + c_{ij} \frac{s(m_b)}{4} (J_{ij}^{(5)} - J_{ij}^{(4)}) + \frac{s(M_W)}{4} (B_i + B_j - J_{ij}^{(5)}) \right] \end{aligned} \quad (\text{XII.31})$$

We conclude this section with a discussion of a few important issues concerning the structure of this formula.

(XII.31), as first obtained in (Herrlich and Nierste, 1994), represents the next-to-leading order generalization of the leading log expression for c_1 given in (Gilman and Wise, 1983). The latter follows as a special case of (XII.31) when the $\mathcal{O}(\alpha_s)$ correction terms are put to zero.

The expression (XII.31) is independent of the renormalization scheme up to terms of the neglected order $\mathcal{O}(\alpha_s^2)$. We have written c_1 in a form, in which this scheme independence becomes manifest: While the various J -terms, B_i and c_{ij} in (XII.31) all depend on the renormalization scheme when considered separately, the combinations $c_{ij} (J_{ij}^{(4)} - J_{ij}^{(5)}) + c_{ij} J_{ij}^{(5)} - J_{ij}^{(4)}$ and $B_i + B_j - J_{ij}^{(5)}$ are scheme invariant.

The product $c_1(\mu_c) x_c(\mu_c)$ is independent of μ_c to the considered order,

$$\frac{d}{d \ln \mu_c} c_1(\mu_c) x_c(\mu_c) = \mathcal{O}(\alpha_s^2) \quad (\text{XII.32})$$

in accordance with the requirements of renormalization group invariance. The cancellation of the μ_c -dependence to $\mathcal{O}(\alpha_s)$ is related to the presence of an explicitly μ_c -dependent term at NLO in (XII.31) and is guaranteed through the identity

$$c_{ij} = c_{ij}^{(0)} + \frac{\alpha_s^{(0)}}{2} \left(\frac{c_i^{(0)}}{2} + \frac{c_j^{(0)}}{2} \right) A \quad (\text{XII.33})$$

which is easily verified using (III.17), (XII.7), (XII.24), (XII.28) and (XII.29).

Also the ambiguity in the scale μ_b , at which W is integrated out, is reduced from $\mathcal{O}(\mu_s)$ to $\mathcal{O}(\mu_s^2)$ when going from leading to next-to-leading order. As mentioned above the dependence on the b -threshold scale μ_b is $\mathcal{O}(\mu_s^2)$ in NLLA as well as in LLA. Numerically the dependence on μ_b is very small. Also the variation of the result with the high energy matching scale μ_W is considerably weaker than the residual dependence on μ_c . Therefore we have set $\mu_b = m_b$ and $\mu_W = M_W$ in (XII.31). In numerical analyses we will take the dominant μ_c -dependence as representative for the short-distance scale ambiguity of \mathcal{S}_1 . The generalization to the case $\mu_W \neq M_W$ is discussed in (Herrlich and Nierste, 1994). The more general case $\mu_b \neq m_b$ is trivially obtained by substituting $m_b \rightarrow \mu_b$ in (XII.31).

Note that due to the GIM structure of Q_{ij} no mixing under infinite renormalization occurs between \mathcal{O}_{ij} and the local operator \mathcal{Q} . This is related to the absence of the logarithm in the function $S_0(x_c)$ in (XII.3).

It is instructive to compare the results obtained for \mathcal{S}_1 and \mathcal{S}_2 . Expanding (XII.31) to first order in μ_s , in this way “switching off” the RG summations, we find

$$\begin{aligned} [\mathcal{S}_1(\mu_s)]^{2=9} &= 1 + \frac{\mu_s}{4} J_3 \mathcal{S}_1 = \\ &= 1 + \frac{\mu_s}{4} \frac{(0)}{2} \ln \frac{\mu_c^2}{M_W^2} + \ln \frac{m_c^2}{M_W^2} = 1 + \frac{2}{9} \mu_c^2 + m_c^0 \ln \frac{\mu_c^2}{m^2} + \frac{1}{3} \mu_c^{\#} \end{aligned} \quad (\text{XII.34})$$

where we have replaced $\mu_c \rightarrow m_c$ and $m_c \rightarrow m$. In deriving (XII.34) besides (XII.33) the following identities are useful

$$\sum_{i,j=+;-} X_{ij} = 1 \quad \sum_{i,j=+;-} X_{ij} \frac{i^{(0)} + j^{(0)}}{2} = i^{(0)} \quad (\text{XII.35})$$

$$\sum_{i,j=+;-} X_{ij} (B_i + B_j) = 2B_+ \quad (\text{XII.36})$$

The same result (XII.34) is obtained from \mathcal{S}_2 as well, if we set $m_c = m_b = \mu_c = \mu_s$, $m_t = m$ in (XII.10) and expand for $m \ll M_W$. This exercise yields a useful cross-check between the calculations for \mathcal{S}_1 and \mathcal{S}_2 . In addition it gives some further insight into the structure of the QCD corrections to $S = 2$ box diagrams, establishing \mathcal{S}_1 and \mathcal{S}_2 as two different generalizations of the same asymptotic limit (XII.34).

D. The Top-Charm Contribution – \mathcal{S}_3

To complete the description of the $K^0 - \bar{K}^0$ effective hamiltonian we now turn to the mixed top-charm component, defined by the contribution \mathcal{S}_{ct} in (XII.1), and the associated QCD correction factor \mathcal{S}_3 . The short distance QCD effects have been first obtained within the leading log approximation by (Gilman and Wise, 1983). The calculation of \mathcal{S}_3 at next-to-leading order is due to the work of (Herrlich and Nierste, 1995a), (Nierste, 1995). As already mentioned, the renormalization group analysis necessary for \mathcal{S}_3 is more involved than in the cases of \mathcal{S}_1 and \mathcal{S}_2 . The characteristic differences will become clear from the following presentation.

We begin by writing down the relevant $S = 1$ hamiltonian, obtained after integrating out W and top, which provides the basis for the construction of the $S = 2$ effective hamiltonian we want to derive. It reads

$$H_{ct}^{(1)} = \frac{G_F}{2} \sum_{q,q'=u,c} V_{q's} V_{qd}^* \sum_{i=1,2} C_i Q_i^{q'q} + \sum_{i=3}^6 C_i Q_i^A \quad (XII.37)$$

with

$$Q_1^{q'q} = (s_i q_j^0)_{V-A} (q_j d_i)_{V-A} \quad Q_2^{q'q} = (s_i q_i^0)_{V-A} (q_j d_j)_{V-A} \quad (XII.38)$$

and corresponds to the hamiltonian (VI.5), discussed in chapter VI, except that we have included the $C = 1$ components Q_i^{uc}, Q_i^{cu} , which contribute in the analysis of γ_3 . By contrast to the simpler case of γ_1 presented in the previous section, now also the penguin operators $Q_i, i = 3; \dots; 6$ (VI.3) have to be considered. Being proportional to $\gamma_t = V_{ts} V_{td}^*$ they will contribute to the $c \rightarrow t$ part of (XII.1). We remark in this context that, on the other hand, the penguin contribution to the γ_t^2 -sector is entirely negligible. Since only light quarks are involved in $Q_3; \dots; Q_6$, the double penguin diagrams, which would contribute to the γ_t^2 -piece of the $S = 2$ amplitude, are suppressed by at least a factor of m_b^2/m_t^2 compared with the dominant top-exchange effects discussed in section XII B.

At second order in (XII.37) $S = 2$ transitions are generated. Inserting (XII.37) in an expression similar to (XII.18), eliminating γ_u by means of $\gamma_u = \gamma_c - \gamma_t$ and collecting the terms proportional to $\gamma_c \gamma_t$, we obtain the top-charm component of the effective $S = 2$ hamiltonian in the form

$$H_{eff,ct}^{S=2} = \frac{G_F^2}{2} \sum_{i=1}^2 \sum_{j=1}^6 C_i C_j Q_{ij} + C_7 Q_7^5 \quad (XII.39)$$

where

$$Q_{ij} = \frac{1}{2} \int d^4x T [2Q_i^{uu}(x) Q_j^{uu}(0) - Q_i^{uc}(x) Q_j^{cu}(0) - Q_i^{cu}(x) Q_j^{uc}(0)] \quad (XII.40)$$

for $j = 1; 2$ and

$$Q_{ij} = \frac{1}{2} \int d^4x T [(Q_i^{uu}(x) - Q_i^{cc}(x)) Q_j(0) + Q_j(x) (Q_i^{uu}(0) - Q_i^{cc}(0))] \quad (XII.41)$$

for $j = 3; \dots; 6$.

In defining these operators we have already omitted bilocal products with flavor structure like $(suud) - (soud)$, which cannot contribute to $S = 2$ box diagrams. Furthermore, for the factor entering the bilocal operators with index i we have changed the basis from $Q_{1,2}^{q'q}$ to $Q^{q'q}$ given in (XII.17). In addition local counterterms proportional to the $S = 2$ operator

$$Q_7 = \frac{m_c^2}{g^2} (sd)_{V-A} (sd)_{V-A} \quad (XII.42)$$

have been added to (XII.39). These are necessary here because the bilocal operators can in general mix into Q_7 under infinite renormalization, a fact related to the logarithm present in the leading

term $x_t \ln x_c$ entering $S_0(x_c; x_t)$ in (XII.5). This behaviour is in contrast to the charm contribution, where the corresponding function $S_0(x_c) = x_c$ does not contain a logarithmic term and consequently no local $S = 2$ counterterm is necessary in (XII.19). On the other hand the situation here is analogous to the case of the charm contribution to the effective hamiltonian for $K^+ \rightarrow \pi^+ \pi^0$ in section XI B which similarly behaves as $x_t \ln x_c$ in lowest order and correspondingly requires a counterterm, as displayed in (XI.21) and (XI.35).

After integrating out top and W at the high energy matching scale $\mu_W = O(M_W)$, the Wilson coefficients C_j , $j = 1; \dots; 6$ of (XII.37) and (XII.39) are given in the NDR-scheme by (see section VI)

$$C^T(\mu_W) = (0; 1; 0; 0; 0; 0) + \frac{s(\mu_W)}{4} \left(6; -2; \frac{2}{9}; \frac{2}{3}; \frac{2}{9}; \frac{2}{3} \right) \ln \frac{\mu_W}{M_W} \\ + \frac{s(\mu_W)}{4} \left(\frac{11}{2}; \frac{11}{6}; \frac{1}{6}E_0(x_t); \frac{1}{2}E_0(x_t); \frac{1}{6}E_0(x_t); \frac{1}{2}E_0(x_t) \right) \quad (XII.43)$$

and $C = C_2 \dots C_1$. $E_0(x_t)$ can be found in (VI.16). The coefficient of Q_7 is obtained through matching the $S = 2$ matrix element of the effective theory (XII.39) to the corresponding full theory matrix element, which is in the required approximation ($x_c \rightarrow 1$) given by (compare (XII.1))

$$A_{full,ct} = \frac{G_F^2}{16} M_W^2 2 c_t S_0(x_c; x_t) h_{Q_i} \quad (XII.44)$$

At next-to-leading order this matching has to be done to one loop, including finite parts. Note that here the loop effect is due to electroweak interactions and QCD does not contribute explicitly in this step. The matching condition determines the sum $C_7 = C_{7+} + C_7$, which in the NDR scheme and with the conventional definition of evanescent operators, (Buras and Weisz, 1990), see also (Herrlich and Nierste, 1995a), (Nierste, 1995), reads

$$C_7(\mu_W) = \frac{s(\mu_W)}{4} \left(8 \ln \frac{\mu_W}{M_W} + 4 \ln x_t - \frac{3x_t}{1-x_t} - \frac{3x_t^2 \ln x_t}{(1-x_t)^2} + 2 \right) \quad (XII.45)$$

at next-to-leading order. In leading log approximation one simply would have $C_7(\mu_W) = 0$. The distribution of C_7 among C_{7+} and C_7 is arbitrary and has no impact on the physics. For example we may choose

$$C_{7+} = C_7 \quad C_7 = 0 \quad (XII.46)$$

Having determined the initial values of the Wilson coefficients

$$C^{(0)T} = (C_1; \dots; C_6; C_7) \quad (XII.47)$$

at a scale μ_W , $C^{(0)}(\mu_W)$, the next step consists in solving the RG equations to determine $C^{(0)}(\mu_c)$ at the charm mass scale $\mu_c = O(m_c)$. The renormalization group evolution of $C^{(0)}$ is given by

$$\frac{d}{d \ln} C^{(0)}(\mu) = -\gamma^{(0)T} C^{(0)}(\mu) \quad (XII.48)$$

$$\gamma^{(0)} = \gamma_s + \frac{1}{\gamma_7} \gamma_7^{(0)} \quad (XII.49)$$

Here s is the standard 6×6 anomalous dimension matrix for the $S = 1$ effective hamiltonian including QCD penguins from (VI.23), (VI.25) and (VI.26) (NDR-scheme). Similarly s_{i1} are the anomalous dimensions of the current-current operators. They can be obtained as $s_{i1} = s_{i11} - s_{i12}$ and are also given in section V.

γ_7 represents the anomalous dimension of Q_7 (XII.42) and reads

$$\gamma_7 = \gamma_7^{(0)} + 2\gamma_7^{(1)} = \frac{s}{4} \gamma_7^{(0)} + \frac{s^2}{4} \gamma_7^{(1)} \quad (\text{XII.50})$$

For $N = 3$ and in NDR

$$\gamma_7^{(0)} = 2 + \frac{4}{3}f \quad \gamma_7^{(1)} = \frac{175}{3} + \frac{152}{9}f \quad (\text{XII.51})$$

Finally $\tilde{\gamma}_7$, the vector of anomalous dimensions expressing the mixing of the bilocal operators Q_i ($i = 1, \dots, 6$) into Q_7 , is given by

$$\tilde{\gamma}_7 = \frac{s}{4} \tilde{\gamma}_7^{(0)} + \frac{s^2}{4} \tilde{\gamma}_7^{(1)} \quad (\text{XII.52})$$

where

$$\tilde{\gamma}_7^{(0)T} = (16; 8; 32; 16; 32; 16) \quad (\text{XII.53})$$

$$\tilde{\gamma}_7^{(1)T} = (8; 0; 16; 0; 16; 0) \quad (\text{XII.54})$$

$$\tilde{\gamma}_7^{(1)T} = (212; 28; 424; 56\frac{1064}{3}; \frac{832}{3}) \quad (\text{XII.55})$$

$$\tilde{\gamma}_7^{(1)T} = (276; 92; 552; 184; \frac{1288}{3}; 0) \quad (\text{XII.56})$$

The scheme-dependent numbers in $\tilde{\gamma}_7^{(1)}$ are given here in the NDR-scheme with the conventional treatment of evanescent operators as described in (Buras and Weisz, 1990), (Herrlich and Nierste, 1995a), (Nierste, 1995).

In order to solve the RG equation (XII.48) it is useful (Herrlich and Nierste, 1995a), (Nierste, 1995) to define the eight-dimensional vector ($C^T = (C_1; \dots; C_6)$)

$$D^T = (C^T; C_7 = C_+; C_7 = C_-) \quad (\text{XII.57})$$

which obeys

$$\frac{d}{d \ln} D = \Gamma_{ct} D \quad (\text{XII.58})$$

where

$$\Gamma_{ct} = \begin{pmatrix} 0 & s & 0 \\ \gamma_7^{(0)T} & \gamma_7^{(1)T} & 0 \\ 0 & 0 & \gamma_7^{(1)} \end{pmatrix} + \begin{pmatrix} 0 & 0 & 1 \\ 0 & 0 & 0 \\ 0 & 0 & 0 \end{pmatrix} \quad (\text{XII.59})$$

The solution of (XII.58) proceeds in the standard fashion as described in section III F 1 and has the form

$$\mathcal{D}(\mu_c) = U_4(\mu_c; \mu_b) M(\mu_b) U_5(\mu_b; \mu_w) \mathcal{D}(\mu_w) \quad (\text{XII.60})$$

similarly to (III.105). The b-quark-threshold matching matrix $M(\mu_b)$ is an 8×8 matrix whose 6×6 submatrix M_{ij} , $i, j = 1; \dots; 6$ is identical to the matrix M described in section VI D. The remaining elements are $M_{77} = M_{88} = 1$ and zero otherwise. From (XII.60) the Wilson coefficients $C_i(\mu_c)$ are obtained as

$$C_i(\mu_c) = D_i(\mu_c) \quad i = 1; \dots; 6 \quad C_7(\mu_c) = C_+(\mu_c) D_7(\mu_c) + C_-(\mu_c) D_8(\mu_c) \quad (\text{XII.61})$$

The final step in the calculation of α_s consists in removing the charm degrees of freedom from the effective theory. Without charm the effective short-distance hamiltonian corresponding to (XII.39) can be written as

$$H_{\text{eff}; \text{ct}}^{S=2} = \frac{G_F^2}{2} \mu_c^{-2} C_{\text{ct}} Q \quad (\text{XII.62})$$

The matching condition is obtained by equating the matrix elements of (XII.39) and (XII.62), evaluated at a scale $\mu_c = O(\mu_c)$. At next-to-leading order one needs the finite parts of the matrix elements of Q_{ij} , which can be written in the form

$$hQ_{ij}(\mu_c) = \frac{m_c^2(\mu_c)}{8} r_{ij}(\mu_c) hQ_i \quad (\text{XII.63})$$

where in the renormalization scheme described above after eq. (XII.56) the r_{ij} are given by

$$r_{ij}(\mu_c) = \begin{cases} 8(4 \ln(\mu_c/\mu_c) - 1) & i, j = 1; 2 \\ 8 \ln(\mu_c/\mu_c) - 4 & i, j = 3; 4 \\ (8 \ln(\mu_c/\mu_c) + 4) & i, j = 5; 6 \end{cases} \quad (\text{XII.64})$$

$$r_1 = r_3 = r_5 = (1 - 3) = 2 \quad (\text{XII.65})$$

$$r_{+j} = 1 \quad r_j = 0 \quad j \text{ even} \quad (\text{XII.66})$$

Using (XII.63), the matching condition at μ_c between (XII.39) and (XII.62) implies

$$C_{\text{ct}}(\mu_c) = \sum_{i=1}^6 \sum_{j=1}^6 C_i(\mu_c) C_j(\mu_c) \frac{m_c^2(\mu_c)}{8} r_{ij}(\mu_c) + C_7(\mu_c) \frac{m_c^2(\mu_c)}{4} \quad (\text{XII.67})$$

Evolving C_{ct} from μ_c to $\mu < \mu_c$ in a three-flavor theory using (XII.8) and comparing (XII.62) with (XII.1), we obtain the final result

$$\alpha_s = \frac{x_c(\mu_c)}{S_0(x_c(\mu_c); x_t(\mu_w))} \alpha_s(\mu_c)^{2=9} \frac{h}{s(\mu_c)} C_7(\mu_c) \left(1 - \frac{s(\mu_c)}{4} J_3 + \dots \right)$$

$$+ \frac{1}{2} \sum_{i=1}^6 \sum_{j=1}^6 C_i(\mu_c) C_j(\mu_c) r_{ij}(\mu_c) \quad (XII.68)$$

One may convince oneself, that $S_0(x_c; x_t)$ is independent of the renormalization scales, in particular of μ_c , up to terms of $O(x_c^{2=9} \mu_c^{-9})$.

Furthermore, using the formulae given in this section, it is easy to see from the explicit expression (XII.68), that $S_0^{2=9} \mu_c^{-9} \rightarrow 1$ in the limit $\mu_c \rightarrow 0$, as it should indeed be the case.

The next-to-leading order formula (XII.68) for S_3 , first calculated in (Herrlich and Nierste, 1995a), (Nierste, 1995), provides the generalization of the leading log result obtained by (Gilman and Wise, 1983). It is instructive to compare (XII.68) with the leading order approximation, which can be written as

$$S_3^{LO} = S(\mu_c)^{2=9} \frac{C_7^{LO}(\mu_c)}{S(\mu_c) \ln x_c} \quad (XII.69)$$

using the notation of (XII.68). C_7^{LO} denotes the coefficient C_7 , restricted to the leading logarithmic approximation. Formula (XII.69), derived here as a special case of (XII.68), is equivalent to the result obtained in (Gilman and Wise, 1983).

If penguin operators and the b-quark threshold in the RG evolution are neglected, it is possible to write down in closed form a relatively simple, explicit expression for S_3 . Using a 4-flavor effective theory for the evolution from the W -scale down to the charm scale, we find in this approximation

$$\begin{aligned} S_3 = & \frac{x_c(\mu_c)}{S_0(x_c(\mu_c); x_t)} S(\mu_c)^{2=9} \\ & \frac{1}{S(\mu_c)} \left(\frac{18}{7} K_{++} + \frac{12}{11} K_+ + \frac{6}{29} K + \frac{7716}{2233} K_7 - 1 - \frac{S(\mu_c)}{4} \frac{307}{162} \right) + \\ & + \ln \frac{\mu_c}{m_c} \left(\frac{1}{4} (3K_{++} + 2K_+ + K) + \right. \\ & + \frac{262497}{35000} K_{++} + \frac{123}{625} K_+ + \frac{1108657}{1305000} K + \frac{277133}{50750} K_7 + \\ & + K \left(\frac{21093}{8750} K_{++} + \frac{13331}{13750} K_+ + \frac{10181}{18125} K + \frac{1731104}{2512125} K_7 \right) + \\ & + \ln x_t \left(\frac{3x_t}{4(1-x_t)} + \frac{3x_t^2 \ln x_t}{4(1-x_t)^2} + \frac{1}{2} K K_7 \right) \end{aligned} \quad (XII.70)$$

where

$$K_{++} = K^{12=25} \quad K_+ = K^{6=25} \quad K = K^{24=25} \quad (XII.71)$$

$$K_7 = K^{1=5} \quad K = \frac{S(M_W)}{S(\mu_c)} \quad (XII.72)$$

Here we have set $\mu_W = M_W$. (XII.70) represents the next-to-leading order generalization of an approximate formula for the leading log S_3 , also omitting gluon penguins, that has been first given in (Gilman and Wise, 1983). The analytical expression for S_3 in (XII.70) provides an excellent approximation, deviating generally by less than 1% from the full result.

E. Numerical Results

1. General Remarks

After presenting the theoretical aspects of the short-distance QCD factors α_1 , α_2 and α_3 in the previous sections, we shall now turn to a discussion of their numerical values. However, before considering explicit numbers, we would like to make a few general remarks. First of all, it is important to recall that in the matrix element $\langle K^0 | \bar{\psi} \gamma_{\mu} \psi \rangle_{\text{eff}}^{S=2} | K^0 \rangle$ (see (XII.1)), only the complete products

$$S_{0i} \alpha_i [\alpha_s(\mu)]^{2=9} \left[1 + \frac{\alpha_s(\mu)}{4} J_3 \right] \langle K^0 | \bar{\psi} \gamma_{\mu} \psi | K^0 \rangle = C_i(\mu) \langle K^0 | \bar{\psi} \gamma_{\mu} \psi | K^0 \rangle \quad (\text{XII.73})$$

are physically relevant. Here S_{0i} denote the appropriate quark mass dependent functions S_0 for the three contributions ($i = 1, 2, 3$) in (XII.1). None of the factors in (XII.73) is physically meaningful by itself. In particular, there is some arbitrariness in splitting the product (XII.73) into the short-distance part and the matrix element of Q (XII.2) containing long distance contributions. This arbitrariness has of course no impact on the physical result. However, it is essential to employ a definition for the operator matrix element that is consistent with the short-distance QCD factor used.

Conventionally, the matrix element $\langle K^0 | \bar{\psi} \gamma_{\mu} \psi | K^0 \rangle$ is expressed in terms of the so-called bag parameter $B_K(\mu)$ defined through

$$\langle K^0 | \bar{\psi} \gamma_{\mu} \psi | K^0 \rangle = \frac{8}{3} F_K^2 m_K^2 B_K(\mu) \quad (\text{XII.74})$$

where m_K is the kaon mass and $F_K = 160 \text{ MeV}$ is the kaon decay constant. In principle, one could just use the scale- and scheme dependent bag factor $B_K(\mu)$ along with the coefficient functions $C_i(\mu)$ as defined by (XII.73), evaluated at the same scale and in the same renormalization scheme. However, it has become customary to define the short-distance QCD correction factors α_i by splitting off from the Wilson coefficient $C_i(\mu)$ the factor $[\alpha_s(\mu)]^{2=9} \left[1 + \frac{\alpha_s(\mu)}{4} J_3 \right]$ which carries the dependence on the renormalization scheme and the scale μ . This factor is then attributed to the matrix element of Q , formally cancelling its scale and scheme dependence. Accordingly one defines a renormalization scale and scheme invariant bag parameter B_K (compare (XII.73), (XII.74))

$$B_K = [\alpha_s(\mu)]^{2=9} \left[1 + \frac{\alpha_s(\mu)}{4} J_3 \right] B_K(\mu) \quad (\text{XII.75})$$

If the α_i as described in this report are employed to describe the short-distance QCD corrections, eq. (XII.75) is the consistent definition to be used for the kaon bag parameter.

Eventually the quantity $B_K(\mu)$ should be calculated within lattice QCD. At present, the analysis of (Sharpe, 1994), for example, gives a central value of $B_K(2 \text{ GeV})_{\text{NDR}} = 0.16$, with some still sizable uncertainty. For a recent review see also (Soni, 1995). This result already incorporates the lattice-continuum theory matching and refers to the usual NDR scheme. It is clear that the NLO calculation of short-distance QCD effects is essential for consistency with this matching and for a proper treatment of the scheme dependence. Both require $O(\alpha_s)$ corrections, which go beyond

the leading log approximation.

To convert to the scheme invariant parameter B_K one uses (XII.75) with the NDR-scheme value for $J_3 = 307/162$ to obtain $B_K = 0.84$. Note that the factor involving J_3 in (XII.75), which appears at NLO, increases the r.h.s. of (XII.75) by 4.5% . The leading factor $s^{2=9}$ is about 1.31 . Of course, the fact that there is presently still a rather large uncertainty in the calculation of the hadronic matrix element is somewhat forgiving, regarding the precise definition of B_K . However, as the lattice calculations improve further and the errors decrease, the issue of a consistent definition of the α_s and B_K will become crucial and it is important to keep relation (XII.75) in mind.

Let us next add a side remark concerning the separation of the full amplitude into the formally RG invariant factors α_s and B_K . This separation is essentially unique, up to trivial constant factors, if the evolution from the charm scale μ_c down to a "hadronic" scale $\mu < \mu_c$ is written in the resummed form as shown in (XII.8) and one requires that all factors depending on the scale μ are absorbed into the matrix element. On the other hand the hadronic scale $\mu = O(1 \text{ GeV})$ is not really much different from the charm scale $\mu_c = O(m_c)$, so that the logarithms $\ln \mu_c$ are not very large. Therefore one could argue that it is not necessary to resum those logarithms. In this case the first two factors on the r.h.s. of (XII.8) could be expanded to first order in α_s and the amplitude (XII.73) would read

$$C_i(\mu_c) = 1 + \frac{\alpha_s}{c} \ln \frac{\mu_c}{\mu} h_K^{(0)} D(\mu) K^{(0)} i \quad (\text{XII.76})$$

From this expression it is obvious, that the separation of the physical amplitude into scheme invariant short-distance factors and a scheme invariant matrix element is in general not unique. This illustrates once more the ambiguity existing for theoretical concepts such as operator matrix elements or QCD correction factors, which only cancels in physical quantities.

For definiteness, we will stick to the RG improved form also for the evolution between μ_c and μ and the definitions for α_s and B_K that we have discussed in detail above.

2. Results for α_1 , α_2 and α_3

We are now ready to quote numerical results for the short-distance QCD corrections α_i at next-to-leading order and to compare them with the leading order approximation.

The factors α_1 and α_3 have been analyzed in detail in (Herrlich and Nierste, 1994) and (Nierste, 1995). Here we summarize briefly their main results. Using our central parameter values $m_c(m_c) = 1.3 \text{ GeV}$, $\frac{(4)}{MS} = 0.325 \text{ GeV}$, $m_t(m_t) = 170 \text{ GeV}$ and fixing the scales as $\mu_c = m_c$, $\mu_W = M_W$ for α_1 , $\mu_W = 130 \text{ GeV}$ for α_3 , one obtains at NLO

$$\alpha_1 = 1.38 \quad \alpha_3 = 0.47 \quad (\text{XII.77})$$

This is to be compared with the LO values corresponding to the same input $\alpha_1^{LO} = 1.12$, $\alpha_3^{LO} = 0.35$. We note that the next-to-leading order corrections are sizable, typically 20% – 30% , but still perturbative. The numbers above may be compared with the leading log values $\alpha_1^{LO} = 0.85$ and $\alpha_3^{LO} = 0.36$ that have been previously used in the literature, based on the choice $m_c = 1.4 \text{ GeV}$, $\mu_{QCD} = 0.2 \text{ GeV}$ and $\mu_W = M_W$. The considerable difference between the two LO values for α_1 mainly reflects the large dependence of α_1 on μ_{QCD} .

In fact, when the QCD scale is allowed to vary within $\frac{(4)}{MS} = (0.325 - 0.110) \text{ GeV}$, the value for

α_s (NLO) changes by $\pm 35\%$. The leading order result α_s^{LO} appears to be slightly less sensitive to μ_{QCD} . However, in this approximation the relation of α_s^{LO} to $\frac{(4)}{MS}$ is not well defined, which introduces an additional source of uncertainty when working to leading logarithmic accuracy.

The situation is much more favorable in the case of α_s , where the sensitivity to $\frac{(4)}{MS}$ is quite small, $\pm 3\%$. Likewise the dependence on the charm quark mass is very small for both α_s and α_s . Using $m_c(m_c) = (1.3 \pm 0.05) \text{ GeV}$ and the central value for $\frac{(4)}{MS}$ it is about $\pm 4\%$ for α_s and entirely negligible for α_s .

Finally, there are the purely theoretical uncertainties due to the renormalization scales. They are dominated by the ambiguity related to μ_c . The products $S_0(x_c(\mu_c)) \alpha_s(\mu_c)$ and $S_0(x_c(\mu_c); x_t) \alpha_s(\mu_c)$ are independent of μ_c up to terms of the neglected order in RG improved perturbation theory. In the case of $S_0(x_c(\mu_c)) \alpha_s(\mu_c) (S_0(x_c(\mu_c); x_t) \alpha_s(\mu_c))$ the remaining sensitivity to μ_c amounts to typically $\pm 15\%$ ($\pm 7\%$) at NLO. These scale dependences are somewhat reduced compared to the leading order calculation, where the corresponding uncertainty is around $\pm 30\%$ ($\pm 10\%$).

To summarize, sizable uncertainties are still associated with the number for the QCD factor α_s , whose central value is found to be $\alpha_s = 1.38$ (Herrlich and Nierste, 1994). On the other hand, the prediction for α_s appears to be quite stable and can be reliably determined as $\alpha_s = 0.47 \pm 0.03$ (Herrlich and Nierste, 1995a), (Nierste, 1995). One should emphasize however, that these conclusions have their firm basis only within the framework of a complete NLO analysis, as the one performed in (Herrlich and Nierste, 1994), (Nierste, 1995). Fortunately the quantity α_s , for which a high precision seems difficult to achieve, plays a less important role in the phenomenology of indirect CP violation.

Finally, we turn to a brief discussion of α_s (Buras *et al.*, 1990), representing the short-distance QCD effects of the top-quark contribution. For central parameter values, in particular $\frac{(4)}{MS} = 0.325 \text{ GeV}$ and $m_t(m_t) = 170 \text{ GeV}$, and for $\mu_t = m_t(m_t)$ the numerical value is

$$\alpha_s = 0.574 \quad (\text{XII.78})$$

Varying the QCD scale within $\frac{(4)}{MS} = (0.325 \pm 0.110) \text{ GeV}$ results in a $\pm 0.5\%$ change in α_s . The dependence on $m_t(m_t)$ is even smaller, only $\pm 0.3\%$ for $m_t(m_t) = (170 \pm 15) \text{ GeV}$. It is worthwhile to compare the NLO results with the leading log approximation. Using the same input as before yields a central value of $\alpha_s^{LO} = 0.612$, about 7% larger as the NLO result (XII.78). However, what is even more important than the difference in central values is the quite striking reduction of scale uncertainty when going from the leading log approximation to the full NLO treatment. Recall that the μ_t -dependence in α_s has to cancel the scale dependence of the function $S_0(x_t(\mu_t))$. Allowing for a typical variation of the renormalization scale $\mu_t = O(m_t)$ from 100 GeV to 300 GeV results in a sizable change in $S_0(x_t(\mu_t)) \alpha_s^{LO}$ of $\pm 9\%$. In fact, in leading order the μ_t -dependence of α_s has even the wrong sign, re-inforcing the scale dependence present in $S_0(x_t(\mu_t))$ instead of reducing it. The large sensitivity to the unphysical parameter μ_t is essentially eliminated (to $\pm 0.4\%$) for $\alpha_s S_0(x_t)$ at NLO, a quite remarkable improvement of the theoretical accuracy. The situation here is similar to the case of the top-quark dominated rare K and B decays discussed in sections XI, XXIV and XXVI. For a further illustration of the reduction in scale uncertainty see the discussion of the analogous case of α_s in section XIII B.

The dependence of α_s on the charm and bottom threshold scales $\mu_c = O(m_c)$ and $\mu_b = O(m_b)$ is also extremely weak. Taking $1 \text{ GeV} < \mu_c < 3 \text{ GeV}$ and $3 \text{ GeV} < \mu_b < 9 \text{ GeV}$ results in a variation of α_s by merely $\pm 0.26\%$ and $\pm 0.06\%$, respectively.

In summary, the NLO result for $\chi^2_{S_0}(\mathbf{x}_t)$ is, by contrast to the leading logarithmic approximation, essentially free from theoretical uncertainties. Furthermore, $\chi^2_{S_0}$ is also rather insensitive to the input parameters \overline{m}_S and m_t . The top contribution plays the dominant role for indirect CP violation in the neutral kaon system. The considerable improvement in the theoretical analysis of the short-distance QCD factor $\chi^2_{S_0}$ brought about by the next-to-leading order calculation is therefore particularly satisfying.

XIII. THE EFFECTIVE HAMILTONIAN FOR $B^0 - \bar{B}^0$ MIXING

A. General Structure

Due to the particular hierarchy of the CKM matrix elements only the top sector can contribute significantly to $B^0 - \bar{B}^0$ mixing. The charm sector and the mixed top-charm contributions are entirely negligible here, in contrast to the $K^0 - \bar{K}^0$ case, which considerably simplifies the analysis.

Referring to our earlier presentation of the top sector for $S = 2$ transitions in section XII B we can immediately write down the effective $B = 2$ hamiltonian. Performing the RG evolution only down to scales $\mu_b = O(m_b)$ and making the necessary replacements ($s \rightarrow b$) we get, in analogy to (XII.1) (Buras *et al.*, 1990)

$$H_{\text{eff}}^{B=2} = \frac{G_F^2}{16} M_W^2 (V_{tb} V_{td})^2 {}_{2B} S_0(x_t) [s(b)]^{6=23} \left(1 + \frac{s(b)}{4} J_5 \right) Q + h.c. \quad (\text{XIII.1})$$

where here

$$Q = (\bar{b}d)_V {}_A (\bar{b}d)_V {}_A \quad (\text{XIII.2})$$

and

$${}_{2B} S_0 = [s(x_t)]^{6=23} \left(1 + \frac{s(x_t)}{4} \frac{S_1(x_t)}{S_0(x_t)} + B_t J_5 + \frac{(0)}{2} \ln \frac{m_t^2}{M_W^2} + m_0 \frac{\partial \ln S_0(x_t)}{\partial \ln x_t} \ln \frac{m_t^2}{M_W^2} \right) \quad (\text{XIII.3})$$

The definitions of the various quantities in (XIII.3) can be found in section XII B. Several important aspects of S_2 in the kaon system have also been discussed in this section. Similar comments apply to the present case of ${}_{2B}$. Here we would still like to supplement this discussion by writing down the formula for ${}_{2B}$ in the limiting case $m_t \rightarrow M_W$,

$${}_{2B} S_0 = [s(x_t)]^{6=23} \left(1 + \frac{s(x_t)}{4} \frac{(0)}{2} \ln \frac{m_t^2}{m_t^2} + m_0 \ln \frac{m_t^2}{m_t^2} + 11 \frac{20}{9} + B_t J_5 + O \left(\frac{M_W^2}{m_t^2} \right) \right) \quad (\text{XIII.4})$$

This expression clarifies the structure of the RG evolution in the limit $m_t \rightarrow M_W$. It also suggests that the renormalization scale is most naturally to be taken as $\mu_t = O(m_t)$ rather than $\mu_t = O(M_W)$, both in the definition of the top quark mass and as the initial scale of the RG evolution. Formula (XIII.4) also holds, with obvious modifications, for the S_2 factor in the kaon system, which has been discussed in sec. XII B.

We finally mention that in the literature the b -dependent factors in (XIII.1) are sometimes not attributed to the matrix elements of Q , as implied by (XIII.1), but absorbed into the definition of the QCD correction factor

$${}_{2B} = {}_{2B} [s(b)]^{6=23} \left(1 + \frac{s(b)}{4} J_5 \right) \quad (\text{XIII.5})$$

Whichever definition is employed, it is important to remember this difference and to evaluate the hadronic matrix element consistently. Note that, in contrast to ${}_{2B}$, ${}_{2B}$ is scale and scheme dependent.

B. Numerical Results

The correction factor $_{2B}$ describes the short-distance QCD effects in the theoretical expression for $B^0 - \bar{B}^0$ mixing. Due to the arbitrariness that exists in dividing the physical amplitude into short-distance contribution and hadronic matrix element, the short-distance QCD factor is strictly speaking an unphysical quantity and hence definition dependent. The B -factor, parametrizing the hadronic matrix element, has to match the convention used for $_{2B}$. With the definition of $_{2B}$ employed in this article and given explicitly in the previous section, the appropriate B -factor to be used is the so-called scheme independent bag-parameter B_B as defined in eq. (XVIII.18), where $\alpha_s = \alpha_b = \alpha(m_b)$. We remark, that the factor $_{2B}$ is identical for $B_d - \bar{B}_d$ and $B_s - \bar{B}_s$ mixing. The effects of $SU(3)$ breaking enter only the hadronic matrix elements. This feature is a consequence of the factorization of short-distance and long-distance contributions inherent to the operator product expansion. For further comments see also the discussion of the analogous case of short-distance QCD factors in the neutral kaon system in section XII E 1.

In the following we summarize the main results of a numerical analysis of $_{2B}$. The factor $_{2B}$ is analogous to $_2$ entering the top contribution to $K^0 - \bar{K}^0$ mixing and both quantities share many important features.

The value of $_{2B}$ for $\frac{(4)}{MS} = 0.325 \text{ GeV}$, $m_t(m_t) = 170 \text{ GeV}$ and with $_t$ set equal to $m_t(m_t)$ reads at NLO

$$_{2B} = 0.551 \quad (\text{XIII.6})$$

This can be compared with $_{2B}^{LO} = 0.580$, obtained, using the same input, in the leading logarithmic approximation. In the latter case the product $_{2B}^{LO}(\alpha_t) S(\alpha_t)$ is, however, affected by a residual scale ambiguity of 9% (for $100 \text{ GeV} < \mu_t < 300 \text{ GeV}$). This uncertainty is reduced to the negligible amount of 0.3% in the complete NLO expression of $_{2B}(\alpha_t) S(\alpha_t)$, corresponding to an increase in accuracy by a factor of 25. The sensitivity to the unphysical scale $_t$ in leading and next-to-leading order is illustrated in fig. 9.

In addition the number shown in (XIII.6) is also very stable against changes in the input parameters. Taking $\frac{(4)}{MS} = (0.325 \pm 0.110) \text{ GeV}$ and $m_t(m_t) = (170 \pm 15) \text{ GeV}$ results in a variation of $_{2B}$ by 1.3% and 0.3%, respectively.

It is clear from this discussion, that the short-distance QCD effects in $B^0 - \bar{B}^0$ mixing are very well under control, once NLO corrections have been properly included, and the remaining uncertainties are extremely small. The effective hamiltonian given in (XIII.1) therefore provides a solid foundation for the incorporation of non-perturbative effects, to be determined from lattice gauge theory, and for further phenomenological investigations related to $B^0 - \bar{B}^0$ mixing phenomena.

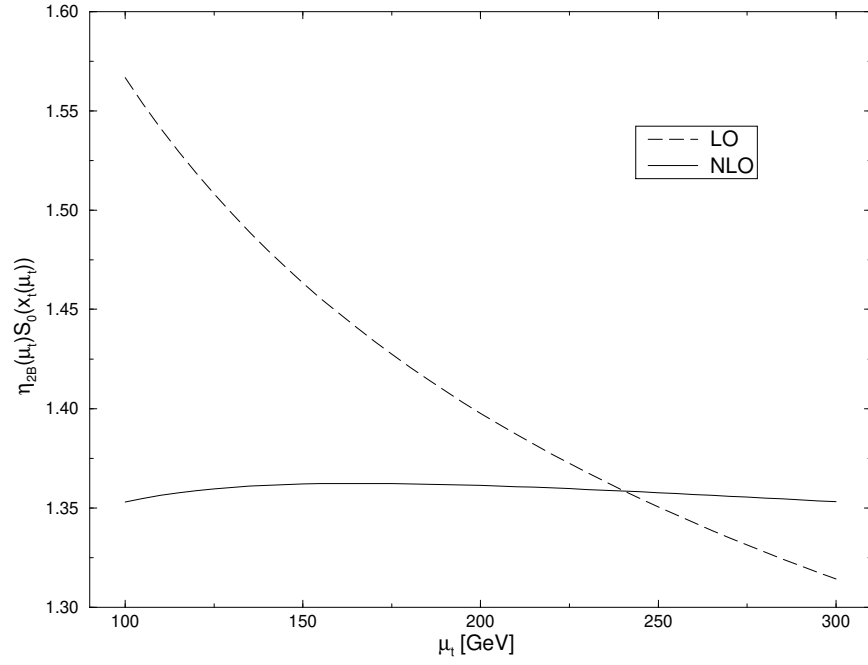


FIG. 9. Scale μ_t dependence of $\eta_{2B}(\mu_t) S_0(x_t(\mu_t))$ in LO and NLO. The quantity $\eta_{2B}(\mu_t) S_0(x_t(\mu_t))$ enters the theoretical expression for m_B , describing $B^0 - \bar{B}^0$ mixing. It is independent of the precise value of the renormalization scale μ_t up to terms of the neglected order in α_s . The remaining sensitivity represents an unavoidable theoretical uncertainty. This ambiguity is shown here for the leading order (dashed) and the next-to-leading order calculation (solid).

XIV. PENGUIN BOX EXPANSION FOR FCNC PROCESSES

An important virtue of OPE and RG is that with $m_t > M_W$ the dependence of weak decays on the top quark mass is very elegantly isolated. It resides only in the initial conditions for the Wilson coefficients at scale M_W i.e. in $C_i(M_W)$. A quick look at the initial conditions in the previous sections reveals the important fact that the leading m_t -dependence in all decays considered is represented universally by the m_t -dependent functions which result from exact calculations of the relevant penguin and box diagrams with internal top quark exchanges. These are the functions

$$S_0(x_t); B_0(x_t); C_0(x_t); D_0(x_t); E_0(x_t); D_0^0(x_t); E_0^0(x_t) \quad (\text{XIV.1})$$

for which explicit expressions are given in (XII.4), eqs. (VII.13)–(VII.15), (VI.15), (IX.12) and (IX.13), respectively. In certain decays some of these functions do not appear because the corresponding penguin or box diagram does not contribute to the initial conditions. However, the function $C_0(x_t)$ resulting from the Z^0 -penguin diagram enters all $F = 1$ decays but $B \rightarrow X_s$. Having a quadratic dependence on m_t , this function is responsible for the dominant m_t -dependence of these decays. Since the non-leading m_t -dependence of $C_0(x_t)$ is gauge dependent, $C_0(x_t)$ is always accompanied by $B_0(x_t)$ or $D_0(x_t)$ in such a way that this dependence cancels. For this reason it is useful to replace the gauge dependent functions $B_0(x_t)$, $C_0(x_t)$ and $D_0(x_t)$ by the gauge independent set (Buchalla *et al.*, 1991)

$$\begin{aligned} X_0(x_t) &= C_0(x_t) - 4B_0(x_t) \\ Y_0(x_t) &= C_0(x_t) - B_0(x_t) \\ Z_0(x_t) &= C_0(x_t) + \frac{1}{4}D_0(x_t) \end{aligned} \quad (\text{XIV.2})$$

as we have already done at various places in this review. The inclusion of NLO QCD corrections to B^0 - B^0 -, K^0 - K^0 -mixing and the rare K - and B -decays of section XI requires the calculation of QCD corrections to penguin and box diagrams in the full theory. This results in the functions $\tilde{S}(x_t) = {}_2S_0(x_t)$, $\tilde{X}(x_t)$ and $\tilde{Y}(x_t)$, with the latter two given in (XI.5) and (XI.45), respectively. It turns out however that if the top quark mass is defined as $m_t = m_t(m_t)$ one has

$$\tilde{S}(x_t) = {}_2S_0(x_t); \quad \tilde{X}(x_t) = {}_X X_0(x_t); \quad \tilde{Y}(x_t) = {}_Y Y_0(x_t) \quad (\text{XIV.3})$$

with ${}_2$, ${}_X$ and ${}_Y$ almost independent of m_t . Numerical values of ${}_X$ and ${}_Y$ are given in part three.

Consequently with this definition of m_t the basic m_t -dependent functions listed in (XIV.1) and (XIV.2) represent the m_t -dependence of weak decays at the NLO level to a good approximation. It should be remarked that the QCD corrections to D_0 , E_0 , D_0^0 and E_0^0 have not been calculated yet. They would however be only required for still higher order corrections (NNLO) in the renormalization group improved perturbation theory as far as D_0 and E_0 are concerned. On the other hand, in the case of D_0^0 and E_0^0 , which are relevant for the $b \rightarrow s$ decay, these corrections are necessary.

An inspection of the effective hamiltonians derived in the previous sections shows that for B^0 - B^0 -mixing, K^0 - K^0 -mixing and the rare decays of section XI the m_t dependence of the effective hamiltonian is explicitly given in terms of the basic functions listed above. Due to the one step evolution from m_t to m_b we have also presented the explicit m_t -dependence for $B \rightarrow X_s$ and $B \rightarrow X_s e^+ e^-$ decays. On the other hand in the case of $K \rightarrow \pi$ and $K_L \rightarrow \pi^0 e^+ e^-$ where

the renormalization group evolution is very complicated the m_t dependence of a given box or penguin diagram is distributed among various Wilson coefficient functions. In other words the m_t -dependence acquired at scale $O(M_W)$ is hidden in a complicated numerical evaluation of $U(\mu; M_W)$.

For phenomenological applications it is more elegant and more convenient to have a formalism in which the final formulae for all amplitudes are given explicitly in terms of the basic m_t -dependent functions discussed above.

In (Buchalla *et al.*, 1991) an approach has been presented which accomplishes this task. It gives the decay amplitudes as linear combinations of the basic, universal, process independent but m_t -dependent functions $F_r(x_t)$ of eq. (XIV.1) with corresponding coefficients P_r characteristic for the decay under consideration. This approach termed ‘‘Penguin Box Expansion’’ (PBE) has the following general form

$$A(\text{decay}) = P_0(\text{decay}) + \sum_r P_r(\text{decay}) F_r(x_t) \quad (\text{XIV.4})$$

where the sum runs over all possible functions contributing to a given amplitude. In (XIV.4) we have separated a m_t -independent term P_0 which summarizes contributions stemming from internal quarks other than the top, in particular the charm quark.

Many examples of PBE appear in this review. Several decays or transitions depend only on a single function out of the complete set (XIV.1). For completeness we give here the correspondence between various processes and the basic functions

B^0 - B^0 -mixing	$S_0(x_t)$
$K^0 \rightarrow \pi^0, B^0 \rightarrow K^0, B^0 \rightarrow \pi^0$	$X(x_t)$
$K^0 \rightarrow \pi^0, B^0 \rightarrow \pi^0$	$Y_0(x_t)$
$K_L^0 \rightarrow \pi^0 e^+ e^-$	$Y_0(x_t), Z_0(x_t), E_0(x_t)$
π^0	$X_0(x_t), Y_0(x_t), Z_0(x_t), E_0(x_t)$
$B^0 \rightarrow X_s$	$D_0^0(x_t), E_0^0(x_t)$
$B^0 \rightarrow X_s e^+ e^-$	$Y_0(x_t), Z_0(x_t), E_0(x_t), D_0^0(x_t), E_0^0(x_t)$

In (Buchalla *et al.*, 1991) an explicit transformation from OPE to PBE has been made. This transformation and the relation between these two expansions can be very clearly seen on the basis of

$$A(P \rightarrow F) = \sum_{ijk} h_F \mathcal{D}_k(\mu) \mathcal{P}_{ijk}(\mu; M_W) C_j(M_W) \quad (\text{XIV.5})$$

where $U_{kj}(\mu; M_W)$ represents the renormalization group transformation from M_W down to μ . As we have seen, OPE puts the last two factors in this formula together, mixing this way the physics around M_W with all physical contributions down to very low energy scales. The PBE is realized on the other hand by putting the first two factors together and rewriting $C_j(M_W)$ in terms of the basic functions (XIV.1). This results in the expansion of eq. (XIV.4). Further technical details and the methods for the evaluation of the coefficients P_r can be found in (Buchalla *et al.*, 1991), where further virtues of PBE are discussed.

Finally, we give approximate formulae having power-like dependence on x_t for the basic, gauge independent functions of PBE

$$\begin{aligned}
S_0(x_t) &= 0.784 x_t^{0.76} & X_0(x_t) &= 0.660 x_t^{0.575} \\
Y_0(x_t) &= 0.315 x_t^{0.78} & Z_0(x_t) &= 0.175 x_t^{0.93} \\
E_0(x_t) &= 0.564 x_t^{0.51} & D_0^0(x_t) &= 0.244 x_t^{0.30} \\
E_0^0(x_t) &= 0.145 x_t^{0.19} :
\end{aligned} \tag{XIV.6}$$

In the range $150 \text{ GeV} \leq m_t \leq 200 \text{ GeV}$ these approximations reproduce the exact expressions to an accuracy better than 1%.

XV. HEAVY QUARK EFFECTIVE THEORY BEYOND LEADING LOGS

A. General Remarks

Since its advent in 1989 heavy quark effective theory (HQET) has developed into an elaborate and well-established formalism, providing a systematic framework for the treatment of hadrons containing a heavy quark. HQET represents a static approximation for the heavy quark, covariantly formulated in the language of an effective field theory. It allows to extract the dependence of hadronic matrix elements on the heavy quark mass and to exploit the simplifications that arise in QCD in the static limit.

There are several excellent reviews on this subject (Neubert, 1994c), (Georgi, 1991), (Grinstein, 1991), (Isgur and Wise, 1992), (Mannel, 1993) and we do not attempt here to cover the details of this extended field. However, we would like to emphasize the close parallels in the general formalism employed to calculate perturbative QCD effects for the effective weak hamiltonians we have been discussing in this review and in the context of HQET. In particular we will concentrate on results that have been obtained in HQET beyond the leading logarithmic approximation in QCD perturbation theory. Such calculations have been done mainly for bilinear current operators involving heavy quark fields, which have important applications in semileptonic decays of heavy hadrons. For the purpose of illustration we will focus on the simplest case of heavy-light currents as an important example. Furthermore, while existing reviews concentrate on semileptonic decays and current operators, we will also include results obtained for nonleptonic transitions and summarize the calculation of NLO QCD corrections to $B^0 - \bar{B}^0$ mixing in HQET (Flynn *et al.*, 1991), (Giménez, 1993). These latter papers generalize the leading-log results first obtained in (Voloshin and Shifman, 1987), (Politzer and Wise, 1988a), (Politzer and Wise, 1988b).

Throughout we will restrict ourselves to the leading order in HQET and not address the question of $1/m$ corrections. For a discussion of this topic we refer the reader to the literature, in particular the above mentioned review articles.

B. Basic Concepts

Let us briefly recall the most important basic concepts underlying the idea of HQET. The Lagrangian describing a quark field Q with mass m and its QCD interactions with gluons reads

$$\mathcal{L} = \bar{Q} i \not{D} Q - m \bar{Q} Q \quad (XV.1)$$

where $D_\mu = \partial_\mu - ig T^a A_\mu^a$ is the gauge-covariant derivative. If Q is a heavy quark, i.e. its mass is large compared to the QCD scale, $m \gg \Lambda_{\text{QCD}}$, it acts approximately like a static color source and its QCD interactions simplify. A heavy quark inside a hadron moving with velocity v has approximately the same velocity. Thus its momentum can be written as $p = m v + k$, where k is a small residual momentum of the order of Λ_{QCD} and subject to changes of the same order through soft QCD interactions. To implement this approximation, the quark field Q is decomposed into

$$Q(x) = e^{im v \cdot x} (h_v(x) + H_v(x)) \quad (XV.2)$$

with h_v and H_v defined by

$$h_v(x) = e^{im_v \frac{1+\not{x}}{2}}(x) \quad (XV.3)$$

$$H_v(x) = e^{im_v \frac{1-\not{x}}{2}}(x) \quad (XV.4)$$

To be specific we consider here the case of a hadron containing a heavy quark, as opposed to a heavy antiquark. In order to describe a heavy antiquark, the definitions (XV.3) and (XV.4) are replaced by

$$h_v^{(\dagger)}(x) = e^{-im_v \frac{1+\not{x}}{2}}(x) \quad (XV.5)$$

$$H_v^{(\dagger)}(x) = e^{-im_v \frac{1-\not{x}}{2}}(x) \quad (XV.6)$$

Consequently, for a heavy antiquark, one only needs to substitute $v \rightarrow -v$ in the expressions given below for the case of a heavy quark.

In the rest frame of the heavy quark h_v and H_v correspond to the upper and lower components of ψ , respectively. In general, for $m \gg 1$ h_v and H_v represent the "large" and "small" components of ψ . In fact, the equations of motion of QCD imply that H_v is suppressed by a factor $\sim 1/m$ in comparison to h_v . The inclusion of an explicit exponential factor $\exp(-im_v \not{x})$ in (XV.2) ensures that the momentum associated with the field h_v is only a small residual momentum of order $\sim 1/m$. Now an effective theory for h_v is constructed by eliminating the small component field H_v from explicitly appearing in the description of the heavy quark. On the classical level this can be done by using the equations of motion or, equivalently, by directly integrating out the H_v degrees of freedom in the context of a path integral formulation (Mannel *et al.*, 1992). The effective Lagrangian one obtains from (XV.1) along these lines is given by ($D_\mu = D_\mu - v_\mu \not{D}$)

$$L_{eff,tot} = h_v i \not{D} h_v + h_v i \not{D} \frac{1}{D + 2m} i \not{D} h_v \quad (XV.7)$$

The first term in (XV.7)

$$L_{eff} = h_v (i \not{D} + g \not{v} T^a A^a) h_v \quad (XV.8)$$

represents the Lagrangian of HQET to lowest order in $1/m$ and will be sufficient for our purposes. The second, nonlocal contribution in (XV.7) can be expanded into a series of local, higher dimension operators, carrying coefficients with increasing powers of $1/m$. To first order it yields the correction due to the residual heavy quark kinetic energy and the chromo-magnetic interaction term, coupling the heavy quark spin to the gluon field.

From (XV.8) one can obtain the Feynman rules of HQET, the propagator of the effective field h_v

$$\frac{i}{v \cdot k} \frac{1+\not{v}}{2} \quad (XV.9)$$

and the h_v - h_v -gluon vertex, $ig \not{v} T^a$. The explicit factor $(1+\not{v})/2$ in (XV.9) arises because the effective field h_v is a constrained spinor, satisfying $\not{v} h_v = h_v$, as is obvious from (XV.3). The

velocity v is a constant in the effective theory and plays the role of a label for the effective field h_v . In principle, a different field h_v has to be considered for every velocity v .

The Lagrangian in (XV.8) exhibits the crucial features of HQET: The quark-gluon coupling is independent of the quark's spin degrees of freedom and the Lagrangian is independent of the heavy quark flavor, since the heavy quark mass has been eliminated. This observation forms the basis for the spin-flavor symmetry of HQET (Isgur and Wise, 1989), (Isgur and Wise, 1990), which gives rise to important simplifications in the strong interactions of heavy quarks and allows to establish relations among the form factors of different heavy hadron matrix elements. The heavy quark symmetries are broken by $1/m$ -contributions as well as radiative corrections.

So far our discussion has been limited to the QCD interactions of the heavy quark. Weak interactions introduce new operators into the theory, which may be current operators, bilinear in quark fields, or four-quark operators, relevant for semileptonic and nonleptonic transitions, respectively. Such operators form the basic ingredients to be studied in weak decay phenomenology. They can as well be expanded in $1/m$ and incorporated into the framework of HQET. For example a heavy-light current operator q (evaluated at the origin, $x = 0$), can be written (XV.2)

$$q = q h_v + O\left(\frac{1}{m}\right) \quad (\text{XV.10})$$

to lowest order in HQET.

Up to now we have restricted our discussion to the classical level. In addition, of course, quantum radiative corrections have to be included. They will for example modify relations such as (XV.10). Technically their effects are taken into account by performing the appropriate matching calculations, relating operators in the effective theory to the corresponding operators in the full theory to the required order in renormalization group improved QCD perturbation theory. The procedure is very similar to the calculation of the usual effective hamiltonians for weak decays. The basic difference consists in the heavy degrees of freedom that are being integrated out in the matching process. In the general case of effective weak hamiltonians the heavy field to be removed as a dynamical variable is the W boson, whereas it is the lower component heavy quark field H_v in the case of HQET. This similarity will become obvious from our presentation below.

At this point some comment might be in order concerning the relationship of the HQET formalism to the general weak effective hamiltonians discussed primarily in this review, in particular those relevant for b-physics.

The effective hamiltonians for $B = 1/2$ nonleptonic transitions are the relevant hamiltonians for scales $\mu = O(m_b)$, which are appropriate for B hadron decays, and their Wilson coefficients incorporate the QCD short distance dynamics between scales of $O(M_W)$ and $O(m_b)$. As already mentioned at the end of section V it is therefore not necessary to invoke HQET. The physics below $\mu = O(m_b)$ is completely contained within the relevant hadronic matrix elements. On the other hand, HQET may be useful in certain cases, like e.g. $B^0 - \bar{B}^0$ mixing, to gain additional insight into the structure of the hadronic matrix elements for scales below m_b , but still large compared to μ_{QCD} . These scales are still perturbative and the related contributions can be extracted analytically within HQET. In particular, this procedure makes the dependence of the matrix element on the heavy quark mass explicit, as we will see on examples below. Furthermore, this approach can be useful e.g. in connection with lattice calculations of hadronic matrix elements, which are easier to perform in the static limit for b-quarks, i.e. employing HQET (Sachrajda, 1992). The simplifications obtained are however at the expense of the approximation due to the expansion in $1/m$.

The most important application of HQET has been to the analysis of exclusive semileptonic transitions involving heavy quarks, where this formalism allows to exploit the consequences of heavy quark symmetry to relate formfactors and provides a basis for systematic corrections to the $m \rightarrow 1$ limit. This area of weak decay phenomenology has been already reviewed in detail (Neubert, 1994c), (Georgi, 1991), (Grinstein, 1991), (Isgur and Wise, 1992), (Mannel, 1993) and will not be covered in the present article.

C. Heavy-Light Currents

As an example of a next-to-leading QCD calculation within the context of HQET, we will now discuss the case of a weak current, composed of one heavy and one light quark field, to leading order in the $1/m$ expansion. For definiteness we consider the axial vector heavy-light current, whose matrix elements determine the decay constants of pseudoscalar mesons containing a single heavy quark, like f_B and f_D .

The axial vector current operator in the full theory is given by

$$A = \bar{q} \gamma_5 h_v \quad (XV.11)$$

where h_v is the heavy and q the light quark field. In HQET this operator can be expanded in the following way

$$A = C_1 \left(\frac{1}{m} \right) \tilde{A}_1 + C_2 \left(\frac{1}{m} \right) \tilde{A}_2 + O\left(\frac{1}{m}\right) \quad (XV.12)$$

where the operator basis in the effective theory reads

$$\tilde{A}_1 = \bar{q} \gamma_5 h_v, \quad \tilde{A}_2 = \bar{q} \gamma_\nu \gamma_5 h_\nu \quad (XV.13)$$

with the heavy quark effective field h_v defined in (XV.3). The use of the expansion (XV.12) is to make the dependence of the matrix elements of A on the heavy quark mass m explicit. The dependence on this mass is two-fold. First, there is a power dependence, which is manifest in the heavy quark expansion in powers of $1/m$. From this series only the lowest order term is shown in (XV.12). Second, there is a logarithmic dependence on m due to QCD radiative corrections, which can be calculated in perturbation theory. This dependence is factorized into the coefficient functions C_1, C_2 in much the same way as the logarithmic dependence of nonleptonic weak decay amplitudes on the W boson mass is factorized into the Wilson coefficients of the usual weak hamiltonians. Since the dynamics of HQET is, by construction, independent of m , no further m dependence is present in the matrix elements of the effective theory operators $\tilde{A}_{1,2}$, except for trivial factors of m related to the normalization of meson states. Consequently the m dependence of (XV.12) is determined explicitly.

We remark that in general the meson states in HQET to be used for the r.h.s. of (XV.12) differ from the meson states in the full theory to be used to sandwich the operator A on the l.h.s.. For the leading order in $1/m$ we are working in this distinction is irrelevant, however.

An important point is that the operators $\tilde{A}_{1,2}$ in the effective theory have anomalous dimensions, although the operator A in the full theory, being an axial vector current operator, does not. As a consequence matrix elements of $\tilde{A}_{1,2}$ will depend on the renormalization scale and scheme. This dependence is canceled however through a corresponding dependence of the coefficients

so that the physical matrix elements of A will be scale and scheme independent as they must be. The existence of anomalous dimensions for the effective theory operators merely reflects the logarithmic dependence on the heavy quark mass m due to QCD effects. This dependence results in logarithmic divergences in the limit $m \rightarrow 1$, corresponding to the effective theory, which require additional infinite renormalizations not present in full QCD. Obviously the situation is completely analogous to the case of constructing effective weak hamiltonians through integrating out the W boson, which we have described in detail in section III. In fact, the extraction of the coefficient functions by factorizing long and short distance contributions to quark level amplitudes and the renormalization group treatment follow exactly the same principles.

The Wilson coefficients at the high matching scale $\mu_h = O(m)$, the initial condition to the RG evolution, can be calculated in ordinary perturbation theory with the result (NDR scheme)

$$C_1(\mu_h) = 1 + \frac{s}{4} \gamma_{h1}^{(0)} \ln \frac{\mu_h}{m} + B_1 \quad (XV.14)$$

$$C_2(\mu_h) = \frac{s}{4} B_2 \quad (XV.15)$$

with

$$B_1 = 4C_F \quad B_2 = 2C_F \quad (XV.16)$$

and $\gamma_{h1}^{(0)}$ given in (XV.18) below. C_F is the QCD color factor $(N^2 - 1)/(2N)$. We remark that the coefficient of the new operator \tilde{A}_2 , generated at $O(s)$, is finite without requiring renormalization. As a consequence no explicit scale dependence appears in (XV.15) and B_2 is a scheme independent constant. For the same reason \tilde{A}_1 and \tilde{A}_2 do not mix under renormalization, but renormalize only multiplicatively. The anomalous dimension of the effective heavy quark currents is independent of the Dirac structure. It is the same for \tilde{A}_1 and \tilde{A}_2 and reads at two-loop order

$$\gamma_{h1} = \gamma_{h1}^{(0)} \frac{s}{4} + \gamma_{h1}^{(1)} \frac{s^2}{4} \quad (XV.17)$$

where

$$\gamma_{h1}^{(0)} = 3C_F \quad (XV.18)$$

$$\begin{aligned} \gamma_{h1}^{(1)} &= \frac{49}{6} + \frac{2}{3} N C_F + \frac{5}{2} \frac{8}{3} C_F^2 + \frac{5}{3} C_F f = \\ &= \frac{254}{9} - \frac{56}{27} N^2 + \frac{20}{9} f \quad (\text{NDR}) \end{aligned} \quad (XV.19)$$

$N(f)$ denotes the number of colors (flavors). The anomalous dimension $\gamma_{h1}^{(0)}$ has been first calculated by (Voloshin and Shifman, 1987) and (Politzer and Wise, 1988a), (Politzer and Wise, 1988b). The generalization to next-to-leading order has been performed in (Ji and Musolf, 1991) and (Broadhurst and Grozin, 1991).

The RG equations are readily solved to obtain the coefficients at a lower but still perturbative scale μ , where, formally, $\mu_h = O(m)$. Using the results of section III F we have

$$C_1(\mu) = 1 + \frac{s(\mu)}{4} J_{h1} - \frac{s(\mu_h)}{s(\mu)} \frac{d_{h1}}{4} \left(1 + \frac{s(\mu_h)}{4} \ln \frac{\mu_h}{\mu} + B_1 \right) J_{h1} \quad (\text{XV.20})$$

$$C_2(\mu) = - \frac{s(\mu_h)}{s(\mu)} \frac{d_{h1}}{4} B_2 \quad (\text{XV.21})$$

with

$$d_{h1} = \frac{d_{h1}^{(0)}}{2} \quad J_{h1} = \frac{d_{h1}^{(1)}}{2} \quad (\text{XV.22})$$

We remark that the corresponding formulae for the vector current can be simply obtained from the above expressions by letting $\mu_h \rightarrow 1$ and changing the sign of B_2 .

In addition to the case of heavy-light currents considered here, the NLO corrections have also been calculated for flavor-conserving and flavor-changing heavy-heavy currents of the type $\bar{\psi}_1 \psi_2$ respectively, where $\psi, \psi_{1,2}$ are heavy quark fields ($\psi = \psi, \psi_s$). In these cases the anomalous dimensions become velocity dependent. Additional complications arise in the analysis of flavor changing heavy-heavy currents due to the presence of two distinct heavy mass scales. For a detailed presentation see (Neubert, 1994c) and references cited therein.

D. The Pseudoscalar Decay Constant in the Static Limit

An important application of the results summarized in the last section is the calculation of the short distance QCD effects, from scales between $\mu_h = O(m)$ and the low scale $\mu = O(1 \text{ GeV})$, for the decay constants f_P of pseudoscalar heavy mesons. Using only the leading term in the expansion (XV.12), omitting all $1/m$ power corrections, corresponds to the static limit for f_P , which plays some role in lattice studies. As already mentioned we will restrict ourselves here to this limit. We should remark however, that non-negligible power corrections are known to exist for the realistic case of B or D meson decay constants (Sachrajda, 1992).

The decay constant f_P is defined through

$$\langle 0 | \bar{\psi} \gamma_5 \psi | P \rangle = i f_P m_P v \quad (\text{XV.23})$$

where the pseudoscalar meson state $|P\rangle$ is normalized in the conventional way ($\langle P | P \rangle = 2E_V$). The matrix elements of $\bar{\psi}_{1,2}$ are related via heavy quark symmetry and are given by

$$\langle 0 | \bar{\psi}_1 \psi | P \rangle = \langle 0 | \bar{\psi}_2 \psi | P \rangle = \bar{f}(\mu) \frac{P}{m_P} v \quad (\text{XV.24})$$

Apart from the explicit mass factor $\frac{P}{m_P}$, which is merely due to the normalization of $|P\rangle$, these matrix elements are independent of the heavy quark mass. The "reduced" decay constant $\bar{f}(\mu)$ is therefore m -independent. It does however depend on the renormalization scale and scheme chosen. The computation of $\bar{f}(\mu)$ is a nonperturbative problem involving strong dynamics below scale μ . Using (XV.12), (XV.20), (XV.21), (XV.23) and (XV.24) we obtain

$$f_P = \frac{\bar{f}(\mu)}{P/m_P} \left(1 + \frac{s(\mu)}{4} J_{h1} - \frac{s(\mu_h)}{s(\mu)} \frac{d_{h1}}{4} \left(1 + \frac{s(\mu_h)}{4} \ln \frac{\mu_h}{\mu} + B_1 \right) J_{h1} - B_2 \right) \quad (\text{XV.25})$$

The dependence of the coefficient function on the renormalization scheme through J_{h1} in the second factor in (XV.25), and its dependence on μ_s cancel the corresponding dependences in the hadronic quantity $\hat{F}(\mu_s)$ to the considered order in α_s . The last factor in (XV.25) is scheme independent. Furthermore the cancellation of the dependence on μ_h to the required order can be seen explicitly. Note also the leading scaling behaviour $f_B \propto \frac{1}{m_B}$, which is manifest in (XV.25). Although $\hat{F}(\mu_s)$ cannot be calculated without nonperturbative input, its independence of the heavy quark mass m implies that \hat{F} will drop out in the ratio of f_B over f_D , if charm is treated as a heavy quark. One thus obtains

$$\frac{f_B}{f_D} = \frac{m_D}{m_B} \frac{s(b)}{s(c)} \left(1 + \frac{s(b)}{4} \frac{s(c)}{s(b)} (B_1 - J_{h1} - B_2) + \frac{s(b)}{4} \ln \frac{b}{m_b} + \frac{s(c)}{4} \ln \frac{c}{m_c} \right) \quad (XV.26)$$

The QCD factor on the right hand side of (XV.26) amounts to 1.14 for $m_b = 4.3 \text{ GeV}$, $m_c = 1.4 \text{ GeV}$ and $\mu_s = 0.2 \text{ GeV}$ if we set $\mu_i = m_i$, $i = b, c$. If we allow for a variation of the renormalization scales as $2 \leq \mu_i \leq 2m_i$, this factor lies within a range of 1.12 to 1.16. This is to be compared with the leading log approximation, where the central value reads 1.12 with a variation from 1.10 to 1.15. Note that due to cancellations in the ratio f_B/f_D the scale ambiguity is not much larger in LLA than in NLLA. However the next-to-leading order QCD effects further enhance f_B/f_D independently of the renormalization scheme.

E. $B = 2$ Transitions in the Static Limit

In section XIII we have described the effective hamiltonian for $B^0 - \bar{B}^0$ mixing. The calculation of the mixing amplitude requires in particular the evaluation of the matrix element $\langle B^0 | \mathcal{O} | \bar{B}^0 \rangle$ of the operator

$$\mathcal{O} = (\bar{b}d)_{V-A} (\bar{b}d)_{V-A} \quad (XV.27)$$

in addition to the short-distance Wilson coefficient. Coefficient function and operator matrix element are to be evaluated at a common renormalization scale, $\mu_b = O(m_b)$, say. In contrast to the determination of the Wilson coefficient, the computation of the hadronic matrix element involves nonperturbative long-distance contributions. Ultimately this problem should be solved using lattice QCD. However, the b quark is rather heavy and it is therefore difficult to incorporate it as a fully dynamical field in the context of a lattice regularization approach. On the other hand QCD effects from scales below $\mu_b = O(m_b)$ down to 1 GeV are still accessible to a perturbative treatment. HQET provides the tool to calculate these contributions. At the same time it allows one to extract the dependence of $\langle B^0 | \mathcal{O} | \bar{B}^0 \rangle$ on the bottom mass m_b explicitly, albeit at the prize of the further approximation introduced by the expansion in inverse powers of m_b .

In a first step the operator \mathcal{O} in (XV.27) is expressed as a linear combination of HQET operators by matching the "full" to the effective theory at a scale $\mu_b = O(m_b)$

$$\langle \mathcal{O}(\mu_b) \rangle = \left(1 + \frac{s(b)}{4} \right) \langle \mathcal{O}^{(0)} \rangle + \frac{s(b)}{4} \ln \frac{b}{m_b} \langle \mathcal{O}^{(0)} \rangle + \mathcal{B} \langle \mathcal{O}(\mu_b) \rangle + \frac{s(b)}{4} \mathcal{B}_s \langle \mathcal{O}_s(\mu_b) \rangle \quad (XV.28)$$

Here

$$\mathcal{Q} = 2 (\bar{h}d)_{V-A} (h^c \bar{d})_{V-A} \quad \mathcal{Q}_s = 2 (\bar{h}d)_{S-P} (h^c \bar{d})_{S-P} \quad (\text{XV.29})$$

$(\bar{h}d)_{S-P}$ and $h(1-\gamma_5)d$ are the necessary operators in HQET relevant for the case of a $B^0 \rightarrow B^0$ transition. The field h creates a heavy quark, while h^c annihilates a heavy antiquark. Since the effective theory field h (h^c) cannot, unlike the full theory field b in \mathcal{Q} , at the same time annihilate (create) the heavy antiquark (heavy quark), explicit factors of two have to appear in (XV.29). Similarly to the case of the heavy-light current discussed in the previous section a new operator \mathcal{Q}_s with scalar-pseudoscalar structure is generated. Its coefficient is finite and hence no operator mixing under infinite renormalization occurs between \mathcal{Q} and \mathcal{Q}_s .

In a second step, the matrix element $\langle \mathcal{Q} \rangle_b$ at the high scale μ_b has to be expressed through the matrix element of \mathcal{Q} evaluated at a lower scale $\mu_s \sim 1 \text{ GeV}$, which is relevant for a nonperturbative calculation, for example using lattice gauge theory. This relation can be obtained through the usual renormalization group evolution and reads in NLLA

$$\langle \mathcal{Q} \rangle_b = \left(\frac{s(\mu_b)}{s(\mu_s)} \right)^{\frac{\gamma_{\mathcal{Q}}}{2}} \left(1 + \frac{s(\mu_s)}{4} \frac{s(\mu_b)}{s(\mu_s)} \mathcal{J} \right) \langle \mathcal{Q} \rangle_s \quad (\text{XV.30})$$

where

$$\gamma_{\mathcal{Q}} = \frac{\gamma^{(0)}}{2} \quad \mathcal{J} = \frac{\gamma^{(1)}}{2} - \frac{\gamma^{(0)}}{2} \quad (\text{XV.31})$$

with the beta-function coefficients γ_0 and γ_1 given in (III.16). The calculation of the one-loop anomalous dimension $\gamma^{(0)}$ of the HQET operator \mathcal{Q} , required for the leading log approximation to (XV.30), has been first performed in (Voloshin and Shifman, 1987) and (Politzer and Wise, 1988a), (Politzer and Wise, 1988b). The computation of the two-loop anomalous dimension $\gamma^{(1)}$ is due to (Giménez, 1993). Finally, the next-to-leading order matching condition (XV.28) has been determined in (Flynn *et al.*, 1991). In the following we summarize the results obtained in these papers.

The scheme dependent next-to-leading order quantities B , \tilde{B} and $\gamma^{(1)}$ refer to the NDR scheme with anticommuting γ_5 and the usual subtraction of evanescent terms as defined in (Buras and Weisz, 1990). For $N_c = 3$ colors we then have

$$\gamma^{(0)} = -8 \quad \gamma^{(1)} = 4 \quad (\text{XV.32})$$

$$\tilde{B} - B = -14 \quad B = \frac{11}{3} \quad \tilde{B}_s = -8 \quad (\text{XV.33})$$

$$\gamma^{(1)} = \frac{808}{9} - \frac{52}{27} n_f^2 + \frac{64}{9} n_f \quad (\text{XV.34})$$

where n_f is the number of active flavors.

At this point we would like to make the following comments.

The logarithmic term in (XV.28) reflects the $\mathcal{O}(\mu_s)$ scale dependence of the matrix elements of \mathcal{Q} and \mathcal{Q}_s . Accordingly its coefficient is given by the difference in the one-loop anomalous dimensions of these operators, $\gamma^{(0)}$ and $\gamma_s^{(0)}$.

The one-loop anomalous dimension of the effective theory operator \mathcal{Q} , $\gamma^{(0)}$, is exactly twice as large as the one-loop anomalous dimension of the heavy-light current discussed in section XV C (see eq. (XV.18)). Therefore the scale dependence of $\langle \mathcal{Q} \rangle$ below μ_b is entirely contained in the scale dependence of the decay constant squared $f^2(\mu)$. This implies the well known result that in leading log approximation the parameter B_B has no perturbative scale dependence in the static theory below μ_b . As the result of (Giménez, 1993) for $\gamma^{(1)}$ shows, this somewhat accidental cancellation is not valid beyond the one-loop level.

The matching condition (XV.28) contains besides the logarithm a scheme dependent constant term in the relation between $\langle \mathcal{Q} \rangle$ and $\langle \mathcal{Q} \rangle$. We have written this coefficient in the form $\mathcal{B} = B$ in order to make the cancellation of scheme dependences, to be discussed below, more transparent. Here B is identical to B_+ introduced in (V.8) and characterizes the scheme dependence of $\langle \mathcal{Q} \rangle$ (see also sections XII and XIII).

The quantity \mathcal{B} has been originally calculated in (Giménez, 1993) using dimensional reduction (DRED) instead of NDR as renormalization scheme. However, \mathcal{B} turns out to be the same in DRED and NDR, implying that also $\gamma^{(1)}$ coincides in these schemes (Giménez, 1993).

Finally we may put together (XV.28) and (XV.30), omitting for the moment the scheme independent, constant correction due to \mathcal{Q}_s , to obtain

$$\langle \mathcal{Q}(\mu_b) \rangle = \frac{s(\mu_b)}{s(\mu)}^{\gamma^{(0)}/4} \left(1 + \frac{s(\mu_b)}{4} (\gamma^{(0)} - \gamma^{(0)}) \ln \frac{\mu_b}{\mu} + \mathcal{B} - B \right) \mathcal{J} + \frac{s(\mu)}{4} \mathcal{J} \langle \mathcal{Q}(\mu) \rangle \quad (\text{XV.35})$$

This relation serves to express the $B^0 \rightarrow B^0$ matrix element of the operator \mathcal{Q} , evaluated at a scale $\mu_b = \mathcal{O}(\mu_b)$, which is the relevant scale for the effective hamiltonian of section XIII, in terms of the static theory matrix element $\langle \mathcal{Q}(\mu) \rangle$ normalized at a low scale $\mu = 1 \text{ GeV}$. The latter is more readily accessible to a nonperturbative lattice calculation than the full theory matrix element $\langle \mathcal{Q}(\mu_b) \rangle$. Note that (XV.35) as it stands is valid in the continuum theory. In order to use lattice results one still has to perform an $\mathcal{O}(\mu_s)$ matching of \mathcal{Q} to its lattice counterpart. This step however does not require any further renormalization group improvement since by means of (XV.35) \mathcal{Q} is already normalized at the appropriate low scale μ . The continuum – lattice theory matching was determined in (Flynn *et al.*, 1991) and is also discussed in (Giménez, 1993).

Of course, the right hand side in (XV.35) gives only the leading contribution in the $1/m$ expansion of the full matrix element $\langle \mathcal{Q}(\mu_b) \rangle$ (apart from \mathcal{Q}_s). Going beyond this approximation would require the consideration of several new operators, which appear at the next order in $1/m$. These contributions have been studied in (Kilian and Mannel, 1993) in the leading logarithmic approximation. On the other hand (XV.35), while restricted to the static limit, includes and resums all leading and next-to-leading logarithmic corrections between the scales $\mu_b = \mathcal{O}(\mu_b)$ and 1 GeV in the relation among \mathcal{Q} and \mathcal{Q} . It is interesting to consider the scale and scheme dependences present in (XV.35). The dependence on μ in the first factor on the r.h.s. of (XV.35) is canceled by the μ -dependence of $\langle \mathcal{Q}(\mu) \rangle$. The dependence on μ_b of this factor is canceled by the explicit $\ln \mu_b$ term proportional to $\gamma^{(0)}$. Hence the only scale dependence remaining on the r.h.s., to the considered order $\mathcal{O}(\mu_s)$, is the one $s(\mu_b)^{\gamma^{(0)}/4} \ln \mu_b$. This is precisely the scale

dependence of the full theory matrix element on the l.h.s., which is required to cancel the corresponding dependence of the Wilson coefficient. Similarly the term $\mathcal{B}_s(\mu_b)B$ represents the correct scheme dependence of $\langle \mathcal{Q}(\mu_b) \rangle$, while the scheme dependence of $\mathcal{B}_s(\mu_s)\mathcal{J}$ cancels with the scheme dependence of $\langle \mathcal{Q}(\mu_s) \rangle$ and the difference $\mathcal{B} - \mathcal{J}$ is scheme independent by itself. This discussion demonstrates explicitly that the transition from full QCD to HQET can be made at an arbitrary scale $\mu_b = \mathcal{O}(\mu_b)$, as we have already emphasized above.

Finally we would like to remark that since the logarithm $\ln \mu_b =$ is not really very large in the present case, one might take the attitude of neglecting higher order resummations of logarithmic terms altogether and restricting oneself to the $\mathcal{O}(\alpha_s)$ corrections alone. Then (XV.28) would be already the final result, as it was used in (Flynn *et al.*, 1991). This approximation is fully consistent from a theoretical point of view. Yet it is useful to have the more complete expression (XV.35) at hand. Of course, as indicated above, the finite $\mathcal{O}(\alpha_s)$ correction due to the matrix element of \mathcal{Q}_s in (XV.28) must still be added to the r.h.s. of (XV.35). However, to complete the NLO renormalization group calculation also the leading logarithmic corrections related to the operator \mathcal{Q}_s should then be resummed. To our knowledge this part of the analysis has not yet been performed in the literature so far.

Part Three –

The Phenomenology of Weak Decays

The third part of our review presents the phenomenological picture of weak decays beyond the leading logarithmic approximation.

There is essentially a one-to-one correspondence between the sections in the second and in the third part of this review. Part three uses heavily the results derived in part two. In spite of this, the third part is meant to be essentially self-contained and can be followed without difficulties by those readers who only scanned the material of the second part and read section II.

The phenomenological part of our review is organized as follows. We begin with a few comments on the input parameters in section XVI. Next, as an application of the NLO corrections in the current-current sector, we summarize the present status of the tree level inclusive B-decays, in particular the theoretical status of the semi-leptonic branching ratio. The issue of exclusive two-body non-leptonic decays and the question of factorization will not be discussed here. The numerical values of the related factors a_i for various renormalization schemes can be found in (Buras, 1995).

The main part of the phenomenology begins in section XVIII where we update the "standard" analysis of the unitarity triangle based on the indirect CP violation in $K \rightarrow \pi\pi$ (the parameter η_K) and the $B_d^0 - \bar{B}_d^0$ mixing described by x_d . We incorporate in this analysis the most recent values of m_t , $V_{ub}=V_{cb}$, V_{cb} , B_K and F_B . In addition to the analysis of the unitarity triangle we determine several quantities of interest. These results will be used frequently in subsequent sections.

In section XIX we present ϵ_K' beyond leading logarithms, summarizing and updating the extensive analysis presented in (Buras *et al.*, 1993b). ϵ_K' measures the size of the direct CP violation in $K \rightarrow \pi\pi$ and its accurate estimate is an important but very difficult task. In section XX we discuss briefly the $K_L - K_S$ mass difference and the $\Delta I = 1/2$ rule. Next, in section XXI we present an update for $K_L \rightarrow \pi^0 e^+ e^-$.

Next in sections XXII and XXIII we consider $B \rightarrow X_s \gamma$ and $B \rightarrow X_s e^+ e^-$, respectively. $B \rightarrow X_s \gamma$ is known only in the LO approximation. However, in view of its importance we summarize the leading order formulae and show the standard model prediction compared with the CLEO II findings. We also summarize the present status of NLO calculations for this decay. The NLO calculations for $B \rightarrow X_s e^+ e^-$ have been completed and we give a brief account of these results.

Sections XXIV–XXVI discuss $K \rightarrow \pi\pi$, $K_L \rightarrow \pi^+ \pi^-$ and rare B-decays ($B \rightarrow X_s \gamma$, $B \rightarrow \pi^+ \pi^-$). Except for $K_L \rightarrow \pi^+ \pi^-$, all these decays have only very small hadronic uncertainties and the dominant theoretical errors are related to various renormalization scale ambiguities. We demonstrate that these uncertainties are considerably reduced by including NLO corrections, which will improve the determination of the CKM matrix in forthcoming experiments. Using the results of section XVIII, we also give updated standard model predictions for these decays.

XVI. COMMENTS ON INPUT PARAMETERS

The phenomenology of weak decays depends sensitively on a number of input parameters. We have collected the numerical values of these parameters in appendix A. To this end we have frequently used the values quoted by (Particle Data Group, 1994). The basis for our choice of the numerical values for various non-perturbative parameters, such as B_K or F_B , will be given in the course of our presentation. In certain cases, like the B-meson life-times and the size of the $B_d^0 - \bar{B}_d^0$ mixing, for which the experimental world averages change constantly we have chosen values, which are in the ball park of those presented at various conferences and workshops during the summer of 1995. Here we would like to comment briefly on three important parameters: $|V_{cb}|$, $|V_{ub}| = |V_{cb}|$ and m_t . The importance of these parameters lies in the fact that many branching ratios and also the CP violation in the Standard Model depend sensitively on them.

A. CKM Element $|V_{cb}|$

During the last two years there has been a considerable progress made by experimentalists (Patterson, 1995) and theorists in the extraction of $|V_{cb}|$ from the exclusive and inclusive B-decays. In these investigations the HQET in the case of exclusive decays and the Heavy Quark Expansions for inclusive decays played a considerable role. In particular we would like to mention the important papers (Neubert, 1994a), (Shifman *et al.*, 1995) and (Ball *et al.*, 1995a) on the basis of which one is entitled to use:

$$|V_{cb}| = 0.040 \pm 0.003 \Rightarrow A = 0.82 \pm 0.06 \quad (\text{XVI.1})$$

This should be compared with an error of ± 0.006 for $|V_{cb}|$ quoted still in 1993. The corresponding reduction of the error in A by a factor of 2 has important consequences for the phenomenology of weak decays.

B. CKM Element Ratio $|V_{ub}| = |V_{cb}|$

Here the situation is much worse and the value

$$\frac{|V_{ub}|}{|V_{cb}|} = 0.08 \pm 0.02 \quad (\text{XVI.2})$$

quoted by (Particle Data Group, 1994) appears to be still valid. There is a hope that the error could be reduced by a factor of 2 to 4 in the coming years both due to the theory (Ball *et al.*, 1995a) and the recent CLEO measurements of the exclusive semileptonic decays $B \rightarrow (\pi, \rho) l \bar{\nu}_l$ (Thorndike, 1995).

C. Top Quark Mass m_t

Next it is important to stress that the discovery of the top quark (Abe *et al.*, 1994a), (Abe *et al.*, 1994b), (Abe *et al.*, 1994c), (Abachi *et al.*, 1995) and its mass measurement had an important impact on the field of rare decays and CP violation reducing considerably one potential uncertainty.

It is however important to keep in mind that the parameter m_t , the top quark mass, used in weak decays is not equal to the one used in the electroweak precision studies at LEP or SLD. In the latter investigations the so-called pole mass is used, whereas in all the NLO calculations listed in table I and used in this review, m_t refers to the running current top quark mass normalized at $\mu = m_t$: $m_t(\mu_t)$. One has

$$m_t^{(\text{pole})} = m_t(\mu_t) \left[1 + \frac{4}{3} \frac{\alpha_s(\mu_t)}{\pi} \right] \quad (\text{XVI.3})$$

so that for $m_t = O(170 \text{ GeV})$, $m_t(\mu_t)$ is typically by 8 GeV smaller than $m_t^{(\text{pole})}$. This difference will matter in a few years.

In principle any definition $m_t(\mu_t)$ with $\mu_t = O(m_t)$ could be used. In the leading order this arbitrariness in the choice of μ_t introduces a potential theoretical uncertainty in those branching ratios which depend sensitively on the top quark mass. The inclusion of NLO corrections reduces this uncertainty considerably so that the resulting branching ratios remain essentially independent of the choice of μ_t . We have discussed this point already in previous sections. Numerical examples will be given in this part below. The choice $\mu_t = m_t$ turns out to be convenient and will be adopted in what follows.

Using the $m_t^{(\text{pole})}$ quoted by CDF (Abe *et al.*, 1994a), (Abe *et al.*, 1994b), (Abe *et al.*, 1994c) together with the relation (XVI.3) we find roughly

$$m_t = m_t(\mu_t) = (170 \pm 15) \text{ GeV} \quad (\text{XVI.4})$$

which we will use in our phenomenological applications. In principle an error of $\pm 11 \text{ GeV}$ could be used but we prefer to be conservative.

XVII. INCLUSIVE B DECAYS

A. General Remarks

Inclusive decays of B mesons constitute an important testing ground for our understanding of strong interaction dynamics in its interplay with the weak forces. At the same time inclusive semileptonic modes provide useful information on \mathcal{H}_{cb} .

Due to quark-hadron duality inclusive decays of heavy mesons can, in general, be calculated more reliably than corresponding exclusive modes. During recent years a systematic formulation for the treatment of inclusive heavy meson decays has been developed. It is based on operator product and heavy quark expansion, which are applied to the B meson inclusive width, expressed as the absorptive part of the B forward scattering amplitude

$$\langle B \rightarrow X \rangle = \frac{1}{2m_B} \text{Im} \int_0^Z d^4x \langle B | \mathcal{H}_{\text{eff}}^{(X)}(x) \mathcal{H}_{\text{eff}}^{(X)}(0) | B \rangle \quad (\text{XVII.1})$$

Here $\mathcal{H}_{\text{eff}}^{(X)}$ is the part of the complete $B = 1$ effective hamiltonian that contributes to the particular inclusive final state X under consideration. E.g. for inclusive semileptonic decays

$$\mathcal{H}_{\text{eff}; B=1}^{(SL)} = \frac{G_F}{2} V_{cb} V_{A\ell}^* \sum_{\ell=e;\mu} (1)_{V-A} + \text{h.c.} \quad (\text{XVII.2})$$

For nonleptonic modes the relevant expression is the $B = 1$ short distance effective hamiltonian given in (VI.32). It has been shown in (Chay *et al.*, 1990), (Bjorken *et al.*, 1992), (Bigi *et al.*, 1992), (Bigi *et al.*, 1993), (Manohar and Wise, 1994), (Blok *et al.*, 1994), (Falk *et al.*, 1994), (Mannel, 1994), (Bigi *et al.*, 1994a), that the leading term in a systematic expansion of (XVII.1) in $1/m_b$ is determined by the decay width of a free b-quark calculated in the parton picture. Furthermore, the nonperturbative corrections to this perturbative result start at order $(\Lambda_{\text{QCD}}/m_b)^2$, where

Λ_{QCD} is a hadronic scale $\sim 1 \text{ GeV}$, and are quite small in the case of B decays. In the light of this formulation it becomes apparent that the perturbative, partonic description of heavy hadron decay is thus promoted from the status of a model calculation to the leading contribution in a systematic expansion based on QCD. We will still comment on the $(\Lambda_{\text{QCD}}/m_b)^2$ corrections below. In the following we will however concentrate on the leading quark level analysis of inclusive B decays. As we shall see, the treatment of short-distance QCD effects at the next-to-leading order level – at least for the dominant modes – is of crucial importance for a proper understanding of these processes.

The calculation of b-quark decay starts from the effective $B = 1$ hamiltonian containing the relevant four-fermion operators multiplied by Wilson coefficients. To obtain the decay rate, the matrix elements (squared) of these operators have to be calculated perturbatively to the required order in α_s . While in LLA a zeroth order evaluation is sufficient, $\mathcal{O}(\alpha_s)$ virtual gluon effects (along with real gluon bremsstrahlung contributions for the proper cancellation of infrared divergences in the inclusive rate) have to be taken into account at NLO. In this way the renormalization scale and scheme dependence present in the coefficient functions is canceled to the considered order ($\mathcal{O}(\alpha_s)$) in the decay rate. Thus, by contrast to low energy decays, in the case of inclusive heavy quark decay, a physical final result can be obtained within perturbation theory alone.

Our goal will be in particular to review the present status of the theoretical prediction for the B meson semileptonic branching ratio B_{SL} . This quantity has received some attention in recent years

since theoretical calculations (Altarelli and Petrarca, 1991), (Tanimoto, 1992), (Palmer and Stech, 1993), (Bigi *et al.*, 1994b), (Falk *et al.*, 1995) tended to yield values around $12.5 \pm 1.5\%$, above the experimental figure $B_{SL} = (10.4 \pm 0.4)\%$ (Particle Data Group, 1994). However, these earlier analyses have not been complete in regard to the inclusion of final state mass effects and NLO QCD corrections in the nonleptonic widths. More precisely, these calculations took into account mass effects appropriate for the leading order in QCD along with NLO QCD corrections obtained for massless final state quarks. Recently the most important of these – so far lacking – mass effects have been properly included in the NLO QCD calculation through the work of (Bagan *et al.*, 1994), (Bagan *et al.*, 1995a), (Bagan *et al.*, 1995b). These $O(m_s)$ mass effects tend to decrease B_{SL} and, according to the analysis of these authors essentially bring it, within theoretical uncertainties, into agreement with the experimental number. Before further discussing these issues, it is appropriate to start with a short overview summarizing the possible b-quark decay modes and classifying their relative importance.

B. b-Quark Decay Modes

First of all, a b-quark can decay *semileptonically* to the final states $c\bar{l}_1$ and $u\bar{l}_1$ with $l = e, \mu$.

In the case of nonleptonic final states we may distinguish three classes: Decays induced through current-current operators alone (class I), decays induced by both current-current and penguin operators (class II) and pure penguin transitions (class III). We have

Class	Final State			
I	$c\bar{u}$, $c\bar{s}$;	$u\bar{c}$, $u\bar{d}$		
II	$c\bar{c}$, $c\bar{d}$;	$u\bar{u}$, $u\bar{s}$		
III	$d\bar{d}$, $d\bar{s}$;	$s\bar{d}$, $s\bar{s}$		

Clearly there is a rich structure of possible decay modes even at the quark level and a complete treatment would be quite complicated. However, not all of these final states are equally important. In order to perform the analysis of b-quark decay, in particular in view of the calculation of B_{SL} , it is useful to identify the most important channels and to introduce appropriate approximations in dealing with less prominent decays. To organize the procedure, we make the following observations:

The dominant, i.e. CKM allowed and tree-level induced, decays are $b \rightarrow c\bar{l}$, $b \rightarrow c\bar{u}$ and $b \rightarrow c\bar{c}$. For these a complete NLO calculation including final state mass effects is necessary.

The channels $c\bar{s}$, $c\bar{d}$, $u\bar{c}$, $u\bar{s}$ may be incorporated with excellent accuracy into the modes $c\bar{u}$, $c\bar{c}$, $u\bar{c}$, $u\bar{d}$, respectively, using the approximate CKM unitarity in the first two generations. The error introduced thereby through the s - d mass difference is entirely negligible.

Penguin transitions are generally suppressed by the smallness of their Wilson coefficient functions, which are typically of the order of a few percent. For this reason, one may neglect the pure penguin decays of class III altogether as their decay rates involve penguin coefficients squared.

Furthermore we may neglect the penguin contributions to the CKM suppressed $b \rightarrow u$ transitions of class II.

In addition one may treat the remaining smaller effects, namely $b \rightarrow u$ transitions and the interference of penguins with the leading current-current contribution in $b \rightarrow ccs$ within the leading log approximation.

Finally, rare, flavor-changing neutral current b -decay modes are negligible in the present context as well.

Next we will write down expressions for the relevant decay rate contributions we have discussed. For the dominant modes $b \rightarrow cl$, $b \rightarrow cud$ and $b \rightarrow ccs$ (without penguin effects) one has at next-to-leading order:

$$\Gamma(b \rightarrow cl) = \Gamma_0 P(x_c; x_1; 0) \left[1 + \frac{2}{3} \frac{s(\mu)}{s(\mu_W)} g(x_c; x_1; 0) \right] \quad (\text{XVII.3})$$

$$\begin{aligned} \Gamma(b \rightarrow cud) = & \Gamma_0 P(x_c; 0; 0) \left[2L_+^2 + L_-^2 + \frac{s(\mu_W)}{2} \frac{s(\mu)}{s(\mu_W)} (2L_+^2 R_+ + L_-^2 R_-) \right] \\ & + \frac{2}{3} \frac{s(\mu)}{s(\mu_W)} \frac{3}{4} (L_+ - L_-)^2 g_{11}(x_c) + \frac{3}{4} (L_+ + L_-)^2 g_{22}(x_c) \\ & + \frac{1}{2} (L_+^2 - L_-^2) (g_{12}(x_c) - 12 \ln \frac{m_b}{m_c}) \end{aligned} \quad (\text{XVII.4})$$

$$\begin{aligned} \Gamma(b \rightarrow ccs) = & \Gamma_0 P(x_c; x_c; x_s) \left[2L_+^2 + L_-^2 + \frac{s(\mu_W)}{2} \frac{s(\mu)}{s(\mu_W)} (2L_+^2 R_+ + L_-^2 R_-) \right] \\ & + \frac{2}{3} \frac{s(\mu)}{s(\mu_W)} \frac{3}{4} (L_+ - L_-)^2 h_{11}(x_c) + \frac{3}{4} (L_+ + L_-)^2 h_{22}(x_c) \\ & + \frac{1}{2} (L_+^2 - L_-^2) (h_{12}(x_c) - 12 \ln \frac{m_b}{m_c}) \end{aligned} \quad (\text{XVII.5})$$

Eq. (XVII.5) neglects small strange quark mass effects in the NLO terms, which have however been included in the numerical analysis in (Bagan *et al.*, 1995b). In the equations above $\Gamma_0 = G_F^2 m_b^5 |V_{cb}|^2 / (192 \pi^3)$ and $P(x_1; x_2; x_3)$ is the leading order phase space factor given for arbitrary masses $x_i = m_i^2/m_b^2$ by

$$P(x_1; x_2; x_3) = 12 \int_0^{(1-x_1)^2} \frac{ds}{s} (s - x_2 - x_3) (1 + x_1^2 - s) w(s; x_2^2; x_3^2) w(s; x_1^2; 1) \quad (\text{XVII.6})$$

$$w(a; b; c) = (a^2 + b^2 + c^2 - 2ab - 2ac - 2bc)^2 \quad (\text{XVII.7})$$

P is a completely symmetric function of its arguments. Furthermore

$$L = L(\mu) = \frac{L_s(M_W)}{L_s(\mu)}^{\#_d} \quad (\text{XVII.8})$$

with $d_+ = 6=23$, $d_- = 12=23$ (see (V.10)) and $\mu = O(m_b)$. The scheme independent R come from the NLO renormalization group evolution and are given by $R = B/J$ (see (V.9)). For $f = 5$ flavors $R_+ = 6473=3174$, $R_- = 9371=1587$. Note that the leading dependence of L on the renormalization scale is canceled to $O(\mu)$ by the explicit μ -dependence in the s -correction terms. Virtual gluon and bremsstrahlung corrections to the matrix elements of four fermion operators are contained in the mass dependent functions g , g_{ij} and h_{ij} .

The function $g(x_1; x_2; x_3)$ is available for arbitrary x_1, x_2, x_3 from (Hokim and Pham, 1983), (Hokim and Pham, 1984). The special case $g(x_1; 0; 0)$ has been analysed also in (Cabibbo and Maiani, 1978). Analytical expressions have been given in (Nir, 1989) for $g(x_1; 0; 0)$ and in (Bagan *et al.*, 1994) for $g(0; x_2; 0)$. The functions $g_{11}(x)$, $g_{12}(x)$ and $g_{22}(x)$ are calculated analytically in (Bagan *et al.*, 1994). Furthermore, as discussed in (Bagan *et al.*, 1994), $h_{11}(x)$ and $h_{22}(x)$ can be obtained from the work of (Hokim and Pham, 1983), (Hokim and Pham, 1984). Finally, $h_{12}(x)$ has been determined in (Bagan *et al.*, 1995b). For the full mass dependence of these functions we refer the reader to the cited literature. Here we quote the results obtained in the massless limit. These have been computed in (Altarelli *et al.*, 1981), (Buchalla, 1993) for g_{ij} , h_{ij} ($g_{ij}(0) = h_{ij}(0)$)

$$g_{11}(0) = g_{22}(0) = \frac{31}{4} \mu^2 \quad g_{12}(0) = g_{11}(0) \frac{19}{2} \quad (\text{XVII.9})$$

Furthermore

$$g(0; 0; 0) = \frac{25}{4} \mu^2 \quad (\text{XVII.10})$$

In table XXXVI we have listed some typical numbers extracted from (Bagan *et al.*, 1995a), (Bagan *et al.*, 1995b) illustrating the impact of charm mass effects (for $x_c = 0.3$) in the NLO correction terms by giving the enhancement factor of the NLO over the LO results. There are of course various ambiguities involved in this comparison. The numbers in table XXXVI are therefore merely intended to show the general trend. Note the sizable enhancement through NLO mass effects in the nonleptonic channels, in particular $b \rightarrow ccs$. A large QCD enhancement in the latter case has also been reported in (Voloshin, 1995).

TABLE XXXVI. Typical values for the ratio of NLO to LO results for dominant b -decay channels with (I) and without (II) including finite charm mass effects in the NLO correction terms. The leading order final state mass effects (through the function P) are taken into account in all cases.

	$b \rightarrow c\bar{e}$	$b \rightarrow c\bar{c}$	$b \rightarrow c\bar{u}d$	$b \rightarrow c\bar{c}s$
I	0.85	0.88	1.06	1.32
II	0.79	0.80	1.01	1.02

To complete the presentation of b decay modes we next write down expressions for the CKM suppressed channels $b \rightarrow u\bar{l}$, $b \rightarrow u\bar{c}s$ and $b \rightarrow u\bar{u}d$ (without penguins) as well as the contribution to the $b \rightarrow c\bar{c}s$ rate due to interference of the leading, current-current type transitions with penguin operators. Restricting ourselves to the LLA for these small contributions we obtain

$$(b \rightarrow u \ell \bar{\ell}) = \frac{V_{ub}}{V_{cb}} \mathcal{F}_1^X(0; x_\ell; 0) \quad (\text{XVII.11})$$

$$(b \rightarrow u cs) = \frac{V_{ub}}{V_{cb}} \mathcal{F}_1^X(0; x_c; x_s) \left[2L_+^2 + L_-^2 \right] \quad (\text{XVII.12})$$

$$(b \rightarrow uud) = \frac{V_{ub}}{V_{cb}} \mathcal{F}_1^X(2L_+^2 + L_-^2) \quad (\text{XVII.13})$$

$$\begin{aligned} \text{penguin } (b \rightarrow ccs) = & 6 \mathcal{P}(x_c; x_c; x_s) \left[c_1 c_3 + \frac{1}{3} c_4 + F \left(c_5 + \frac{1}{3} c_6 \right) \right. \\ & \left. + c_2 \left[\frac{1}{3} c_3 + c_4 + F \left(\frac{1}{3} c_5 + c_6 \right) \right] \right] \end{aligned} \quad (\text{XVII.14})$$

where c_1, \dots, c_6 are the leading order Wilson coefficients and

$$F = \frac{6x_c^2}{\mathcal{P}(x_c; x_c; x_s)} \frac{(1 - x_c)^2}{(x_c + x_s)^2} \frac{ds}{s^2} (s + x_s^2 - x_c^2) (1 + s - x_c^2) w(s; x_c^2; x_s^2) w(1; s; x_c^2) \quad (\text{XVII.15})$$

Numerically we have for $V_{ub}/V_{cb} = 0.1$

$$(b \rightarrow u \ell \bar{\ell}) = 0.024_0 \quad (b \rightarrow u cs) = 0.017_0 \quad (\text{XVII.16})$$

$$(b \rightarrow uud) = 0.034_0 \quad \text{penguin } (b \rightarrow ccs) = 0.041_0 \quad (\text{XVII.17})$$

Note that the contribution due to the interference with penguin transitions in $b \rightarrow ccs$ is negative. Hence, in addition to being small the effects in (XVII.16) and (XVII.17) tend to cancel each other in the total nonleptonic width.

Finally one may also incorporate nonperturbative corrections. These have been derived in (Bigi *et al.*, 1992) and are also discussed in (Bagan *et al.*, 1994). As mentioned above, nonperturbative effects are suppressed by two powers of the heavy b-quark mass and amount typically to a few percent. For details we refer the reader to the cited articles.

C. The B Meson Semileptonic Branching Ratio

An important application of the results described in the previous section is the theoretical prediction for the inclusive semileptonic branching ratio of B mesons

$$B_{SL} = \frac{\Gamma(B \rightarrow X \ell \bar{\ell})}{\Gamma_{\text{tot}}(B)} \quad (\text{XVII.18})$$

On the parton level $\Gamma(B \rightarrow X \ell \bar{\ell})' = \Gamma(b \rightarrow c \ell \bar{\ell})$ and

$$\Gamma_{\text{tot}}(B) = \sum_{\text{lepton}} \left[\Gamma(b \rightarrow cl) + \Gamma(b \rightarrow cud) + \Gamma(b \rightarrow ccs) + \Gamma_{\text{penguin}}(b \rightarrow ccs) + \Gamma(b \rightarrow u) \right] \quad (\text{XVII.19})$$

Here we have applied the approximations discussed above. $\Gamma(b \rightarrow u)$ summarizes the $b \rightarrow u$ transitions.

Based on a similar treatment of the partonic rates, including in particular next-to-leading QCD corrections for the dominant channels and also incorporating nonperturbative corrections, the authors of (Bagan *et al.*, 1995a), (Bagan *et al.*, 1995b) have carried out an analysis of B_{SL} and estimated the theoretical uncertainties. They obtain (Bagan *et al.*, 1995b)

$$B_{SL} = (12.0 \pm 1.4)\% \quad \text{and} \quad B_{SL} = (11.2 \pm 1.7)\% \quad (\text{XVII.20})$$

using pole and $\overline{M_S}$ masses, respectively. The error is dominated in both cases by the renormalization scale uncertainty ($m_b = 2 < \mu < 2m_b$). Note also the sizable scheme ambiguity.

Within existing uncertainties, the theoretical prediction does not disagree significantly with the experimental value $B_{SL, \text{exp}} = (10.4 \pm 0.4)\%$ (Particle Data Group, 1994), although it seems to lie still somewhat on the high side.

It is amusing to note, that the naive mode counting estimate for B_{SL} , neglecting QCD and final state mass effects completely, yields $B_{SL} = 1/9 = 11.1\%$ in (almost) "perfect agreement" with experiment. Including the final state masses, still neglecting QCD, enhances this number to $B_{SL} = 15.2\%$. Incorporating in addition QCD effects at the leading log level *increases* the hadronic modes, thus leading to a *decrease* in B_{SL} , resulting typically in $B_{SL} = 14.7\%$. A substantial further decrease is finally brought about through the NLO QCD corrections, which both further enhance hadronic channels, in particular $b \rightarrow ccs$, and simultaneously reduce $b \rightarrow ce$. As pointed out in (Bagan *et al.*, 1995a), (Bagan *et al.*, 1995b) and illustrated in table XXXVI final state mass effects in the NLO correction terms play a nonnegligible role for this enhancement of hadronic decays. The nonperturbative effects also lead to a slight decrease of B_{SL} .

In short, leading final state mass effects and QCD corrections, acting in opposite directions on B_{SL} , tend to cancel each other, resulting in a number for B_{SL} not too different from the simple modecounting guess.

We finally mention that, besides a calculation of B_{SL} , the partonic treatment of heavy meson decay has further important applications, such as the determination of $\langle N_{cb} \rangle$ from inclusive semileptonic B decay, $B \rightarrow X_{ce}$. Analyses of this type have been presented in (Luke and Savage, 1994), (Bigi and Uraltsev, 1994), (Ball and Nierste, 1994), (Shifman *et al.*, 1995).

Exact results beyond the presently known NLO accuracy seem extremely difficult to obtain, even for relatively simple quantities like the semileptonic b-quark decay rate. There exist however calculations in the literature devoted to the investigation of these higher order perturbative effects. Due to the severe technical difficulties, those calculations require additional assumptions. For instance, in an interesting study (Ball *et al.*, 1995a) have investigated the effects of the running of α_s on the semileptonic b-quark decay rate to all orders in perturbation theory. This calculation is equivalent to a resummation of all terms of the form $\alpha_s^n (\ln \mu / \mu_s)^n$, which are related to one-gluon exchange diagrams containing an arbitrary number n of fermion bubbles. The work of (Ball *et al.*, 1995a) applies the renormalon techniques developed in (Beneke and Braun, 1995), (Ball *et al.*, 1995b) and generalizes the $O(\alpha_s^2)$ results computed in (Luke *et al.*, 1995). The underlying idea is similar in spirit to the BLM approach (Brodsky *et al.*, 1983). An important application of the

result is the extraction of \mathcal{V}_{cb} (Ball *et al.*, 1995a). The formalism has also been used to study higher order QCD corrections to the lepton hadronic width (Ball *et al.*, 1995b). Irrespective of the ultimate reliability of the approximation, these investigations are useful from a conceptual point of view as they help to illustrate important features of the higher order behavior of the perturbative expansion.

In principle the discussion we have given for b-decays may of course, with appropriate modifications, be applied to the case of charm as well. However here the nonperturbative corrections to the parton picture, which scale like $1/m_Q^2$ with the heavy quark mass m_Q , are by an order of magnitude larger than for B mesons and accurate theoretical predictions are much more difficult to obtain (Blok and Shifman, 1993).

XVIII. $\epsilon_K, B^0\text{-}B^0$ MIXING AND THE UNITARITY TRIANGLE

A. Basic Formula for ϵ_K

The indirect CP violation in $K \rightarrow \pi\pi$ is described by the well known parameter ϵ_K . The general formula for ϵ_K is given as follows

$$\epsilon_K = \frac{\exp(i\phi_K)}{2\Delta M_K} (\text{Im } M_{12} + 2\text{Re } M_{12}) \quad (\text{XVIII.1})$$

where

$$\phi_K = \frac{\text{Im } A_0}{\text{Re } A_0} \quad (\text{XVIII.2})$$

with $A_0 = A(K \rightarrow \pi\pi)_{J=0}$ and ΔM_K being the K_L - K_S mass difference. The off-diagonal element M_{12} in the neutral K -meson mass matrix represents the K^0 - \bar{K}^0 mixing. It is given by

$$2m_K M_{12} = \langle K^0 | H_{\text{eff}}(S=2) | \bar{K}^0 \rangle \quad (\text{XVIII.3})$$

where $H_{\text{eff}}(S=2)$ is the effective hamiltonian of eq. (XII.1). Defining the renormalization group invariant parameter B_K by

$$B_K = \langle \pi | \bar{s} s | K \rangle_{\text{eff}}^2 / (2\Delta M_K) = 1 + \frac{J_3}{4} \quad (\text{XVIII.4})$$

$$\langle \pi | \bar{s} s | K \rangle_{\text{eff}}^2 = \frac{8}{3} B_K^2 F_K^2 m_K^2 \quad (\text{XVIII.5})$$

and using (XII.1) we find

$$M_{12} = \frac{G_F^2}{12} F_K^2 B_K m_K \Delta M_K^2 \left[S_0(x_c) + \frac{1}{2} S_0(x_t) + 2 S_0(x_c, x_t) \right] \quad (\text{XVIII.6})$$

where the functions $S_0(x_i)$ and $S_0(x_i, x_j)$ are those of eq. (XII.3)–(XII.5). F_K is the K -meson decay constant and m_K the K -meson mass. The coefficient J_3 is given in (XII.9) and the QCD factors S_i have been discussed in section XII. Their numerical values are

$$J_1 = 1.38, \quad J_2 = 0.57, \quad J_3 = 0.47 \quad (\text{XVIII.7})$$

The last term in (XVIII.1) constitutes at most a 2% correction to ϵ_K and consequently can be neglected in view of other uncertainties, in particular those connected with B_K . Inserting (XVIII.6) into (XVIII.1) we find

$$\epsilon_K = C \epsilon B_K \frac{\text{Im } M_{12}}{\Delta M_K} = C \epsilon B_K \frac{\text{Im } M_{12}}{\Delta M_K} \quad (\text{XVIII.8})$$

where we have used the unitarity relation $\text{Im } M_{12} = \text{Im } M_{21}$ and we have neglected $\text{Re } M_{12} = \text{Re } M_{21} = 0$ in evaluating $\text{Im } M_{12}$. The numerical constant C is given by

$$C_{\pi} = \frac{G_F^2 F_K^2 m_K M_W^2}{6^2 2^2 M_K} = 3.78 \quad (10) \quad (\text{XVIII.9})$$

Using the standard parametrization of (II.13) to evaluate $\text{Im } i$ and $\text{Re } i$, setting the values for s_{12} , s_{13} , s_{23} and m_t in accordance with appendix A and taking a value for B_K (see below) one can determine the phase δ by comparing (XVIII.8) with the experimental value for θ_K .

Once δ has been determined in this manner one can find the corresponding point $(\theta; \delta)$ by using (II.19) and (II.22). Actually for a given set $(s_{12}, s_{13}, s_{23}, m_t, B_K)$ there are two solutions for δ and consequently two solutions for $(\theta; \delta)$. In order to see this clearly it is useful to use the Wolfenstein parametrization in which $\text{Im } t$, $\text{Re } c$ and $\text{Re } t$ are given to a very good approximation by (II.23)–(II.25). We then find that (XVIII.8) and the experimental value for θ_K specify a hyperbola in the $(\theta; \delta)$ plane given by

$$(1 - \theta)^2 A^2 S_0(x_t) + P_0(\theta) A^2 B_K = 0.226 : \quad (\text{XVIII.10})$$

where

$$P_0(\theta) = [3S_0(x_c; x_t) - x_c] \frac{1}{4} : \quad (\text{XVIII.11})$$

The hyperbola (XVIII.10) intersects the circle given by (II.32) in two points which correspond to the two solutions for δ mentioned earlier.

The position of the hyperbola (XVIII.10) in the $(\theta; \delta)$ plane depends on m_t , \mathcal{V}_{cb} and B_K . With decreasing m_t , \mathcal{V}_{cb} and B_K the θ_K -hyperbola moves away from the origin of the $(\theta; \delta)$ plane. When the hyperbola and the circle (II.32) touch each other lower bounds consistent with θ_K^{exp} for m_t , \mathcal{V}_{cb} and B_K can be found. The lower bound on m_t is discussed in (Buras, 1993). Corresponding results for \mathcal{V}_{cb} and B_K are shown in fig. 11 and 12, respectively. They will be discussed below.

Moreover approximate analytic expressions for these bounds can be derived. One has

$$(m_t)_{\min} = M_W \frac{1}{2A^2} \frac{1}{A^2 B_K R_b} \quad 1.4 \quad 0.658 \quad (\text{XVIII.12})$$

$$\mathcal{V}_{ub} = \mathcal{V}_{cb} \frac{1}{1 - 2A^2 B_K} \quad 2x_t^{0.76} A^2 + 1.4 \quad i \quad 1 \quad (\text{XVIII.13})$$

$$(B_K)_{\min} = A^2 R_b \quad 2x_t^{0.76} A^2 + 1.4 \quad i \quad 1 \quad (\text{XVIII.14})$$

Concerning the parameter B_K , the analyses of (Sharpe, 1994), (Ishizuka, 1993) ($B_K = 0.83 \pm 0.03$) using the lattice method and of (Bijnens and Prades, 1995) using a somewhat modified form of the $1=N$ approach of (Bardeen *et al.*, 1988), (Gérard, 1990) give results in the ballpark of the $1=N$ result $B_K = 0.70 \pm 0.10$ obtained some time ago in (Bardeen *et al.*, 1988), (Gérard, 1990). In particular the analysis of (Bijnens and Prades, 1995) seems to have explained the difference between these values for B_K and the lower values obtained using the QCD Hadronic Duality approach (Pich and de Rafael, 1985), (Prades *et al.*, 1991) ($B_K = 0.39 \pm 0.10$) or using SU(3) symmetry and PCAC ($B_K = 1/3$) (Donoghue *et al.*, 1982). These higher values of B_K are also found in the most recent lattice analysis (Crisafulli *et al.*, 1995) ($B_K = 0.86 \pm 0.15$) and in the lattice calculations of Bernard and Soni ($B_K = 0.78 \pm 0.11$) and the JLQCD group ($B_K = 0.67 \pm 0.07$) with the quoted values obtained on the basis on the review by (Soni, 1995). In our numerical analysis we will use

$$B_K = 0.75 \pm 0.15 : \quad (\text{XVIII.15})$$

B. Basic Formula for B^0 - B^0 Mixing

The B^0 - B^0 mixing is usually described by

$$x_{d;s} = \frac{(M)_{B_{d;s}}}{B_{d;s}} = \frac{2M_{12}}{B_{d;s}} \quad (\text{XVIII.16})$$

where $(M)_{B_{d;s}}$ is the mass difference between the mass eigenstates in the B_d^0 - B_d^0 system and the B_s^0 - B_s^0 system, respectively, and $B_{d;s} = 1/\tau_{B_{d;s}}$ with $\tau_{B_{d;s}}$ being the corresponding lifetimes. The off-diagonal term M_{12} in (XVIII.16) is given by

$$2m_B M_{12} = \langle B^0 | H_e (B=2) | \bar{B}^0 \rangle \quad (\text{XVIII.17})$$

where $H_e (B=2)$ is the effective hamiltonian of (XIII.1). Defining the renormalization group invariant parameter B_B by

$$B_B = B_B(\mu) \left(\frac{\alpha_s(\mu)}{\alpha_s(\mu_0)} \right)^{\frac{1}{6-2\beta_1}} \left(1 + \frac{\alpha_s(\mu)}{4} J_5 \right) \quad (\text{XVIII.18})$$

$$\langle B^0 | j(\bar{d})_V \gamma_\mu (d)_V \gamma_\mu | \bar{B}^0 \rangle = \frac{8}{3} B_B(\mu) F_B^2 m_B^2 \quad (\text{XVIII.19})$$

and using (XIII.1) we find

$$x_{d;s} = B_{d;s} \frac{G_F^2}{6} m_B m_{B_{d;s}} (B_{B_{d;s}} F_{B_{d;s}}^2) M_W^2 S_0(x_t) \mathcal{V}_{td} \mathcal{V}_{ts}^* \quad (\text{XVIII.20})$$

with the QCD factor B_B discussed in section XIII and given by $B_B = 0.55$.

The measurement of B_d^0 - B_d^0 mixing allows then to determine \mathcal{V}_{td} or R_t of (II.33)

$$\mathcal{V}_{td} = A^3 R_t \quad R_t = 1.52 \frac{R_0}{S_0(x_t)} \quad (\text{XVIII.21})$$

where

$$R_0 = \frac{0.040}{\mathcal{V}_{cb}} \left(\frac{200 \text{ MeV}}{B_{B_d} F_{B_d}} \right)^2 \frac{x_d^{0.5}}{0.75} \frac{1.6 \text{ ps}}{B}^{0.5} \frac{0.55}{B}^{0.5} \quad (\text{XVIII.22})$$

which gives setting $B_B = 0.55$

$$\mathcal{V}_{td} = 8.56 \cdot 10^3 \frac{170 \text{ GeV}}{m_t(m_t)} \left(\frac{200 \text{ MeV}}{B_{B_d} F_{B_d}} \right)^2 \frac{x_d^{0.5}}{0.75} \frac{1.6 \text{ ps}}{B}^{0.5} \quad (\text{XVIII.23})$$

There is a vast literature on the lattice calculations of F_B . The most recent results are somewhat lower than quoted a few years ago. Based on a review by (Sachrajda, 1994), the recent extensive study by (Duncan *et al.*, 1995) and the analyses in (Bernard *et al.*, 1994), (Draper and McNeile, 1994) we conclude that $F_{B_d} = (180 \pm 40) \text{ MeV}$. This together with the earlier result of the European Collaboration (Abada *et al.*, 1992) for B_B , gives $F_{B_d} B_{B_d} = 194 \pm 45 \text{ MeV}$. A

reduction of the error in this important quantity is desirable. These results for F_B are compatible with the results obtained using QCD sum rules (e.g. (Bagan *et al.*, 1992), (Neubert, 1992)). An interesting upper bound $F_{B_d} < 195 \text{ MeV}$ using QCD dispersion relations has also recently been obtained (Boyd *et al.*, 1995). In our numerical analysis we will use

$$F_{B_d} = (200 \pm 40) \text{ MeV} : \quad (\text{XVIII.24})$$

The accuracy of the determination of R_t can be considerably improved by measuring simultaneously the B_s^0 - B_d^0 mixing described by x_s . We have

$$R_t = \frac{1}{R_{ds}} \frac{x_d}{x_s} \frac{1}{1 \pm 2\%} \quad R_{ds} = \frac{B_d}{B_s} \frac{m_{B_d}}{m_{B_s}} \frac{F_{B_d}}{F_{B_s}} \frac{B_{B_d}}{B_{B_s}} : \quad (\text{XVIII.25})$$

Note that m_t and V_{cb} have been eliminated in this way and that R_{ds} depends only on SU (3)-flavour breaking effects which contain much smaller theoretical uncertainties than the hadronic matrix elements in x_d and x_s separately. Provided $x_d = x_s$ has been accurately measured a determination of R_t within 10% should be possible. Indeed the most recent lattice results (Duncan *et al.*, 1995), (Baxter *et al.*, 1994) give $F_{B_s} = F_{B_d} = 1.22 \pm 0.04$. A similar result $F_{B_s} = F_{B_d} = 1.16 \pm 0.05$ has been obtained using QCD sum rules (Narison, 1994). It would be useful to know $B_{B_s} = B_{B_d}$ with a similar precision. For $B_{B_s} = B_{B_d}$ we find using the lattice result $R_{ds} = 0.66 \pm 0.07$.

C. $\sin(2\beta)$ from π_K and B^0 - B^0 Mixing

Combining (XVIII.10) and (XVIII.20) one can derive an analytic formula for $\sin(2\beta)$ (Buras *et al.*, 1994b)

$$\sin(2\beta) = \frac{1}{1.16 A^2 R_0^2} \frac{0.226}{A^2 B_K} P_0(\beta) : \quad (\text{XVIII.26})$$

$P_0(\beta)$ is weakly dependent on m_t and for $155 \text{ GeV} < m_t < 185 \text{ GeV}$ one has $P_0(\beta) = 0.31 \pm 0.02$. As 0.45 for $V_{cb} = 0.1$ the first term in parenthesis is generally by a factor of 2–3 larger than the second term. Since this dominant term is independent of m_t , the values for $\sin(2\beta)$ extracted from π_K and B^0 - B^0 mixing show only a weak dependence on m_t as stressed in particular in (Rosner, 1992).

Since in addition $A^2 R_0^2$ is independent of V_{cb} the dominant uncertainty in this determination of $\sin(2\beta)$ resides in $A^2 B_K$ in the first term in the parenthesis and in $F_{B_d} = B_{B_d}$ contained in R_0^2 .

D. Phenomenological Analysis

We will now combine the analyses of π_K and of B_d^0 - B_d^0 mixing to obtain allowed ranges for several quantities of interest. We consider two sets of input parameters, which are collected in the appendix. The first set represents the present situation. The second set can be considered as a “future vision” in which the errors on various input parameters have been decreased. It is plausible that such errors will be achieved at the end of this decade, although one cannot guarantee that the central values will remain. In table XXXVII we show the results for β , $\sin 2\beta$, $\sin 2\alpha$, $\sin 2\gamma$,

\mathcal{V}_{td} and x_s . They correspond to the two sets of parameters in question, with and without the constraint from $B_d^0 - \bar{B}_d^0$ mixing. The results for $\mathcal{I}m_{\tau}$ and \mathcal{V}_{td} will play an important role in the phenomenology of rare decays and CP violation. For completeness we also show the expectations for $\sin 2\beta$, $\sin 2\beta_c$ and $\sin \beta$ which enter various CP asymmetries in B-decays. As already discussed in detail in (Buras *et al.*, 1994b), $\sin 2\beta$ cannot be predicted accurately this way. On the other hand $\sin 2\beta_c$ and $\sin \beta$ are more constrained and the resulting ranges for these quantities indicate that large CP asymmetries should be observed in a variety of B-decays.

TABLE XXXVII. Predictions for various quantities using present and future input parameter ranges given in appendix A. $\mathcal{I}m_{\tau}$ and \mathcal{V}_{td} are given in units of 10^{-4} and 10^{-3} , respectively. β is in degrees.

	no x_d constraint		with x_d constraint	
	Present	Future	Present	Future
$\mathcal{I}m_{\tau}$	37.7 – 160.0	57.4 – 144.9	37.7 – 140.2	58.5 – 93.3
\mathcal{V}_{td}	0.64 – 1.75	0.82 – 1.50	0.87 – 1.75	1.12 – 1.50
\mathcal{V}_{td}	6.7 – 13.5	7.7 – 12.1	6.7 – 11.9	7.8 – 9.3
x_s	–	–	11.1 – 47.0	19.6 – 29.6
$\sin 2\beta$	–0.86 – 1.00	–0.323 – 1.00	–0.86 – 1.00	–0.30 – 0.73
$\sin 2\beta_c$	0.21 – 0.80	0.34 – 0.73	0.34 – 0.80	0.57 – 0.73
$\sin \beta$	0.34 – 1.00	0.58 – 1.00	0.61 – 1.00	0.85 – 1.00

In fig. 10 we show $\mathcal{I}m_{\tau}$ as a function of m_{τ} . In fig. 11 the lower bound on $\mathcal{V}_{ub} = \mathcal{V}_{cb}$ resulting from the ϵ_K -constraint is shown as a function of \mathcal{V}_{cb} for various values of B_K . To this end we have set $m_{\tau} = 185 \text{ GeV}$. For lower values of m_{τ} the lower bound on $\mathcal{V}_{ub} = \mathcal{V}_{cb}$ is stronger. A similar analysis has been made by (Herrlich and Nierste, 1995a). The latter work and the plot in fig. 11 demonstrate clearly the impact of the ϵ_K constraint on the allowed values of $\mathcal{V}_{ub} = \mathcal{V}_{cb}$ and \mathcal{V}_{cb} . Simultaneously small values of $\mathcal{V}_{ub} = \mathcal{V}_{cb}$ and \mathcal{V}_{cb} although still consistent with tree-level decays, are not allowed by the size of the indirect CP violation observed in $K \rightarrow \pi \ell \ell$. Another representation of this behaviour is shown in fig. 12 where we plot the minimal value of B_K consistent with the experimental value of ϵ_K as a function of \mathcal{V}_{cb} for different $\mathcal{V}_{ub} = \mathcal{V}_{cb}$ and $m_{\tau} < 185 \text{ GeV}$.

Finally in fig. 13 we show the allowed ranges in the $(\beta; \beta_c)$ plane obtained using the information from \mathcal{V}_{cb} , $\mathcal{V}_{ub} = \mathcal{V}_{cb}$, ϵ_K and $B_d^0 - \bar{B}_d^0$ mixing. In this plot we also show the impact of a future measurement of $B_s^0 - \bar{B}_s^0$ mixing with $x_s = 10, 15, 25, 40$, which by means of the formula (XVIII.25) gives an important measurement of the side R_t of the unitarity triangle. Whereas at present a broad range in the $(\beta; \beta_c)$ plane is allowed, the situation might change in the future allowing only the values $0 \leq \beta \leq 0.2$ and $0.30 \leq \beta_c \leq 0.40$. This results in smaller ranges for various quantities of interest as explicitly seen in table XXXVII.

Other analyses of the unitarity triangle can be found in (Peccei and Wang, 1995), (Ciuchini *et al.*, 1995), (Herrlich and Nierste, 1995a), (Ali and London, 1995).

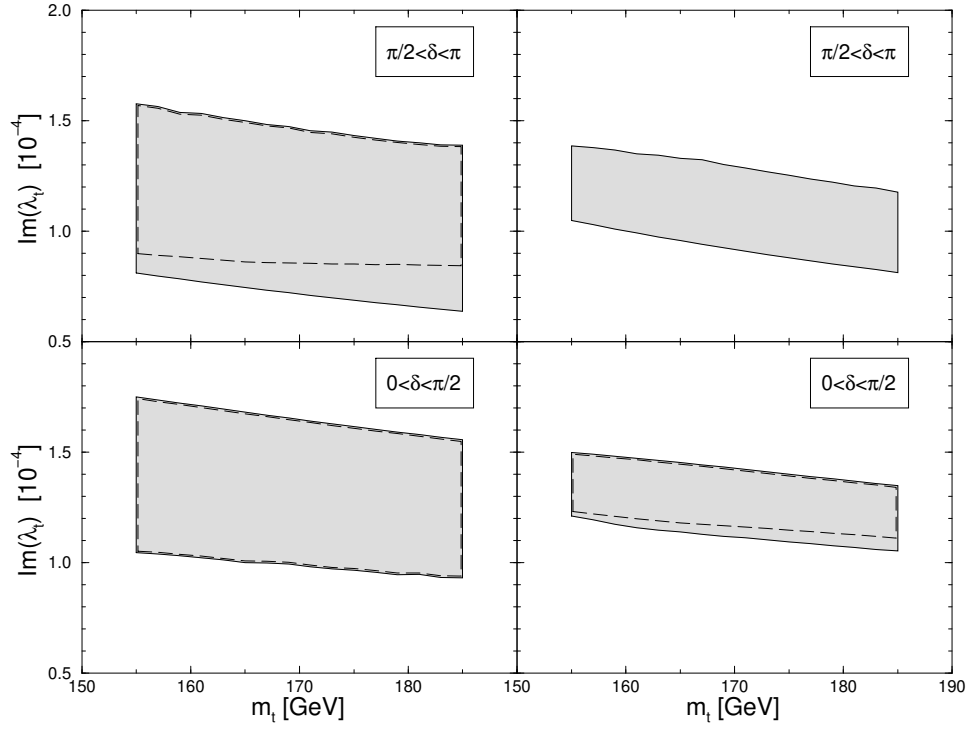


FIG. 10. Present (left) and future (right) allowed ranges for $\text{Im}(\lambda_i)$. The ranges have been obtained by fitting μ_K in (XVIII.8) to the experimental value. Input parameter ranges are given in appendix A. The impact of the additional constraint coming from x_d is illustrated by the dashed lines. With the x_d constraint imposed the solution $\approx 2 < \dots$ is completely eliminated for the future scenario.

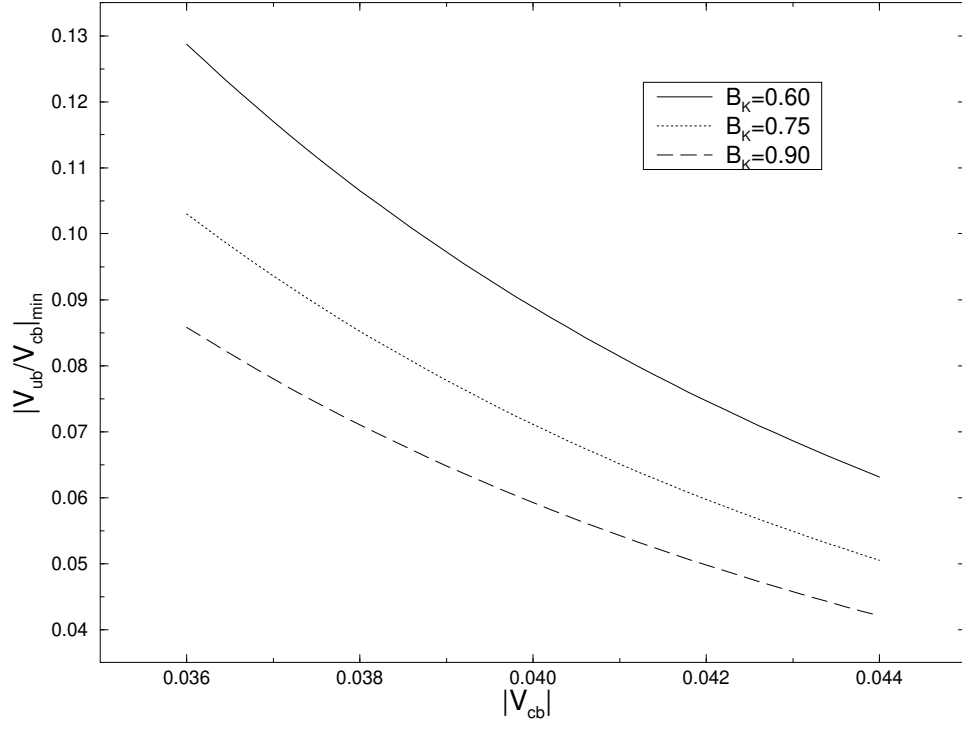


FIG. 11. $|V_{ub}/V_{cb}|_{\min}$ for $m_t = 185 \text{ GeV}$ and various choices of B_K .

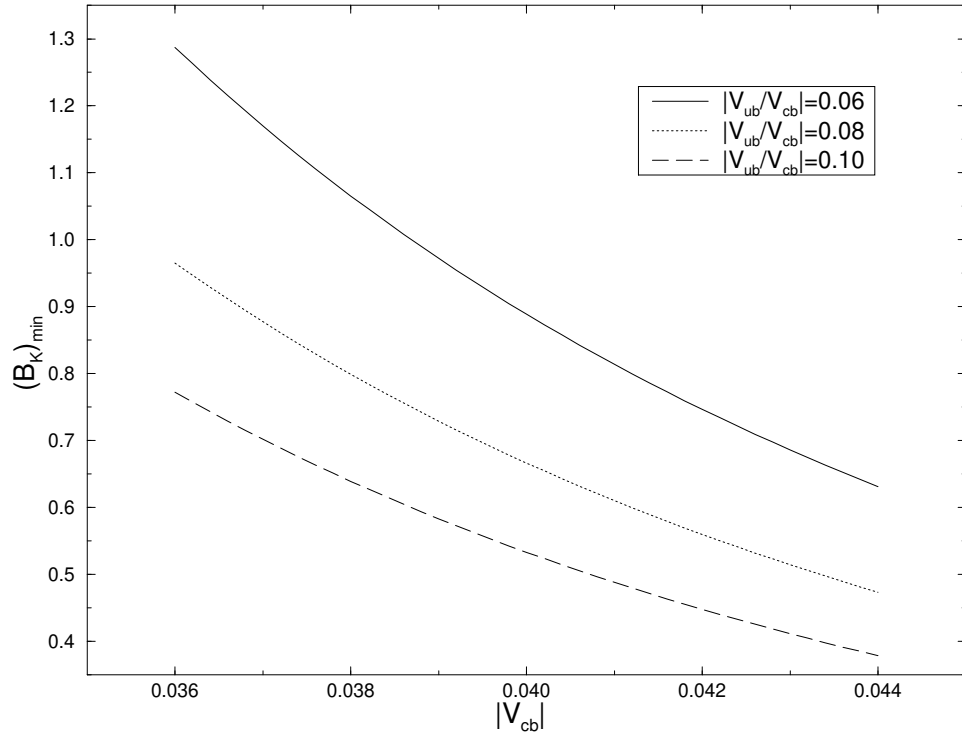


FIG. 12. $(B_K)_{\min}$ of eq. (XVIII.14) for $m_t = 185 \text{ GeV}$ and various choices of $|V_{ub}/V_{cb}|$.

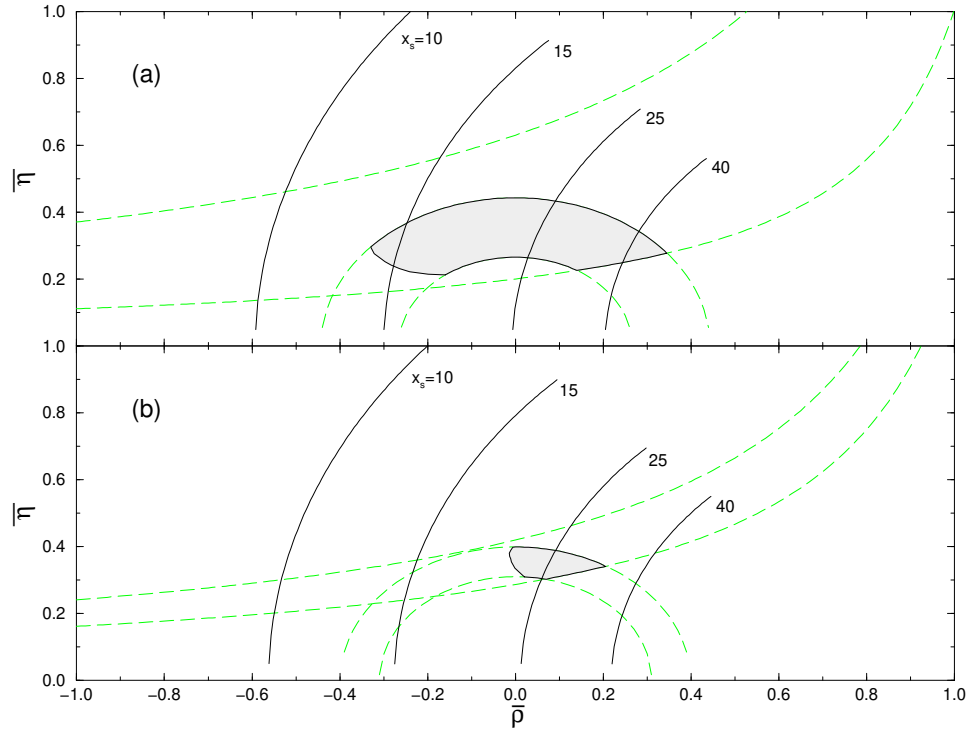


FIG. 13. Present (a) and future (b) allowed ranges for the upper corner A of the UT using data from $K^0 \rightarrow K^0$, $B^0 \rightarrow B^0$ -mixing and tree-level B-decays. Input parameter ranges are given in appendix A. The solid lines correspond to $(R_t)_{\max}$ from eq.(XVIII.25) using $R_{ds} = 0.66$ and $x_s = 10; 15; 25$ and 40, respectively.

XIX. "0=" BEYOND LEADING LOGARITHMS

A. Basic Formulae

The direct CP violation in $K \rightarrow \pi\pi$ is described by ϵ_0 . The parameter ϵ_0 is given in terms of the amplitudes $A_0 = A(K \rightarrow \pi\pi)_{I=0}$ and $A_2 = A(K \rightarrow \pi\pi)_{I=2}$ as follows

$$\epsilon_0 = \frac{1}{\sqrt{2}} (1 - \frac{A_2}{A_0}) \exp(i\phi); \quad (XIX.1)$$

where

$$\frac{A_2}{A_0} = \frac{\text{Im } A_0}{\text{Re } A_0}; \quad \phi = \frac{\text{Re } A_2}{\text{Re } A_0}; \quad \frac{1}{\sqrt{2}} \frac{\text{Im } A_2}{\text{Im } A_0} \quad (XIX.2)$$

and $\phi = \phi_2 + \phi_0 = 4$.

When using (XIX.1) and (XIX.2) in phenomenological applications one usually takes $\text{Re } A_0$ and ϕ from experiment, i.e.

$$\text{Re } A_0 = 3.33 \cdot 10^7 \text{ GeV} \quad \text{Re } A_2 = 1.50 \cdot 10^8 \text{ GeV} \quad \phi = 0.045 \quad (XIX.3)$$

where the last relation reflects the so-called $I = 1/2$ rule. The main reason for this strategy is the unpleasant fact that until today nobody succeeded in fully explaining this rule which to a large extent is believed to originate in the long-distance QCD contributions. We will be more specific about this in the next section. On the other hand the imaginary parts of the amplitudes in (XIX.2) being related to CP violation and the top quark physics should be dominated by short-distance contributions. Therefore $\text{Im } A_0$ and $\text{Im } A_2$ are usually calculated using the effective hamiltonian given in (VII.1). Using this hamiltonian and the experimental values for ϕ , $\text{Re } A_0$ and ϕ the ratio ϵ_0 can be written as follows

$$\epsilon_0 = \frac{\text{Im}}{\text{Re}} \frac{h}{t} P^{(1=2)} \quad P^{(3=2)} \quad (XIX.4)$$

where

$$P^{(1=2)} = \sum_i P_i^{(1=2)} = r \sum_i y_i h_{i1} (1 + \phi) \quad (XIX.5)$$

$$P^{(3=2)} = \sum_i P_i^{(3=2)} = \frac{r}{t} \sum_i y_i h_{i2} \quad (XIX.6)$$

with

$$r = \frac{G_F \phi}{2\sqrt{2} \text{Re } A_0} \quad (XIX.7)$$

Here the hadronic matrix element shorthand notation is

$$h_{i1} = h(\pi\pi)_{i1} \quad (XIX.8)$$

and the sum in (XIX.5) and (XIX.6) runs over all contributing operators. This means for $\phi > m_c$ also contributions from operators $Q_{1,2}^c$ to $P^{(1=2)}$ and $P^{(3=2)}$ have to be taken into account. These are necessary for $P^{(1=2)}$ and $P^{(3=2)}$ to be independent of the renormalization scale μ . Next,

$$+0 = \frac{1}{!} \frac{(\text{Im } A_2)_{\text{IB}}}{\text{Im } A_0} \quad (\text{XIX.9})$$

represents the contribution stemming from isospin breaking in the quark masses ($m_u \neq m_d$). For $+0$ we will take

$$+0 = 0.25 \quad 0.05 \quad (\text{XIX.10})$$

which is in the ball park of the values obtained in the $1=N_c$ approach (Buras and Gérard, 1987) and in chiral perturbation theory (Donoghue *et al.*, 1986), (Lusignoli, 1989). $+0$ is independent of m_t .

The numerical values of the Wilson coefficients y_i have been already given in section VII E. We therefore turn now our attention to the hadronic matrix elements (XIX.8) which constitute the main source of uncertainty in the calculation of $"0"$.

B. Hadronic Matrix Elements for $K \rightarrow \pi$

The hadronic matrix elements $\langle Q_i \rangle_{\pi}$ depend generally on the renormalization scale μ and on the scheme used to renormalize the operators Q_i . These two dependences are canceled by those present in the Wilson coefficients $C_i(\mu)$ so that the resulting physical amplitudes do not depend on μ and on the renormalization scheme of the operators. Unfortunately the accuracy of the present non-perturbative methods used to evaluate $\langle Q_i \rangle_{\pi}$, like lattice methods or $1=N_c$ expansion, is not sufficient to obtain the required μ and scheme dependences of $\langle Q_i \rangle_{\pi}$. A review of the existing methods and their comparison can be found in (Buras *et al.*, 1993b), (Ciuchini *et al.*, 1995). In view of this situation it has been suggested (Buras *et al.*, 1993b) to determine as many matrix elements $\langle Q_i \rangle_{\pi}$ as possible from the leading CP conserving $K \rightarrow \pi$ decays, for which the experimental data are summarized in (XIX.3). To this end it turned out to be very convenient to determine $\langle Q_i \rangle_{\pi}$ at a scale $\mu = m_c$. Using the renormalization group evolution one can then find $\langle Q_i \rangle_{\pi}$ at any other scale $\mu \neq m_c$. The details of this procedure can be found in (Buras *et al.*, 1993b). Here we simply summarize the results of this work.

We first express the matrix elements $\langle Q_i \rangle_{\pi}$ in terms of the non-perturbative parameters $B_i^{(1=2)}$ and $B_i^{(3=2)}$ for $\langle Q_i \rangle_{\pi_0}$ and $\langle Q_i \rangle_{\pi_2}$, respectively. For $\mu = m_c$ we have (Buras *et al.*, 1993b)

$$\langle Q_1 \rangle_{\pi_0} = \frac{1}{9} X B_1^{(1=2)} ; \quad (\text{XIX.11})$$

$$\langle Q_2 \rangle_{\pi_0} = \frac{5}{9} X B_2^{(1=2)} ; \quad (\text{XIX.12})$$

$$\langle Q_3 \rangle_{\pi_0} = \frac{1}{3} X B_3^{(1=2)} ; \quad (\text{XIX.13})$$

$$\langle Q_4 \rangle_{\pi_0} = \langle Q_3 \rangle_{\pi_0} + \langle Q_2 \rangle_{\pi_0} - \langle Q_1 \rangle_{\pi_0} ; \quad (\text{XIX.14})$$

$$\langle Q_5 \rangle_{\pi_0} = \frac{1}{3} B_5^{(1=2)} \overline{\langle Q_6 \rangle_{\pi_0}} ; \quad (\text{XIX.15})$$

$$\langle Q_6 \rangle_{\pi_0} = \frac{1}{4} \frac{\frac{3}{2} \frac{m_K^2}{m_s(\mu) + m_d(\mu)}}{\frac{3}{2} \frac{m_K^2}{m_s(\mu) + m_d(\mu)}} \frac{\#_2 F}{B_6^{(1=2)}} ; \quad (\text{XIX.16})$$

$$\langle Q_7 \rangle_{\pi_0} = \frac{1}{6} \overline{\langle Q_6 \rangle_{\pi_0}} (\frac{1}{3} + 1) - \frac{X}{2} B_7^{(1=2)} ; \quad (\text{XIX.17})$$

$$h_{Q_8 i_0} = \frac{1}{2} \overline{h_{Q_6 i_0}} (+ 1) \frac{X}{6} B_8^{(1=2)} ; \quad (\text{XIX.18})$$

$$h_{Q_9 i_0} = \frac{3}{2} h_{Q_1 i_0} - \frac{1}{2} h_{Q_3 i_0} ; \quad (\text{XIX.19})$$

$$h_{Q_{10} i_0} = h_{Q_2 i_0} + \frac{1}{2} h_{Q_1 i_0} - \frac{1}{2} h_{Q_3 i_0} ; \quad (\text{XIX.20})$$

$$h_{Q_1 i_2} = h_{Q_2 i_2} = \frac{4}{9} \frac{p}{2} X B_1^{(3=2)} ; \quad (\text{XIX.21})$$

$$h_{Q_i i_2} = 0 ; \quad i = 3 ; \dots ; 6 ; \quad \# \quad (\text{XIX.22})$$

$$h_{Q_7 i_2} = \frac{p}{6} \frac{p}{2} \overline{h_{Q_6 i_0}} + \frac{X}{2} B_7^{(3=2)} ; \quad (\text{XIX.23})$$

$$h_{Q_8 i_2} = \frac{p}{2} \frac{p}{2} \overline{h_{Q_6 i_0}} + \frac{p}{6} \frac{p}{2} X B_8^{(3=2)} ; \quad (\text{XIX.24})$$

$$h_{Q_9 i_2} = h_{Q_{10} i_2} = \frac{3}{2} h_{Q_1 i_2} ; \quad (\text{XIX.25})$$

where

$$= \frac{2}{m_K^2 m^2} = \frac{F}{F_K F} ; \quad (\text{XIX.26})$$

$$X = \frac{s}{2} \frac{3}{2} F m_K^2 m^2 ; \quad (\text{XIX.27})$$

and

$$\overline{h_{Q_6 i_0}} = \frac{h_{Q_6 i_0}}{B_6^{(1=2)}} ; \quad (\text{XIX.28})$$

The actual numerical values used for m_K , m , F_K , F are collected in appendix A.

In the vacuum insertion method $B_i = 1$ independent of . In QCD, however, the hadronic parameters B_i generally depend on the renormalizations scale and the renormalization scheme considered.

C. $h_{Q_i} () i_2$ for $(V - A) (V - A)$ Operators

The matrix elements $h_{Q_1 i_2}$, $h_{Q_2 i_2}$, $h_{Q_9 i_2}$ and $h_{Q_{10} i_2}$ can to a very good approximation be determined from $Re A_2$ in (XIX.3) as functions of $\frac{1}{m^2}$, and the renormalization scheme considered. To this end it is useful to set $\epsilon = 0$, as the $O ()$ effects in CP conserving amplitudes, such as the contributions of electroweak penguins, are very small. One then finds

$$h_{Q_1} () i_2 = h_{Q_2} () i_2 = \frac{10^6 \text{ GeV}^2 Re A_2}{1.77 Z_+ ()} = \frac{8.47 \cdot 10^3 \text{ GeV}^3}{Z_+ ()} \quad (\text{XIX.29})$$

and comparing with (XIX.21)

$$B_1^{(3=2)}(\mu_c) = \frac{0.363}{z_+(\mu_c)} \quad (\text{XIX.30})$$

with $z_+ = z_1 + z_2$. Since $z_+(\mu_c)$ depends on the scale and the renormalization scheme used, (XIX.30) gives automatically the scheme and dependence of $B_1^{(3=2)}$ and of the related matrix elements $hQ_1 i_2$, $hQ_2 i_2$, $hQ_9 i_2$ and $hQ_{10} i_2$. The impact of $O(\alpha_s)$ corrections on this result has been analysed in (Buras *et al.*, 1993b). It amounts only to a few percent as expected. These corrections are of course included in the numerical analysis presented in this reference and here as well. Using $m_c = 1.3 \text{ GeV}$, $\frac{(4)}{MS} = 325 \text{ MeV}$ and $z_+(\mu_c)$ of table XIX we find according to (XIX.30)

$$B_{1,NDR}^{(3=2)}(\mu_c) = 0.453 \quad B_{1,HV}^{(3=2)}(\mu_c) = 0.472 : \quad (\text{XIX.31})$$

The following comments should be made:

$B_1^{(3=2)}(\mu_c)$ decreases with increasing μ_c .

The extracted value for $B_1^{(3=2)}$ is by more than a factor of two smaller than the vacuum insertion estimate.

It is compatible with the $1/N_c$ value $B_1^{(3=2)}(1 \text{ GeV}) = 0.55$ (Bardeen *et al.*, 1987a) and somewhat smaller than the lattice result $B_1^{(3=2)}(2 \text{ GeV}) = 0.6$ (Ciuchini *et al.*, 1995).

D. $hQ_i(\mu_c) i_0$ for $(V-A) \times (V-A)$ Operators

The determination of $hQ_i(\mu_c) i_0$ matrix elements is more involved because several operators may contribute to $R\bar{A}_0$. The main idea of (Buras *et al.*, 1993b) is then to set $\mu_c = m_c$, as at this scale only Q_1 and Q_2 operators contribute to $R\bar{A}_0$ in the HV scheme. One then finds $hQ_1(\mu_c) i_0$ as a function of $hQ_2(\mu_c) i_0$

$$hQ_1(\mu_c) i_0 = \frac{10^6 \text{ GeV}^2}{1.77} \frac{R\bar{A}_0}{z_1(\mu_c)} - \frac{z_2(\mu_c)}{z_1(\mu_c)} hQ_2(\mu_c) i_0 \quad (\text{XIX.32})$$

where the reference in $hQ_{1,2}(\mu_c) i_0$ to the HV scheme has been suppressed for convenience. Using next the relations (XIX.14), (XIX.19) and (XIX.20) one is able to obtain $hQ_4(\mu_c) i_0$, $hQ_9(\mu_c) i_0$ and $hQ_{10}(\mu_c) i_0$ as functions of $hQ_2(\mu_c) i_0$ and $hQ_3(\mu_c) i_0$. Because $hQ_3(\mu_c) i_0$ is colour suppressed it is less essential for this analysis than $hQ_2(\mu_c) i_0$. Moreover its Wilson coefficient is small and similarly to $hQ_9(\mu_c) i_0$ and $hQ_{10}(\mu_c) i_0$ also $hQ_3(\mu_c) i_0$ has only a small impact on $\langle \bar{u}u \rangle$. On the other hand the coefficient Y_4 is substantial and consequently $hQ_4(\mu_c) i_0$ plays a considerable role in the analysis of $\langle \bar{u}u \rangle$. The matrix element $hQ_3(\mu_c) i_0$ has then an indirect impact on $\langle \bar{u}u \rangle$ through relation (XIX.14). For numerical evaluation, $hQ_3(\mu_c) i_0$ of (XIX.13) with $B_3^{(1=2)} = 1$ can be used keeping in mind that this may introduce a small uncertainty in the final analysis. This uncertainty has been investigated in (Buras *et al.*, 1993b).

Once the matrix elements in question have been determined as functions of $hQ_2(\mu_c) i_0$ in the HV scheme, they can be found by a finite renormalization in any other scheme. Details can be found in (Buras *et al.*, 1993b).

If one in addition makes the very plausible assumption valid in all known non-perturbative approaches that $hQ_-(m_c) i_0 = hQ_+(m_c) i_0 = 0$ the experimental value of R_{EA_0} in (XIX.3) together with (XIX.32) and table XIX implies for $\frac{(4)}{M_S} = 325 \text{ MeV}$

$$B_{2;L_0}^{(1=2)}(m_c) = 5.7 \pm 1.1 \quad B_{2;N_D R}^{(1=2)}(m_c) = 6.6 \pm 1.0 \quad B_{2;H V}^{(1=2)}(m_c) = 6.2 \pm 1.0 : \quad (\text{XIX.33})$$

The extraction of $B_1^{(1=2)}(m_c)$ and of an analogous parameter $B_4^{(1=2)}(m_c)$ are presented in detail in (Buras *et al.*, 1993b). $B_1^{(1=2)}(m_c)$ depends very sensitively on $B_2^{(1=2)}(m_c)$ and its central value is as high as 15. $B_4^{(1=2)}(m_c)$ is less sensitive and typically by (10–15) % lower than $B_2^{(1=2)}(m_c)$. In any case this analysis shows very large departures from the results of the vacuum insertion method.

E. $hQ_i(\cdot) i_{0,2}$ for $(V - A) - (V + A)$ Operators

The matrix elements of the $(V - A) - (V + A)$ operators $Q_5 - Q_8$ cannot be constrained by CP conserving data and one has to rely on existing non-perturbative methods to calculate them. Fortunately, there are some indications that the existing non-perturbative estimates of $hQ_i(\cdot) i_{0,2}$, $i = 5; \dots; 8$ are more reliable than the corresponding calculations for $(V - A) - (V + A)$ operators.

First of all, the parameters $B_{5,6}^{(1=2)}$ (Kilcup, 1991), (Sharpe, 1991) and $B_{7,8}^{(3=2)}$ (Franco *et al.*, 1989), (Kilcup, 1991), (Sharpe, 1991), (Bernard and Soni, 1991) calculated in the lattice approach

$$B_{5,6}^{(1=2)} = 1.0 \pm 0.2 \quad B_{7,8}^{(3=2)} = 1.0 \pm 0.2 \quad (\text{XIX.34})$$

agree well with the vacuum insertion values ($B_i = 1$) and in the case of $B_6^{(1=2)}$ and $B_8^{(3=2)}$ with the $1=N_c$ approach ($B_6^{(1=2)} = B_8^{(3=2)} = 1$) (Bardeen *et al.*, 1987b), (Buras and Gérard, 1987).

We note next that with fixed values for $B_{5,6}^{(1=2)}$ and $B_{7,8}^{(3=2)}$ the β -dependence of $hQ_{5,6} i_0$ and $hQ_{7,8} i_2$ is governed by the β -dependence of $m_s(\beta)$. For $hQ_6 i_0$ and $hQ_8 i_2$ this property has been first found in the $1=N_c$ approach (Buras and Gérard, 1987): in the large- N_c limit the anomalous dimensions of Q_6 and Q_8 are simply twice the anomalous dimension of the mass operator leading to

$1=m_s^2(\beta)$ for the corresponding matrix elements. Another support comes from a renormalization study in (Buras *et al.*, 1993b). In this analysis the B_i -factors in (XIX.34) have been set to unity at $\mu = m_c$. Subsequently the evolution of the matrix elements in the range $1 \text{ GeV} < \mu < 4 \text{ GeV}$ has been calculated showing that for the NDR scheme $B_{5,6}^{(1=2)}$ and $B_{7,8}^{(3=2)}$ were β -independent within an accuracy of (2–3) %. The β -dependence in the HV scheme has been found to be stronger but still below 10 %.

Concerning $B_{7,8}^{(1=2)}$ one can simply set $B_{7,8}^{(1=2)} = 1$ as the matrix elements $hQ_{7,8} i_0$ play only a minor role in the " $\theta=0$ " analysis.

In summary, our treatment of $hQ_i i_{0,2}$, $i = 5; \dots; 8$ follows the one used in (Buras *et al.*, 1993b). We will set

$$B_{7,8}^{(1=2)}(m_c) = 1 \quad B_5^{(1=2)}(m_c) = B_6^{(1=2)}(m_c) \quad B_7^{(3=2)}(m_c) = B_8^{(3=2)}(m_c) \quad (\text{XIX.35})$$

and we will treat $B_6^{(1=2)}(m_c)$ and $B_8^{(3=2)}(m_c)$ as free parameters in the neighbourhood of the values given in (XIX.34). Then the main uncertainty in the values of $hQ_i i_{0,2}$, $i = 5; \dots; 8$ results from the value of the strange quark mass $m_s(m_c)$. The present estimates give

$$m_s(m_c) = (170 \pm 20) \text{ MeV} \quad (\text{XIX.36})$$

with the lower values coming from recent lattice calculations (Allton *et al.*, 1994) and the higher ones from QCD sum rules (Jamin and Münz, 1995), (Chetyrkin *et al.*, 1995).

F. The Four Dominant Contributions to R_{B}

$P^{(1=2)}$ and $P^{(3=2)}$ in (XIX.4) can be written as linear combinations of two independent hadronic parameters $B_6^{(1=2)}$ and $B_8^{(3=2)}$ (Buras *et al.*, 1993b). This B_i -expansion reads

$$P^{(1=2)} = a_0^{(1=2)} + \frac{178 \text{ MeV}}{m_s(m_c) + m_d(m_c)} a_6^{(1=2)} B_6^{(1=2)} \quad (\text{XIX.37})$$

$$P^{(3=2)} = a_0^{(3=2)} + \frac{178 \text{ MeV}}{m_s(m_c) + m_d(m_c)} a_8^{(3=2)} B_8^{(3=2)} : \quad (\text{XIX.38})$$

Here $a_0^{(1=2)}$ and $a_0^{(3=2)}$ effectively summarize all dependences other than $B_6^{(1=2)}$ and $B_8^{(3=2)}$, especially $B_2^{(1=2)}$ in the case of $a_0^{(1=2)}$. Note that in contrast to (Buras *et al.*, 1993b) we have absorbed the dependence on $B_2^{(1=2)}$ into $a_0^{(1=2)}$ and we have exhibited the dependence on m_s which was not shown explicitly there. The residual m_s dependence present in $a_0^{(1=2)}$ and $a_0^{(3=2)}$ is negligible. Setting $\mu = m_c$, and using the strategy for hadronic matrix elements outlined above one finds the coefficients $a_i^{(1=2)}$ and $a_i^{(3=2)}$ as functions of $\frac{4}{M_S}$, m_t and the renormalization scheme considered. These dependences are given in tables XXXVIII and XXXIX. We should however stress that $P^{(1=2)}$ and $P^{(3=2)}$ are independent of μ and the renormalization scheme considered.

TABLE XXXVIII. B_i -expansion coefficients for $P^{(1=2)}$.

$\frac{4}{M_S} [\text{MeV}]$	$m_t [\text{GeV}]$	LO		NDR		HV	
		$a_0^{(1=2)}$	$a_6^{(1=2)}$	$a_0^{(1=2)}$	$a_6^{(1=2)}$	$a_0^{(1=2)}$	$a_6^{(1=2)}$
215	155	-2.138	5.110	-2.251	4.676	-2.215	4.159
	170	-2.070	5.138	-2.187	4.698	-2.150	4.181
	185	-1.996	5.162	-2.117	4.716	-2.081	4.200
325	155	-2.231	6.540	-2.414	6.255	-2.362	5.389
	170	-2.161	6.576	-2.350	6.282	-2.298	5.416
	185	-2.085	6.606	-2.281	6.306	-2.229	5.439
435	155	-2.288	8.171	-2.549	8.417	-2.473	6.972
	170	-2.212	8.214	-2.482	8.451	-2.406	7.005
	185	-2.130	8.251	-2.409	8.480	-2.333	7.035

Inspecting (XIX.37), (XIX.38) and tables XXXVIII, XXXIX we identify the following four contributions which govern the ratio R_{B} at scales $\mu = O(m_c)$:

- The contribution of $(\bar{V} \quad A) \quad (\bar{V} \quad A)$ operators to $P^{(1=2)}$ is dominantly represented by $a_0^{(1=2)}$. This term is to a large extent fixed by the experimental value of A_0 and consequently

TABLE XXXIX. B_1 -expansion coefficients for $P^{(3=2)}$.

$\frac{(4)}{M_S}$ [M eV]	m_t [G eV]	LO		NDR		HV	
		$a_0^{(3=2)}$	$a_8^{(3=2)}$	$a_0^{(3=2)}$	$a_8^{(3=2)}$	$a_0^{(3=2)}$	$a_8^{(3=2)}$
215	155	-0.797	1.961	-0.819	1.887	-0.838	2.114
	170	-0.880	2.602	-0.900	2.438	-0.919	2.666
	185	-0.965	3.296	-0.983	3.036	-1.002	3.263
325	155	-0.788	2.645	-0.814	2.639	-0.837	2.894
	170	-0.870	3.422	-0.895	3.305	-0.917	3.560
	185	-0.956	4.264	-0.978	4.027	-1.000	4.281
435	155	-0.779	3.425	-0.809	3.622	-0.835	3.899
	170	-0.861	4.360	-0.889	4.435	-0.915	4.712
	185	-0.947	5.372	-0.971	5.316	-0.998	5.593

is only very weakly dependent on $\frac{(4)}{M_S}$ and the renormalization scheme considered. The weak dependence on m_t results from small contributions of electroweak penguin operators. Taking $\frac{(4)}{M_S} = 325 \text{ M eV}$, $m_c = m_c$ and $m_t = 170 \text{ G eV}$ we have $a_0^{(1=2)} = 2.3$ for both schemes considered. We observe that the contribution of $(V - A) - (V + A)$ operators, in particular Q_4 , to $"0="$ is *negative*.

- ii. The contribution of $(V - A) - (V + A)$ QCD penguin operators to $P^{(1=2)}$ is given by the second term in (XIX.37). This contribution is large and *positive*. The coefficient $a_6^{(1=2)}$ depends sensitively on $\frac{(4)}{M_S}$ which results from the strong dependence of y_6 on the QCD scale. The dependence on m_t is very weak on the other hand. Taking $\frac{(4)}{M_S} = 325 \text{ M eV}$, $m_s(m_c) = 170 \text{ M eV}$ and $m_t = 170 \text{ G eV}$ and setting as an example $B_6^{(1=2)} = 1$ in the NDR and HV schemes we find a positive contribution to $"0="$ amounting to 6.3 and 5.4 in the NDR and HV scheme, respectively.
- iii. The contribution of the $(V - A) - (V + A)$ electroweak penguin operators Q and Q_{10} to $P^{(3=2)}$ is represented by $a_0^{(3=2)}$. As in the case of the contribution i, the matrix elements contributing to $a_0^{(3=2)}$ are fixed by the CP conserving data, this time by the amplitude A_2 . Consequently, the scheme and the $\frac{(4)}{M_S}$ dependence of $a_0^{(3=2)}$ is very weak. The sizeable m_t dependence of $a_0^{(3=2)}$ results from the m_t dependence of $y_9 + y_{10}$. $a_0^{(3=2)}$ contributes *positively* to $"0="$. For $m_t = 170 \text{ G eV}$ this contribution is roughly 0.9 for both renormalization schemes and the full range of $\frac{(4)}{M_S}$ considered.
- iv. The contribution of the $(V - A) - (V + A)$ electroweak penguin operators Q and Q_8 to $P^{(3=2)}$ is represented by the second term in (XIX.38). This contribution depends sensitively on m_t and $\frac{(4)}{M_S}$ as could be expected on the basis of y_7 and y_8 . Taking again $B_8^{(3=2)} = 1$ in both renormalization schemes we find for the central values of $\frac{(4)}{M_S}$, m_t and m_c a *negative* contribution to $"0="$ equal to -3.9 and -3.6 for the NDR and HV scheme, respectively.

Before analysing $"0="$ numerically in more detail, let us just set $\text{Im } m_t = 1.3 \cdot 10^4$ and $B_6^{(1=2)} =$

$B_8^{(3=2)} = 1$ in both schemes. Then for the central values of the remaining parameters one obtains $"^0=" = 2.0 \cdot 10^4$ and $"^0=" = 0.6 \cdot 10^4$ for the NDR and HV scheme, respectively. This strong scheme dependence can only be compensated for by having $B_6^{(1=2)}$ and $B_8^{(3=2)}$ different in the two schemes considered. As we will see below the strong cancellations between various contributions at $m_t = 170 \text{ GeV}$ make the prediction for $"^0="$ rather uncertain. One should also stress that the formulation presented here does not exhibit analytically the m_t dependence. As the coefficients $a_0^{(3=2)}$ and $a_8^{(3=2)}$ depend very sensitively on m_t it is useful to display this dependence in an analytic form.

G. An Analytic Formula for $"^0="$

As shown in (Buras and Lautenbacher, 1993) it is possible to cast the above discussion into an analytic formula which exhibits the m_t dependence together with the dependence on m_s , $B_6^{(1=2)}$ and $B_8^{(3=2)}$. Such an analytic formula should be useful for those phenomenologists and experimentalists who are not interested in getting involved with the technicalities discussed in preceding sections.

In order to find an analytic expression for $"^0="$ which exactly reproduces the results discussed above one uses the PBE presented in section XIV. The resulting analytic expression for $"^0="$ is then given as follows

$$"^0=" = \text{Im}_t F(\mathbf{x}_t) \quad (\text{XIX.39})$$

where

$$F(\mathbf{x}_t) = P_0 + P_X X_0(\mathbf{x}_t) + P_Y Y_0(\mathbf{x}_t) + P_Z Z_0(\mathbf{x}_t) + P_E E_0(\mathbf{x}_t) \quad (\text{XIX.40})$$

with the m_t dependent functions listed in section XIV. The coefficients P_i are given in terms of $B_6^{(1=2)}$, $B_6^{(1=2)}(m_c)$, $B_8^{(3=2)}$, $B_8^{(3=2)}(m_c)$ and $m_s(m_c)$ as follows

$$P_i = r_i^{(0)} + \frac{178 \text{ MeV}}{m_s(m_c) + m_d(m_c)} \#_2 \quad r_i^{(6)} B_6^{(1=2)} + r_i^{(8)} B_8^{(3=2)} : \quad (\text{XIX.41})$$

The P_i are and renormalization scheme independent. They depend however on $\overline{m_s}$. In table XL we give the numerical values of $r_i^{(0)}$, $r_i^{(6)}$ and $r_i^{(8)}$ for different values of $\overline{m_s}$ at $\mu = m_c$ in the NDR renormalization scheme. Analogous results in the HV scheme are given in table XLI. The coefficients $r_i^{(0)}$, $r_i^{(6)}$ and $r_i^{(8)}$ do not depend on $m_s(m_c)$ as this dependence has been factored out. $r_i^{(0)}$ does, however, depend on the particular choice for the parameter $B_2^{(1=2)}$ in the parametrization of the matrix element $\langle \bar{u} \gamma_5 d \rangle_0$. The values given in the tables correspond to the central values in (XIX.33). Variation of $B_2^{(1=2)}$ in the full allowed range introduces an uncertainty of at most 18 % in the $r_i^{(0)}$ column of the tables. Since the parameters $r_i^{(0)}$ give only subdominant contributions to $"^0="$ keeping $B_2^{(1=2)}$ and $r_i^{(0)}$ at their central values is a very good approximation.

For different scales the numerical values in the tables change without modifying the values of the P_i 's as it should be. To this end also $B_6^{(1=2)}$ and $B_8^{(3=2)}$ have to be modified as they depend albeit weakly on μ .

Concerning the scheme dependence we note that whereas r_0 coefficients are scheme dependent, the coefficients r_i , $i = X; Y; Z; E$ do not show any scheme dependence. This is related to the fact that the m_t dependence in Γ^0 enters first at the NLO level and consequently all coefficients r_i in front of the m_t dependent functions must be scheme independent. That this turns out to be indeed the case is a nice check of our calculations.

Consequently when changing the renormalization scheme one is only obliged to change appropriately $B_6^{(1=2)}$ and $B_8^{(3=2)}$ in the formula for P_0 in order to obtain a scheme independence of Γ^0 . In calculating P_i where $i \neq 0$, $B_6^{(1=2)}$ and $B_8^{(3=2)}$ can in fact remain unchanged, because their variation in this part corresponds to higher order contributions to Γ^0 which would have to be taken into account in the next order of perturbation theory.

For similar reasons the NLO analysis of Γ^0 is still insensitive to the precise definition of m_t . In view of the fact that the NLO calculations of Γ_{m_t} have been done with $m_t = \overline{m}_t(m_t)$ we will also use this definition in calculating $F(x_t)$.

TABLE XL. $S = 1$ PBE coefficients for various \overline{m}_S in the NDR scheme.

i	$\overline{m}_S = 215 \text{ M eV}$			$\overline{m}_S = 325 \text{ M eV}$			$\overline{m}_S = 435 \text{ M eV}$		
	$r_i^{(0)}$	$r_i^{(6)}$	$r_i^{(8)}$	$r_i^{(0)}$	$r_i^{(6)}$	$r_i^{(8)}$	$r_i^{(0)}$	$r_i^{(6)}$	$r_i^{(8)}$
0	-2.644	4.784	0.876	-2.749	6.376	0.689	-2.845	8.547	0.436
X	0.555	0.008	0	0.521	0.012	0	0.495	0.017	0
Y	0.422	0.037	0	0.385	0.046	0	0.356	0.057	0
Z	0.074	-0.007	-4.798	0.149	-0.009	-5.789	0.237	-0.011	-7.064
E	0.209	-0.591	0.205	0.181	-0.727	0.265	0.152	-0.892	0.342

TABLE XLI. $S = 1$ PBE coefficients for various \overline{m}_S in the HV scheme.

i	$\overline{m}_S = 215 \text{ M eV}$			$\overline{m}_S = 325 \text{ M eV}$			$\overline{m}_S = 435 \text{ M eV}$		
	$r_i^{(0)}$	$r_i^{(6)}$	$r_i^{(8)}$	$r_i^{(0)}$	$r_i^{(6)}$	$r_i^{(8)}$	$r_i^{(0)}$	$r_i^{(6)}$	$r_i^{(8)}$
0	-2.631	4.291	0.668	-2.735	5.548	0.457	-2.830	7.163	0.185
X	0.555	0.008	0	0.521	0.012	0	0.495	0.017	0
Y	0.422	0.037	0	0.385	0.046	0	0.356	0.057	0
Z	0.074	-0.007	-4.798	0.149	-0.009	-5.789	0.237	-0.011	-7.064
E	0.209	-0.591	0.205	0.181	-0.727	0.265	0.152	-0.892	0.342

The inspection of tables XL and XLI shows that the terms involving $r_0^{(6)}$ and $r_Z^{(8)}$ dominate the ratio Γ^0 . The function $Z_0(x_t)$ representing a gauge invariant combination of Z^0 - and γ -penguins grows rapidly with m_t and due to $r_Z^{(8)} < 0$ these contributions suppress Γ^0 strongly for large m_t (Flynn and Randall, 1989b), (Buchalla *et al.*, 1990). These two dominant terms $r_0^{(6)}$ and $r_Z^{(8)}$ correspond essentially to the second terms in (XIX.37) and (XIX.38), respectively. The first term in (XIX.37) corresponds roughly to $r_0^{(0)}$ given here, while the first term in (XIX.38) is represented

to a large extent by the positive contributions of $X_0(x_t)$ and $Y_0(x_t)$. The last term in (XIX.40) representing the residual m_t dependence of QCD penguins plays only a minor role in the full analysis of $"0="$.

H. Numerical Results

Let us define two effective B-factors:

$$(B_i^{(j)}(m_c))_{\text{eff}} = \frac{178 \text{ MeV}}{m_s(m_c) + m_d(m_c)} \#_2 B_i^{(j)}(m_c) \quad (\text{XIX.42})$$

In fig. 14 we show $"0="$ for $m_t = 170 \text{ GeV}$ as a function of $\frac{1}{m_s}$ for different choices of the effective B_i factors. We show here only the results in the NDR scheme. As discussed above $"0="$ is generally lower in the HV scheme, if the same values for $B_6^{(1=2)}$ and $B_8^{(3=2)}$ are used in both schemes. In view of the fact that the differences between NDR and HV schemes are smaller than the uncertainties in $B_6^{(1=2)}$ and $B_8^{(3=2)}$ we think it is sufficient to present only the results in the NDR scheme here. The results in the HV scheme can be found in (Buras *et al.*, 1993b), (Ciuchini *et al.*, 1995).

Fig. 14 shows strong dependence of $"0="$ on $\frac{1}{m_s}$. However the main uncertainty originates in the poor knowledge of $(B_i)_{\text{eff}}$. In case a) in which the QCD-penguin contributions dominate, $"0="$ can reach values as high as $1 \cdot 10^3$. However, in case c) the electroweak penguin contributions are large enough to cancel essentially the QCD-penguin contributions completely. Consequently in this case $"0=" < 2 \cdot 10^5$ and the standard model prediction of $"0="$ cannot be distinguished from a superweak theory. As shown in fig. 15 higher values of $"0="$ can be obtained for $m_t = 155 \text{ GeV}$ although still $"0=" < 13 \cdot 10^4$.

For $m_t = 185 \text{ GeV}$ the values of $"0="$ are correspondingly smaller and in case c) small negative values are found for $"0="$. In figs. 14–16 the dark grey regions refer to the future ranges for $\frac{1}{m_s}$. Of course one should hope that also the knowledge of $(B_i)_{\text{eff}}$ and of $\frac{(4)}{m_s}$ will be improved in the future so that a firmer prediction for $"0="$ can be obtained.

Finally, fig. 17 shows the interrelated influence of m_t and the two most important hadronic matrix elements for penguin operators on the theoretical prediction of $"0="$. For a dominant QCD penguin matrix element $\langle Q_6 \rangle_0$ $"0="$ stays positive for all m_t values considered. $"0=" = 0$ becomes possible for equally weighted matrix elements $\langle Q_6 \rangle_0$ and $\langle Q_8 \rangle_2$ around $m_t = 205 \text{ GeV}$. A dominant electroweak penguin matrix element $\langle Q_8 \rangle_2$ shifts the point $"0=" = 0$ to $m_t = 165 \text{ GeV}$ and even allows for a negative $"0="$ for higher values of m_t . The key issue to understand this behaviour of $"0="$ is the observation that the Q_6 contribution to $"0="$ is positive and only weakly m_t dependent. On the other hand the contribution coming from Q_8 is negative and shows a strong m_t dependence.

The results in fig. 14–17 use only the $"_K$ constraint. In order to complete our analysis we want to impose also the x_d -constraint and vary $m_s(m_c)$, $B_6^{(1=2)}$ and $B_8^{(3=2)}$ in the full ranges given in (XIX.34) and (XIX.36).

This gives for the “present” scenario

$$2:1 \cdot 10^4 \leq "0=" \leq 13:2 \cdot 10^4 \quad (\text{XIX.43})$$

to be compared with

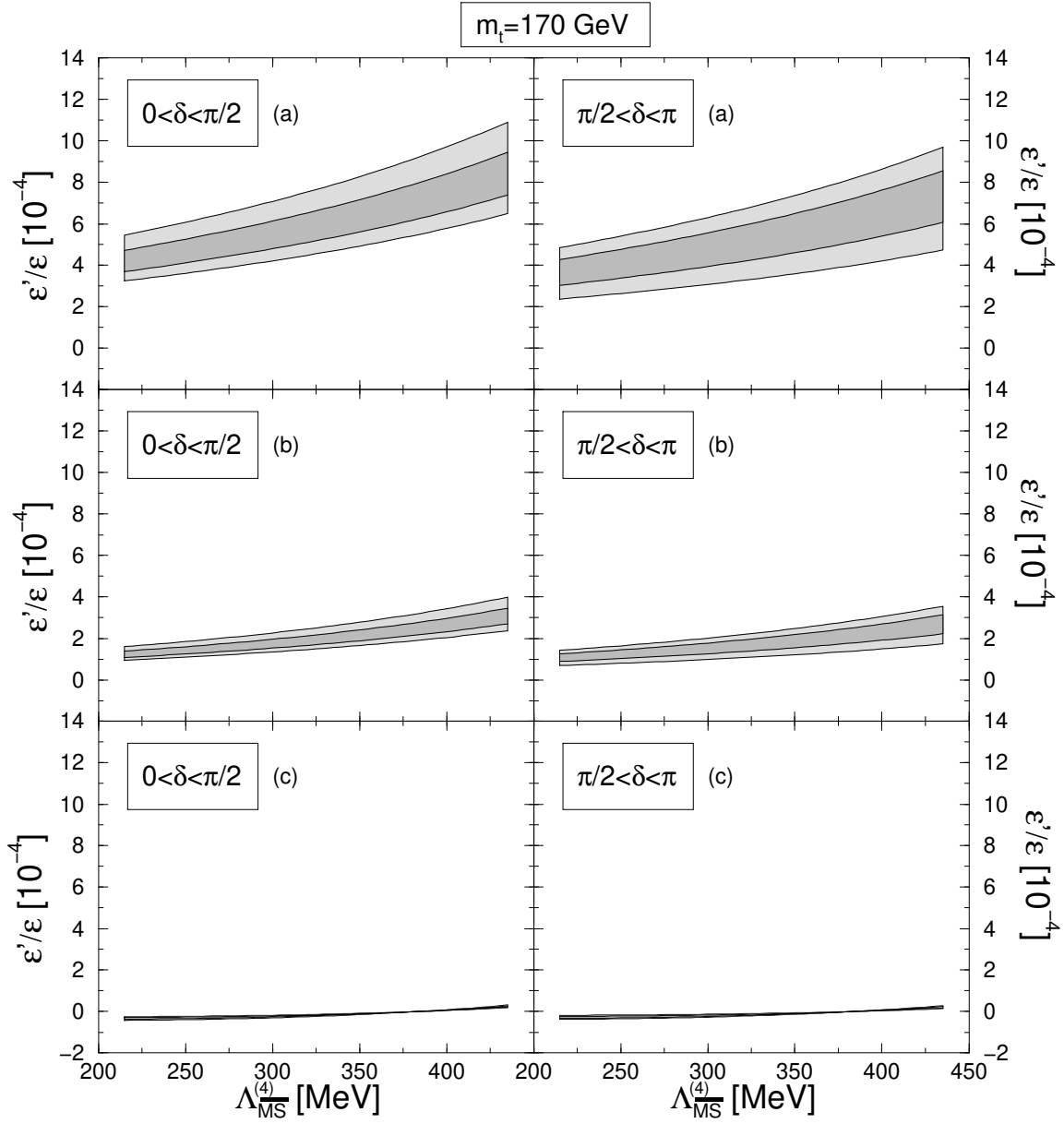


FIG. 14. The ranges of ϵ'/ϵ in the NDR scheme as a function of $\Lambda_{\overline{MS}}^{(4)}$ for $m_t = 170 \text{ GeV}$ and present (light grey) and future (dark grey) parameter ranges given in appendix A. The three pairs of ϵ'/ϵ plots correspond to hadronic parameter sets (a) $(B_6^{(1=2)}(m_c))_e = 1.5$, $(B_8^{(3=2)}(m_c))_e = 1.0$, (b) $(B_6^{(1=2)}(m_c))_e = 1.0$, $(B_8^{(3=2)}(m_c))_e = 1.0$, and (c) $(B_6^{(1=2)}(m_c))_e = 1.0$, $(B_8^{(3=2)}(m_c))_e = 1.5$, respectively.

$$1:1 \quad 10 \quad \epsilon'/\epsilon \quad 10:4 \quad 10 \quad (XIX.44)$$

in the case of the “future” scenario. In both cases the x_d -constraint has essentially no impact on the predicted range for ϵ'/ϵ .

Finally, extending the “future” scenario to $m_s(m_c) = (170 \quad 10) \text{ MeV}$, $\Lambda_{\overline{MS}}^{(4)} = (325 \quad 50) \text{ MeV}$ and $B_6^{(1=2)}; B_8^{(3=2)} = 1.0 \quad 0.1$ would give

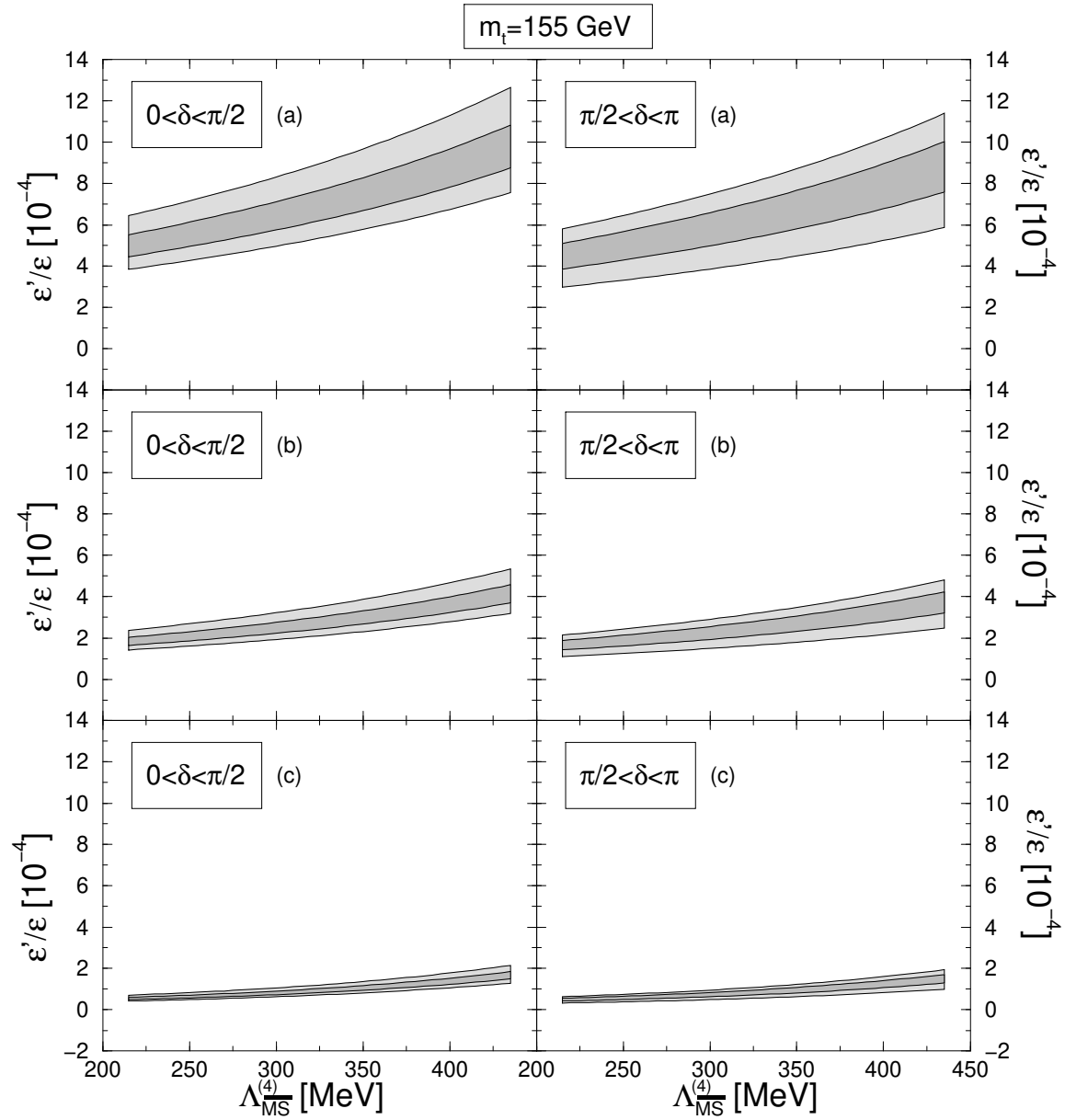


FIG. 15. Same as fig. 14 but for $m_t = 155 \text{ GeV}$.

$$0.3 \quad 10^4 \quad \alpha_s = 5.4 \quad 10^4 \quad (\text{XIX.45})$$

again with no impact from imposing the α_s -constraint.

Allowing for the additional variation $B_{2\pi^0 \text{ DR}}^{(1=2)}(m_c) = 6.6 \quad 1.0$ extends ranges (XIX.43)–(XIX.45) to $2.5 \quad 10^4 \quad \alpha_s = 13.7 \quad 10^4$, $1.5 \quad 10^4 \quad \alpha_s = 10.8 \quad 10^4$ and $0.1 \quad 10^4 \quad \alpha_s = 5.8 \quad 10^4$, respectively.

An analysis of the Rome group (Ciuchini *et al.*, 1995) gives $\text{Re}(\alpha_s) = (3.1 \quad 2.5) \quad 10^4$ which is compatible with our results. Similar results are found with hadronic matrix elements calculated in the chiral quark model (Bertolini *et al.*, 1995a), (Bertolini *et al.*, 1995b).

The difference in the range for α_s presented here by us and the Rome group is related to the

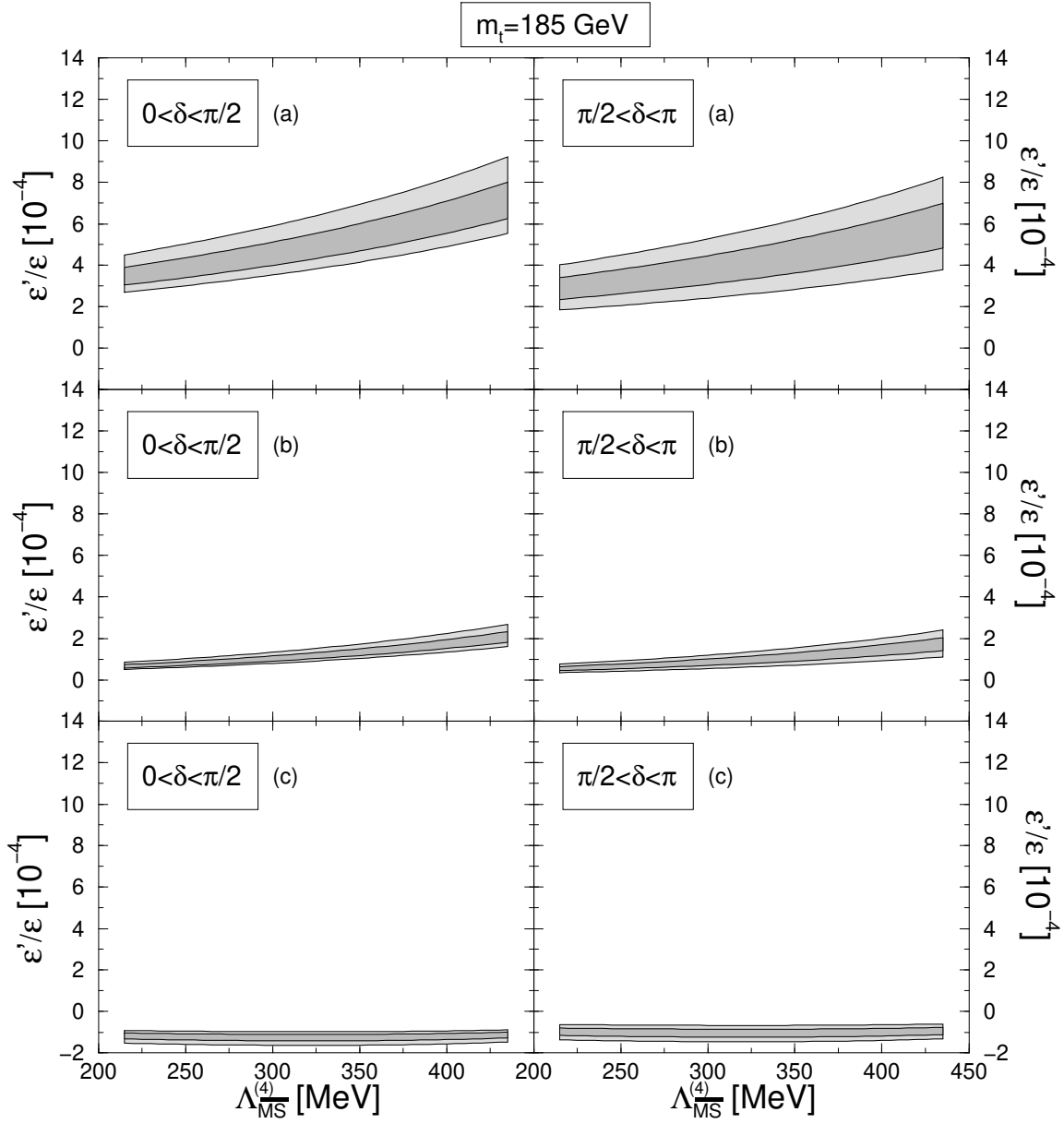


FIG. 16. Same as fig. 14 but for $m_t = 185 \text{ GeV}$.

different treatment of theoretical and experimental errors. Whereas we simply scan all parameters within one standard deviation, (Ciuchini *et al.*, 1995) use Gaussian distributions in treating the experimental errors. Consequently our procedure is more conservative. We agree however with these authors that values for ϵ'/ϵ above $1 \cdot 10^3$ although not excluded are very improbable. This should be contrasted with the work of the Dortmund group (Fröhlich *et al.*, 1991), (Heinrich *et al.*, 1992) which finds values for ϵ'/ϵ in the ball park of $(2 \cdot 3) \cdot 10^3$. We do not know any consistent framework for hadronic matrix elements which would give such high values within the Standard Model.

The experimental situation on $\text{Re}(\epsilon'/\epsilon)$ is unclear at present. While the result of the NA31

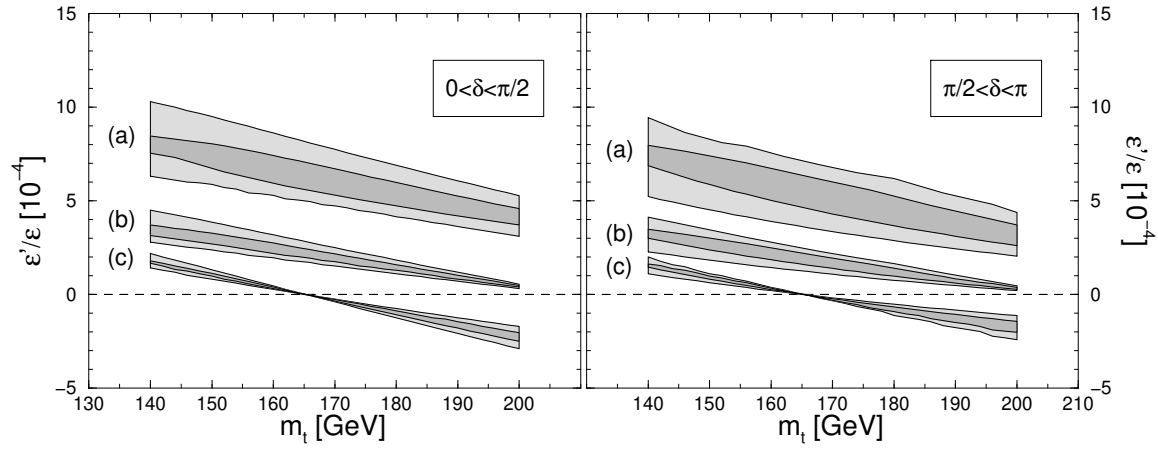


FIG. 17. The ranges of ϵ'/ϵ in the NDR scheme as a function of m_t for $\frac{(4)}{M_S} = 325 \text{ MeV}$ and present (light grey) and future (dark grey) parameter ranges given in appendix A. The three bands correspond to hadronic parameter sets (a) $(B_6^{(1=2)}(m_c))_e = 1.5$, $(B_8^{(3=2)}(m_c))_e = 1.0$, (b) $(B_6^{(1=2)}(m_c))_e = 1.0$, $(B_8^{(3=2)}(m_c))_e = 1.0$, and (c) $(B_6^{(1=2)}(m_c))_e = 1.0$, $(B_8^{(3=2)}(m_c))_e = 1.5$, respectively.

collaboration at CERN with $\text{Re}(\epsilon'/\epsilon) = (23 \pm 7) \cdot 10^{-4}$ (Barr *et al.*, 1993) clearly indicates direct CP violation, the value of E731 at Fermilab, $\text{Re}(\epsilon'/\epsilon) = (7.4 \pm 5.9) \cdot 10^{-4}$ (Gibbons *et al.*, 1993), is compatible with superweak theories (Wolfenstein, 1964) in which $\epsilon'/\epsilon = 0$. The E731 result is in the ballpark of the theoretical estimates. The NA31 value appears a bit high compared to the range given in (XIX.43) above.

Hopefully, in about three years the experimental situation concerning ϵ'/ϵ will be clarified through the improved measurements by the two collaborations at the 10^{-4} level and by experiments at the ϕ factory in Frascati. One should also hope that the theoretical situation of ϵ'/ϵ will improve by then to confront the new data.

XX. $K_L - K_S$ MASS DIFFERENCE AND $I = 1=2$ RULE

It is probably a good moment to make a few comments on the $K_L - K_S$ mass difference given by

$$M = M(K_L) - M(K_S) = 3.51 \cdot 10^{15} \text{ GeV} \quad (\text{XX.1})$$

and the approximate $I = 1=2$ rule in $K \rightarrow \pi$ decays. As we have already briefly mentioned in the beginning of section XIX A, this empirical rule manifests itself in the dominance of $I = 1=2$ over $I = 3=2$ decay amplitudes. It can be expressed as

$$\frac{\text{Re}A_0}{\text{Re}A_2} = 22.2 \quad (\text{XX.2})$$

using the notation of section XIX A.

$$\mathbf{A.} \quad M(K_L - K_S)$$

The $K_L - K_S$ mass difference can be written as

$$M = 2\text{Re}M_{12} + (M)_{LD} \quad (\text{XX.3})$$

with M_{12} given in (XVIII.6) and $(M)_{LD}$ representing long distance contributions, corresponding for instance to the exchange of intermediate light pseudoscalar mesons (π^0, η). The first term in (XX.3), the so-called short distance contribution, is dominated by the first term in (XVIII.6) so that

$$(M)_{SD} = \frac{G_F^2}{6} F_K^2 B_K m_K M_W^2 \left[\frac{1}{c} + \frac{m_c^2}{M_W^2} \right] + \text{top} \quad (\text{XX.4})$$

where top represents the two top dependent terms in (XVIII.6). In writing (XX.4) we are neglecting the tiny imaginary part in $\frac{1}{c} = V_{cs}V_{cd}$. A very extensive numerical analysis of (XX.4) has been presented by (Herrlich and Nierste, 1994), who calculated the NLO corrections to $\frac{1}{c}$ and also to $\frac{1}{3}$ (Herrlich and Nierste, 1995a) which enters top . The NLO calculation of the short distance contributions improves the matching to the non-perturbative matrix element parametrized by B_K and clarifies the proper definition of B_K to be used along with the QCD factors $\frac{1}{c}$. In addition the NLO study reveals an enhancement of $\frac{1}{c}$ over its LO estimate by about 20%. Although sizable, this enhancement can still be considered being perturbative, as required by the consistency of the calculation. This increase in $\frac{1}{c}$, reinforced by updates in input parameters ($\frac{1}{M_S}$), brings $(M)_{SD}$ closer to the experimental value in (XX.1). With $\frac{(4)}{M_S} = 325 \text{ MeV}$ and $m_c = 1.3 \text{ GeV}$, giving $\frac{1}{c}^{\text{NLO}} = 1.38$, one finds that typically 70% of M can be described by the short distance component. The exact value is still somewhat uncertain because $\frac{1}{c}$ is rather sensitive to $\frac{1}{M_S}$. Further uncertainties are introduced by the error in B_K and due to the renormalization scale ambiguity, which is still quite pronounced even at NLO. Yet the result is certainly more reliable than previous LO estimates. Using the old value $\frac{1}{c}^{\text{LO}} = 0.85$, corresponding to $m_c = 1.4 \text{ GeV}$ and $\frac{1}{QCD} = 200 \text{ MeV}$, $(M)_{SD} = M$ would be below 50%, suggesting a dominance of long distance contributions in M . As discussed in (Herrlich and Nierste, 1994), such a situation would

be "unnatural" since the long distance component is formally suppressed by $\frac{2}{Q_{CD}} \approx m_c^2$. Hence the short distance dominance indicated by the NLO analysis is also gratifying in this respect.

The long distance contributions, to which one can attribute the remaining 30% in M not explained by the short distance part, are nicely discussed in (Bijnens *et al.*, 1991).

In summary, the observed $K_L - K_S$ mass difference can be roughly described within the standard model after the NLO corrections have been taken into account. The remaining theoretical uncertainties in the dominant part in (XX.4) and the uncertainties in $(M)_{LD}$ do not allow however to use M as a constraint on the CKM parameters.

B. The $I = 1=2$ Rule

Using the effective hamiltonian in (VII.1) and keeping only the dominant terms one has

$$\frac{R\epsilon A_0}{R\epsilon A_2} = \frac{z_1(\mu)hQ_1(\mu)i_0 + z_2(\mu)hQ_2(\mu)i_0 + z_6(\mu)hQ_6(\mu)i_0}{z_1(\mu)hQ_1(\mu)i_2 + z_2(\mu)hQ_2(\mu)i_2} \quad (XX.5)$$

where $hQ_{i1,2}$ are defined in (XIX.8). The coefficients $z_i(\mu)$ can be found in table XVIII. For the hadronic matrix elements we use the formulae (XIX.11), (XIX.12), (XIX.16) and (XIX.21), which have been discussed in section XIX B. We find then, separating current-current and penguin contributions

$$\frac{R\epsilon A_0}{R\epsilon A_2} = R_c + R_p \quad (XX.6)$$

$$R_c = \frac{5z_2(\mu)B_2^{(1=2)} + z_4(\mu)B_1^{(1=2)}}{4 + 2z_+(\mu)B_1^{(3=2)}} \quad z_+ = z_1 + z_2 \quad (XX.7)$$

$$R_p = 11.9 \frac{z_6(\mu)B_6^{(1=2)}}{z_+(\mu)B_1^{(3=2)}} \left(\frac{178 \text{ MeV}}{m_s(\mu) + m_d(\mu)} \right)^{\#_2} \quad (XX.8)$$

The factor 11.9 expresses the enhancement of the matrix elements of the penguin operator Q_6 over $hQ_{1,2}i$ first pointed out in (Vainshtein *et al.*, 1977). It is instructive to calculate R_c and R_p using the vacuum insertion estimate for which $B_1^{(1=2)} = B_2^{(1=2)} = B_1^{(3=2)} = B_6^{(1=2)} = 1$. Without QCD effects one finds then $R_c = 0.9$ and $R_p = 0$ in complete disagreement with the data. In table XLII we show the values of R_c and R_p at $\mu = 1 \text{ GeV}$ using the results of table XVIII. We have set $m_s + m_d = 178 \text{ MeV}$.

The inclusion of QCD effects enhances both R_c and R_p (Gaillard and Lee, 1974a), (Altarelli and Maiani, 1974), however even for the highest values of $\frac{(4)}{M_S}$ the ratio $R\epsilon A_0/R\epsilon A_2$ is by at least a factor of 8 smaller than the experimental value in (XX.2). Moreover a considerable scheme dependence is observed. Lowering μ would improve the situation, but for $\mu < 1 \text{ GeV}$ the perturbative calculations of $z_i(\mu)$ can no longer be trusted. Similarly lowering m_s down to 100 MeV would increase the penguin contribution. In view of the most recent estimates in (XIX.36) such a low value of m_s seems to be excluded however. We conclude therefore, as already known since many years, that the vacuum insertion estimate fails completely in explaining the $I = 1=2$ rule.

TABLE XLII. The quantities R_c and R_p contributing to $R_{\Theta A_0} = R_{\Theta A_2}$ as described in the text, calculated using the vacuum insertion estimate for the hadronic matrix elements. The Wilson coefficient functions are evaluated for various $\frac{(4)}{M_S}$ in leading logarithmic approximation as well as in next-to-leading order in two different schemes (NDR and HV).

	$\frac{(4)}{M_S} = 215 \text{ M eV}$			$\frac{(4)}{M_S} = 325 \text{ M eV}$			$\frac{(4)}{M_S} = 435 \text{ M eV}$		
Scheme	LO	NDR	HV	LO	NDR	HV	LO	NDR	HV
R_c	1.8	1.4	1.6	2.0	1.6	1.8	2.4	1.8	2.2
R_p	0.1	0.3	0.1	0.2	0.5	0.2	0.3	1.0	0.4

As we have discussed in section XIX the vacuum insertion estimate $B_6^{(1=2)} = 1$ is supported by the $1=N$ expansion approach and by lattice calculations. Consequently the only solution to the $I = 1=2$ rule problem appears to be a change in the values of the remaining B_i factors. For instance repeating the above calculation with $B_1^{(3=2)} = 0.48$, $B_2^{(1=2)} = 5$ and $B_1^{(1=2)} = 10$ would give in the NDR scheme $R_c = 20$, $R_p = 2$ and $R_{\Theta A_0} = R_{\Theta A_2} = 22$ in accordance with the experimental value.

There have been several attempts to explain the $I = 1=2$ rule, which basically use the effective hamiltonian in (VII.1) but employ different methods for the hadronic matrix elements. In particular we would like to mention the $1=N$ approach (Bardeen *et al.*, 1987a), the work of (Pich and de Rafael, 1991) based on an effective action for four-quark operators, the diquark approach in (Neubert and Stech, 1991), QCD sum rules (Jamin and Pich, 1994), the chiral perturbation calculations in (Kambor *et al.*, 1990), (Kambor *et al.*, 1991) and very recently an analysis (Antonelli *et al.*, 1995) in the framework of the chiral quark model (Cohen and Manohar, 1984).

With these methods values for $R_{\Theta A_0} = R_{\Theta A_2}$ in the range 15–20 can be obtained. It is beyond the scope of this review to discuss the weak and strong points of each method, although at least one of us believes that the "meson evolution" picture advocated in (Bardeen *et al.*, 1987a) represents the main bulk of the physics behind the number 22. In view of the uncertainties present in these approaches, we have not used them in our analysis of " π^0 ", but have constrained the hadronic matrix elements so that they satisfy the $I = 1=2$ rule exactly.

XXI. THE DECAY $K_L \rightarrow \pi^0 e^+ e^-$

A. General Remarks

Let us next move on to discuss the rare decay $K_L \rightarrow \pi^0 e^+ e^-$. Whereas in $K \rightarrow \pi \ell \ell$ decays the CP violating contribution is only a tiny part of the full amplitude and the direct CP violation as we have just seen is expected to be at least by three orders of magnitude smaller than the indirect CP violation, the corresponding hierarchies are very different for $K_L \rightarrow \pi^0 e^+ e^-$. At lowest order in electroweak interactions (one-loop photon penguin, Z^0 -penguin and W-box diagrams), this decay takes place only if CP symmetry is violated. The CP conserving contribution to the amplitude comes from a two photon exchange, which although of higher order in α could in principle be sizable. Extensive studies of several groups indicate however that the CP conserving part is likely to be smaller than the CP violating contributions. We will be more specific about this at the end of this section.

The CP violating part can again be divided into a direct and an indirect one. The latter is given by the $K_S \rightarrow \pi^0 e^+ e^-$ amplitude times the CP violating parameter ϵ_K . The amplitude $A(K_S \rightarrow \pi^0 e^+ e^-)$ can be written as

$$A(K_S \rightarrow \pi^0 e^+ e^-) = \langle \pi^0 e^+ e^- | H_{eff} | K_S \rangle \quad (XXI.1)$$

where H_{eff} can be found in (VIII.1) with the operators $Q_1; \dots; Q_6$ defined in (VI.3), the operators Q_{7V} and Q_{7A} given by

$$Q_{7V} = (sd)_V (ee)_V \quad Q_{7A} = (sd)_V (ee)_A \quad (XXI.2)$$

and the Wilson coefficients z_i and y_i calculated in section VIII.

Let us next note that the coefficients of Q_{7V} and Q_{7A} are $O(\alpha^2)$, but their matrix elements $\langle \pi^0 e^+ e^- | Q_{7V/A} | K_S \rangle$ are $O(1)$. In the case of $Q_i (i=1; \dots; 6)$ the situation is reversed: the Wilson coefficients are $O(1)$, but the matrix elements $\langle \pi^0 e^+ e^- | Q_i | K_S \rangle$ are $O(\alpha^2)$. Consequently at $O(\alpha^2)$ all operators contribute to $A(K_S \rightarrow \pi^0 e^+ e^-)$. However because $K_S \rightarrow \pi^0 e^+ e^-$ is CP conserving, the coefficients y_i multiplied by $\epsilon_K = O(\alpha^4)$ can be fully neglected and the operator Q_{7A} drops out in this approximation. Now whereas $\langle \pi^0 e^+ e^- | Q_{7V} | K_S \rangle$ can be trivially calculated, this is not the case for $\langle \pi^0 e^+ e^- | Q_i | K_S \rangle$ with $i=1; \dots; 6$ which can only be evaluated using non-perturbative methods. Moreover it is clear from the short-distance analysis of section VIII that the inclusion of Q_i in the estimate of $A(K_S \rightarrow \pi^0 e^+ e^-)$ cannot be avoided. Indeed, whereas $\langle \pi^0 e^+ e^- | Q_{7V} | K_S \rangle$ is independent of μ and the renormalization scheme, the coefficient z_{7V} shows very strong scheme and μ -dependences. They can only be canceled by the contributions from the four-quark operators Q_i . All this demonstrates that the estimate of the indirect CP violation in $K_L \rightarrow \pi^0 e^+ e^-$ cannot be done very reliably at present. Some estimates in the framework of chiral perturbation theory will be discussed below. On the other hand, a much better assessment of the importance of indirect CP violation in $K_L \rightarrow \pi^0 e^+ e^-$ will become possible after a measurement of $B(K_S \rightarrow \pi^0 e^+ e^-)$.

Fortunately the directly CP violating contribution can be fully calculated as a function of m_t , CKM parameters and the QCD coupling constant α_s . There are practically no theoretical uncertainties related to hadronic matrix elements because $\langle \pi^0 | j(sd)_V | K_L \rangle$ can be extracted using isospin symmetry from the well measured decay $K^+ \rightarrow \pi^0 e^+ \nu$. In what follows, we will concentrate on this contribution.

B. Analytic Formula for $B(K_L \rightarrow \pi^0 e^+ e^-)_{\text{dir}}$

The directly CP violating contribution is governed by the coefficients y_i and consequently only the penguin operators Q_3, \dots, Q_6, Q_{7V} and Q_{7A} have to be considered. Since $y_i = O(\alpha_s)$ for $i = 3, \dots, 6$, the contribution of QCD penguins to $B(K_L \rightarrow \pi^0 e^+ e^-)_{\text{dir}}$ is really $O(\alpha_s)$ to be compared with the $O(1)$ contributions of Q_{7V} and Q_{7A} . In deriving the final formula we will therefore neglect the contributions of the operators Q_3, \dots, Q_6 , i.e. we will assume that

$$\sum_{i=3}^6 y_i \langle \pi^0 | h^0 e^+ e^- | K_L \rangle = y_{7V} \langle \pi^0 | h^0 e^+ e^- | K_L \rangle \quad (\text{XXI.3})$$

This assumption is supported by the corresponding relation for the quark-level matrix elements

$$\sum_{i=3}^6 y_i \langle \pi^0 | h d e^+ e^- | \bar{s} i \rangle = y_{7V} \langle \pi^0 | h d e^+ e^- | \bar{s} i \rangle \quad (\text{XXI.4})$$

that can be easily verified perturbatively.

The neglect of the QCD penguin operators is compatible with the scheme and α_s -independence of the resulting branching ratio. Indeed y_{7A} does not depend on α_s and the renormalization scheme at all and the corresponding dependences in y_{7V} are at the level of 1% as discussed in section VIII E. Introducing the numerical constant

$$c_e = \frac{1}{V_{us}^2} \frac{\langle K_L \rangle}{\langle K^+ \rangle} \frac{1}{2} B(K^+ \rightarrow \pi^0 e^+ e^-) = 6.3 \cdot 10^6 \quad (\text{XXI.5})$$

one then finds

$$B(K_L \rightarrow \pi^0 e^+ e^-)_{\text{dir}} = c_e (\text{Im } \tau_t)^2 (y_{7V}^2 + y_{7A}^2) \quad (\text{XXI.6})$$

where

$$y_i = \frac{1}{2} Y_i \quad (\text{XXI.7})$$

Using next the method of the penguin-box expansion (section XIV) we can write similarly to (X.5) and (X.3)

$$y_{7V} = P_0 + \frac{Y_0(x_t)}{\sin^2 \theta_w} - 4Z_0(x_t) + P_E E_0(x_t) \quad (\text{XXI.8})$$

$$y_{7A} = \frac{1}{\sin^2 \theta_w} Y_0(x_t) \quad (\text{XXI.9})$$

with Y_0 , Z_0 and E_0 given in (XI.46), (XIV.2) and (VI.15). P_E is $O(10^{-2})$ and consequently the last term in (XXI.8) can be neglected. P_0 is given for different values of α_s and $\frac{1}{M_S}$ in table XLIII. There we also show the leading order results and the case without QCD corrections.

The analytic expressions in (XXI.8) and (XXI.9) are useful as they display not only the explicit m_t -dependence, but also isolate the impact of leading and next-to-leading QCD effects. These effects modify only the constants P_0 and P_E . As anticipated from the results of section VIII E, P_0

TABLE XLIII. PBE coefficient P_0 of y_{7V} for various values of $\frac{(4)}{M_S}$ and μ . In the absence of QCD $P_0 = 8 \ln(M_W/m_c) = 3.664$ holds universally.

		P_0		
$\frac{(4)}{M_S} [M \text{ eV}]$	$\mu [G \text{ eV}]$	LO	NDR	HV
215	0.8	2.073	3.159	3.110
	1.0	2.048	3.133	3.084
	1.2	2.027	3.112	3.063
325	0.8	1.863	3.080	3.024
	1.0	1.834	3.053	2.996
	1.2	1.811	3.028	2.970
435	0.8	1.672	2.976	2.914
	1.0	1.640	2.965	2.899
	1.2	1.613	2.939	2.872

is strongly enhanced relatively to the LO result. This enhancement amounts roughly to a factor of 1.6 ± 0.1 . Partially this enhancement is however due to the fact that for $\mu_{LO} = \overline{M_S}$ the QCD coupling constant in the leading order is 20–30% larger than its next-to-leading order value. Calculating P_0 in LO but with the full α_s of (III.19) we have found that the enhancement then amounts to a factor of 1.33 ± 0.06 . In any case the inclusion of NLO QCD effects and a meaningful use of $\overline{M_S}$ show that the next-to-leading order effects weaken the QCD suppression of y_{7V} . As seen in table XLIII, the suppression of P_0 by QCD corrections amounts to about 15% in the complete next-to-leading order calculation.

C. Numerical Analysis

In fig. 8 of section VIII E we have shown $y_{7V} = \hat{y}$ and $y_{7A} = \hat{y}$ as functions of m_t together with the leading order result for $y_{7V} = \hat{y}$ and the case without QCD corrections. From there it is obvious that the dominant m_t -dependence of $B(K_L \rightarrow 0e^+e^-)_{\text{dir}}$ originates from the coefficient of the operator Q_{7A} . Another noteworthy feature was that accidentally for $m_t = 175 \text{ GeV}$ one finds $y_{7V} = y_{7A}$.

In fig. 18 the ratio $B(K_L \rightarrow 0e^+e^-)_{\text{dir}}/(\text{Im } t)^2$ is shown as a function of m_t . The enhancement of the directly CP violating contribution through NLO corrections relatively to the LO estimate is clearly visible on this plot. As we will see below, due to large uncertainties present in $\text{Im } t$ this enhancement cannot yet be fully appreciated phenomenologically.

The very weak dependence on $\overline{M_S}$ should be contrasted with the very strong dependence found in the case of $"0="$. Therefore, provided the other two contributions to $K_L \rightarrow 0e^+e^-$ can be shown to be small or can be reliably calculated one day, the measurement of $B(K_L \rightarrow 0e^+e^-)$ should offer a good determination of $\text{Im } t$.

Next we would like to comment on the possible uncertainties due to the definition of m_t . At the level of accuracy at which we work we cannot fully address this question yet. In order to be able to do it, one needs to know the perturbative QCD corrections to $Y_0(x_t)$ and $Z_0(x_t)$ and for

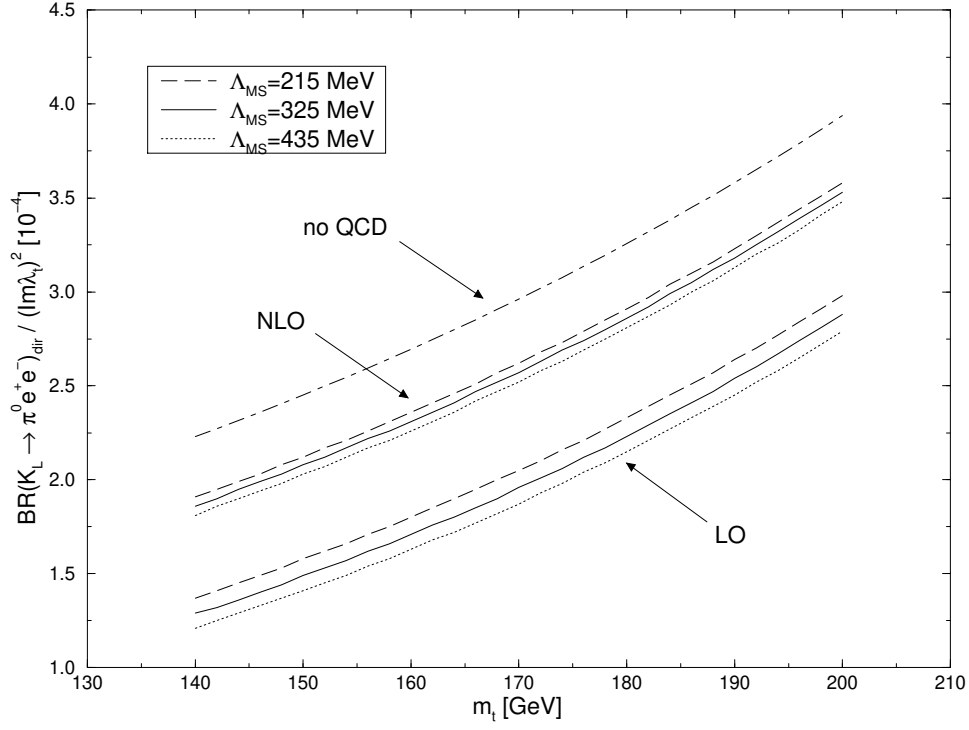


FIG. 18. $B(K_L \rightarrow \pi^0 e^+ e^-)_{\text{dir}} = (\text{Im } \lambda_t)^2$ as a function of m_t for various values of $\frac{(4)}{M_S}$ at scale $\mu = 10 \text{ GeV}$.

consistency an additional order in the renormalization group improved calculation of P_0 . Since the m_t -dependence of Y_{7V} is rather moderate, the main concern in this issue is the coefficient Y_{7A} whose m_t -dependence is fully given by $Y(x_t)$. Fortunately the QCD corrected function $Y(x_t)$ is known from the analysis of $K_L \rightarrow \pi^+ \pi^-$ and can be directly used here. As we will discuss in section XXV, for $m_t = m_t(m_t)$ the QCD corrections to $Y_0(x_t)$ are around 2%. On this basis we believe that if $m_t = m_t(m_t)$ is chosen, the additional QCD corrections to $B(K_L \rightarrow \pi^0 e^+ e^-)_{\text{dir}}$ should be small.

Finally we give the predictions for the present and future sets of input parameters as described in appendix A. It should be emphasized that the uncertainties in these predictions result entirely from the CKM parameters. This situation will improve considerably in the era of dedicated B-physics experiments in the next decade, allowing a precise prediction for $B(K_L \rightarrow \pi^0 e^+ e^-)_{\text{dir}}$.

We find

$$B(K_L \rightarrow \pi^0 e^+ e^-)_{\text{dir}} = \begin{pmatrix} 4.26 & 3.03 & 10^2 \text{ no } x_d \text{ constraint} \\ 4.48 & 2.77 & 10^2 \text{ with } x_d \text{ constraint} \end{pmatrix} \quad (\text{XXI.10})$$

$$B(K_L \rightarrow \pi^0 e^+ e^-)_{\text{dir}} = \begin{pmatrix} 3.71 & 1.61 & 10^2 \text{ no } x_d \text{ constraint} \\ 4.32 & 0.96 & 10^2 \text{ with } x_d \text{ constraint} \end{pmatrix} \quad (\text{XXI.11})$$

These results are compatible with those found in (Buras *et al.*, 1994a), (Donoghue and Gabbiani, 1995), (Köhler and Paschos, 1995) with differences originating in various choices of CKM parameters.

D. The Indirectly CP Violating and CP Conserving Parts

Now we want to compare the results obtained for the direct CP violating part with the estimates made for the indirect CP-violating contribution and the CP-conserving one. The most recent discussions have been presented in (Cohen *et al.*, 1993), (Heiliger and Seghal, 1993), (Donoghue and Gabbiani, 1995), (Köhler and Paschos, 1995) where references to earlier papers can be found.

The indirect CP violating amplitude is given by the $K_S \rightarrow \pi^0 e^+ e^-$ amplitude times the CP parameter ϵ_K . Once $B(K_S \rightarrow \pi^0 e^+ e^-)$ has been accurately measured, it will be possible to calculate this contribution precisely. Using chiral perturbation theory it is however possible to get an estimate by relating $K_S \rightarrow \pi^0 e^+ e^-$ to the $K^+ \rightarrow \pi^+ e^+ e^-$ transition (Ecker *et al.*, 1987), (Ecker *et al.*, 1988). To this end one can write

$$B(K_L \rightarrow \pi^0 e^+ e^-)_{\text{indir}} = B(K^+ \rightarrow \pi^+ e^+ e^-) \frac{(K_L)}{(K^+)} \epsilon_K r^2 \quad (\text{XXI.12})$$

where

$$r^2 = \frac{(K_S \rightarrow \pi^0 e^+ e^-)}{(K^+ \rightarrow \pi^+ e^+ e^-)} \quad (\text{XXI.13})$$

With $B(K^+ \rightarrow \pi^+ e^+ e^-) = (2.74 \pm 0.23) \cdot 10^{-8}$ (Alliegro *et al.*, 1992) and the most recent chiral perturbation theory estimate $\epsilon_K = 0.5$ (Ecker *et al.*, 1988), (Bruno and Prades, 1993) one has

$$B(K_L \rightarrow \pi^0 e^+ e^-)_{\text{indir}} = (5.9 \pm 0.5) \cdot 10^{-2} r^2 = 1.6 \pm 10^{-2}; \quad (\text{XXI.14})$$

i.e. a branching ratio more than a factor of 2 below the direct CP violating contribution.

Yet as emphasized recently in (Donoghue and Gabbiani, 1995) and also in (Heiliger and Seghal, 1993) the knowledge of r is very uncertain at present. In particular the estimate in (XXI.14) is based on a relation between two non-perturbative parameters, which is rather ad hoc and certainly not a consequence of chiral symmetry. As shown in (Donoghue and Gabbiani, 1995) a small deviation from this relation increases r to values above unity so that $B(K_L \rightarrow \pi^0 e^+ e^-)_{\text{indir}}$ could be comparable or even large than $B(K_L \rightarrow \pi^0 e^+ e^-)_{\text{dir}}$. It appears then that this enormous uncertainty in the indirectly CP violating part can only be removed by measuring the rate of $K_S \rightarrow \pi^0 e^+ e^-$.

It should also be stressed, that in reality the CP indirect amplitude may interfere with the vector part of the CP direct amplitude. The full CP violating amplitude can then be written following (Dib *et al.*, 1989a), (Dib *et al.*, 1989b) as follows

$$B(K_L \rightarrow \pi^0 e^+ e^-)_{\text{CP}} = 2.43 \cdot 10^{-6} \text{re}^{i=4} \left[\frac{1}{1} \text{Im}(\tau_{7V})^2 + \epsilon (\text{Im}(\tau))^2 \gamma_A^2 \right] \quad (\text{XXI.15})$$

As an example we show in fig. 19 $B(K_L \rightarrow \pi^0 e^+ e^-)_{\text{CP}}$ for $m_t = 170 \text{ GeV}$, $\frac{(4)}{MS} = 325 \text{ MeV}$ and $\text{Im}(\tau) = 1.3 \cdot 10^4$ as a function of r . We observe that whereas for $0 < r < 1$ the dependence of $B(K_L \rightarrow \pi^0 e^+ e^-)_{\text{CP}}$ on r is moderate, it is rather strong otherwise and already for $r < 0.6$ values as high as 10^{-11} are found.

The estimate of the CP conserving contribution is also difficult. We refer the reader to (Cohen *et al.*, 1993), (Heiliger and Seghal, 1993) and (Donoghue and Gabbiani, 1995) where further references to an extensive literature on this subject can be found. The measurement of the branching ratio

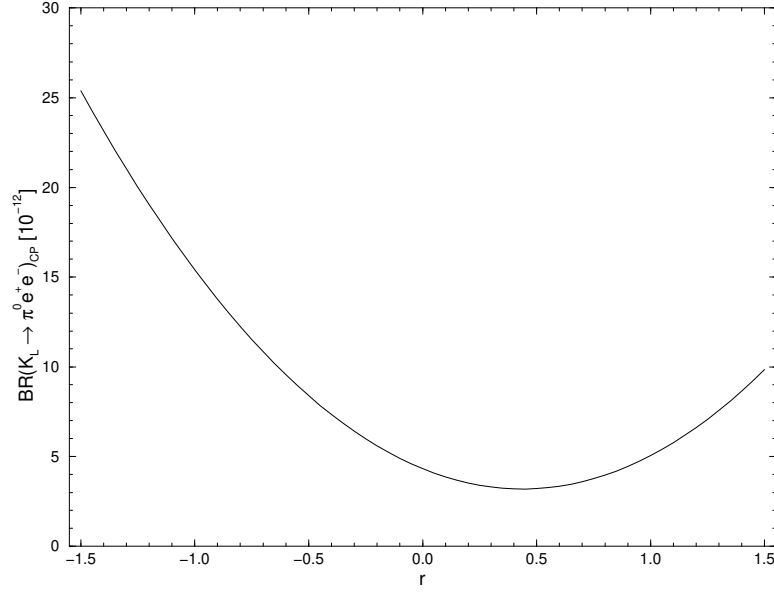


FIG. 19. $\text{BR}(K_L \rightarrow \pi^0 e^+ e^-)_{\text{CP}}$ for $m_t = 170 \text{ GeV}$, $\frac{(4)}{M_S} = 325 \text{ MeV}$ and $\text{Im } t = 1.3 \cdot 10^4$ as a function of r .

$$\text{BR}(K_L \rightarrow \pi^0) \begin{pmatrix} (1.7 \quad 0.3) & 1\theta \text{ (Barr et al., 1992)} \\ (2.0 \quad 1.0) & 1\theta \text{ (Papadimitriou et al., 1991)} \end{pmatrix} \quad (\text{XXI.16})$$

and of the shape of the π^0 mass spectrum plays an important role in this estimate. The most recent analyses give

$$\text{BR}(K_L \rightarrow \pi^0 e^+ e^-)_{\text{cons}} \begin{cases} \gtrsim (0.3 \quad 1.8) & 1\theta^2 \text{ (Cohen et al., 1993)} \\ \gtrsim 4.0 & 10^{12} \text{ (Heiliger and Seghal, 1993)} \\ \gtrsim (5 \quad 5) & 1\theta^2 \text{ (Donoghue and Gabbiani, 1995)} \end{cases} \quad (\text{XXI.17})$$

i.e. not necessarily below the CP violating contribution. An improved estimate of this component is certainly desirable. It should be noted that there is no interference in the rate between the CP conserving and CP violating contributions so that the results in fig. 19 and (XXI.17) can simply be added.

E. Outlook

The results discussed above indicate that within the Standard Model $\text{BR}(K_L \rightarrow \pi^0 e^+ e^-)$ could be as high as $1 \cdot 10^{11}$. Moreover the direct CP violating contribution is found to be important and could even be dominant. Unfortunately the large uncertainties in the remaining two contributions will probably not allow an easy identification of the direct CP violation by measuring the branching ratio only. The future measurements of $\text{BR}(K_S \rightarrow \pi^0 e^+ e^-)$ and improvements in the estimate of the CP conserving part may of course change this unsatisfactory situation. Alternatively the measurements of the electron energy asymmetry (Heiliger and Seghal, 1993), (Donoghue and Gabbiani, 1995) and the study of the time evolution of $K^0 \rightarrow \pi^0 e^+ e^-$ (Littenberg, 1989b), (Donoghue and

Gabbiani, 1995), (Köhler and Paschos, 1995) could allow for a refined study of CP violation in this decay.

The present experimental bounds

$$B(\bar{K}_L \rightarrow \pi^0 e^+ e^-) \begin{cases} 4.3 & 10^9 \text{ (Harris } et al., 1993) \\ 5.5 & 10^9 \text{ (Ohl } et al., 1990) \end{cases} \quad (XXI.18)$$

are still by three orders of magnitude away from the theoretical expectations. Yet the prospects of getting the required sensitivity of order 10^{-11} – 10^{-12} in five years are encouraging (Littenberg and Valencia, 1993), (Winstein and Wolfenstein, 1993), (Ritchie and Wojcicki, 1993).

XXII. THE DECAY $B \rightarrow X_s$

A. General Remarks

The $B \rightarrow X_s$ decay is known to be extremely sensitive to the structure of fundamental interactions at the electroweak scale. As any FCNC process, it does not arise at the tree level in the Standard Model. The one-loop W-exchange diagrams that generate this decay at the lowest order in the Standard Model are small enough to be comparable to possible nonstandard contributions (charged scalar exchanges, SUSY one loop diagrams, W_R exchanges in the L–R symmetric models, etc.).

The $B \rightarrow X_s$ decay is particularly interesting because its rate is of order G_F^2 , while most of the other FCNC processes involving leptons or photons are of order $G_F^2 \alpha^2$. The long-range strong interactions are expected to play a minor role in the inclusive $B \rightarrow X_s$ decay. This is because the mass of the b-quark is much larger than the QCD scale. Moreover, the only relevant intermediate hadronic states X_s are expected to give very small contributions, as long as we assume no interference between short- and long-distance terms in the inclusive rate. Therefore, it has become quite common to use the following approximate equality to estimate the $B \rightarrow X_s$ rate:

$$\frac{\Gamma(B \rightarrow X_s)}{\Gamma(B \rightarrow X_{ce})}, \quad \frac{\Gamma(b \rightarrow s)}{\Gamma(b \rightarrow ce)} = R(m_t; m_s) \quad (\text{XXII.1})$$

where the quantities on the r.h.s are calculated in the spectator model corrected for short-distance QCD effects. The normalization to the semileptonic rate is usually introduced in order to cancel the uncertainties due to the Cabibbo-Kobayashi-Maskawa (CKM) matrix elements and factors of m_b^5 in the r.h.s. of eq. (XXII.1). Additional support for the approximation given above comes from the heavy quark expansions. Indeed the spectator model has been shown to correspond to the leading order approximation of an expansion in $1/m_b$. The first corrections appear at the $O(1/m_b^2)$ level. The latter terms have been studied by several authors (Chay *et al.*, 1990), (Bjorken *et al.*, 1992), (Bigi *et al.*, 1992), (Bigi *et al.*, 1993), (Manohar and Wise, 1994), (Blok *et al.*, 1994), (Falk *et al.*, 1994), (Mannel, 1994), (Bigi *et al.*, 1994a) with the result that they affect $\Gamma(B \rightarrow X_s)$ and $\Gamma(B \rightarrow X_{ce})$ by only a few percent.

As indicated above, the ratio R depends only on m_t and m_s in the Standard Model. In extensions of the Standard Model, additional parameters are present. They have been commonly denoted by λ . The main point to be stressed here is that R is a calculable function of its parameters in the framework of a renormalization group improved perturbation theory. Consequently, the decay in question is particularly suited for tests of the Standard Model and its extensions.

One of the main difficulties in analyzing the inclusive $B \rightarrow X_s$ decay is calculating the short-distance QCD effects due to hard gluon exchanges between the quark lines of the leading one-loop electroweak diagrams. These effects are known (Bertolini *et al.*, 1987), (Deshpande *et al.*, 1987), (Grinstein *et al.*, 1990), (Grigjanis *et al.*, 1988), (Grigjanis *et al.*, 1992), (Misiak, 1991) to enhance the $B \rightarrow X_s$ rate in the Standard Model by a factor of 2–3, depending on the top quark mass. So the $B \rightarrow X_s$ decay appears to be the only known short distance process in the Standard Model that is dominated by two-loop contributions.

The $B \rightarrow X_s$ decay has already been measured. In 1993 CLEO reported (Ammar *et al.*, 1993) the following branching ratio for the exclusive $B \rightarrow K$ decay

$$\mathcal{B}(B \rightarrow K) = (4.5 \pm 1.5 \pm 0.9) \cdot 10^{\pm 1} \quad (\text{XXII.2})$$

In 1994 a first measurement of the inclusive rate has been presented (Alam *et al.*, 1995)

$$\mathcal{B}(B \rightarrow X_s) = (2.32 \pm 0.57 \pm 0.35) \cdot 10^{\pm 1} \quad (\text{XXII.3})$$

where the first error is statistical and the second is systematic.

As we will see below these experimental findings are in the ball park of the Standard Model expectations based on the leading logarithmic approximation.

In fact a complete leading order analysis of $\mathcal{B}(B \rightarrow X_s)$ in the Standard Model has been presented almost a year before the CLEO result giving (Buras *et al.*, 1994c)

$$\mathcal{B}(B \rightarrow X_s)_{\text{TH}} = (2.8 \pm 0.8) \cdot 10^{\pm 1} \quad (\text{XXII.4})$$

where the error is dominated by the uncertainty in the choice of the renormalization scale $m_b = 2 < \mu < 2m_b$ as first stressed by Ali and Greub (Ali and Greub, 1993) and confirmed in (Buras *et al.*, 1994c). Since $B \rightarrow X_s$ is dominated by QCD effects, it is not surprising that this scale-uncertainty in the leading order is particularly large. Such an uncertainty, inherent in any finite order of perturbation theory can be reduced by including next-to-leading order corrections. Unfortunately, it will take some time before the μ -dependences present in $B \rightarrow X_s$ can be reduced in the same manner as it was done for the other decays (Buras *et al.*, 1990), (Buchalla and Buras, 1993a), (Buchalla and Buras, 1994a), (Herrlich and Nierste, 1994). As we already stated in section IX B, a full next-to-leading order computation of $B \rightarrow X_s$ would require calculation of three-loop mixings between the operators $Q_1; \dots; Q_6$ and the magnetic penguin operators $Q_7; Q_8$. Moreover, certain two-loop matrix elements of the relevant operators should be calculated in the spectator model. A formal analysis at the next-to-leading level (Buras *et al.*, 1994c) is however very encouraging and shows that the μ -dependence can be considerably reduced once all the necessary calculations have been performed. We will return to this issue below.

B. The Decay $B \rightarrow X_s$ in the Leading Log Approximation

The leading logarithmic calculations (Grinstein *et al.*, 1990), (Misiak, 1993), (Ali and Greub, 1993), (Ciuchini *et al.*, 1994c), (Cella *et al.*, 1994a), (Misiak, 1995), (Buras *et al.*, 1994c) can be summarized in a compact form, as follows:

$$\mathcal{R} = \frac{\langle b \rightarrow s \rangle}{\langle b \rightarrow c e \rangle} = \frac{\mathcal{V}_{ts} \mathcal{V}_{tb}^2}{\mathcal{V}_{cb}^2} \frac{6}{f(z)} \mathcal{C}_7^{(0)\text{eff}}(z) f^2 \quad (\text{XXII.5})$$

where $\mathcal{C}_7^{(0)\text{eff}}(z)$ is the effective coefficient given in (IX.23) and table XXVIII, $z = \frac{m_c}{m_b}$, and

$$f(z) = 1 - 8z^2 + 8z^6 - z^8 - 24z^4 \ln z \quad (\text{XXII.6})$$

is the phase space factor in the semileptonic b -decay. Note, that at this stage one should not include the $\mathcal{O}(\alpha_s)$ corrections to $\langle b \rightarrow c e \rangle$ since they are part of the next-to-leading effects. For the same reason we do not include the $\mathcal{O}(\alpha_s)$ QCD corrections to the matrix element of the operator Q_7 (the QCD bremsstrahlung $b \rightarrow s + g$ and the virtual corrections to $b \rightarrow s$) which

are known (Ali and Greub, 1991a), (Ali and Greub, 1991b), (Pott, 1995) and will be a part of a future NLO analysis.

Formula (XXII.5) and the expression (IX.23) for $C_7^{(0)\text{eff}}(\mu)$ summarize the complete leading logarithmic (LO) approximation for the $B \rightarrow X_s$ rate in the Standard Model. Their important property is that they are exactly the same in many interesting extensions of the Standard Model, such as the Two-Higgs-Doublet Model (2HDM) (Grinstein *et al.*, 1990), (Hewett, 1993), (Barger *et al.*, 1993), (Hayashi *et al.*, 1993), (Buras *et al.*, 1994c) or the Minimal Supersymmetric Standard Model (MSSM) (Bertolini *et al.*, 1991a), (Barbieri and Giudice, 1993), (Borzumati, 1994). The only quantities that change are the coefficients $C_2^{(0)}(\mu_W)$, $C_7^{(0)}(\mu_W)$ and $C_{8G}^{(0)}(\mu_W)$. On the other hand in a general $SU(2)_L \times SU(2)_R \times U(1)$ model additional modifications are necessary, because new operators enter (Cho and Misiak, 1994).

A critical analysis of theoretical and experimental uncertainties present in the prediction for $B \rightarrow X_s$ based on the above formulae has been made (Buras *et al.*, 1994c). Here we just briefly list the main findings:

First of all, eq. (XXII.5) is based on the spectator model. As we have mentioned above the heavy quark expansion gives a strong support for this model in inclusive B-decays. On a conservative side one can assume the error due to the use of the spectator model in $B \rightarrow X_s$ to amount to at most 10%.

The uncertainty coming from the ratio $z = \frac{m_c}{m_b}$ in the phase-space factor $f(z)$ for the semileptonic decay is estimated to be around 6%.

The error due to the ratio of the CKM parameters in eq. (XXII.5) is small. Assuming unitarity of the 3×3 CKM matrix and imposing the constraints from the CP-violating parameter ϵ_K and $B^0 - \bar{B}^0$ mixing one finds

$$\frac{\mathcal{V}_{ts}\mathcal{V}_{tb}}{\mathcal{V}_{cb}} = 0.95 \pm 0.03 \quad (\text{XXII.7})$$

There exists an uncertainty due to the determination of α_s . This uncertainty is not small because of the importance of QCD corrections in the considered decay. For instance the difference between the ratios R of eq. (XXII.5) obtained with help of $\overline{\alpha_s}(\mu_Z) = 0.11$ and 0.13 , respectively, is roughly 20%.

The dominant uncertainty in eq. (XXII.5) comes from the unknown next-to-leading order contributions. This uncertainty is best signaled by the strong μ -dependence of the leading order expression (XXII.5), which is shown by the solid line in fig. 20, for the case $m_t = 170 \text{ GeV}$.

One can see that when μ is varied by a factor of 2 in both directions around $m_b = 5 \text{ GeV}$, the ratio (XXII.5) changes by around 25%, i.e. the ratios R obtained for $\mu = 2.5 \text{ GeV}$ and $\mu = 10 \text{ GeV}$ differ by a factor of 1.6 (Ali and Greub, 1993).

The dashed lines in fig. 20 show the expected μ -dependence of the ratio (XXII.5) once a complete next-to-leading calculation is performed. The μ -dependence is then much weaker, but until one performs the calculation explicitly one cannot say which of the dashed curves is the proper one. The way the dashed lines are obtained is described in (Buras *et al.*, 1994c).

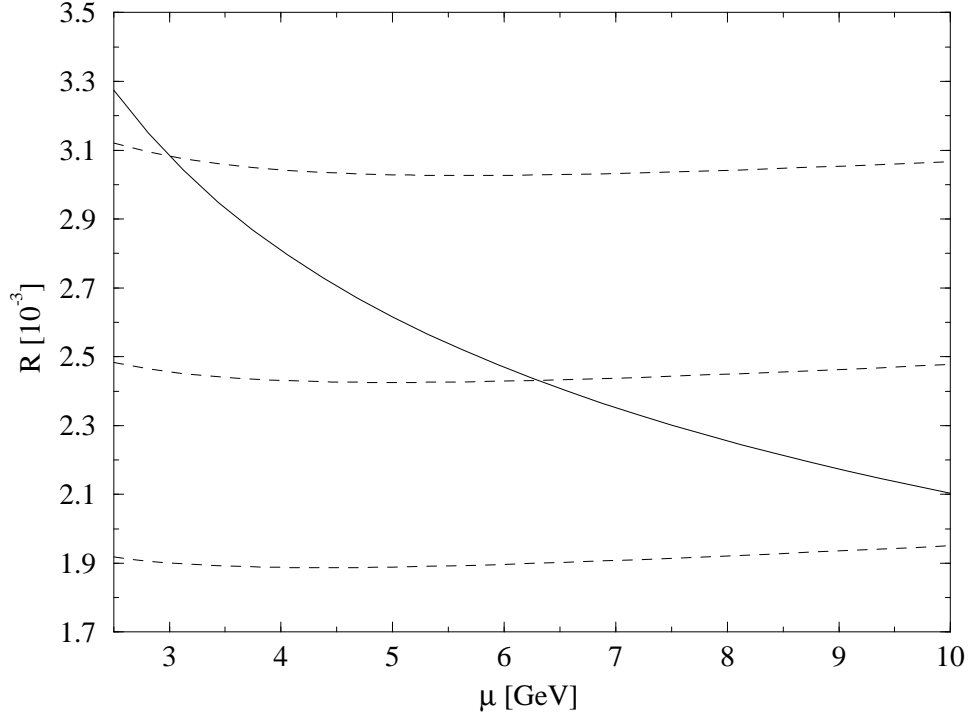


FIG. 20. μ -dependence of the theoretical prediction for the ratio R for $m_t = 170 \text{ GeV}$ and $\frac{(5)}{M_S} = 225 \text{ MeV}$. The solid line corresponds to the leading order prediction. The dashed lines describe possible next-to-leading results.

Finally, there exists a 2.4% error in determining $B(B \rightarrow X_s)$ from eq. (XXII.1), which is due to the error in the experimental measurement of $B(B \rightarrow X_{ce}) = (10.43 \pm 0.24)\%$ (Particle Data Group, 1994).

The uncertainty due to the value of m_t is small as is shown explicitly below.

Fig. 21 based on (Buras *et al.*, 1994c) presents the Standard Model prediction for the inclusive $B \rightarrow X_s$ branching ratio including the errors listed above as a function of m_t together with the CLEO result.

We stress that the theoretical curves have been obtained prior to the experimental result. Since the theoretical error is dominated by scale ambiguities a complete NLO analysis is very desirable.

C. Looking at $B \rightarrow X_s$ Beyond Leading Logarithms

In this section we describe briefly a complete next-to-leading calculation of $B \rightarrow X_s$ in general terms. This section collects the most important findings of section 4 of (Buras *et al.*, 1994c).

Let us first enumerate what has been already calculated in the literature and which calculations are still required in order to complete the next-to-leading calculation of $B(B \rightarrow X_s)$. The present status is as follows:

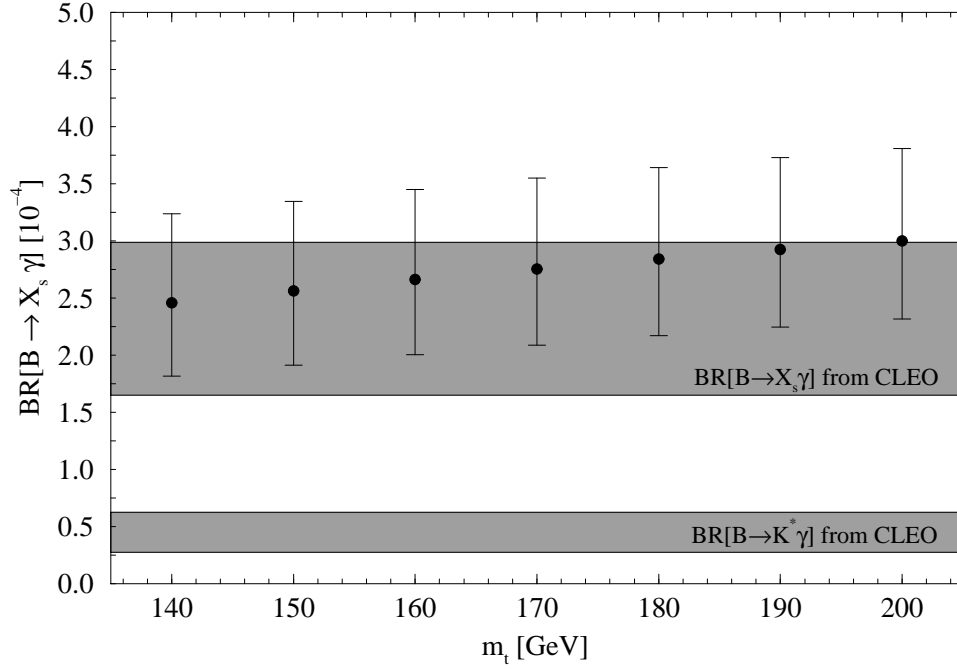


FIG. 21. Predictions for $B \rightarrow X_s \gamma$ in the SM as a function of the top quark mass with the theoretical uncertainties taken into account.

The 6×6 submatrix of $^{(1)}$ describing the two-loop mixing of $(Q_1; \dots; Q_6)$ and the corresponding $O(s)$ corrections in $C(M_W)$ have been already calculated. They are given in section VI.

The two-loop mixing in the $(Q_7; Q_{8G})$ sector of $^{(1)}$ is known (Misiak and Münz, 1995) and given in section IX C.

The $O(s)$ corrections to the matrix element of the operators Q_7 and Q_{8G} have been calculated (Ali and Greub, 1991a), (Ali and Greub, 1991b). They have been recently confirmed by (Pott, 1995) who also presents the results for the matrix elements of the remaining operators.

The remaining ingredients of a next-to-leading analysis of $B(B \rightarrow X_s \gamma)$ are:

The three-loop mixing between the sectors $(Q_1; \dots; Q_6)$ and $(Q_7; Q_{8G})$ which, with our normalizations, contributes to $^{(1)}$.

The $O(s)$ corrections to $C_7(M_W)$ and $C_{8G}(M_W)$ in (IX.12) and (IX.13). This requires evaluation of two-loop penguin diagrams with internal W and top quark masses and a proper matching with the effective five-quark theory. An attempt to calculate the necessary two-loop Standard Model diagrams has been made in (Adel and Yao, 1994).

The finite parts of the effective theory two-loop diagrams with the insertions of the four-quark operators.

All these calculations are very involved, and the necessary three-loop calculation is a truly formidable task! Yet, as stressed in (Buras *et al.*, 1994c) all these calculations have to be done if we want to reduce the theoretical uncertainties in $b \rightarrow s$ to around 10%.

As demonstrated formally in (Buras *et al.*, 1994c) the cancellation of the dominant α_s -dependence in the leading order can be achieved by calculating the relevant two-loop matrix element of the dominant four-quark operator Q_2 . This matrix element is however renormalization-scheme dependent and moreover mixing with other operators takes place. This scheme dependence can only be canceled by calculating $\alpha_s^{(1)}$ in the same renormalization scheme. This point has been extensively discussed in this review and we will not repeat this discussion here. However, it is clear from these remarks, that in order to address the α_s -dependence and the renormalization-scheme dependence as well as their cancellations, it is necessary to perform a complete next-to-leading order analysis of $C(\mu)$ and of the corresponding matrix elements.

In this context we would like to comment on an analysis of (Ciuchini *et al.*, 1994b) in which the known two-loop mixing of $Q_1; \dots; Q_6$ has been added to the leading order analysis of $B \rightarrow X_s$. Strong renormalization scheme dependence of the resulting branching ratio has been found, giving the branching ratio $(1.7 \pm 0.2) \cdot 10^4$ and $(2.3 \pm 0.2) \cdot 10^4$ at $\mu = 5 \text{ GeV}$ for HV and NDR schemes, respectively. It has also been observed that whereas in the HV scheme the dependence has been weakened, it remained still strong in the NDR scheme. In our opinion this partial cancellation of the α_s -dependence in the HV scheme is rather accidental and has nothing to do with the cancellation of the α_s -dependence discussed above. The latter requires the evaluation of finite parts in two-loop matrix elements of the four-quark operators $Q_1; \dots; Q_6$. On the other hand the strong scheme dependence in the partial NLO analysis presented in (Ciuchini *et al.*, 1994b) demonstrates very clearly the need for a full analysis. In view of this discussion we think that the decrease of the branching ratio for $B \rightarrow X_s$ relative to the LO prediction, found in (Ciuchini *et al.*, 1994b), and given by $B(B \rightarrow X_s) = (1.9 \pm 0.2 \pm 0.5) \cdot 10^4$ is still premature and one should wait until the full NLO analysis has been done.

XXIII. THE DECAY $B \rightarrow X_s e^+ e^-$

A. General Remarks

The rare decay $B \rightarrow X_s e^+ e^-$ has been the subject of many theoretical studies in the framework of the Standard Model and its extensions such as the two Higgs doublet models and models involving supersymmetry (Hou *et al.*, 1987), (Grinstein *et al.*, 1989), (Jaus and Wyler, 1990), (Bertolini *et al.*, 1991b), (Ali *et al.*, 1991), (Deshpande *et al.*, 1993), (Ali *et al.*, 1995), (Greub *et al.*, 1995). In particular the strong dependence of $B \rightarrow X_s e^+ e^-$ on m_t has been stressed in (Hou *et al.*, 1987). It is clear that once $B \rightarrow X_s e^+ e^-$ has been observed, it will offer a useful test of the Standard Model and its extensions. To this end the relevant branching ratio, the dilepton invariant mass distribution and other distributions of interest should be calculated with sufficient precision. In particular the QCD effects should be properly taken into account.

The central element in any analysis of $B \rightarrow X_s e^+ e^-$ is the effective hamiltonian for this decay given in section X where a detailed analysis of the Wilson coefficients has been presented. However, the actual calculation of $B \rightarrow X_s e^+ e^-$ involves not only the evaluation of Wilson coefficients of the relevant local operators but also the calculation of the corresponding matrix elements of these operators relevant for $B \rightarrow X_s e^+ e^-$. The latter part of the analysis can be done in the

spectator model, which, as indicated by the heavy quark expansion should offer a good approximation to QCD for B-decays. One can also include the non-perturbative $O(1/m_b^2)$ corrections to the spectator model which enhance the rate for $B \rightarrow X_s e^+ e^-$ by roughly 10% (Falk *et al.*, 1994). A realistic phenomenological analysis should also include the long-distance contributions which are mainly due to the J/ψ and ψ' resonances (Lim *et al.*, 1989), (Deshpande *et al.*, 1989), (O'Donnell and Tung, 1991). Since in this review we are mainly interested in the next-to-leading short-distance QCD effects we will not include these complications in what follows. This section closely follows (Buras and Münz, 1995) except that the numerical results in figs. 22–24 have been slightly changed in accordance with the input parameters of appendix A.

We stress again that in a consistent NLO analysis of the decay $B \rightarrow X_s e^+ e^-$, one should on one hand calculate the Wilson coefficient of the operator $Q_{9V} = (sb)_{V-A} (\bar{e}e)_V$ including leading and next-to-leading logarithms, but on the other hand only leading logarithms should be kept in the remaining Wilson coefficients. Only then a scheme independent amplitude can be obtained. As already discussed in section X, this special treatment of Q_9 is related to the fact that strictly speaking in the leading logarithmic approximation only this operator contributes to $B \rightarrow X_s e^+ e^-$. The contributions of the usual current-current operators, QCD penguin operators, magnetic penguin operators and of $Q_{10A} = (sb)_{V-A} (\bar{e}e)_A$ enter only at the NLO level and to be consistent only the leading contributions to the corresponding Wilson coefficients should be included.

B. The Differential Decay Rate

Introducing

$$\hat{s} = \frac{(p_{e^+} + p_{e^-})^2}{m_b^2}; \quad z = \frac{m_c}{m_b} \quad (\text{XXIII.1})$$

and calculating the one-loop matrix elements of Q_i using the spectator model in the NDR scheme one finds (Misiak, 1995), (Buras and Münz, 1995)

$$\begin{aligned} R(\hat{s}) &= \frac{d\Gamma(B \rightarrow X_s e^+ e^-)}{d\hat{s}} = \frac{1}{4} \frac{V_{ts}^2}{V_{cb}^2} \frac{(1 - \hat{s})^2}{f(z)} \\ &= (1 + 2\hat{s}) \mathcal{C}_9^{\text{eff}} + \mathcal{C}_{10}^2 + 4 \left(1 + \frac{2}{\hat{s}}\right) \mathcal{C}_7^{(0)\text{eff}} + 12\mathcal{C}_7^{(0)\text{eff}} \text{Re}\mathcal{C}_9^{\text{eff}} \end{aligned} \quad (\text{XXIII.2})$$

where

$$\begin{aligned} \mathcal{C}_9^{\text{eff}} &= \mathcal{C}_9^{\text{NDR}} \sim (\hat{s}) + h(z; \hat{s}) \left[3\mathcal{C}_1^{(0)} + \mathcal{C}_2^{(0)} + 3\mathcal{C}_3^{(0)} + \mathcal{C}_4^{(0)} + 3\mathcal{C}_5^{(0)} + \mathcal{C}_6^{(0)} \right. \\ &\quad \left. + \frac{1}{2} h(1; \hat{s}) \left[4\mathcal{C}_3^{(0)} + 4\mathcal{C}_4^{(0)} + 3\mathcal{C}_5^{(0)} + \mathcal{C}_6^{(0)} \right] \right. \\ &\quad \left. + \frac{1}{2} h(0; \hat{s}) \left[\mathcal{C}_3^{(0)} + 3\mathcal{C}_4^{(0)} + \frac{2}{9} \left(3\mathcal{C}_3^{(0)} + \mathcal{C}_4^{(0)} + 3\mathcal{C}_5^{(0)} + \mathcal{C}_6^{(0)} \right) \right] \right] : \end{aligned} \quad (\text{XXIII.3})$$

The general expression (XXIII.2) with $f(z) = 1$ has been first presented by (Grinstein *et al.*, 1989) who in their approximate leading order renormalization group analysis kept only the operators $Q_1; Q_2; Q_7; Q_{9V}; Q_{10A}$.

The various entries in (XXIII.2) are given as follows

$$h(z; \hat{s}) = \frac{8}{9} \ln \frac{m_b}{\mu} - \frac{8}{9} \ln z + \frac{8}{27} + \frac{4}{9} x \quad (XXIII.4)$$

$$\frac{2}{9} (2+x) \ln \frac{1-x+1}{1-x-1} : 2 \arctan \frac{1}{x-1}; \quad \text{for } x = 4z^2/\hat{s} < 1$$

$$\frac{2}{9} (2+x) \ln \frac{1-x+1}{1-x-1} : 2 \arctan \frac{1}{x-1}; \quad \text{for } x = 4z^2/\hat{s} > 1;$$

$$h(0; \hat{s}) = \frac{8}{27} - \frac{8}{9} \ln \frac{m_b}{\mu} - \frac{4}{9} \ln \hat{s} + \frac{4}{9} i : \quad (XXIII.5)$$

$$f(z) = 1 - \frac{8z^2 + 8z^6}{z^8} - \frac{24z^4}{z^8} \ln z; \quad (XXIII.6)$$

$$(z) = 1 - \frac{2}{3} \left(\frac{s}{\mu^2} \right) \left(1 - \frac{31}{4} \right) (1 - z^2) + \frac{3}{2} \quad (XXIII.7)$$

$$\sim (\hat{s}) = 1 + \frac{s}{\mu^2} \ln \left(\frac{s}{\mu^2} \right) : \quad (XXIII.8)$$

with

$$\ln(\hat{s}) = \frac{2}{9} \ln^2 \hat{s} - \frac{4}{3} \text{Li}_2(s) - \frac{2}{3} \ln s \ln(1-s) - \frac{5+4s}{3(1+2s)} \ln(1-s)$$

$$\frac{2s(1+s)(1-2s)}{3(1-s)^2(1+2s)} \ln s + \frac{5+9s-6s^2}{6(1-s)(1+2s)} : \quad (XXIII.9)$$

Here $f(z)$ is the phase-space factor for $b \rightarrow c \gamma$. (z) is the corresponding single gluon QCD correction (Cabibbo and Maiani, 1978) in the approximation of (Kim and Martin, 1989). \sim on the other hand represents single gluon corrections to the matrix element of Q_9 with $m_s = 0$ (Jezabek and Kühn, 1989), (Misiak, 1995). For consistency reasons this correction should only multiply the leading logarithmic term in $\mathcal{C}_9^{\text{NDR}}$.

In the HV scheme the one-loop matrix elements are different and one finds an additional explicit contribution to (XXIII.3) given by (Buras and Münz, 1995)

$$\mathcal{C}_9^{\text{HV}} = \frac{4}{9} (3C_1^{(0)} + C_2^{(0)} - C_3^{(0)} - 3C_4^{(0)}) : \quad (XXIII.10)$$

However $\mathcal{C}_9^{\text{NDR}}$ has to be replaced by $\mathcal{C}_9^{\text{HV}}$ given in (X.5) and (X.9) and consequently $\mathcal{C}_9^{\text{eff}}$ is the same in both schemes.

The first term in the function $h(z; \hat{s})$ in (XXIII.4) represents the leading \hat{s} -dependence in the matrix elements. It is canceled by the \hat{s} -dependence present in the leading logarithm in \mathcal{C}_9 . This is precisely the type of cancellation of the \hat{s} -dependence which one would like to achieve in the case of $B \rightarrow X_s \gamma$. The \hat{s} -dependence present in the coefficients of the other operators can only be canceled by going to still higher order in the renormalization group improved perturbation theory. To this end the matrix elements of four-quark operators should be evaluated at two-loop level. Also certain unknown three-loop anomalous dimensions should be included in the evaluation of $\mathcal{C}_7^{\text{eff}}$ and \mathcal{C}_{9V} . Certainly this is beyond the scope of this review and we will only investigate the left-over \hat{s} -dependence below.

C. Numerical Analysis

A detailed numerical analysis of the formulae above has been presented in (Buras and Münz, 1995). We give here a brief account of this work. We set first $V_{ts}/V_{cb} = 1$ which in view of

(XXII.7) is a good approximation. We keep in mind that for $\hat{s} = m_b^2$, $\hat{s} = m_{D^*}^2$ etc. the spectator model cannot be the full story and additional long-distance contributions discussed in (Lim *et al.*, 1989), (Deshpande *et al.*, 1989), (O'Donnell and Tung, 1991) have to be taken into account in a phenomenological analysis. Similarly we do not include $1/m_b^2$ corrections calculated in (Falk *et al.*, 1994) which typically enhance the differential rate by about 10%.

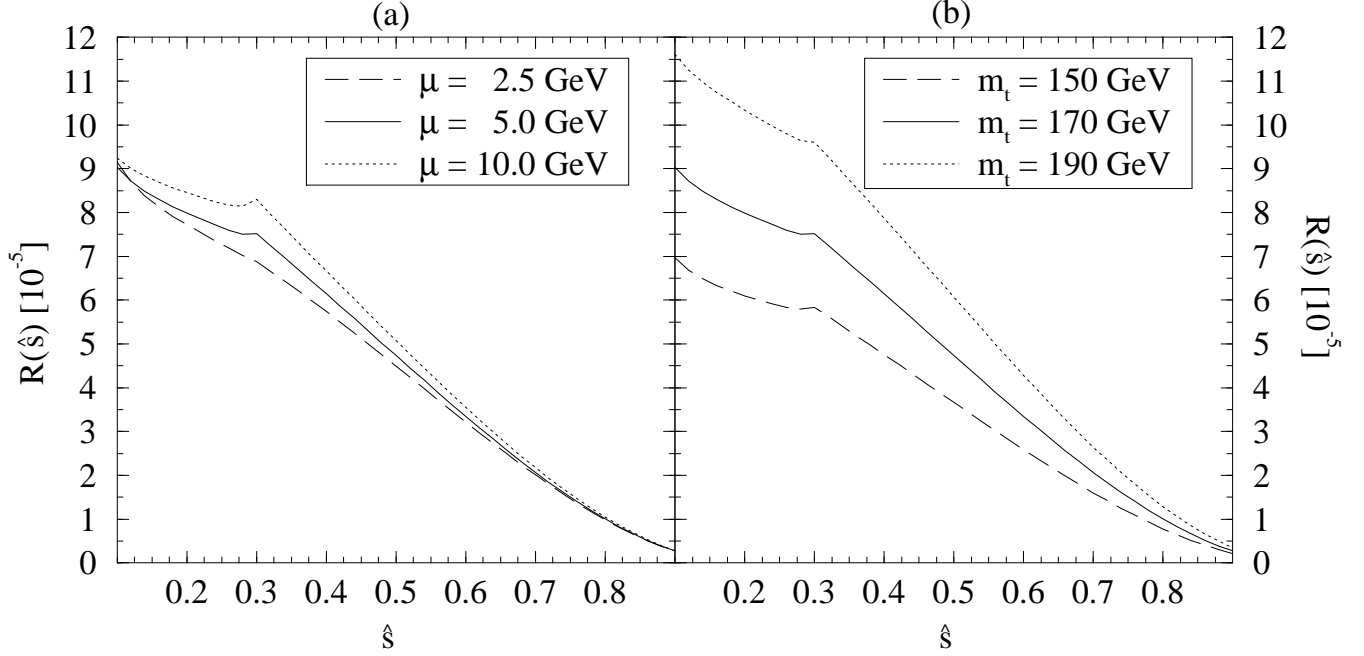


FIG. 22. (a) $R(\hat{s})$ for $m_t = 170 \text{ GeV}$, $\frac{(5)}{M_S} = 225 \text{ MeV}$ and different values of μ .
(b) $R(\hat{s})$ for $\mu = 5 \text{ GeV}$, $\frac{(5)}{M_S} = 225 \text{ MeV}$ and various values of m_t .

In fig. 22 (a) we show $R(\hat{s})$ for $m_t = 170 \text{ GeV}$, $\frac{(5)}{M_S} = 225 \text{ MeV}$ and different values of μ . In fig. 22 (b) we set $\mu = 5 \text{ GeV}$ and vary m_t from 150 GeV to 190 GeV . The remaining μ dependence is rather weak and amounts to at most 8% in the full range of parameters considered. The m_t dependence of $R(\hat{s})$ is sizeable. Varying m_t between 150 GeV and 190 GeV changes $R(\hat{s})$ by typically 60–65% which in this range of m_t corresponds to $R(\hat{s}) \propto m_t^2$. It is easy to verify that this strong m_t dependence originates in the coefficient \mathcal{C}_{10} given in (X.3) as already stressed by several authors in the past (Hou *et al.*, 1987), (Grinstein *et al.*, 1989), (Bertolini *et al.*, 1991b), (Deshpande *et al.*, 1993), (Greub *et al.*, 1995), (Ali *et al.*, 1995), (Ali *et al.*, 1991), (Jaus and Wyler, 1990).

We do not show the $\frac{(5)}{M_S}$ dependence as it is very weak. Typically, changing $\frac{(5)}{M_S}$ from 140 MeV to 310 MeV decreases $R(\hat{s})$ by about 5%.

$R(\hat{s})$ is governed by three coefficients, $\mathcal{C}_9^{\text{eff}}$, \mathcal{C}_{10} and $C_7^{(0)\text{eff}}$. The importance of various contributions has been investigated in (Buras and Münz, 1995). To this end one sets $\frac{(5)}{M_S} = 225 \text{ GeV}$, $m_t = 170 \text{ GeV}$ and $\mu = 5 \text{ GeV}$. In fig. 23 we show $R(\hat{s})$ keeping only $\mathcal{C}_9^{\text{eff}}$, \mathcal{C}_{10} , $C_7^{(0)\text{eff}}$ and the $C_7^{(0)\text{eff}} - \mathcal{C}_9^{\text{eff}}$ interference term, respectively. Denoting these contributions by R_9 , R_{10} , R_7 and $R_{7=9}$ we observe that the term R_7 plays only a minor role in $R(\hat{s})$. On the other hand the presence of $C_7^{(0)\text{eff}}$ cannot be ignored because the interference term $R_{7=9}$ is significant.

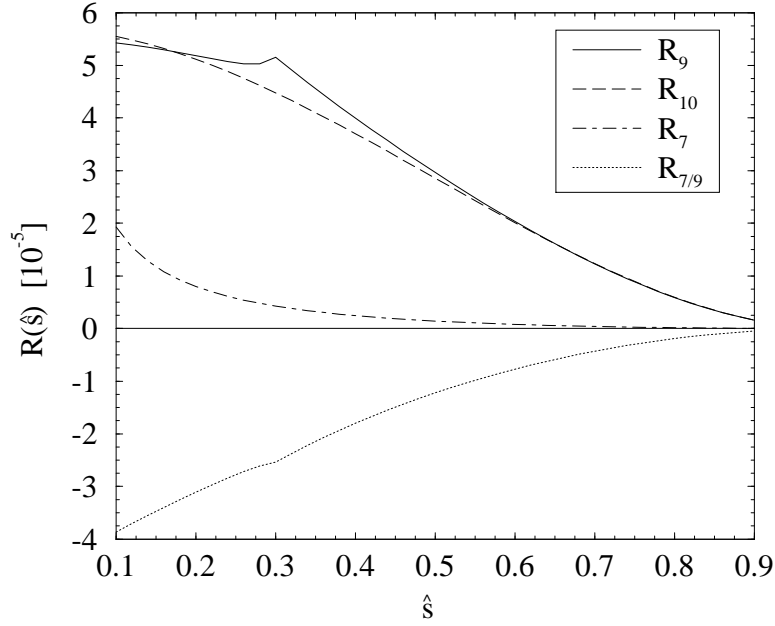


FIG. 23. Comparison of the four different contributions to $R(\hat{s})$ according to eq. (XXIII.2).

In fact the presence of this large interference term could be used to measure experimentally the relative sign of $C_7^{(0)\text{eff}}$ and $\text{Re } C_9^{\text{eff}}$ (Grinstein *et al.*, 1989), (Jaus and Wyler, 1990), (Ali *et al.*, 1991), (Greub *et al.*, 1995), (Ali *et al.*, 1995) which as seen in fig. 23 is negative in the Standard Model. However, the most important contributions are R_9 and R_{10} in the full range of \hat{s} considered. For $m_t = 170 \text{ GeV}$ these two contributions are roughly of the same size. Due to a strong m_t dependence of R_{10} , this contribution dominates for higher values of m_t and is less important than R_9 for $m_t < 170 \text{ GeV}$.

Next, in fig. 24 we show $R(\hat{s})$ for $\sqrt{s} = 5 \text{ GeV}$, $m_t = 170 \text{ GeV}$ and $\overline{M_S} = 225 \text{ MeV}$ compared to the case of no QCD corrections and to the results (Grinstein *et al.*, 1989) would obtain for our set of parameters using their approximate leading order formulae.

The discussion of the definition of m_t used here is identical to the one in the case of $K_L \rightarrow \pi^0 e^+ e^-$ and will not be repeated here. On the basis of the arguments given there we believe that if $m_t = \overline{m}_t(m_t)$ is chosen, the additional short-distance QCD corrections to $B \rightarrow X_s e^+ e^-$ should be small.

Our discussion has been restricted to $B \rightarrow X_s \gamma$. Also the photon spectrum has been the subject of several papers. We just refer to the most recent articles (Neubert, 1994b), (Shifman *et al.*, 1994), (Dikeman *et al.*, 1995), (Kapustin and Ligeti, 1995), (Kapustin *et al.*, 1995), (Ali and Greub, 1995), (Pott, 1995) where further references can be found.

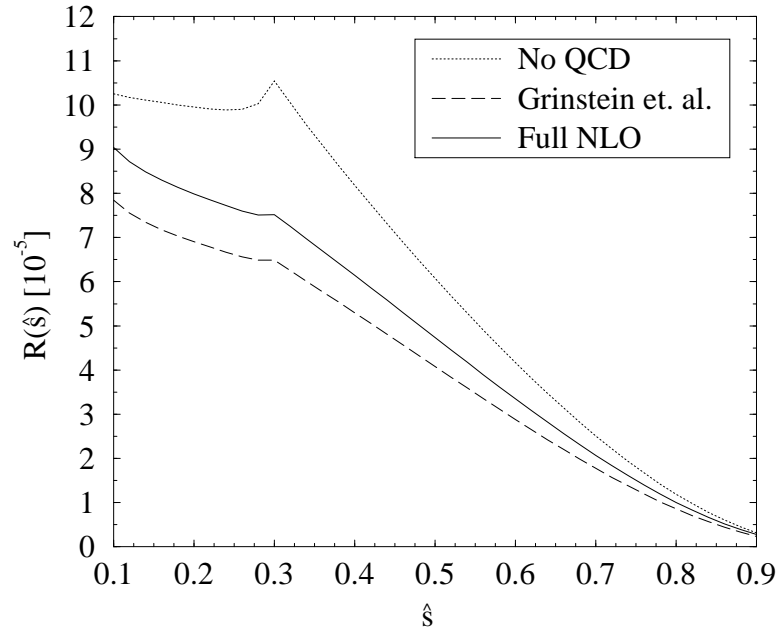


FIG. 24. $R(\hat{s})$ for $m_t = 170 \text{ GeV}$, $\frac{(5)}{M_S} = 225 \text{ MeV}$ and $\mu = 5 \text{ GeV}$.

XXIV. THE DECAYS $K^+ \rightarrow \pi^+ \nu \bar{\nu}$ AND $K_L \rightarrow \pi^0 \nu \bar{\nu}$

A. General Remarks on $K^+ \rightarrow \pi^+ \nu \bar{\nu}$

The rare decay $K^+ \rightarrow \pi^+ \nu \bar{\nu}$ is one of the theoretically cleanest decays. As such it is very well suited for the determination of CKM parameters, in particular of the element V_{td} . $K^+ \rightarrow \pi^+ \nu \bar{\nu}$ is CP conserving and receives contributions from both internal top and charm exchanges. The inclusion of next-to-leading QCD corrections incorporated in the effective hamiltonian in (XI.4) and discussed in detail in section XI B reduces considerably the theoretical uncertainties due to the choice of the renormalization scales present in the leading order expressions. We will illustrate this below. Since in addition the relevant hadronic matrix element of the weak current $(sd)_V$ can be measured in the leading decay $K^+ \rightarrow \pi^0 e^+ \nu$, the resulting theoretical expression for $B(K^+ \rightarrow \pi^+ \nu \bar{\nu})$ is only a function of the CKM parameters, the QCD scale $\frac{1}{M_S}$ and the quark masses m_t and m_c . The long-distance contributions to $K^+ \rightarrow \pi^+ \nu \bar{\nu}$ have been found to be very small: a few percent of the charm contribution to the amplitude at most, which is safely negligible (Rein and Sehgal, 1989), (Hagelin and Littenberg, 1989) and (Lu and Wise, 1994).

Conventionally the branching fraction $B(K^+ \rightarrow \pi^+ \nu \bar{\nu})$ is related to the experimentally well known quantity $B(K^+ \rightarrow \pi^0 e^+ \nu)$ using isospin symmetry. Corrections to this approximation have recently been studied in (Marciano and Parsa, 1995). The breaking of isospin is due to quark mass effects and electroweak radiative corrections. In the case of $K^+ \rightarrow \pi^+ \nu \bar{\nu}$ these effects result in a decrease of the branching ratio by 10%. The corresponding corrections in $K_L \rightarrow \pi^0 \nu \bar{\nu}$ lead to a 5.6% reduction of $B(K_L \rightarrow \pi^0 \nu \bar{\nu})$. We have checked the analysis of (Marciano and Parsa, 1995) and agree with their findings. Once calculated, the inclusion of these effects is straightforward as they only amount to an overall factor for the branching ratio and do not affect the short-distance structure of $K \rightarrow \pi \nu \bar{\nu}$. We shall neglect the isospin violating corrections in the following chapters, where the focus is primarily on the short-distance physics. The effects are however incorporated in the final prediction quoted in our summary table in section XXVII.

In the following we shall concentrate on a discussion of $K^+ \rightarrow \pi^+ \nu \bar{\nu}$ within the framework of the standard model. The impact of various scenarios of new physics on this decay has been considered for instance in (Bigi and Gabbiani, 1991).

B. Master Formulae for $K^+ \rightarrow \pi^+ \nu \bar{\nu}$

Using the effective hamiltonian (XI.4) and summing over the three neutrino flavors one finds

$$B(K^+ \rightarrow \pi^+ \nu \bar{\nu}) = \frac{1}{4} \left[\frac{\text{Im}(t_c)}{5} X(x_t) + \frac{\text{Re}(c)}{P_0} X(x_c) + \frac{\text{Re}(t_c)}{5} X(x_t) \right]^2 \quad (\text{XXIV.1})$$

$$+ \frac{3}{2} \frac{B(K^+ \rightarrow \pi^0 e^+ \nu)}{\sin^4 \theta_w} = 4.57 \cdot 10^{11} \quad (\text{XXIV.2})$$

where we have used

$$\frac{1}{129} \sin^2 \theta_w = 0.23 \quad B(K^+ \rightarrow \pi^0 e^+ \nu) = 4.82 \cdot 10^2 \quad (\text{XXIV.3})$$

Here $\gamma_i = V_{is}V_{id}$ with γ_c being real to a very high accuracy. The function X of (XI.5) can also be written as

$$X(x) = x \tilde{X}(x) \quad x = 0.985 \quad (\text{XXIV.4})$$

where x summarizes the NLO corrections discussed in section XI B. With $m_t \rightarrow m_t(m_t)$ the QCD factor X is practically independent of m_t and $\frac{1}{M_S}$. Next

$$P_0(X) = \frac{1}{4} \frac{2}{3} X_{NL}^e + \frac{1}{3} X_{NL} \quad (\text{XXIV.5})$$

with the numerical values for X_{NL}^1 given in table XXXIII. The corresponding values for $P_0(X)$ as a function of $\frac{1}{M_S}$ and $m_c \rightarrow m_c(m_c)$ are collected in table XLIV. We remark that a negligibly small term $(X_{NL}^e - X_{NL})^2$ ($\sim 0.2\%$ effect on the branching ratio) has been discarded in formula (XXIV.1).

TABLE XLIV. The function $P_0(X)$ for various $\frac{(4)}{M_S}$ and m_c .

	$P_0(X)$		
$\frac{(4)}{M_S} \text{ n } m_c$	1.25 GeV	1.30 GeV	1.35 GeV
215 MeV	0.402	0.436	0.472
325 MeV	0.366	0.400	0.435
435 MeV	0.325	0.359	0.393

Using the improved Wolfenstein parametrization and the approximate formulae (II.23) – (II.25) we can next write

$$B(K^+ \rightarrow \pi^+ \pi^0) = 4.57 \cdot 10^{-1} A^4 X^2(x_t) \frac{1}{2} \left(\frac{1}{2} + \left(\frac{\gamma_0}{\gamma} \right)^2 \right) \quad (\text{XXIV.6})$$

where

$$= \frac{1}{1 - \frac{1}{2}} \quad (\text{XXIV.7})$$

The measured value of $B(K^+ \rightarrow \pi^+ \pi^0)$ then determines an ellipse in the $(\gamma; \gamma_0)$ plane centered at $(\gamma_0; 0)$ with (Buras *et al.*, 1994b)

$$\gamma_0 = 1 + \frac{P_0(X)}{A^2 X(x_t)} \quad (\text{XXIV.8})$$

and having the squared axes

$$\gamma_1^2 = r_0^2 \quad \frac{1}{2} = \frac{r_0}{2} \quad (\text{XXIV.9})$$

where

$$r_0^2 = \frac{1}{A^4 X^2(x_t)} \frac{B R(K^+ \rightarrow \pi^+ \pi^0)}{4.57 \cdot 10^{11}} \quad (\text{XXIV.10})$$

The departure of ρ_0 from unity measures the relative importance of the internal charm contributions.

The ellipse defined by r_0 , ρ_0 and ϕ given above intersects with the circle (II.32). This allows to determine ρ and ϕ with

$$\rho = \frac{1}{1 - \frac{r_0^2}{2\rho_0^2}} \rho_0 \sqrt{\frac{2\rho_0^2 + (1 - \frac{r_0^2}{2\rho_0^2})(r_0^2 - 2R_b^2)}{R_b^2 - \rho_0^2}} = \frac{r_0}{R_b^2 - \rho_0^2} \quad (\text{XXIV.11})$$

and consequently

$$R_t^2 = 1 + R_b^2 - 2\rho \quad (\text{XXIV.12})$$

where ϕ is assumed to be positive.

In the leading order of the Wolfenstein parametrization

$$\rho \approx 1 - \frac{1}{2} \quad \phi \approx \frac{\pi}{2} \quad (\text{XXIV.13})$$

and $B(K^+ \rightarrow \pi^+ \pi^0)$ determines a circle in the $(\rho; \phi)$ plane centered at $(\frac{1}{2}; 0)$ and having the radius r_0 of (XXIV.10) with $\phi = 1$. Formulae (XXIV.11) and (XXIV.12) then simplify to (Buchalla and Buras, 1994a)

$$R_t^2 = 1 + R_b^2 + \frac{r_0^2}{\rho_0} R_b^2 \quad \rho = \frac{1}{2} \rho_0 + \frac{R_b^2}{\rho_0} r_0^2 \quad (\text{XXIV.14})$$

Given ρ and ϕ one can determine V_{td} :

$$V_{td} = A^{-3} (1 - \rho - i\phi) \quad |V_{td}| = A^{-3} R_t \quad (\text{XXIV.15})$$

Before proceeding to the numerical analysis a few remarks are in order:

The determination of $|V_{ub}|$ and of the unitarity triangle requires the knowledge of V_{cb} (or A) and of $|V_{ub}| = |V_{cb}|$. Both values are subject to theoretical uncertainties present in the existing analyses of tree level decays. Whereas the dependence on $|V_{ub}| = |V_{cb}|$ is rather weak, the very strong dependence of $B(K^+ \rightarrow \pi^+ \pi^0)$ on A or V_{cb} makes a precise prediction for this branching ratio difficult at present. We will return to this below.

The dependence of $B(K^+ \rightarrow \pi^+ \pi^0)$ on m_t is also strong. However m_t should be known already in this decade within 5% and consequently the uncertainty in m_t will soon be less serious for $B(K^+ \rightarrow \pi^+ \pi^0)$ than the corresponding uncertainty in V_{cb} .

Once ρ and ϕ are known precisely from CP asymmetries in B decays, some of the uncertainties present in (XXIV.6) related to $|V_{ub}| = |V_{cb}|$ (but not to V_{cb}) will be removed.

A very clean determination of $\sin 2\beta$ without essentially any dependence on m_t and V_{cb} can be made by combining $B(K^+ \rightarrow \pi^+ \pi^0)$ with $B(K_L \rightarrow \pi^0 \pi^0)$ discussed below. We will present an analysis of this type in section XXIV H.

C. Numerical Analysis of $K^+ \rightarrow \pi^+ \pi^0$

1. Renormalization Scale Uncertainties

We will now investigate the uncertainties in $X(x_t)$, X_{NL} , $B(K^+ \rightarrow \pi^+ \pi^0)$, \mathcal{V}_{cb} and in the determination of the unitarity triangle related to the choice of the renormalization scales μ_t and μ_c (see section XI B). To this end we will fix the remaining parameters as follows

$$m_c = m_c(m_c) = 1.3 \text{ GeV} \quad m_t = m_t(m_t) = 170 \text{ GeV} \quad (\text{XXIV.16})$$

$$V_{cb} = 0.040 \quad \mathcal{V}_{ub} = V_{cb} = 0.08 \quad (\text{XXIV.17})$$

In the case of $B(K^+ \rightarrow \pi^+ \pi^0)$ we need the values of both α_s and β . Therefore in this case we will work with

$$\alpha_s = 0 \quad \beta = 0.36 \quad (\text{XXIV.18})$$

rather than with $\mathcal{V}_{ub} = V_{cb}$. Finally we will set $\frac{(4)}{M_S} = 0.325 \text{ GeV}$ and $\frac{(5)}{M_S} = 0.225 \text{ GeV}$ for the charm part and top part, respectively. We then vary the scales μ_c and μ_t , entering $m_c(\mu_c)$ and $m_t(\mu_t)$ respectively, in the ranges

$$1 \text{ GeV} < \mu_c < 3 \text{ GeV} \quad 100 \text{ GeV} < \mu_t < 300 \text{ GeV} \quad (\text{XXIV.19})$$

In fig. 25 we show the charm function X_{NL} (for $m_1 = 0$) compared to the leading-log result X_L and the case without QCD as functions of μ_c . We observe the following features:

The residual slope of X_{NL} is considerably reduced in comparison to X_L , which exhibits a quite substantial dependence on the unphysical scale μ_c . The variation of X (defined as $(X(1 \text{ GeV}) - X(3 \text{ GeV})) / X(m_c)$) is 24.5% in NLLA compared to 56.6% in LLA.

The suppression of the uncorrected function through QCD effects is somewhat less pronounced in NLLA.

The next-to-leading effects amount to a $\sim 10\%$ correction relative to X at $\mu_c = m_c$. However the size of this correction strongly depends on μ_c due to the scale ambiguity of the leading order result. This means that the question of how large the next-to-leading effects compared to the LLA really are cannot be answered uniquely. Therefore the relevant result is actually the reduction of the μ_c -dependence in NLLA.

In fig. 26 we show the analogous results for the top function $X(x_t)$ as a function of μ_t . We observe:

Due to $\mu_t \sim \mu_c$ the scale dependences in the top function are substantially smaller than in the case of charm. Note in particular how the yet appreciable scale dependence of X_0 gets flattened out almost perfectly when the $O(\alpha_s^2)$ effects are taken into account. The total variation of $X(x_t)$ with $100 \text{ GeV} < \mu_t < 300 \text{ GeV}$ is around 1% in NLLA compared to 10% in LLA.

As already stated above after (XXIV.4), with the choice $\mu_t = m_t$ the NLO correction is very small. It is substantially larger for μ_t very different from m_t .

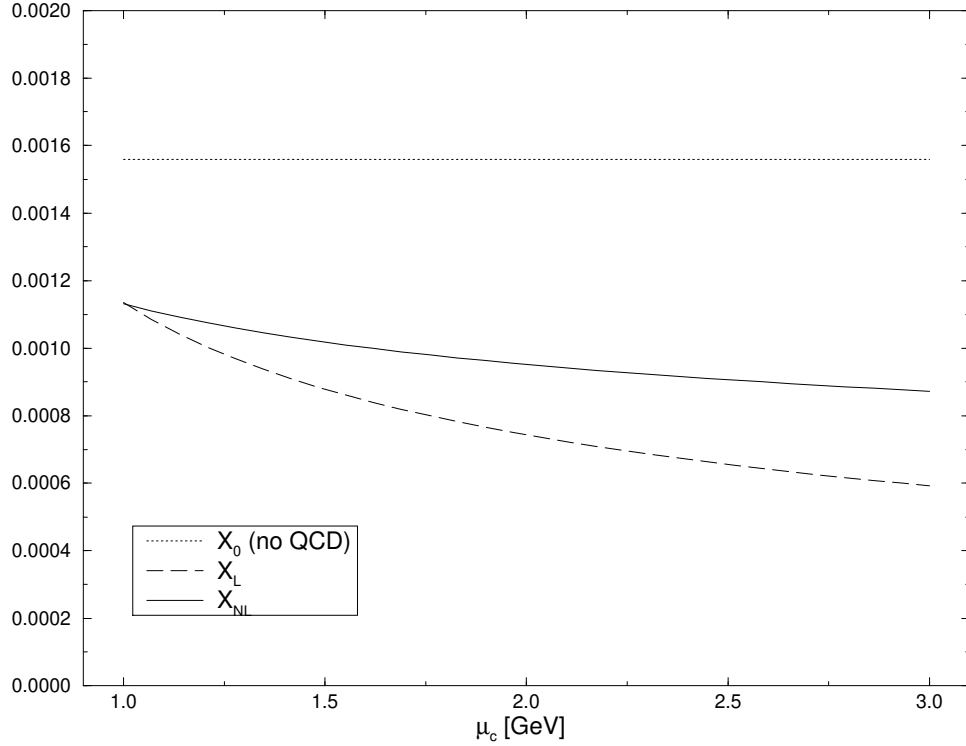


FIG. 25. Charm quark function X_{NL} (for $m_l = 0$) compared to the leading-log result X_L and the case without QCD as functions of μ_c .

Using (XXIV.1) and varying c_{τ} in the ranges (XXIV.19) we find that for the above choice of the remaining parameters the uncertainty in $B(K^+ \rightarrow \pi^+)$

$$0.76 \cdot 10^{10} B(K^+ \rightarrow \pi^+) = 1.20 \cdot 10^9 \quad (XXIV.20)$$

present in the leading order is reduced to

$$0.88 \cdot 10^{10} B(K^+ \rightarrow \pi^+) = 1.02 \cdot 10^9 \quad (XXIV.21)$$

after including NLO corrections. Similarly we obtain

$$8.24 \cdot 10^3 \mathcal{M}_{td} = 10.97 \cdot 10^3 \quad \text{LLA} \quad (XXIV.22)$$

$$9.23 \cdot 10^3 \mathcal{M}_{td} = 10.10 \cdot 10^3 \quad \text{NLLA} \quad (XXIV.23)$$

where we have set $B(K^+ \rightarrow \pi^+) = 1 \cdot 10^9$. We observe that including the full next-to-leading corrections reduces the uncertainty in the determination of \mathcal{M}_{td} from 14% (LLA) to 4.6% (NLLA) in the present example. The main bulk of this theoretical error stems from the charm sector. Indeed, keeping $\mu_c = m_c$ fixed and varying only c_{τ} , the uncertainties in the determination of \mathcal{M}_{td} would shrink to 4.7% (LLA) and 0.6% (NLLA). Similar comments apply to $B(K^+ \rightarrow \pi^+)$ where, as seen in (XXIV.20) and (XXIV.21), the theoretical uncertainty due to c_{τ} is reduced from 22% (LLA) to 7% (NLLA).

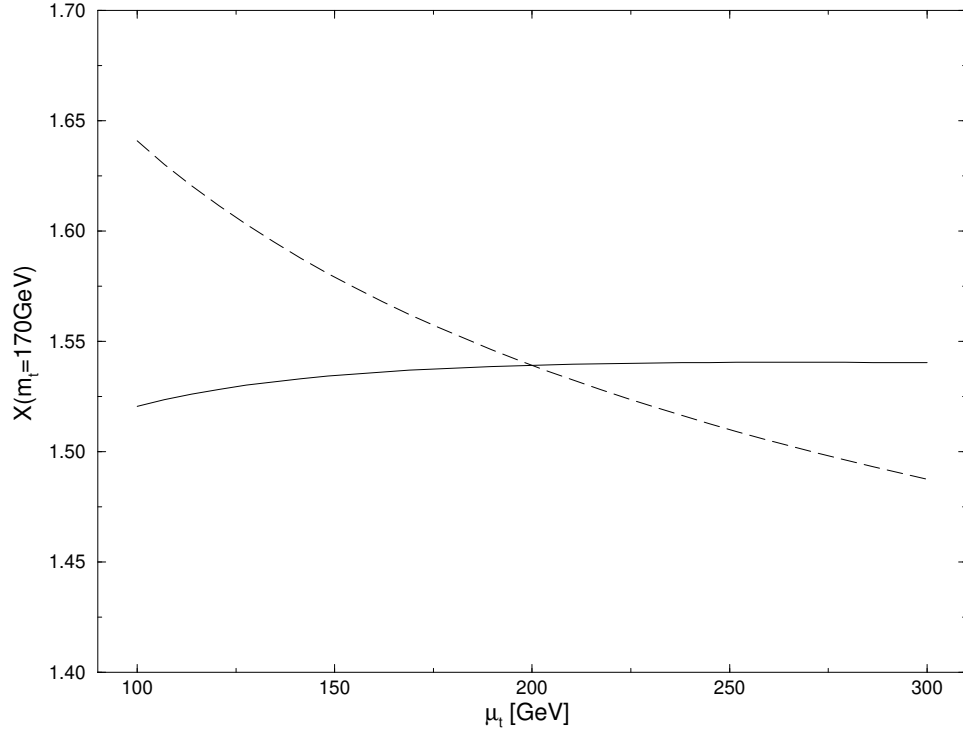


FIG. 26. Top quark function $X(x_t)$ as a function of μ_t for fixed $m_t(m_t) = 170 \text{ GeV}$ with (solid curve) and without (dashed curve) $O(\alpha_s)$ corrections.

Finally in fig. 27 we show the position of the point $(\%, \quad)$ which determines the unitarity triangle. To this end we have fixed all parameters as stated above except for R_b , for which we have chosen three representative numbers, $R_b = 0.25, 0.36, 0.47$. The full and the reduced ranges represent LLA and NLLA respectively. The impact of the inclusion of NLO corrections on the accuracy of determining the unitarity triangle is clearly visible.

2. Expectations for $B(K^+ \rightarrow \pi^+)$

The purely theoretical uncertainties discussed so far should be distinguished from the uncertainties coming from the input parameters such as $m_t, V_{cb}, |V_{ub}|=V_{cb}$ etc.. As we will see the latter uncertainties are still rather large to date. Consequently the progress achieved by the NLO calculations (Buchalla and Buras, 1994a) cannot yet be fully exploited phenomenologically at present. However the determination of the relevant parameters should improve in the future. Once the precision in the input parameters will have attained the desired level, the gain in accuracy of the theoretical prediction for $K^+ \rightarrow \pi^+$ in NLLA by a factor of more than 3 compared to the LLA will become very important.

Using our standard set of input parameters specified in appendix A and the constraints implied by the analysis of B_K and $B_d - B_d$ mixing as described in section XVIII, we find for the $K^+ \rightarrow \pi^+$ branching fraction the range

$$0.6 \cdot 10^{10} \leq B(K^+ \rightarrow \pi^+) \leq 1.5 \cdot 10^{10} \quad (\text{XXIV.24})$$

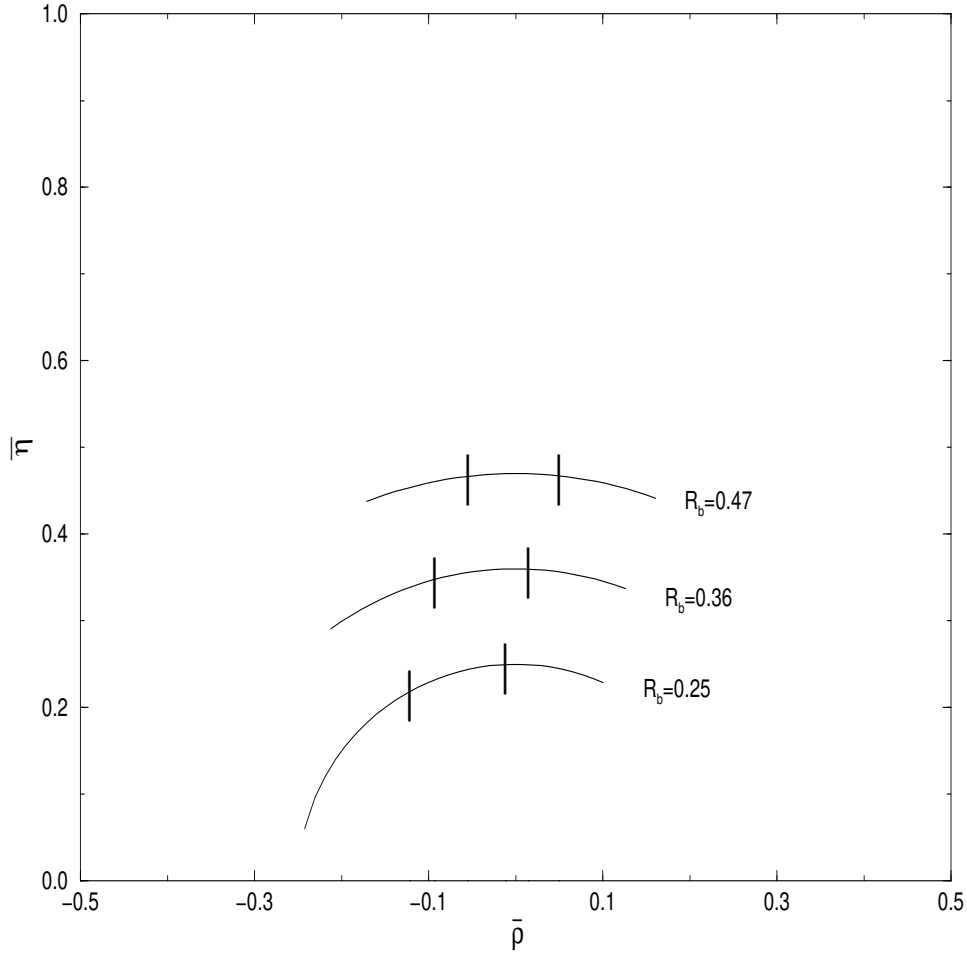


FIG. 27. The theoretical uncertainties in the determination of the unitarity triangle (UT) in the $(\bar{\rho}; \bar{\eta})$ plane from $B(\bar{K}^+ \rightarrow \pi^+ \pi^0)$. With fixed input parameters the vertex of the UT has to lie on a circle around the origin with radius R_b . A variation of the scales μ_c, μ_t within $1 \text{ GeV} \leq \mu_c \leq 3 \text{ GeV}$ and $100 \text{ GeV} \leq \mu_t \leq 300 \text{ GeV}$ then yields the indicated ranges in LLA (full) and NLLA (reduced). We show the cases $R_b = 0.25; 0.36; 0.47$.

Eq. (XXIV.24) represents the current standard model expectation for $B(\bar{K}^+ \rightarrow \pi^+ \pi^0)$ (neglecting small isospin breaking corrections). To obtain this estimate we have allowed for a variation of the parameters $m_t, |V_{cb}|, |V_{ub}|=|V_{cb}| B_K, F_B^2 B_B, x_d$ within their uncertainties as summarized in appendix A. The uncertainties in m_c and $\overline{M_S}$, on the other hand, are small in comparison and have been neglected in this context. The above range would be reduced to

$$0.8 \cdot 10^{10} \leq B(\bar{K}^+ \rightarrow \pi^+ \pi^0) \leq 1.0 \cdot 10^{10} \quad (\text{XXIV.25})$$

if the uncertainties in the input parameters could be decreased as assumed by our “future” scenario in appendix A.

It should be remarked that the x_d -constraint, excluding a part of the second quadrant for the CKM phase β , plays an essential role in obtaining the upper bounds given above, without essentially any effect on the lower bounds. Without the x_d -constraint the upper bounds in (XXIV.24) and (XXIV.25) are relaxed to $2.3 \cdot 10^{10}$ and $1.6 \cdot 10^{10}$, respectively.

D. General Remarks on $K_L \rightarrow \pi^0$

The rare decay $K_L \rightarrow \pi^0$ is even cleaner than $K^+ \rightarrow \pi^+ \pi^-$. It proceeds almost entirely through direct CP violation (Littenberg, 1989a) and is completely dominated by short-distance loop diagrams with top quark exchanges. In fact the m_t -dependence of $B(K_L \rightarrow \pi^0)$ is again described by $X(x_t)$. Since the charm contribution can be fully neglected also the theoretical uncertainties present in $K^+ \rightarrow \pi^+ \pi^-$ due to m_c , α_s and \overline{MS} are absent here. For this reason $K_L \rightarrow \pi^0$ is very well suited for the determination of CKM parameters, in particular the Wolfenstein parameter λ .

E. Master Formulae for $K_L \rightarrow \pi^0$

Using the effective hamiltonian (XI.56) and summing over three neutrino flavors one finds

$$B(K_L \rightarrow \pi^0) = \frac{1}{5} \text{Im} \frac{m_t}{m_c} X(x_t) \quad (XXIV.26)$$

$$\frac{1}{5} = \frac{B(K_L)}{B(K^+)} = 1.91 \cdot 10^{10} \quad (XXIV.27)$$

with $\frac{1}{5}$ given in (XXIV.2). Using the Wolfenstein parametrization we can rewrite (XXIV.26) as

$$B(K_L \rightarrow \pi^0) = 1.91 \cdot 10^{10} A^4 X^2(x_t) \quad (XXIV.28)$$

or

$$B(K_L \rightarrow \pi^0) = 3.48 \cdot 10^9 V_{cb}^4 X^2(x_t) \quad (XXIV.29)$$

A few remarks are in order:

The determination of λ using $B(K_L \rightarrow \pi^0)$ requires the knowledge of V_{cb} and m_t . The very strong dependence on V_{cb} or A makes a precise prediction for this branching ratio difficult at present.

It has been pointed out (Buras, 1994) that the strong dependence of $B(K_L \rightarrow \pi^0)$ on V_{cb} , together with the clean nature of this decay, can be used to determine this element without any hadronic uncertainties. To this end λ and m_t have to be known with sufficient precision in addition to $B(K_L \rightarrow \pi^0)$. λ should be measured accurately in CP asymmetries in B decays and the value of m_t known to better than $\pm 5 \text{ GeV}$ from TEVATRON and future LHC experiments. Inverting (XXIV.29) and using a very accurate approximation for $X(x_t)$ (valid for $m_t = \overline{m}_t(m_t)$) as given by (XXIV.4) and (XIV.6)

$$X(x_t) = 0.65 \cdot x_t^{5.75} \quad (XXIV.30)$$

one finds

$$V_{cb} = 39.3 \cdot 10^3 \frac{s}{0.39} \frac{170 \text{ GeV}}{m_t}^{0.575} \frac{B(K_L \rightarrow \pi^0)}{3 \cdot 10^{11}}^{\#_{1=4}} \quad (\text{XXIV.31})$$

We note that the weak dependence of V_{cb} on $B(K_L \rightarrow \pi^0)$ allows to achieve a high precision for this CKM element even when $B(K_L \rightarrow \pi^0)$ is known with only relatively moderate accuracy, e.g. 10–15%. Needless to say that any measurement of $B(K_L \rightarrow \pi^0)$ is extremely challenging. A numerical analysis of (XXIV.31) can be found in (Buras, 1994).

F. Numerical Analysis of $K_L \rightarrow \pi^0$

1. Renormalization Scale Uncertainties

The scale ambiguities present in the function $X(x_t)$ have already been discussed in connection with $K^+ \rightarrow \pi^+ \pi^-$. After the inclusion of NLO corrections they are so small that they can be neglected for all practical purposes. Effectively they could also be taken into account by introducing an additional error $m_t = 1 \text{ GeV}$. At the level of $B(K_L \rightarrow \pi^0)$ the ambiguity in the choice of m_t is reduced from 10% (LLA) down to 1% (NLLA), which considerably increases the predictive power of the theory. Varying m_t according to (XXIV.19) and using the input parameters of section XXIV C we find that the uncertainty in $B(K_L \rightarrow \pi^0)$

$$2.68 \cdot 10^{11} B(K_L \rightarrow \pi^0) = 3.26 \cdot 10^{11} \quad (\text{XXIV.32})$$

present in the leading order is reduced to

$$2.80 \cdot 10^{11} B(K_L \rightarrow \pi^0) = 2.88 \cdot 10^{11} \quad (\text{XXIV.33})$$

after including NLO corrections. This means that the theoretical uncertainty in the determination of $B(K_L \rightarrow \pi^0)$ amounts to only 0.7% in NLLA which is safely negligible. The reduction of the scale ambiguity for $B(K_L \rightarrow \pi^0)$ is further illustrated in fig. 28.

2. Expectations for $B(K_L \rightarrow \pi^0)$

From an analysis of $B(K_L \rightarrow \pi^0)$ similar to the one described for $K^+ \rightarrow \pi^+ \pi^-$ in section XXIV C 2 we obtain the standard model expectation

$$1.1 \cdot 10^{11} B(K_L \rightarrow \pi^0) = 5.0 \cdot 10^{11} \quad (\text{XXIV.34})$$

corresponding to present day errors in the relevant input parameters. This would change into

$$2.2 \cdot 10^{11} B(K_L \rightarrow \pi^0) = 3.6 \cdot 10^{11} \quad (\text{XXIV.35})$$

if the parameter uncertainties would decrease as anticipated by our “future” scenario defined in appendix A.

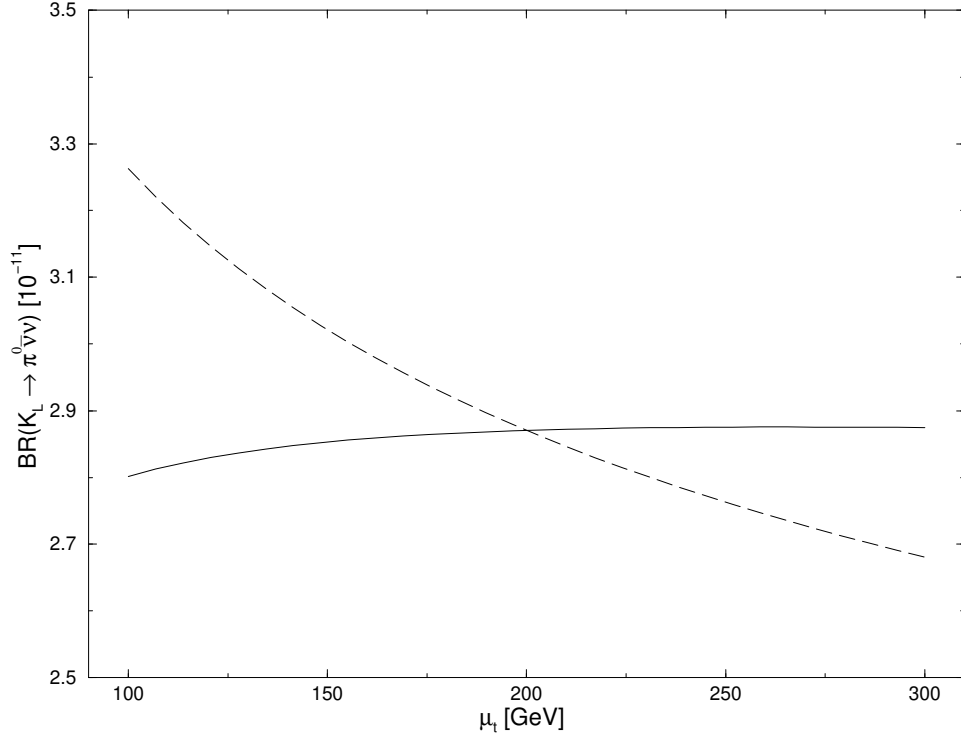


FIG. 28. The μ_t -dependence of $B(K_L^0 \rightarrow \pi^0 \nu \bar{\nu}) = 10^{-11}$ with (solid curve) and without (dashed curve) $O(\alpha_s)$ corrections for $m_t (m_t) = 170 \text{ GeV}$, $|V_{cb}| = 0.04$ and $\beta = 0.36$.

G. Unitarity Triangle from $K \rightarrow \pi \nu \bar{\nu}$

The measurement of $B(K^+ \rightarrow \pi^+ \nu \bar{\nu})$ and $B(K_L^0 \rightarrow \pi^0 \nu \bar{\nu})$ can determine the unitarity triangle completely provided m_t and V_{cb} are known. Using these two branching ratios simultaneously allows to eliminate $|V_{ub}| = |V_{cb}|$ from the analysis which removes considerable uncertainty. Indeed it is evident from (XXIV.1) and (XXIV.26) that, given $B(K^+ \rightarrow \pi^+ \nu \bar{\nu})$ and $B(K_L^0 \rightarrow \pi^0 \nu \bar{\nu})$, one can extract both $\text{Im } \lambda_t$ and $\text{Re } \lambda_t$. We get

$$\text{Im } \lambda_t = \frac{P \overline{B_2}}{X(x_t)} \quad \text{Re } \lambda_t = \frac{5 \frac{\text{Re } c}{P_0(X)} + P \overline{B_1 B_2}}{X(x_t)} \quad (\text{XXIV.36})$$

where we have defined the “reduced” branching ratios

$$B_1 = \frac{B(K^+ \rightarrow \pi^+ \nu \bar{\nu})}{4.57 \cdot 10^{-11}} \quad B_2 = \frac{B(K_L^0 \rightarrow \pi^0 \nu \bar{\nu})}{1.91 \cdot 10^{-10}} \quad (\text{XXIV.37})$$

Using next the expressions for $\text{Im } \lambda_t$, $\text{Re } \lambda_t$ and $\text{Re } c$ given in (II.23) – (II.25) we find

$$\eta = 1 + \frac{P_0(X) \sqrt{(B_1 - B_2)}}{A^2 X(x_t)} = \frac{P \overline{B_2}}{A^2 X(x_t)} \quad (\text{XXIV.38})$$

with η defined in (XXIV.7). An exact treatment of the CKM matrix shows that the formulae (XXIV.38) are rather precise (Buchalla and Buras, 1994c). The error in η is below 0.1% and η may deviate from the exact expression by at most $\eta = 0.02$ with essentially negligible error for

0 % 0.25.

As an illustrative example, let us consider the following scenario. We assume that the branching ratios are known to within 10%

$$B(K^+ \rightarrow \pi^+ \gamma) = (1.0 \pm 0.1) \cdot 10^{-6} \quad B(K_L \rightarrow \pi^0 \gamma) = (2.5 \pm 0.25) \cdot 10^{-6} \quad (\text{XXIV.39})$$

Next we take (m_t, m_c, V_{cb})

$$m_t = (170 \pm 5) \text{ GeV} \quad m_c = (1.30 \pm 0.05) \text{ GeV} \quad V_{cb} = 0.040 \pm 0.001 \quad (\text{XXIV.40})$$

where the quoted errors are quite reasonable if one keeps in mind that it will take at least ten years to achieve the accuracy assumed in (XXIV.39). Finally, we use

$$\frac{(4)}{M_S} = (200 \pm 350) \text{ MeV} \quad \mu_c = (1 \pm 3) \text{ GeV} \quad (\text{XXIV.41})$$

where μ_c is the renormalization scale present in the analysis of the charm contribution. Its variation gives an indication of the theoretical uncertainty involved in the calculation. In comparison to this error we neglect the effect of varying $\mu_W = O(M_W)$, the high energy matching scale at which the W boson is integrated out, as well as the very small scale dependence of the top quark contribution. As reference parameters we use the central values in (XXIV.39) and (XXIV.40) and $\frac{(4)}{M_S} = 300 \text{ MeV}$, $\mu_c = m_c$. The results that would be obtained in such a scenario for β , γ_{td} and γ are collected in table XLV.

TABLE XLV. β , γ_{td} and γ determined from $K^+ \rightarrow \pi^+ \gamma$ and $K_L \rightarrow \pi^0 \gamma$ for the scenario described in the text together with the uncertainties related to various parameters.

		(BR)	(m_t, V_{cb})	$(m_c, \frac{(4)}{M_S})$	(μ_c)	total
	0.33	0.02	0.03	0.00	0.00	0.05
$\gamma_{td} = 10^{-3}$	9.3	0.6	0.6	0.5	0.4	2.1
γ	0.00	0.08	0.09	0.06	0.04	0.27

There we have also displayed separately the associated, symmetrized errors (\pm) coming from the uncertainties in the branching ratios, m_t and V_{cb} , m_c and $\frac{(4)}{M_S}$, μ_c , as well as the total uncertainty.

We observe that respectable determinations of β and γ_{td} can be obtained. On the other hand the determination of γ is rather poor. We also note that a sizable part of the total uncertainty results in each case from the strong dependence of both branching ratios on m_t and V_{cb} . There is however one important quantity for which the strong dependence of $B(K^+ \rightarrow \pi^+ \gamma)$ and $B(K_L \rightarrow \pi^0 \gamma)$ on m_t and V_{cb} does not matter at all.

H. $\sin 2\beta$ from $K \rightarrow \pi \gamma$

Using (XXIV.38) one finds (Buchalla and Buras, 1994c)

$$r_s = r_s(B_1; B_2) \quad \frac{1}{r_s} = \cot \sin 2 = \frac{2r_s}{1 + r_s^2} \quad (\text{XXIV.42})$$

with

$$r_s(B_1; B_2) = \frac{P_0(X)}{P_{B_2}} \quad (\text{XXIV.43})$$

Thus within the approximation of (XXIV.38) $\sin 2$ is independent of V_{cb} (or A) and m_t . An exact treatment of the CKM matrix confirms this finding to a high accuracy. The dependence on V_{cb} and m_t enters only at order $O(\epsilon^2)$ and as a numerical analysis shows this dependence can be fully neglected.

It should be stressed that $\sin 2$ determined this way depends only on two measurable branching ratios and on the function $P_0(X)$ which is completely calculable in perturbation theory. Consequently this determination is free from any hadronic uncertainties and its accuracy can be estimated with a high degree of confidence. To this end we use the input given in (XXIV.39) – (XXIV.41) to find

$$\sin 2 = 0.60 \pm 0.06 \pm 0.03 \pm 0.02 \quad (\text{XXIV.44})$$

where the first error comes from $B(K^+ \rightarrow \pi^+)$ and $B(K_L \rightarrow \pi^0)$, the second from m_c and $\overline{M_S}$ and the last one from the uncertainty due to ϵ_c . We note that the largest partial uncertainty results from the branching ratios themselves. It can be probably reduced with time as is the case with the 0.03 uncertainty related to $\overline{M_S}$ and m_c . Note that the theoretical uncertainty represented by (ϵ_c) , which ultimately limits the accuracy of the analysis, is small. This reflects the clean nature of the $K \rightarrow \pi$ decays. However the small uncertainty of 0.02 is only achieved by including next-to-leading order QCD corrections. In the leading logarithmic approximation the corresponding error would amount to 0.05 , larger than the one coming from m_c and $\overline{M_S}$. The accuracy to which $\sin 2$ can be obtained from $K \rightarrow \pi$ is, in our example, comparable to the one expected in determining $\sin 2$ from CP asymmetries in B decays prior to LHC experiments. In this case $\sin 2$ is determined best by measuring the time integrated CP violating asymmetry in $B_d^0 \rightarrow K_S$ which is given by

$$\begin{aligned} A_{CP}(K_S) &= \frac{R_1^h(B \rightarrow K_S) - R_1^i(B \rightarrow K_S)}{R_1^h(B \rightarrow K_S) + R_1^i(B \rightarrow K_S)} \frac{dt}{dt} \\ &= \sin 2 \frac{x_d}{1 + x_d^2} \end{aligned} \quad (\text{XXIV.45})$$

where $x_d = m =$ gives the size of $B_d^0 - \bar{B}_d^0$ mixing. Combining (XXIV.42) and (XXIV.45) we obtain an interesting connection between rare K decays and B physics

$$\frac{2r_s(B_1; B_2)}{1 + r_s^2(B_1; B_2)} = A_{CP}(K_S) \frac{1 + x_d^2}{x_d} \quad (\text{XXIV.46})$$

which must be satisfied in the Standard Model. We stress that except for $P_0(X)$ given in table XLIV all quantities in (XXIV.46) can be directly measured in experiment and that this relationship is essentially independent of m_t and V_{cb} .

XXV. THE DECAYS $K_L \rightarrow \pi^+ \pi^-$ AND $K^+ \rightarrow \pi^+ \pi^- \pi^0$

A. General Remarks on $K_L \rightarrow \pi^+ \pi^-$

The rare decay $K_L \rightarrow \pi^+ \pi^-$ is CP conserving and in addition to its short-distance part receives important contributions from the two-photon intermediate state, which are difficult to calculate reliably (Geng and Ng, 1990), (Bélanger and Geng, 1991), (Ko, 1992).

This latter fact is rather unfortunate because the short-distance part is, similarly to $K^+ \rightarrow \pi^+ \pi^- \pi^0$, free of hadronic uncertainties and if extracted from the data would give a useful determination of the Wolfenstein parameter λ . The separation of the short-distance from the long-distance piece in the measured rate is very difficult however.

In spite of all this we will present here the analysis of the short-distance contribution because on one hand it may turn out to be useful one day for $K_L \rightarrow \pi^+ \pi^-$ and on the other hand it also plays an important role in a parity violating asymmetry, which can be measured in $K^+ \rightarrow \pi^+ \pi^- \pi^0$. We will discuss this latter topic later on in this section.

The analysis of $(K_L \rightarrow \pi^+ \pi^-)_{SD}$ proceeds in essentially the same manner as for $K^+ \rightarrow \pi^+ \pi^- \pi^0$. The only difference enters through the lepton line in the box contribution. This change introduces two new functions Y_{NL} and $Y(\chi_t)$ for the charm and top contributions respectively (section XI C), which will be discussed in detail below.

B. Master Formulae for $(K_L \rightarrow \pi^+ \pi^-)_{SD}$

Using the effective hamiltonian (XI.44) and relating $\langle \pi^+ \pi^- | H_{SD} | K_L \rangle$ to $B(K^+ \rightarrow \pi^+ \pi^-)$ we find

$$B(K_L \rightarrow \pi^+ \pi^-)_{SD} = \frac{1}{2} \left(\text{Re } c_{P_0}(Y) + \frac{\text{Re } e_t}{5} Y(\chi_t) \right) \quad (\text{XXV.1})$$

$$= \frac{2 B(K^+ \rightarrow \pi^+ \pi^- \pi^0)}{2 \sin^4 \theta_w} \frac{(K_L)}{(K^+)} = 1.68 \cdot 10^9 \quad (\text{XXV.2})$$

where we have used

$$\frac{1}{129} \sin^2 \theta_w = 0.23 \quad B(K^+ \rightarrow \pi^+ \pi^- \pi^0) = 0.635 \quad (\text{XXV.3})$$

The function $Y(\chi)$ of (XI.45) can also be written as

$$Y(\chi) = Y_0 \tilde{Y}(\chi) \quad Y_0 = 1.026 \cdot 0.006 \quad (\text{XXV.4})$$

where Y_0 summarizes the NLO corrections discussed in section XI C. With $m_t = m_t(m_t)$ this QCD factor depends only very weakly on m_t . The range in (XXV.4) corresponds to $150 \text{ GeV} < m_t < 190 \text{ GeV}$. The dependence on $\frac{Y_{NL}}{M_S}$ can be neglected. Next

$$P_0(Y) = \frac{Y_{NL}}{4} \quad (\text{XXV.5})$$

TABLE XLVI. The function $P_0(Y)$ for various $\frac{(4)}{M_S}$ and m_c .

	$P_0(Y)$		
$\frac{(4)}{M_S} / m_c$	1.25 GeV	1.30 GeV	1.35 GeV
215 MeV	0.132	0.141	0.151
325 MeV	0.140	0.149	0.159
435 MeV	0.145	0.156	0.166

with Y_{N_L} calculated in section XIC. Values for $P_0(Y)$ as a function of $\frac{(4)}{M_S}$ and m_c are collected in table XLVI.

Using the improved Wolfenstein parametrization and the approximate formulae (II.23) – (II.25) we can next write

$$B(K_L \rightarrow \pi^+ \pi^-)_{SD} = 1.68 \cdot 10^9 A^4 Y^2(x_t) \frac{1}{(1 - \frac{1}{2})^2} \quad (XXV.6)$$

with

$$\%_0 = 1 + \frac{P_0(Y)}{A^2 Y^2(x_t)} = \frac{1}{1 - \frac{1}{2}} \quad (XXV.7)$$

The "experimental" value of $B(K_L \rightarrow \pi^+ \pi^-)_{SD}$ determines the value of $\%$ given by

$$\% = \%_0 \cdot \kappa \quad \kappa^2 = \frac{1}{A^4 Y^2(x_t)} \frac{B(K_L \rightarrow \pi^+ \pi^-)_{SD}}{1.68 \cdot 10^9} \quad (XXV.8)$$

Similarly to r_0 in the case of $K^+ \rightarrow \pi^+ \pi^-$, the value of κ is fully determined by the top contribution which has only a very weak renormalization scale ambiguity after the inclusion of $O(\alpha_s)$ corrections. The main scale ambiguity resides in $\%_0$ whose departure from unity measures the relative importance of the charm contribution.

C. Numerical Analysis of $(K_L \rightarrow \pi^+ \pi^-)_{SD}$

1. Renormalization Scale Uncertainties

We will now investigate the uncertainties in $Y(x_t)$, Y_{N_L} , $B(K_L \rightarrow \pi^+ \pi^-)_{SD}$ and $\%$ related to the dependence of these quantities on the choice of the renormalization scales μ_t and μ_c . To this end we proceed as in section XXIV C 1. We fix all the remaining parameters as given in (XXIV.16) and (XXIV.17) and we vary μ_c and μ_t within the ranges stated in (XXIV.19).

Fig. 29 shows the charm function Y_{N_L} compared to the leading-log result Y_L and the case without QCD as a function of μ_c . We note the following points:

The residual slope of Y_{N_L} is considerably smaller than in Y_L although still sizable. The variation of Y with μ_c defined as $(Y(1 \text{ GeV}) - Y(3 \text{ GeV})) / Y(\mu_c)$ is 53% in NLLA compared to 92% in LLA.

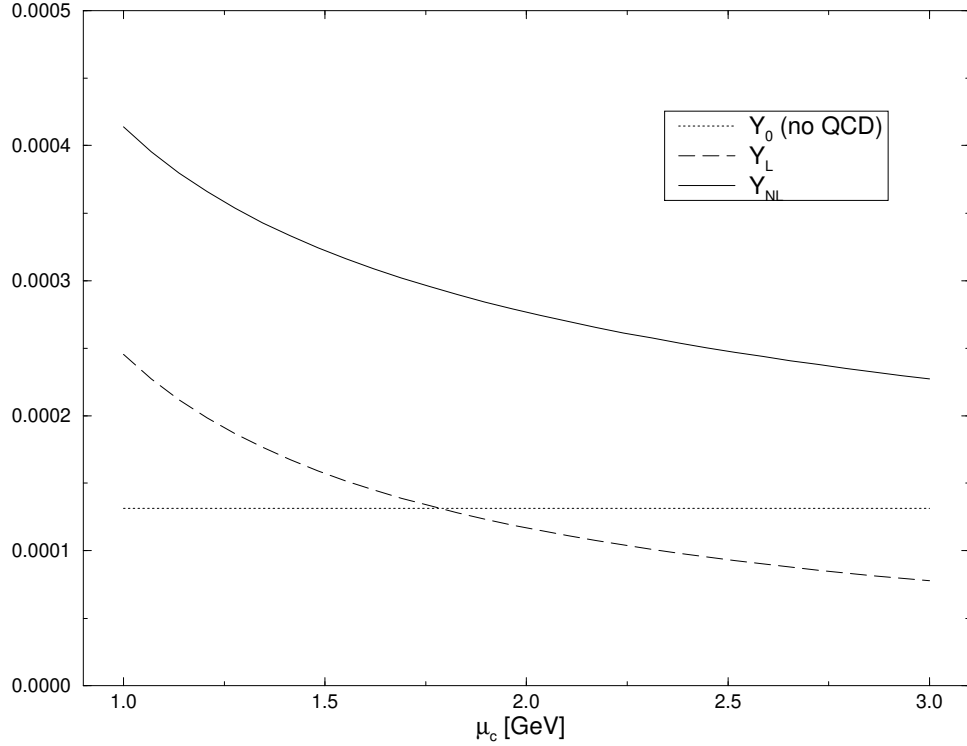


FIG. 29. Charm quark function Y_{NL} compared to the leading-log result Y_L and the case without QCD as functions of μ_c .

There is a strong enhancement of χ through QCD corrections in contrast to the suppression found in the case of X_0 .

In fig. 30 we show the analogous results for $Y(x_t)$ as a function of x_t . The observed features are similar to the ones found in the case of $X(x_t)$:

Considerable reduction of the scale uncertainties in NLLA relative to the LLA with a tiny residual uncertainty after the inclusion of NLO corrections.

Small NLO correction for the choice $x_t = m_t$ as summarized by Y in (XXV.4).

Using (XXV.1) and varying $\mu_{c\bar{t}}$ in the ranges (XXIV.19) we find that for our choice of input parameters the uncertainty in $B(K_L \rightarrow \pi^+ \pi^-)_{SD}$

$$0.316 \cdot 10^9 \cdot B(K_L \rightarrow \pi^+ \pi^-)_{SD} = 1.33 \cdot 10^8 \quad (XXV.9)$$

present in the leading order is reduced to

$$1.02 \cdot 10^9 \cdot B(K_L \rightarrow \pi^+ \pi^-)_{SD} = 1.25 \cdot 10^8 \quad (XXV.10)$$

after including NLO corrections. Here we have assumed $\% = 0$. Similarly we find

$$0.117 \cdot \% = 0.165 \quad \text{LLA} \quad (XXV.11)$$

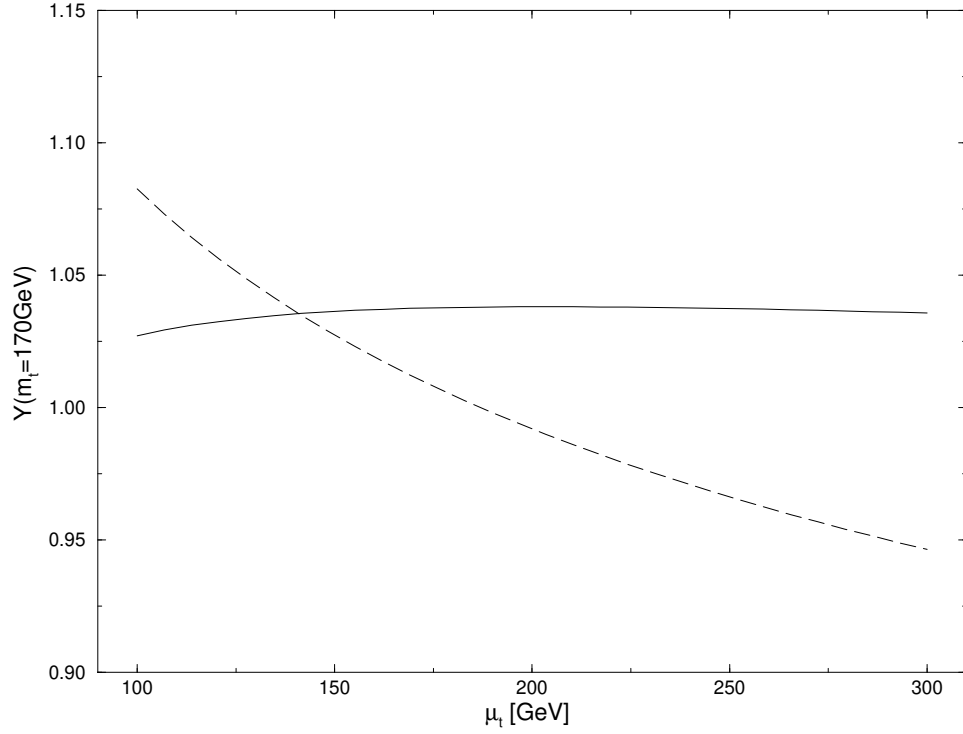


FIG. 30. Top quark function $Y(x_t)$ as a function of μ_t for fixed $m_t(m_t) = 170 \text{ GeV}$ with (solid curve) and without (dashed curve) $O(\alpha_s)$ corrections.

$$0.011 \pm 0.0134 \text{ NLLA} \quad (\text{XXV.12})$$

where we have set $B(K_L \rightarrow \pi^+ \pi^-)_{SD} = 1 \cdot 10^9$. We observe again a considerable reduction of the theoretical error when the NLO effects are included in the analyses. Also in this case the remaining ambiguity is largely dominated by the uncertainty in the charm sector.

2. Expectations for $B(K_L \rightarrow \pi^+ \pi^-)_{SD}$

We finally quote the standard model expectation for the short-distance contribution to the $K_L \rightarrow \pi^+ \pi^-$ branching ratio. Using the analysis of π_K and the constraint implied by $B_d \rightarrow B_d$ mixing in analogy to the case of $K^+ \rightarrow \pi^+ \pi^0$ described in section XXIV C 2, we find

$$0.6 \cdot 10^9 \leq B(K_L \rightarrow \pi^+ \pi^-)_{SD} \leq 2.0 \cdot 10^9 \quad (\text{XXV.13})$$

and

$$0.9 \cdot 10^9 \leq B(K_L \rightarrow \pi^+ \pi^-)_{SD} \leq 1.2 \cdot 10^9 \quad (\text{XXV.14})$$

for present parameter uncertainties and our "future" scenario, respectively. The relevant sets of input parameters and their errors are collected in appendix A. Removing the x_d constraint would increase the upper bounds in (XXV.13) and (XXV.14) to $3.5 \cdot 10^9$ and $2.2 \cdot 10^9$, respectively.

D. General Remarks on $K^+ \rightarrow \mu^+ \nu_\mu$

Obviously, the short distance effective hamiltonian in (XI.44) also gives rise to an amplitude for the transition $K^+ \rightarrow \mu^+ \nu_\mu$. This amplitude, however, is by three orders of magnitude smaller than the dominant contribution to $K^+ \rightarrow \mu^+ \nu_\mu$ given by the one-photon exchange diagram (Ecker *et al.*, 1987) and is therefore negligible in the total decay rate. On the other hand the coupling to the muon pair is purely vector-like for the one-photon amplitude, whereas it contains an axial vector part in the case of the SD contribution mediated by Z^0 -penguin and W-box diagrams. Thus, as was pointed out by (Savage and Wise, 1990) and discussed in detail in (Lu *et al.*, 1992), the *interference* of the one-photon and the SD contribution, which is odd under parity, generates a parity violating longitudinal muon polarization asymmetry

$$A_{LR} = \frac{R - L}{R + L} \quad (\text{XXV.15})$$

in the decay $K^+ \rightarrow \mu^+ \nu_\mu$. Here R (L) denotes the rate of producing a right- (left-) handed μ^+ , that is a μ^+ with spin along (opposite to) its three-momentum direction. In this way a measurement of the asymmetry A_{LR} could probe the phenomenologically interesting short distance physics, which is not visible in the total rate.

The $K^+ \rightarrow \mu^+ \nu_\mu$ vertex is described by a form factor $f(s)$ (s being the invariant mass squared of the muon pair), that determines the one-photon amplitude and hence the total rate of $K^+ \rightarrow \mu^+ \nu_\mu$, but also enters the asymmetry A_{LR} . This formfactor has been analyzed in detail in (Ecker *et al.*, 1987) within the framework of chiral perturbation theory. The imaginary part $\text{Im } f(s)$ turns out to be much smaller than $\text{Re } f(s)$ and can safely be neglected in the calculation of A_{LR} . For this reason $f(s) \approx \text{Re } f(s)$, which depends on a constant not fixed by chiral perturbation theory, may also be directly extracted from experimental data on $K^+ \rightarrow \mu^+ e^+ e^-$ (Alliegro *et al.*, 1992), sensitive to $f(s)$. We follow (Lu *et al.*, 1992) in adopting this procedure.

The dominance of $\text{Re } f(s)$ further implies that A_{LR} actually measures the real part of the short distance amplitude. As emphasized in (Bélanger *et al.*, 1993), A_{LR} is therefore closely related to the short distance part of $K_L \rightarrow \mu^+ \nu_\mu$ and could possibly yield useful information on this contribution, which is difficult to extract from experimental results on $K_L \rightarrow \mu^+ \nu_\mu$. Like $(K_L \rightarrow \mu^+ \nu_\mu)_{SD}$, A_{LR} is in particular a measure of the Wolfenstein parameter ρ .

The authors of (Lu *et al.*, 1992) have also considered potential long distance contributions to A_{LR} originating from two-photon exchange amplitudes. Unfortunately these are very difficult to calculate in a reliable manner. The discussion in (Lu *et al.*, 1992) indicates however, that they are likely to be much smaller than the short distance contributions considered above. We will focus here on the short distance part, keeping in mind the uncertainty due to possible non-negligible long distance corrections.

One should stress that the short distance part by itself, although calculable in a well defined perturbative framework, is not completely free from theoretical uncertainty. The natural context to discuss this issue is a next-to-leading order analysis, which for A_{LR} has been presented in (Buchalla and Buras, 1994b), generalizing the previous leading log calculations (Savage and Wise, 1990), (Lu *et al.*, 1992), (Bélanger *et al.*, 1993). We will summarize the results of (Buchalla and Buras, 1994b) below.

We finally mention that other asymmetries in $K^+ \rightarrow \mu^+ \nu_\mu$, which are odd under time reversal and are also sensitive to short distance contributions, have been discussed in the literature

(Savage and Wise, 1990), (Lu *et al.*, 1992), (Agrawal *et al.*, 1991), (Agrawal *et al.*, 1992). They involve both the $+$ and $-$ polarizations and are considerably more difficult to measure than A_{LR} . Possibilities for measuring the polarization of muons from $K^+ \rightarrow \pi^+ \mu^+ \nu_\mu$ in future experiments, based on studying the angular distribution of e^- from muon decay, are described in (Kuno, 1992).

E. Master Formulae for A_{LR}

The absolute value of the asymmetry A_{LR} can be written as

$$|A_{LR}| = r |Re_t| \quad (XXV.16)$$

The factor r arises from phase space integrations. It depends only on the particle masses m_K , m_π and m_μ , on the form factors of the matrix element $\langle \pi^+ | j_\mu | K^+ \rangle$, as well as on the form factor of the $K^+ \rightarrow \pi^+ \mu^+ \nu_\mu$ transition, relevant for the one-photon amplitude. In addition r depends on a possible cut which may be imposed on $\cos \theta$, the angle between the three-momenta of the μ^+ and the pion in the rest frame of the $\mu^+ \nu_\mu$ pair. Without any cuts one has $r = 2/3$ (Lu *et al.*, 1992). If $\cos \theta$ is restricted to lie in the region $0.5 \leq \cos \theta \leq 1.0$, this factor is increased to $r = 4/3$. As discussed in (Lu *et al.*, 1992), such a cut in $\cos \theta$ could be useful since it enhances A_{LR} by 80% with only a 22% decrease in the total number of events.

Re_t is a function containing the information on the short distance physics. It depends on CKM parameters, the QCD scale $\overline{m_s}$, the quark masses m_t and m_c and is given by

$$Re_t = \frac{Re_c}{P_0(Y)} + \frac{Re_t}{5} Y(x_t) \quad (XXV.17)$$

$$= \frac{4}{2 \sin^2 \theta_W (1 - \frac{2}{3})} = 1.66 \cdot 10^3 \quad (XXV.18)$$

Here $\langle j_{us} \rangle = 0.22$, $\sin^2 \theta_W = 0.23$, $x_t = m_t^2 / \overline{m_s}^2$, $V_{is} = V_{is} V_{id}$ and

$$P_0(Y) = \frac{Y_{NL}}{4} \quad (XXV.19)$$

The functions Y_{NL} and $Y(x_t)$ represent the charm and the top contribution, respectively. They are to next-to-leading logarithmic accuracy given in (XI.48) and (XI.45) and have already been discussed in chapter XI C and in the previous sections on the phenomenology of $(K_L \rightarrow \pi^+ \mu^+ \nu_\mu)_{SD}$. Numerical values for $P_0(Y)$ can be found in table XLVI. From (XXV.16) and (XXV.17) we can obtain Re_t expressed as a function of $|A_{LR}|$

$$Re_t = \frac{5 |A_{LR}| r}{Y(x_t)} \left(1 - \frac{2}{3} P_0(Y) \right) \quad (XXV.20)$$

Since Re_t is related to the Wolfenstein parameter ρ (see section II), one may use (XXV.20) to extract ρ from a given value of $|A_{LR}|$

F. Numerical Analysis of α_{LR}

To illustrate the phenomenological implications of the next-to-leading order calculation, let us consider the following scenario. We assume a typical value for α_{LR} , allowing for an uncertainty of 10%

$$\alpha_{LR} = (6.0 \pm 0.6) \cdot 10^{-3} \quad (XXV.21)$$

Here a cut on $\cos \theta_{\ell\ell} \geq 0.5$ is understood. Next we take $(m_t, m_i, m_{\bar{i}})$

$$m_t = (170 \pm 5) \text{ GeV} \quad m_c = (1.30 \pm 0.05) \text{ GeV} \quad V_{cb} = 0.040 \pm 0.001 \quad (XXV.22)$$

$$\frac{(4)}{M_S} = (300 \pm 50) \text{ MeV} \quad (XXV.23)$$

Table XLVII shows the central value of α that is extracted from α_{LR} in our example together with the uncertainties associated to the relevant input. Combined errors due to a simultaneous variation of several parameters can be obtained to a good approximation by simply adding the errors in table XLVII.

TABLE XLVII. α determined from α_{LR} for the scenario described in the text together with the uncertainties related to various input parameters.

	(α_{LR})	(m_t)	(V_{cb})	(m_c)	$(\frac{(4)}{M_S})$
α	0.06	0.13	0.05	0.01	0.00

These errors should be compared with the purely theoretical uncertainty of the short distance calculation, estimated by a variation of the renormalization scales μ_c and μ_t . Varying these scales as given in (XXIV.19) and keeping all other parameters at their central values we find

$$0.15 \pm 0.03 \text{ (NLLA)} \quad (XXV.24)$$

$$0.31 \pm 0.02 \text{ (LLA)} \quad (XXV.25)$$

We observe that at NLO the scale ambiguity is reduced by almost a factor of 3 compared to the leading log approximation. However, even in the NLLA the remaining uncertainty is still sizable, though moderate in comparison with the errors in table XLVII. Note that the remaining error in (XXV.24) is almost completely due to the charm sector, since the scale uncertainty in the top contribution is practically eliminated at NLO.

We remark that for definiteness we have incorporated the numerically important piece $x_c=2$ in the leading log expression for the charm function Y , although this is strictly speaking a next-to-leading order term. This procedure corresponds to a central value of $\alpha = 0.12$ in LLA. Omitting the $x_c=2$ term and employing the strict leading log result shifts this value to $\alpha = 0.20$. Within NLLA this ambiguity is avoided in a natural way.

Finally we give the Standard Model expectation for α_{LR} , based on the short distance contribution

in (XXV.16), for the Wolfenstein parameter λ in the range $0.25 \geq \lambda \geq 0.25$, $V = 0.040 \pm 0.004$ and $m_t = (170 \pm 20) \text{ GeV}$. Including the uncertainties due to m_c , $\overline{M_S}$, α_s and μ_t and imposing the cut $0.5 \leq \cos \theta \leq 1$, we find

$$3.0 \times 10^3 \leq \Gamma_{LR} \leq 9.6 \times 10^3 \quad (\text{XXV.26})$$

employing next-to-leading order formulae. Anticipating improvements in V_{cb} , m_t and λ we also consider a future scenario in which $\lambda = 0.00 \pm 0.02$, $V_{cb} = 0.040 \pm 0.001$ and $m_t = (170 \pm 5) \text{ GeV}$. The very precise determination of λ used here should be achieved through measuring CP asymmetries in B decays in the LHC era (Buras, 1994). Then (XXV.26) reduces to

$$4.8 \times 10^3 \leq \Gamma_{LR} \leq 6.6 \times 10^3 \quad (\text{XXV.27})$$

One should mention that although the top contribution dominates the short distance prediction for Γ_{LR} the charm part is still important and should not be neglected, as done in (Bélanger *et al.*, 1993). It is easy to convince oneself that the charm sector contributes to λ the sizable amount $\lambda_{\text{charm}} \approx 0.2$. Furthermore, as we have shown above, the charm part is the dominant source of theoretical uncertainty in the short distance calculation of Γ_{LR} .

To summarize, we have seen that the scale ambiguity in the perturbative short distance contribution to Γ_{LR} can be considerably reduced by incorporating next-to-leading order QCD corrections. The corresponding theoretical error in the determination of λ from an anticipated measurement of Γ_{LR} is then decreased by a factor of 3, in a typical example. Unfortunately the remaining scale uncertainty is quite visible even at NLO. In addition there are further uncertainties due to various input parameters and due to possible long distance effects. Together this implies that the accuracy to which λ can be extracted from Γ_{LR} appears to be limited and Γ_{LR} can not fully compete with the "gold-plated" $K \rightarrow \pi \ell \ell$ decay modes. Still, a measurement of Γ_{LR} might give interesting constraints on SM parameters, λ in particular, and we feel it is worthwhile to further pursue this interesting additional possibility.

XXVI. THE DECAYS $B \rightarrow X$ AND $B \rightarrow \pi^+$

A. General Remarks

The rare decays $B \rightarrow X_s$, $B \rightarrow X_d$ and $B_s \rightarrow \pi^+$, $B_d \rightarrow \pi^+$ are fully dominated by internal top quark contributions. The relevant effective hamiltonians are given in (XI.56) and (XI.57) respectively. Only the top functions $X(x_t)$ and $Y(x_t)$ enter these expressions and the uncertainties due to m_c and $\frac{1}{M_S}$ affecting $K^+ \rightarrow \pi^+$ and $K_L \rightarrow \pi^+$ are absent here. Consequently these two decays are theoretically very clean. In particular the residual renormalization scale dependence of the relevant branching ratios, though sizable in leading order, can essentially be neglected after the inclusion of next-to-leading order corrections. On the other hand a measurement of these rare B decays, in particular of $B \rightarrow X_s$ and $B \rightarrow X_d$, is experimentally very challenging. In addition, as we will see below, $B(B_s \rightarrow \pi^+)$ and $B(B_d \rightarrow \pi^+)$ is subject to the uncertainties in the values of the B meson decay constants F_{B_s} and F_{B_d} , which hopefully will be removed one day.

B. The Decays $B \rightarrow X_s$ and $B \rightarrow X_d$

The branching fraction for $B \rightarrow X_s$ is given by

$$\frac{\mathcal{B}(B \rightarrow X_s)}{\mathcal{B}(B \rightarrow X_{ce})} = \frac{3^2}{4^2 \sin^4 \theta_w} \frac{V_{ts}^2 X^2(x_t)}{V_{cb}^2 f(z)} \quad (XXVI.1)$$

Here $f(z)$, $z = m_c/m_b$ is the phase-space factor for $B \rightarrow X_{ce}$ defined already in (XXII.6) and $\frac{3^2}{4^2 \sin^4 \theta_w}$ is the corresponding QCD correction (Cabibbo and Maiani, 1978) given in (XXIII.7). The factor V_{ts}^2 represents the QCD correction to the matrix element of the $b \rightarrow s$ transition due to virtual and bremsstrahlung contributions and is given by the well known expression

$$V_{ts}^2 = 1 + \frac{2}{3} \frac{m_s(m_b)}{m_b^2} \approx 0.83 \quad (XXVI.2)$$

For the numerical analysis we will use $\alpha_{QCD}^{(5)} = 225 \text{ MeV}$, (XXIV.3), $V_{ts} = V_{cb} m_t(m_t) = 170 \text{ GeV}$, $\mathcal{B}(B \rightarrow X_{ce}) = 0.104$, $f(z) = 0.49$ and $\frac{3^2}{4^2 \sin^4 \theta_w} = 0.88$, keeping in mind the QCD uncertainties in $B \rightarrow X_{ce}$ discussed in section XVII.

Varying m_t as in (XXIV.19) we find that the ambiguity

$$3.82 \cdot 10^5 \mathcal{B}(B \rightarrow X_s) \approx 4.65 \cdot 10^5 \quad (XXVI.3)$$

present in the leading order is reduced to

$$3.99 \cdot 10^5 \mathcal{B}(B \rightarrow X_s) \approx 4.09 \cdot 10^5 \quad (XXVI.4)$$

after the inclusion of QCD corrections (Buchalla and Buras, 1993a).

It should be noted that $\mathcal{B}(B \rightarrow X_s)$ as given in (XXVI.1) is in view of $V_{ts} = V_{cb} \frac{m_t}{m_b} \approx 0.95$ 0.03 essentially independent of the CKM parameters and the main uncertainty resides in the value of m_t . Setting all parameters as given above and in appendix A, and using (XXIV.30) we have

$$B(B \rightarrow X_s) = 4.1 \cdot 10^{-5} \frac{|V_{ts}|^2}{|V_{cb}|^2} \left(\frac{m_t}{170 \text{ GeV}} \right)^{2.30} : \quad (\text{XXVI.5})$$

In view of a new interest in this decay (Grossman *et al.*, 1995) we quote the Standard Model expectation for $B(B \rightarrow X_s)$ based on the input parameters collected in the appendix A. We find

$$3.1 \cdot 10^{-5} \leq B(B \rightarrow X_s) \leq 4.9 \cdot 10^{-5} \quad (\text{XXVI.6})$$

for the “present day” uncertainties in the input parameters and

$$3.6 \cdot 10^{-5} \leq B(B \rightarrow X_s) \leq 4.2 \cdot 10^{-5} \quad (\text{XXVI.7})$$

for our “future” scenario.

In the case of $B \rightarrow X_d$ one has to replace V_{ts} by V_{td} which results in a decrease of the branching ratio by roughly an order of magnitude.

C. The Decays $B_s \rightarrow \ell^+ \ell^-$ and $B_d \rightarrow \ell^+ \ell^-$

The branching ratio for $B_s \rightarrow \ell^+ \ell^-$ is given by (Buchalla and Buras, 1993a)

$$B(B_s \rightarrow \ell^+ \ell^-) = (B_s) \frac{G_F^2}{4 \sin^2 \theta_w} F_{B_s}^2 m_\ell^2 m_{B_s}^2 \frac{|V_{ts}|^2}{1 - \frac{m_\ell^2}{m_{B_s}^2} |V_{tb} V_{ts}|^2 Y^2(x_t)} \quad (\text{XXVI.8})$$

where B_s denotes the flavor eigenstate ($\bar{b}s$) and F_{B_s} is the corresponding decay constant (normalized as $F = 131 \text{ MeV}$). Using (XXIV.3), (XXV.4) and (XIV.6) we find in the case of $B_s \rightarrow \ell^+ \ell^-$

$$B(B_s \rightarrow \ell^+ \ell^-) = 4.18 \cdot 10^{-9} \frac{(B_s)^2}{1.6 \text{ ps}} \frac{F_{B_s}^2}{230 \text{ MeV}} \frac{|V_{ts}|^2}{0.040} \left(\frac{m_t}{170 \text{ GeV}} \right)^{3.12} \quad (\text{XXVI.9})$$

which approximates the next-to-leading order result.

Taking the central values for (B_s) , F_{B_s} , $|V_{ts}|$ and m_t and varying m_t as in (XXIV.19) we find that the uncertainty

$$3.44 \cdot 10^{-9} \leq B(B_s \rightarrow \ell^+ \ell^-) \leq 4.50 \cdot 10^{-9} \quad (\text{XXVI.10})$$

present in the leading order is reduced to

$$4.05 \cdot 10^{-9} \leq B(B_s \rightarrow \ell^+ \ell^-) \leq 4.14 \cdot 10^{-9} \quad (\text{XXVI.11})$$

when the QCD corrections are included. This feature is once more illustrated in fig. 31.

Finally, we quote the standard model expectation for $B(B_s \rightarrow \ell^+ \ell^-)$ based on the input parameters collected in the Appendix. We find

$$1.7 \cdot 10^{-9} \leq B(B_s \rightarrow \ell^+ \ell^-) \leq 8.4 \cdot 10^{-9} \quad (\text{XXVI.12})$$

using present day uncertainties in the parameters and $F_{B_s} = 230 \pm 40 \text{ MeV}$. With reduced errors for the input quantities, corresponding to our second scenario as defined in Appendix A, and taking $F_{B_s} = 230 \pm 10 \text{ MeV}$ this range would shrink to

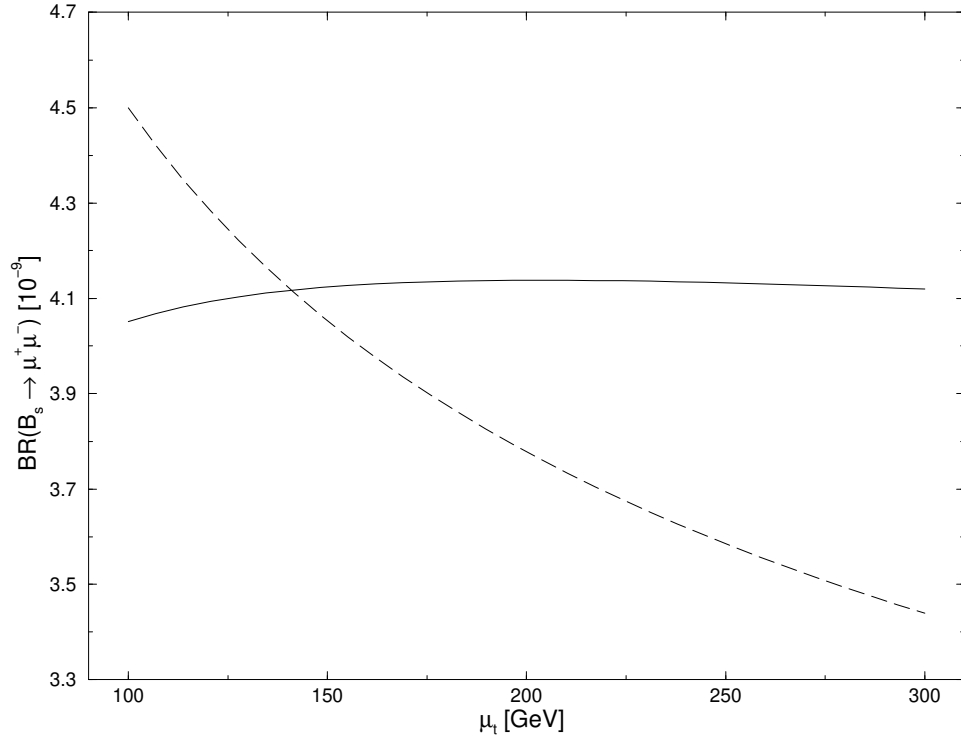


FIG. 31. The μ_t -dependence of $B(B_s \rightarrow \mu^+ \mu^-) [10^{-9}]$ with (solid curve) and without (dashed curve) $O(\mu_s)$ corrections for fixed parameter values as described in the text.

$$3.1 \cdot 10^9 \leq B(B_s \rightarrow \mu^+ \mu^-) \leq 5.0 \cdot 10^8 \quad (\text{XXVI.13})$$

For the case of $B_d \rightarrow \mu^+ \mu^-$ similar formulae hold with obvious replacements of labels ($s \rightarrow d$). Provided the decay constants F_{B_s} and F_{B_d} will have been calculated reliably by non-perturbative methods or measured in leading leptonic decays one day, the rare processes $B_s \rightarrow \mu^+ \mu^-$ and $B_d \rightarrow \mu^+ \mu^-$ should offer clean determinations of $|V_{ts}|$ and $|V_{td}|$. The accuracy of the related analysis will profit considerably from the reduction of theoretical ambiguity achieved through the inclusion of short-distance QCD effects. In particular $B(B_s \rightarrow \mu^+ \mu^-)$, which is expected to be $O(4 \cdot 10^9)$, should be attainable at hadronic machines such as HERA-B, Tevatron and LHC.

XXVII. SUMMARY

In this review we have described in detail the present status of higher order QCD corrections to weak decays of hadrons. We have emphasized that during the last years considerable progress has been made in this field through the calculation of the next-to-leading QCD corrections to essentially all of the most interesting and important processes. This effort reduced considerably the theoretical uncertainties in the relevant formulae and thereby improves the determination of the CKM parameters to be achieved in future experiments. We have illustrated this with several examples.

In this review we have concentrated on weak decays in the Standard Model. The structure of weak decays in extensions of the Standard Model will generally be modified. Although we do not expect substantial effects due to "new physics" in tree level decays, the picture of loop induced processes, such as rare and CP violating decays, may turn out to be different from the one presented here. The basic structure of QCD calculations will remain valid, however. In certain extensions of the Standard Model, in which no new local operators occur, only the initial conditions to the renormalization group evolution will have to be modified. In more complicated extensions additional operators can be present and in addition to the change of the initial conditions, also the evolution matrix will have to be generalized.

Yet in order to be able to decide whether modifications of the standard theory are required by the data, it is essential that the theoretical calculations within the Standard Model itself reach the necessary precision. As far as the *short distance* contributions are concerned, we think that in most cases such a precision has been already achieved.

Important exceptions are the $b \rightarrow s$ and $b \rightarrow sg$ transitions for which the complete NLO corrections are not yet available. On the other hand the status of *long distance* contributions represented by the hadronic matrix elements of local operators or equivalently by various B_i parameters, is much less satisfactory. This is in particular the case of non-leptonic decays, where the progress is very slow. Yet without these difficult non-perturbative calculations it is impossible to give reliable theoretical predictions for non-leptonic decays even if the Wilson coefficients of the relevant operators have been calculated with high precision. Moreover these coefficients have unphysical renormalization scale and renormalization scheme dependences which can only be canceled by the corresponding dependences in the hadronic matrix elements. All efforts should be made to improve the status of non-perturbative calculations.

The next ten years should be very exciting for the field of weak decays. The experimental efforts in several laboratories will provide many new results for the rare and CP violating decays which will offer new tests of the Standard Model and possibly signal some "new physics". As we have stressed in this review the NLO calculations presented here will play undoubtedly an important role in these investigations. Let us just imagine that $B_s^0 \rightarrow B_s^0$ mixing and the branching ratios for $K^+ \rightarrow \pi^+ \pi^0$, $K_L \rightarrow \pi^0 \pi^0$, $B \rightarrow X_s \gamma$ and $B_s \rightarrow \mu^+ \mu^-$ have been measured to an acceptable accuracy. Having in addition at our disposal accurate values of $V_{ub} = V_{cb} \tan \theta_c$, F_B , B_B and B_K as well as respectable results for the angles $(\alpha; \beta; \gamma)$ from the CP asymmetries in B-decays, we could really get a great insight into the physics of quark mixing and CP violation. One should hope that this progress on the experimental side will be paralleled by the progress in the calculations of hadronic matrix elements as well as by the calculations of QCD corrections in potential extensions of the Standard Model.

We would like to end our review with a summary of theoretical predictions and present exper-

imental results for the rare and CP violating decays discussed by us. This summary is given in table XLVIII.

TABLE XLVIII. Summary of theoretical predictions and experimental results for the rare and CP violating processes discussed in this review. The entry “input” indicates that the corresponding measurement is used to determine or to constrain CKM parameters needed for the calculation of other decays. For $B(K_L \rightarrow \pi^+ \pi^-)$ the theoretical value refers only to the short-distance contribution. In the case of $B(K_L \rightarrow \pi^0 e^+ e^-)$ the SM prediction corresponds to the contribution from direct CP violation. The SM predictions for $K^+ \rightarrow \pi^+ \pi^-$ and $K_L \rightarrow \pi^0 \pi^0$ include the isospin breaking corrections considered in (Marciano and Parsa, 1995).

Quantity	SM Prediction	Experiment	Exp. Reference
K-Decays			
$\mathcal{B}(K \rightarrow \pi \pi)$	input	$(2.266 \pm 0.023) \cdot 10^3$	(Particle Data Group, 1994)
$\mathcal{B}(K_S \rightarrow \pi^0 \pi^0)$	$(5.6 \pm 7.7) \cdot 10^4$	$(15 \pm 8) \cdot 10^4$	(Particle Data Group, 1994)
$\mathcal{B}(K_L \rightarrow \pi^0 e^+ e^-)$	$(4.5 \pm 2.8) \cdot 10^{12}$ [CP _{dir}]	$< 4.3 \cdot 10^9$	(Harris <i>et al.</i> , 1993))
$\mathcal{B}(K^+ \rightarrow \pi^+ \pi^-)$	$(1.0 \pm 0.4) \cdot 10^{10}$	$< 2.4 \cdot 10^9$	(Adler <i>et al.</i> , 1995)
$\mathcal{B}(K_L \rightarrow \pi^0 \pi^0)$	$(2.9 \pm 1.9) \cdot 10^{11}$	$< 5.8 \cdot 10^5$	(Weaver <i>et al.</i> , 1994)
$\mathcal{B}(K_L \rightarrow \pi^+ \pi^-)$	$(1.3 \pm 0.7) \cdot 10^9$ [SD]	$(7.4 \pm 0.4) \cdot 10^9$	(Particle Data Group, 1994)
$\mathcal{B}(K_{LR} \rightarrow \pi^+ \pi^- \pi^+ \pi^-)$	$(6 \pm 3) \cdot 10^3$	—	—
B-Decays			
x_d	input	0.75 ± 0.06	(Browder and Honscheid, 1995)
$\mathcal{B}(B \rightarrow X_s \gamma)$	$(2.8 \pm 0.8) \cdot 10^4$	$(2.32 \pm 0.67) \cdot 10^4$	(Alam <i>et al.</i> , 1995)
$\mathcal{B}(B \rightarrow X_s \gamma)$	$(4.0 \pm 0.9) \cdot 10^5$	$< 3.9 \cdot 10^4$	(Grossman <i>et al.</i> , 1995)
$\mathcal{B}(B_s \rightarrow \pi^+ \pi^-)$	$(1.1 \pm 0.7) \cdot 10^6$	—	—
$\mathcal{B}(B_s \rightarrow \pi^+ \pi^-)$	$(5.1 \pm 3.3) \cdot 10^9$	$< 8.4 \cdot 10^6$	(Kroll <i>et al.</i> , 1995)
$\mathcal{B}(B_s \rightarrow e^+ e^-)$	$(1.2 \pm 0.8) \cdot 10^{13}$	—	—
$\mathcal{B}(B_d \rightarrow \pi^+ \pi^-)$	10^{10}	$< 1.6 \cdot 10^6$	(Kroll <i>et al.</i> , 1995)
$\mathcal{B}(B_d \rightarrow e^+ e^-)$	10^{14}	$< 5.9 \cdot 10^6$	(Ammar <i>et al.</i> , 1994)

Let us hope that the next ten years will bring a further reduction of uncertainties in the theoretical predictions and will provide us with accurate measurements of various branching ratios for which, as seen in table XLVIII, only upper bounds are available at present.

ACKNOWLEDGMENTS

We would like to thank M. Jamin for extensive discussions and numerical checks in sections VII and XIX, M. Münz for providing the updated figures in sections XXII and XXIII, and S. Herrlich and U. Nierste for valuable comments on section XII.

Thanks are also due to B. Bardeen, M. Beneke, G. Burdman, I. Dunietz, A. El-Khadra, B. Gough, C. Greub, C. Hill, B. Kayser, W. Kilian, A. Kronfeld, A. Lenz, L. Littenberg, M. Misiak, T. Onogi, S. Parke, J. Simone and B. Winstein for useful discussions. M.E.L. acknowledges support by the Deutsche Forschungsgemeinschaft (DFG) and the hospitality of the SLAC theory group during parts of this work.

This work has been supported by the German Bundesministerium für Bildung und Forschung under contract 06 TM 743, the CEC Science project SC1-CT91-0729 and DFG contracts La 924/1-1 and ESMEX Li 519/2-1.

Fermilab is operated by Universities Research Association, Inc., under contract DE-AC02-76CHO3000 with the United States Department of Energy.

APPENDIX A: COMPILATION OF NUMERICAL INPUT PARAMETERS

Below we give for the convenience of the reader a compilation of input parameters that were used in the numerical parts of this review.

Running quark masses:

$$\begin{aligned}\overline{m}_d(m_c) &= 8 \text{ M eV} & \overline{m}_s(m_c) &= (170 \text{ } 20) \text{ M eV} \\ \overline{m}_c(m_c) &= 1.3 \text{ G eV} \\ \overline{m}_b(m_b) &= 4.4 \text{ G eV} & m_b^{(\text{pole})} &= 4.8 \text{ G eV}\end{aligned}$$

Scalar meson masses and decay constants:

$$\begin{aligned}m &= 135 \text{ M eV} & F &= 131 \text{ M eV} \\ m_K &= 498 \text{ M eV} & F_K &= 160 \text{ M eV} \\ m_{B_d} &= 5.28 \text{ G eV} & (B_d) &= 1.6 \text{ } 10^{12} \text{ s} \\ m_{B_s} &= 5.38 \text{ G eV} & (B_s) &= 1.6 \text{ } 10^{12} \text{ s}\end{aligned}$$

QCD and electroweak parameters:

$$\begin{aligned}\alpha_s(M_Z) &= 0.117 \text{ } 0.007 & \frac{(5)}{M_S} &= (225 \text{ } 85) \text{ M eV} \\ &= 1.129 & M_W &= 80.2 \text{ G eV} \\ \sin \theta_W &= 0.23\end{aligned}$$

CKM elements:

$$|V_{us}| = 0.22 \quad |V_{ud}| = 0.975$$

K⁰ -decays, K⁰ K⁰ and B⁰ B⁰ mixing:

$$\begin{aligned}(K_L) &= 5.17 \text{ } 10^8 \text{ s} & (K^+) &= 1.237 \text{ } 10^8 \text{ s} \\ \text{BR}(K^+ \rightarrow e^+ \nu_e) &= 0.0482 \\ |V_{K^+}| &= (2.266 \text{ } 0.023) \text{ } 10^0 & M_K &= 3.51 \text{ } 10^{15} \text{ G eV} \\ \text{Re} A_0 &= 3.33 \text{ } 10^7 \text{ G eV} & \text{Re} A_2 &= 1.50 \text{ } 10^8 \text{ G eV} \\ \text{Im} A_0 &= 0.25 \\ \text{Im} A_1 &= 1.38 & \text{Im} A_2 &= 0.57 \\ \text{Im} A_3 &= 0.47 & \text{Im} A_B &= 0.55\end{aligned}$$

The values for $\text{Re} A_{0,2}$ have been obtained from PDG using isospin analysis.

Hadronic matrix element parameters for K⁰ → π⁰ :

$$\begin{aligned}B_{2\pi^0}^{(1=2)}(m_c) &= 5.7 \text{ } 1.1 & B_{2\pi^0\pi^0}^{(1=2)}(m_c) &= 6.6 \text{ } 1.0 & \text{for } \frac{(4)}{M_S} &= 325 \text{ M eV} \\ B_{2\pi^0\pi^0}^{(1=2)}(m_c) &= 6.2 \text{ } 1.0\end{aligned}$$

$$B_3^{(1=2)} = B_5^{(1=2)} = B_6^{(1=2)} = B_7^{(1=2)} = B_8^{(1=2)} = B_7^{(3=2)} = B_8^{(3=2)} = 1 \quad (\text{central values})$$

In numerical investigations we have for illustrative purposes sometimes used actual present as well as estimated future errors for various input parameters. In the table below this is indicated by labels “present” and “future”.

Quantity	Central	Present	Future
\mathcal{V}_{cb}	0.040	0.003	0.001
$\mathcal{V}_{ub} = \mathcal{V}_{cb}$	0.08	0.02	0.01
B_K	0.75	0.15	0.05
$P_{\overline{B_d} F_{B_d}}$	200 M eV	40 M eV	10 M eV
x_d	0.75	0.06	0.03
m_t	170 G eV	15 G eV	5 G eV

REFERENCES

- Abachi, S. *et al.*, 1995, Phys. Rev. Lett. **74**, 2632.
- Abada, A. *et al.*, 1992, Nucl. Phys. **B376**, 172.
- Abe, F. *et al.*, 1994a, Phys. Rev. **D50**, 2966.
- Abe, F. *et al.*, 1994b, Phys. Rev. Lett **73**, 225.
- Abe, F. *et al.*, 1994c, Phys. Rev. **D51**, 4623.
- Adel, K. and Y. P. Yao, 1993, Mod. Phys. Lett. **A8**, 1679.
- Adel, K. and Y. P. Yao, 1994, Phys. Rev. **D49**, 4945.
- Adler, S. *et al.*, 1995, BNL preprint, **BNL-62327; hep-ex/9510006**.
- Agrawal, P., J. Ng, G. Bélanger, and C. Geng, 1991, Phys. Rev. Lett. **67**, 537.
- Agrawal, P., J. Ng, G. Bélanger, and C. Geng, 1992, Phys. Rev. **D45**, 2383.
- Alam, M. S. *et al.*, 1995, Phys. Rev. Lett. **74**, 2885.
- Ali, A. and C. Greub, 1991a, Z. Phys. **C49**, 431.
- Ali, A. and C. Greub, 1991b, Phys. Lett. **B259**, 182.
- Ali, A. and C. Greub, 1993, Z. Phys. **C60**, 433.
- Ali, A. and C. Greub, 1995, Phys. Lett. **B361**, 146.
- Ali, A. and D. London, 1995, DESY preprint **DESY-95-148; hep-ph/9508272**.
- Ali, A., T. Mannel, and T. Morozumi, 1991, Phys. Lett. **B273**, 505.
- Ali, A., G. F. Giudice, and T. Mannel, 1995, Z. Phys. **C67**, 417.
- Alliegro, C. *et al.*, 1992, Phys. Rev. Lett. **68**, 278.
- Allton, C. R., M. Ciuchini, M. Crisafulli, V. Lubicz, and G. Martinelli, 1994, Nucl. Phys. **B431**, 667.
- Altarelli, G. and L. Maiani, 1974, Phys. Lett. **B52**, 351.
- Altarelli, G. and S. Petrarca, 1991, Phys. Lett. **B261**, 303.
- Altarelli, G., G. Curci, G. Martinelli, and S. Petrarca, 1981, Nucl. Phys. **B187**, 461.
- Ammar, R. *et al.*, 1993, Phys. Rev. Lett. **71**, 674.
- Ammar, R. *et al.*, 1994, Phys. Rev. **D49**, 5701.
- Antonelli, V., S. Bertolini, M. Fabrichesi, and E. I. Lashin, 1995, SISSA preprint, **SISSA 102/95/EP**.
- Ashmore, J. F., 1972, Lett. Nuovo Cim. **4**, 289.
- Bagan, E., P. Ball, V. Braun, and H. G. Dosch, 1992, Phys. Lett. **B278**, 457.
- Bagan, E., P. Ball, V. Braun, and P. Gosdzinsky, 1994, Nucl. Phys. **B432**, 3.
- Bagan, E., P. Ball, V. Braun, and P. Gosdzinsky, 1995a, Phys. Lett. **B342**, 362.
- Bagan, E., P. Ball, B. Fiol, and P. Gosdzinsky, 1995b, Phys. Lett. **B351**, 546.
- Ball, P. and U. Nierste, 1994, Phys. Rev. **D50**, 5841.
- Ball, P., M. Beneke, and V. M. Braun, 1995a, Phys. Rev. **D52**, 3929.
- Ball, P., M. Beneke, and V. M. Braun, 1995b, Nucl. Phys. **D452**, 563.
- Barbieri, R. and G. F. Giudice, 1993, Phys. Lett. **B309**, 86.
- Bardeen, W. A., A. J. Buras, D. W. Duke, and T. Muta, 1978, Phys. Rev. **D18**, 3998.
- Bardeen, W. A., A. J. Buras, and J.-M. Gérard, 1987a, Phys. Lett. **B192**, 138.
- Bardeen, W. A., A. J. Buras, and J.-M. Gérard, 1987b, Nucl. Phys. **B293**, 787.
- Bardeen, W. A., A. J. Buras, and J.-M. Gérard, 1988, Phys. Lett. **B211**, 343.
- Barger, V., M. S. Berger, and R. J. N. Phillips, 1993, Phys. Rev. Lett. **70**, 1368.
- Barr, G. D. *et al.*, 1992, Phys. Lett. **B284**, 440.
- Barr, G. D. *et al.*, 1993, Phys. Lett. **B317**, 233.

- Baxter, R. M. *et al.*, 1994, Phys. Rev. **D49**, 1594.
- Bélanger, G. and C. Q. Geng, 1991, Phys. Rev. **D43**, 140.
- Bélanger, G., C. Geng, and P. Turcotte, 1993, Nucl. Phys. **B390**, 253.
- Beneke, M. and V. Braun, 1995, Phys. Lett. **B348**, 513.
- Bernard, C. and A. Soni, 1991, Nucl. Phys. (**Proc. Suppl.**) **9**, 155.
- Bernard, C., J. Labrenz, and A. Soni, 1994, Phys. Rev. **D49**, 2536.
- Bertolini, S., F. Borzumati, and A. Masiero, 1987, Phys. Rev. Lett. **59**, 180.
- Bertolini, S., F. Borzumati, A. Masiero, and G. Ridolfi, 1991a, Nucl. Phys. **B353**, 591.
- Bertolini, S., F. Borzumati, A. Masiero, and G. Ridolfi, 1991b, Nucl. Phys. **B353**, 591.
- Bertolini, S., J. Eeg, and M. Fabbrichesi, 1995a, Nucl. Phys. **B449**, 197.
- Bertolini, S., J. O. Eeg, and M. Fabbrichesi, 1995b, SISSA preprint, **SISSA 103/95/EP**.
- Bethke, S., 1994, talk presented at the QCD '94 Conference, Montpellier, France, July 7–13.
- Bigi, I. I. and F. Gabbiani, 1991, Nucl. Phys. **B367**, 3.
- Bigi, I. I. and N. Uraltsev, 1994, Z. Phys. **C62**, 623.
- Bigi, I. I., N. G. Uraltsev, and A. I. Vainshtein, 1992, Phys. Lett. **B293**, 430; erratum *ibid.* *Phys. Lett.* **B297** (1993) 477.
- Bigi, I. I. *et al.*, 1993, Phys. Rev. Lett. **71**, 496.
- Bigi, I. I., B. Blok, M. Shifman, N. G. Uraltsev, and A. I. Vainshtein, 1994a, in *B-Decays* (2nd Edition), editor S. L. Stone, World Scientific, Singapore, (1994) p. 132; (1992), p. 610.
- Bigi, I. I., B. Blok, M. Shifman, and A. Vainshtein, 1994b, Phys. Lett. **B323**, 408.
- Bijnens, J. and J. Prades, 1995, Nucl. Phys. **B444**, 523.
- Bijnens, J. and M. B. Wise, 1984, Phys. Lett. **B137**, 245.
- Bijnens, J., J.-M. Gérard, and G. Klein, 1991, Phys. Lett. **B257**, 191.
- Bjorken, J. D., I. Dunietz, and J. Taron, 1992, Nucl. Phys. **B371**, 111.
- Blok, B. and M. Shifman, 1993, talk presented at the 3rd Workshop on the Tau-Charm Factory, Marbella, Spain, 1-6 June, 1993, **hep-ph/9311331**.
- Blok, B., L. Koyrakh, M. Shifman, and A. I. Vainshtein, 1994, Phys. Rev. **D49**, 3356.
- Bollini, C. G. and J. J. Giambiagi, 1972a, Phys. Lett. **B40**, 566.
- Bollini, C. G. and J. J. Giambiagi, 1972b, Nuovo Cim. **12B**, 20.
- Borzumati, F., 1994, Z. Phys. **C63**, 291.
- Boyd, C., B. Grinstein, and R. Lebed, 1995, Phys. Rev. Lett. **74**, 4603.
- Breitenlohner, P. and D. Maison, 1977, Commun. Math. Phys. **52**, 11, 39, 55.
- Broadhurst, D. and A. Grozin, 1991, Phys. Lett. **B267**, 105.
- Brodsky, S. J., G. P. Lepage, and P. B. Mackenzie, 1983, Phys. Rev. **D28**, 228.
- Browder, T. E. and K. Honscheid, 1995, Prog. Part. Nucl. Phys. **35**, 81.
- Bruno, C. and J. Prades, 1993, Z. Phys. **C57**, 585.
- Buchalla, G. and A. J. Buras, 1993a, Nucl. Phys. **B400**, 225.
- Buchalla, G. and A. J. Buras, 1993b, Nucl. Phys. **B398**, 285.
- Buchalla, G. and A. J. Buras, 1994a, Nucl. Phys. **B412**, 106.
- Buchalla, G. and A. J. Buras, 1994b, Phys. Lett. **B336**, 263.
- Buchalla, G. and A. J. Buras, 1994c, Phys. Lett. **B333**, 221.
- Buchalla, G., A. J. Buras, and M. K. Harlander, 1990, Nucl. Phys. **B337**, 313.
- Buchalla, G., A. J. Buras, and M. K. Harlander, 1991, Nucl. Phys. **B349**, 1.
- Buchalla, G., 1993, Nucl. Phys. **B391**, 501.
- Buras, A. J. and J.-M. Gérard, 1987, Phys. Lett. **B192**, 156.

- Buras, A. J. and M. K. Harlander, 1992, in Heavy Flavours, editors A. J. Buras and M. Lindner, World Scientific, Singapore, (1992), p. 58.
- Buras, A. J. and M. E. Lautenbacher, 1993, Phys. Lett. **B318**, 212.
- Buras, A. J. and M. Münz, 1995, Phys. Rev. **D52**, 186.
- Buras, A. J. and P. H. Weisz, 1990, Nucl. Phys. **B333**, 66.
- Buras, A. J., M. Jamin, and P. H. Weisz, 1990, Nucl. Phys. **B347**, 491.
- Buras, A. J., M. Jamin, M. E. Lautenbacher, and P. H. Weisz, 1992, Nucl. Phys. **B370**, 69; addendum *ibid.* Nucl. Phys. **B375** (1992) 501.
- Buras, A. J., M. Jamin, and M. E. Lautenbacher, 1993a, Nucl. Phys. **B400**, 75.
- Buras, A. J., M. Jamin, and M. E. Lautenbacher, 1993b, Nucl. Phys. **B408**, 209.
- Buras, A. J., M. Jamin, M. E. Lautenbacher, and P. H. Weisz, 1993c, Nucl. Phys. **B400**, 37.
- Buras, A. J., M. E. Lautenbacher, M. Misiak, and M. Münz, 1994a, Nucl. Phys. **B423**, 349.
- Buras, A. J., M. E. Lautenbacher, and G. Ostermaier, 1994b, Phys. Rev. **D50**, 3433.
- Buras, A. J., M. Misiak, M. Münz, and S. Pokorski, 1994c, Nucl. Phys. **B424**, 374.
- Buras, A. J., 1980, Rev. Mod. Phys. **52**, 199.
- Buras, A. J., 1993, Phys. Lett. **B317**, 449.
- Buras, A. J., 1994, Phys. Lett. **B333**, 476.
- Buras, A. J., 1995, Nucl. Phys. **B434**, 606.
- Cabibbo, N. and L. Maiani, 1978, Phys. Lett. **B79**, 109.
- Callan Jr, C. G., 1970, Phys. Rev. **D2**, 1541.
- Cella, G., G. Curci, G. Ricciardi, and A. Viceré, 1990, Phys. Lett. **B248**, 181.
- Cella, G., G. Ricciardi, and A. Viceré, 1991, Phys. Lett. **B258**, 212.
- Cella, G., G. Curci, G. Ricciardi, and A. Viceré, 1994a, Phys. Lett. **B325**, 227.
- Cella, G., G. Curci, G. Ricciardi, and A. Viceré, 1994b, Nucl. Phys. **B431**, 417.
- Chay, J., H. Georgi, and B. Grinstein, 1990, Phys. Lett. **B247**, 399.
- Chetyrkin, K. G., C. A. Dominguez, D. Pirjol, and K. Schilcher, 1995, Phys. Rev. **D51**, 5090.
- Cho, P. and M. Misiak, 1994, Phys. Rev. **D49**, 5894.
- Cicuta, G. M. and E. Montaldi, 1972, Lett. Nuovo Cim. **4**, 329.
- Ciuchini, M., E. Franco, G. Martinelli, and L. Reina, 1993a, Phys. Lett. **B301**, 263.
- Ciuchini, M., E. Franco, G. Martinelli, L. Reina, and L. Silvestrini, 1993b, Phys. Lett. **B316**, 127.
- Ciuchini, M., E. Franco, G. Martinelli, and L. Reina, 1994a, Nucl. Phys. **B415**, 403.
- Ciuchini, M., E. Franco, G. Martinelli, L. Reina, and L. Silvestrini, 1994b, Phys. Lett. **B334**, 137.
- Ciuchini, M., E. Franco, L. Reina, and L. Silvestrini, 1994c, Nucl. Phys. **B421**, 41.
- Ciuchini, M., E. Franco, G. Martinelli, L. Reina, and L. Silvestrini, 1995, Z. Phys. **C68**, 239.
- Cohen, A. G. and A. Manohar, 1984, Phys. Lett. **B143**, 481.
- Cohen, A. G., G. Ecker, and A. Pich, 1993, Phys. Lett. **B304**, 347.
- Crisafulli, M. *et al.*, 1995, preprint, **hep-lat/9509029**.
- Datta, A., J. Fröhlich, and E. A. Paschos, 1990, Z. Phys. **C46**, 63.
- Datta, A., E. A. Paschos, J.-M. Schwarz, and M. N. S. Roy, 1995, University of Dortmund preprint, **DO-TH 95/12**.
- Deshpande, N. G. and X.-G. He, 1995, Phys. Rev. Lett. **74**, 26; erratum *ibid.* Phys. Rev. Lett. **74** (1995) 4099.
- Deshpande, N. G., P. Lo, J. Trampetić, G. Eilam, and P. Singer, 1987, Phys. Rev. Lett. **59**, 183.

Deshpande, N. G., J. Trampetić, and K. Panose, 1989, Phys. Rev. **D39**, 1461.
 Deshpande, N. G., K. Panose, and J. Trampetić, 1993, Phys. Lett. **B308**, 322.
 Deshpande, N. G., X.-G. He, and J. Trampetić, 1995, Phys. Lett. **B345**, 547.
 Dib, C. O., I. Dunietz, and F. J. Gilman, 1989a, Phys. Lett. **B218**, 487.
 Dib, C. O., I. Dunietz, and F. J. Gilman, 1989b, Phys. Rev. **D39**, 2639.
 Dib, C. O., I. Dunietz, F. J. Gilman, and Y. Nir, 1990, Phys. Rev. **D 41**, 1522.
 Dib, C. O., I. Dunietz, and F. J. Gilman, 1991, Mod. Phys. Lett. **A6**, 3573.
 Dikeman, R. D., M. Shifman, and N. G. Uraltsev, 1995, University of Minnesota preprint **TPI-MINN-95/9-T; hep-ph/9505397**.
 Donoghue, J. F. and F. Gabbiani, 1995, Phys. Rev. **D51**, 2187.
 Donoghue, J. F., E. Golowich, and B. R. Holstein, 1982, Phys. Lett. **B119**, 412.
 Donoghue, J. F., E. Golowich, B. R. Holstein, and J. Trampetić, 1986, Phys. Lett. **B179**, 361.
 Draper, T. and C. McNeile, 1994, Nucl. Phys. **B (Proc. Suppl.) 34**, 453.
 Dugan, M. J. and B. Grinstein, 1991, Phys. Lett. **B256**, 239.
 Duncan, A., E. Eichten, J. Flynn, B. Hill, G. Hockney, and H. Thacker, 1995, Phys. Rev. **D51**, 5101.
 Ecker, G., A. Pich, and E. de Rafael, 1987, Nucl. Phys. **B291**, 692.
 Ecker, G., A. Pich, and E. de Rafael, 1988, Nucl. Phys. **B303**, 665.
 Eeg, J. O. and I. Picek, 1988, Phys. Lett. **B214**, 651.
 Ellis, J. and J. S. Hagelin, 1983, Nucl. Phys. **B217**, 189.
 Falk, A., M. Luke, and M. J. Savage, 1994, Phys. Rev. **D49**, 3367.
 Falk, A., M. Wise, and I. Dunietz, 1995, Phys. Rev. **D51**, 1183.
 Fleischer, R., 1994a, Z. Phys. **C62**, 81.
 Fleischer, R., 1994b, Phys. Lett. **B332**, 419.
 Floratos, E. G., D. A. Ross, and C. T. Sachrajda, 1977, Nucl. Phys. **B129**, 66.
 Flynn, J. M. and L. Randall, 1989a, Nucl. Phys. **B326**, 31.
 Flynn, J. M. and L. Randall, 1989b, Phys. Lett. **B224**, 221; erratum *ibid. Phys. Lett.* **B235** (1990) 412.
 Flynn, J., O. Hernández, and B. Hill, 1991, Phys. Rev. **D43**, 3709.
 Flynn, J. M., 1990, Mod. Phys. Lett. **A5**, 877.
 Franco, E., L. Maiani, G. Martinelli, and A. Morelli, 1989, Nucl. Phys. **B317**, 63.
 Fröhlich, J., J. Heinrich, E. A. Paschos, and J.-M. Schwarz, 1991, University of Dortmund preprint, **DO-TH 02/91**.
 Gaillard, M. K. and B. W. Lee, 1974a, Phys. Rev. Lett. **33**, 108.
 Gaillard, M. K. and B. W. Lee, 1974b, Phys. Rev. **D10**, 897.
 Gell-Mann, M. and F. E. Low, 1954, Phys. Rev. **95**, 1300.
 Geng, C. Q. and J. N. Ng, 1990, Phys. Rev. **D41**, 2351.
 Georgi, H., 1991, in *Proceedings of TASI-91*, editors R.K. Ellis et al., World Scientific, Singapore, (1991), p589.
 Gérard, J.-M., 1990, Acta Physica Polonica **B21**, 257.
 Gibbons, L. K. *et al.*, 1993, Phys. Rev. Lett. **70**, 1203.
 Gilman, F. J. and M. B. Wise, 1979, Phys. Rev. **D20**, 2392.
 Gilman, F. J. and M. B. Wise, 1980, Phys. Rev. **D21**, 3150.
 Gilman, F. J. and M. B. Wise, 1983, Phys. Rev. **D27**, 1128.
 Giménez, V., 1993, Nucl. Phys. **B401**, 116.

Greub, C., A. Ioannissian, and D. Wyler, 1995, Phys. Lett. **B346**, 149.
 Grigjanis, R., P. J. O'Donnell, M. Sutherland, and H. Navelet, 1988, Phys. Lett. **B213**, 355.
 Grigjanis, R., P. J. O'Donnell, M. Sutherland, and H. Navelet, 1989, Phys. Lett. **B223**, 239.
 Grigjanis, R., P. O'Donnell, M. Sutherland, and H. Navelet, 1992, Phys. Lett. **B286**, 413E.
 Grinstein, B., M. J. Savage, and M. B. Wise, 1989, Nucl. Phys. **B319**, 271.
 Grinstein, B., R. Springer, and M. B. Wise, 1990, Nucl. Phys. **B339**, 269.
 Grinstein, B., 1989, Phys. Lett. **B229**, 280.
 Grinstein, B., 1991, in *High Energy Phenomenology*, editors R. Huerta and M.A. Pérez, World Scientific, Singapore, (1991), p161.
 Gross, D., 1976, in *Methods In Field Theory* (Les Houches 1975, Proceedings), editors R. Balian and J. Zinn-Justin, North-Holland, Amsterdam, (1976), p. 141.
 Grossman, Y., Z. Ligeti, and E. Nardi, 1995, CALTEC preprint, **CALT-68-2022; hep-ph/9510378**.
 Guberina, B. and R. D. Peccei, 1980, Nucl. Phys. **B163**, 289.
 Hagelin, J. S. and L. S. Littenberg, 1989, Prog. Part. Nucl. Phys. **23**, 1.
 Harris, G. R. and J. L. Rosner, 1992, Phys. Rev. **D45**, 946.
 Harris, D. A. *et al.*, 1993, Phys. Rev. Lett. **71**, 3918.
 Hayashi, T., M. Matsuda, and M. Tanimoto, 1993, Prog. Theo. Phys. **89**, 1047.
 Heiliger, P. and L. Seghal, 1993, Phys. Rev. **D47**, 4920.
 Heinrich, J., E. A. Paschos, J.-M. Schwarz, and Y. L. Wu, 1992, Phys. Lett. **B279**, 140.
 Herrlich, S. and U. Nierste, 1994, Nucl. Phys. **B419**, 292.
 Herrlich, S. and U. Nierste, 1995a, Phys. Rev. **D52**, 6505.
 Herrlich, S. and U. Nierste, 1995b, Nucl. Phys. **B455**, 39.
 Herrlich, S., 1994, Ph.D. dissertation, Munich Technical University (unpublished).
 Hewett, J. L., 1993, Phys. Rev. Lett. **70**, 1045.
 Hokim, Q. and X. Pham, 1983, Phys. Lett. **B122**, 297.
 Hokim, Q. and X. Pham, 1984, Ann. Phys. **155**, 202.
 Hou, W. S., R. I. Willey, and A. Soni, 1987, Phys. Rev. Lett. **58**, 1608.
 Inami, T. and C. S. Lim, 1981, Progr. Theor. Phys. **65**, 297.
 Isgur, N. and M. Wise, 1989, Phys. Lett. **B232**, 113.
 Isgur, N. and M. Wise, 1990, Phys. Lett. **B237**, 527.
 Isgur, N. and M. Wise, 1992, in *Heavy Flavours*, editors A. J. Buras and M. Lindner, World Scientific, Singapore, (1992), p. 234.
 Ishizuka, N., 1993, Phys. Rev. Lett. **71**, 24.
 Jamin, M. and M. Münz, 1995, Z. Phys. **C66**, 633.
 Jamin, M. and A. Pich, 1994, Nucl. Phys. **B425**, 15.
 Jaus, W. and D. Wyler, 1990, Phys. Rev. **D41**, 3405.
 Jezabek, M. and J. H. Kühn, 1989, Nucl. Phys. **B320**, 20.
 Ji, X. and M. Musolf, 1991, Phys. Lett. **B257**, 409.
 Kambor, J., J. Missimer, and D. Wyler, 1990, Nucl. Phys. **B346**, 17.
 Kambor, J., J. Missimer, and D. Wyler, 1991, Phys. Lett. **B261**, 496.
 Kapustin, A. and Z. Ligeti, 1995, Phys. Lett. **B355**, 318.
 Kapustin, A., Z. Ligeti, and H. D. Politzer, 1995, Phys. Lett. **B357**, 653.
 Kaufman, W. A., H. Steger, and Y. P. Yao, 1989, Mod. Phys. Lett. **A3**, 1479.
 Kilcup, G. W., 1991, Nucl. Phys. **B (Proc. Suppl.) 20**, 417.

Kilian, W. and T. Mannel, 1993, Phys. Lett. **B301**, 382.

Kim, C. S. and A. D. Martin, 1989, Phys. Lett. **B225**, 186.

Ko, P., 1992, Phys. Rev. **D45**, 174.

Köhler, G. O. and E. A. Paschos, 1995, Phys. Rev. **D52**, 175.

Kroll, J. *et al.*, 1995, Fermilab preprint, **FERMILAB-CONF-95/229-E**.

Kuno, Y., 1992, KEK-preprint 92-190, published in Proc. 10th Int. Symp. on High Energy Spin Physics, Nagoya, Japan (1992), p. 769.

Lim, C. S., T. Morozumi, and A. I. Sanda, 1989, Phys. Lett. **B218**, 343.

Littenberg, L. and G. Valencia, 1993, Ann. Rev. Nucl. Part. Sci. **43**, 729.

Littenberg, L., 1989a, Phys. Rev. **D39**, 3322.

Littenberg, L. S., 1989b, in *Proceedings of the Workshop on CP Violation at a Kaon Factory*, editor J.N. Ng, TRIUMF, Vancouver, Canada (1989), p. 19.

Lu, M. and M. Wise, 1994, Phys. Lett. **B324**, 461.

Lu, M., M. Wise, and M. Savage, 1992, Phys. Rev. **D46**, 5026.

Luke, M. and M. Savage, 1994, Phys. Lett. **B321**, 88.

Luke, M., M. Savage, and M. B. Wise, 1995, Phys. Lett. **B343**, 329.

Lusignoli, M., 1989, Nucl. Phys. **B325**, 33.

Mannel, T., W. Roberts, and Z. Ryzak, 1992, Nucl. Phys. **B368**, 204.

Mannel, T., 1993, in *QCD – 20 Years Later*, editors P.M. Zerwas and H.A. Kastrup, World Scientific, Singapore, (1993), p. 634.

Mannel, T., 1994, Nucl. Phys. **B413**, 396.

Manohar, A. and M. Wise, 1994, Phys. Rev. **D49**, 1310.

Marciano, W. and Z. Parsa, 1995, preprint, **DOE/ER/40561-224-INT95-17-09**.

Misiak, M. and M. Münz, 1995, Phys. Lett. **B344**, 308.

Misiak, M., 1991, Phys. Lett. **B269**, 161.

Misiak, M., 1993, Nucl. Phys. **B393**, 23.

Misiak, M., 1994, Phys. Lett. **B321**, 113.

Misiak, M., 1995, Nucl. Phys. **B439**, 461E.

Narison, S., 1994, Phys. Lett. **B322**, 247.

Neubert, M. and B. Stech, 1991, Phys. Rev. **D44**, 775.

Neubert, M., 1992, Phys. Rev. **D45**, 2451.

Neubert, M., 1994a, Phys. Lett. **B338**, 84.

Neubert, M., 1994b, Phys. Rev. **D49**, 4623.

Neubert, M., 1994c, Phys. Rept. **245**, 259.

Nierste, U., 1995, Ph.D. dissertation, Munich Technical University **hep-ph/9510323**.

Nir, Y., 1989, Phys. Lett. **B221**, 184.

Nir, Y., 1992, in *Proceedings of the the 20th Annual SLAC Summer Institute on Particle Physics*, Stanford, CA, 13-24 July 1992, p. 81.

Novikov, V. A., A. I. Vainshtein, V. I. Zakharov, and M. A. Shifman, 1977, Phys. Rev. **D16**, 223.

O'Donnell, P. J. and H. K. K. Tung, 1991, Phys. Rev. **D43**, R2067.

Ohl, K. E. *et al.*, 1990, Phys. Rev. Lett. **64**, 2755.

Ovsyannikov, L. V., 1956, Dokl. Acad. Nauk SSSR **109**, 1112.

Palmer, W. and B. Stech, 1993, Phys. Rev. **D48**, 4174.

Papadimitriou, V. *et al.*, 1991, Phys. Rev. **D44**, 573.

- Particle Data Group, 1994, Phys. Rev. **D50**.
- Patterson, R., 1995, proceedings of the XXVII. International Conference on High Energy Physics, Glasgow, 1994, editors P.J. Bussey and I.G. Knowles, IOP Publications Ltd., Bristol, 1995, p149.
- Peccei, R. D. and K. Wang, 1995, Phys. Lett. **B349**, 220.
- Pich, A. and E. de Rafael, 1985, Phys. Lett. **B158**, 477.
- Pich, A. and E. de Rafael, 1991, Nucl. Phys. **B358**, 311.
- Politzer, H. and M. Wise, 1988a, Phys. Lett. **B206**, 681.
- Politzer, H. and M. Wise, 1988b, Phys. Lett. **B208**, 504.
- Ponce, W., 1981, Phys. Rev. **D23**, 1134.
- Pott, N., 1995, Technical University Munich preprint **TUM-T31-93/95**.
- Prades, J., C. Dominguez, J. Penarrocha, A. Pich, and E. de Rafael, 1991, Z. Phys. **C51**, 287.
- Rein, D. and L. M. Sehgal, 1989, Phys. Rev. **D39**, 3325.
- Ritchie, J. L. and S. G. Wojcicki, 1993, Rev. Mod. Phys. **65**, 1149.
- Rosner, J. L., 1992, in *B-Decays*, editor S. L. Stone, World Scientific, Singapore, (1992).
- Sachrajda, C. T., 1992, in *Heavy Flavours*, editors A. J. Buras and M. Lindner, World Scientific, Singapore, (1992), p. 415.
- Sachrajda, C., 1994, in *B-Decays* (2nd Edition), editor S. L. Stone, World Scientific, Singapore, (1994), p. 602.
- Savage, M. and M. Wise, 1990, Phys. Lett. **B250**, 151.
- Schmidtler, M. and K. R. Schubert, 1992, Z.Phys. **C 53**, 347.
- Sharpe, S. R., 1991, Nucl. Phys. **B (Proc. Suppl.) 20**, 429.
- Sharpe, S. R., 1994, Nucl. Phys. **B (Proc. Suppl.) 34**, 403.
- Shifman, M., N. G. Uraltsev, and A. I. Vainshtein, 1994, Int. J. Mod. Phys. **A9**, 2467.
- Shifman, M., N. G. Uraltsev, and A. I. Vainshtein, 1995, Phys. Rev. **D51**, 2217.
- Soni, A., 1995, preprint, **hep-lat 9510036**.
- Stueckelberg, E. C. G. and A. Petermann, 1953, Helv. Phys. Acta **26**, 499.
- Symanzik, K., 1970, Comm. Math. Phys. **18**, 227.
- 't Hooft, G. and M. Veltman, 1972a, Nucl. Phys. **B50**, 318.
- 't Hooft, G. and M. Veltman, 1972b, Nucl. Phys. **B44**, 189.
- 't Hooft, G., 1973, Nucl. Phys. **B61**, 455.
- Tanimoto, M., 1992, Phys. Lett. **B274**, 463.
- Thorndike, E., 1995, talk presented at the EPS-HEP Conference, Brussels, Belgium, July 1995.
- Vainshtein, A. I., V. I. Zakharov, V. A. Novikov, and M. A. Shifman, 1976, Sov. J. Nucl. Phys. **23**, 540.
- Vainshtein, A. I., V. I. Zakharov, and M. A. Shifman, 1977, JEPT **45**, 670.
- Voloshin, M. and M. Shifman, 1987, Sov. J. Nucl. Phys. **45**, 292.
- Voloshin, M., 1995, Phys. Rev. **D51**, 3948.
- Vysotskij, M. I., 1980, Sov. J. Nucl. Phys. **31**, 797.
- Weaver, M. *et al.*, 1994, Phys. Rev. Lett. **72**, 3758.
- Webber, B. R., 1994, talk presented at the International Conference on High Energy Physics, Glasgow, Scotland, July 20–27.
- Weinberg, S., 1973, Phys. Rev. **D8**, 3497.
- Wilson, K. G. and W. Zimmermann, 1972, Comm. Math. Phys. **24**, 87.
- Winstein, B. and L. Wolfenstein, 1993, Rev. Mod. Phys. **65**, 1113.

Witten, E., 1977, Nucl. Phys. **B122**, 109.
Wolfenstein, L., 1964, Phys. Rev. Lett. **13**, 562.
Wolfenstein, L., 1983, Phys. Rev. Lett. **51**, 1841.